



UNIVERSITY OF
BIRMINGHAM

**Development of Novel Implantable Hydrogels and Aerogels
for Localised Cancer Treatment**

By
SHAKER THABIT ALSHARIF

A thesis submitted to the University of Birmingham for the degree of
DOCTOR OF PHILOSOPHY

School of Pharmacy
College of Medical and Dental Sciences
University of Birmingham
April 2022

UNIVERSITY OF
BIRMINGHAM

University of Birmingham Research Archive

e-theses repository

This unpublished thesis/dissertation is copyright of the author and/or third parties. The intellectual property rights of the author or third parties in respect of this work are as defined by The Copyright Designs and Patents Act 1988 or as modified by any successor legislation.

Any use made of information contained in this thesis/dissertation must be in accordance with that legislation and must be properly acknowledged. Further distribution or reproduction in any format is prohibited without the permission of the copyright holder.

Abstract

Pancreatic and bladder cancers are common types of cancer and related to a considerable rate of morbidity and mortality if not managed properly. The adjuvant chemotherapy following the surgical tumour resection is required for both cancer types in order to eliminate any remaining malignant cells to prevent cancer metastasis. Hydrogels and aerogels are promising strategies that can be designed and used to improve the drug delivery into the pancreas and bladder. In the first study, caffeine-loaded agar hydrogels, pre- and post-loaded aerogels were developed as potential implantable drug delivery systems. Several hydrogel and aerogel formulations were prepared by either sol-gel or post-loading methods using increasing concentrations of agar polymer and caffeine as model drug. These two variables were investigated for their impacts on hydrogels and aerogels physical properties, drug content homogeneity and release profiles to determine the optimized formulations. Irinotecan Hydrochloride (IRN)-loaded agar hydrogels pre- and post-loaded aerogel formulations were developed using the optimized formulations as implantable drug delivery systems to improve IRN delivery to the tumour resection sites and increase their efficacy as post-surgical localised treatment for pancreatic cancer. The formulations variables based on the amount of agar and IRN were investigated for their effects on the hydrogels and aerogels physical properties, drug content distribution and release profiles, as well as their cytotoxicity using different pancreatic cancer cell lines. The IRN-loaded hydrogels and aerogels showed stronger mechanical strength and lower levels of hydrogel adhesion, as well as IRN distribution for both formulations with higher agar concentration, while better IRN distribution and more flexible aerogels were associated with lower agar concentration. The *in vitro* release of IRN from all hydrogel and

aerogel formulations demonstrated concentration dependent prolonged release over 4 days. The hydrogels and preloaded aerogels showed faster sustained release rate as the agar concentration decreased due to the increased porosity, while post-loaded aerogels demonstrated slower release profiles as IRN loading rate decreased resulted from lower level of drug distribution. The cytotoxicity assay of IRN pre- and post-loaded agar aerogels against MIA PaCa-2 cells demonstrated more time and concentration dependent reduced cell viability compared to their cytotoxic effect against Panc-1 cells.

In the second study, the development of Infigratinib (INF)-loaded HEC and HPMC hydrogels was established to possibly enhance the INF delivery to the bladder through intravesical administration and potentially increase its efficacy as localised treatment of non-muscle invasive bladder cancer (NMIBC). Based on varying concentrations of HEC and HPMC polymers, as well as INF loading, several hydrogel formulations were prepared by sol-gel method. The effects of these varying concentrations on both sets of hydrogels rheological properties, drug content distribution and release profiles were assessed. The hydrogels with lower HEC and HPMC concentrations, as well as INF loading demonstrated reduced viscosity, suitable shear thinning behaviour making them easier to deliver through a catheter based the rheological analysis and injectability assessment. They showed acceptable drug content distribution. The INF-loaded HEC hydrogels showed better concentration dependent mucoadhesive features compared to the INF-loaded HPMC hydrogels. The release of INF from the HEC and HPMC hydrogels showed a rapid 'burst' release associated with the low HEC and HPMC concentrations, as well as INF loading over 24 hours, while as the HEC and HPMC concentrations and INF loading increased the percent release of INF from the hydrogels reduces. The cytotoxicity of the optimised INF-loaded HEC hydrogel against FGFR mutant and non-mutant cancer cells demonstrated a similar

cytotoxic effect to the free INF and selectively inhibited FGFR mutant cancer cells proliferation. Overall, the results demonstrate that the IRN-loaded agar hydrogels and aerogels have the potential to be effective for the post-operative localised treatment of pancreatic cancer. The targeted therapy using INF-loaded HEC hydrogel through intravesical administration is promising for NMIBC cases associated with FGFR mutations.

Acknowledgement

This project consumed huge amount of work, research, and dedication. Still, implementation would not have been possible if I did not have a support of many individuals. Therefore, I would like to extend my sincere gratitude to all of them.

First and foremost, I would like to express gratitude and sincere thanks to my inspiring mentor Dr. Christopher McConville, who has given me his valuable guidance, advice, encouragement, and read my numerous revisions and helped make some sense of the confusion.

My deepest gratitude goes to all of my family members. It would not be possible to write this thesis without the support from them. I would like to thank my parents Thabit and Fatimah Alsharif who devoted their lives for me, my wife Randa who has been always supportive in my hard times.

I offer my special thanks to the Bladder Cancer Research Centre at the University of Birmingham, who helped me by performing all the cell culture work. I would sincerely like to thank all my lab mates in the Pharmacy School for their kind cooperation.

I am thankful to Saudi Arabian Cultural Bureau, Royal Embassy of Saudi Arabia for their financial, logistical support, and for providing necessary guidance concerning projects implementation.

Last but not least, I am grateful to Prof. Stephen Britland and Dr. Marie-Christine Jones for accepting evaluating my thesis.

Covid-19 impact statement

As the Covid-19 pandemic started at the beginning of the second year of my PhD, there have been some impacts on my project as a result of the lockdown restrictions and the precautionary measures.

The main impacts are listed below:

- I did not get to test the IRN-loaded agar hydrogels cytotoxicity.
- I did not get to investigate the co-loading of other FOLFIRINOX drugs into the IRN-loaded agar hydrogels and aerogels.
- I did not get to investigate the increased residence time of INF-loaded HEC hydrogel *in vitro*.
- I did not get to test the INF-loaded HEC hydrogel in animal study.

Table of contents

Abstract.....	I
Acknowledgement.....	IV
Covid-19 impact statement.....	V
Table of contents	VI
List of tables.....	XIII
List of figures.....	XIV
List of abbreviations	XIX
Chapter 1 : Introduction	1
1. Hydrogels and aerogels: opportunities for localised treatment of cancer	1
1.1 Pancreatic cancer.....	1
1.1.1. Treatment of pancreatic cancer	4
1.1.2. Limitations of systemic chemotherapy in the treatment of pancreatic cancer	8
1.2. Bladder cancer.....	9
1.2.1. Treatment of muscle invasive bladder cancer MIBC.....	12
1.2.2. Treatment of non-muscle invasive bladder cancer NMIBC	13
1.2.3. Challenges of intravesical drug delivery for bladder cancer treatment	15
1.2.4. Strategies for drug delivery to the urinary bladder	16
1.3. Hydrogels as a controlled drug delivery system	19
1.3.1. Biomimetic hydrogels.....	20
1.3.2. Biodegradable hydrogels	22
1.3.3. Smart hydrogels	23
1.3.4. Hydrogel technologies for localised cancer chemotherapy	27

1.4. Aerogels as a controlled delivery system.....	32
1.4.1. Aerogels as a wound healing technology.....	34
1.4.2. Aerogels as a regenerative medicine technology.....	35
1.4.3. Aerogels for localised cancer treatment.....	39
1.5. Limitations of available hydrogels and aerogels as controlled drug delivery systems..	40
1.6. Hypothesis and objectives.....	41
Chapter 2: Development and Optimization of Implantable Agar Hydrogels as a Localised Drug Delivery System	44
2.1 Introduction.....	44
2.2 Materials and method.....	46
2.2.1 Materials	46
2.2.2 Preparation of caffeine-loaded agar hydrogels	46
2.2.3 Characterization of the agar hydrogel formulations	47
2.2.3.1 Hydrogel mechanical strength	47
2.2.3.2 Hydrogel mucoadhesive properties.....	48
2.2.3.3 Hydrogels rheology.....	48
2.2.3.4 Caffeine content distribution in hydrogels.....	49
2.2.4 In vitro release of caffeine from the hydrogel formulations	49
2.2.5 HPLC analysis	50
2.2.5.1 HPLC chromatographic conditions.....	50
2.2.5.2 Stock solution and calibration curve.....	50
2.2.6 Statistical analysis.....	51
2.3 Results.....	51

2.3.1 Hydrogel mechanical and mucoadhesive properties.....	51
2.3.2 Hydrogel rheology	54
2.3.3 HPLC analysis of caffeine	58
2.3.4 Caffeine content distribution in hydrogels.....	59
2.3.5 In vitro release of caffeine from the agar hydrogel formulations	60
2.4 Discussion	63
2.5 Conclusion	68
Chapter 3: Development and Optimization of Implantable Agar Aerogels as a Localised Drug Delivery System	70
3.1 Introduction.....	70
3.2 Materials and methods	71
3.2.1 Materials	71
3.2.2 Preparation of caffeine preloaded and post-loaded agar aerogels.....	72
3.2.3 Characterization of the agar aerogel formulations.....	74
3.2.3.1 Aerogels mechanical strength.....	74
3.2.3.2 Aerogels porosity and swelling ratios.....	75
3.2.3.3 Raman mapping of caffeine post-loaded aerogels	76
3.2.3.4 Caffeine content distribution of the preloaded aerogel formulations	76
3.2.4 In vitro release of caffeine from pre- and post-loaded aerogels	76
3.2.5 HPLC analysis	77
3.2.5.1 HPLC chromatographic conditions, stock solution and calibration curve..	77
3.2.6 Statistical analysis.....	77
3.3 Results.....	78

3.3.1 Aerogels mechanical properties	78
3.3.2 Aerogel porosity and swelling ratios	80
3.3.3 Raman mapping of the caffeine post-loaded aerogels	81
3.3.4 HPLC analysis of caffeine	83
3.3.5 Caffeine content distribution of preloaded agar aerogel formulations	84
3.3.6 In vitro release of caffeine from preloaded agar aerogels.....	85
3.3.7 In vitro release of caffeine from post-loaded aerogels.....	87
3.4 Discussion	92
3.5 Conclusion	101
Chapter 4: Development and Optimization of Implantable Agar Hydrogels and Aerogels for The Localised Treatment of Pancreatic Cancer	102
4.1 Introduction.....	102
4.2 Materials and methods	103
4.2.1 Materials	103
4.2.2 Preparation of IRN-loaded agar hydrogels and aerogels	104
4.2.3 Characterization of the IRN-loaded hydrogels and preloaded aerogels	105
4.2.3.1 IRN-loaded hydrogels and preloaded aerogels mechanical strength.....	105
4.2.3.2 IRN-loaded hydrogels mucoadhesive properties	106
4.2.3.3 IRN-loaded hydrogels rheology.....	106
4.2.3.4 Raman mapping spectroscopy of IRN-preloaded aerogels.....	106
4.2.3.5 IRN content distribution in the agar hydrogel formulations	106
4.2.4 In vitro release of the IRN from agar hydrogels, pre- and post-loaded aerogels	107
4.2.5 HPLC analysis	107

4.2.5.1 HPLC chromatographic conditions.....	107
4.2.5.2 Stock solution and calibration curve.....	108
4.2.6 Cytotoxicity of the IRN pre- and post-loaded agar aerogels against MIA PaCa-2 and Panc-1 cells	108
4.2.7 Statistical analysis.....	109
4.3 Results.....	109
4.3.1 IRN-loaded hydrogels and preloaded aerogels mechanical properties.....	109
4.3.2 IRN-loaded hydrogel rheology	111
4.3.3 Raman mapping spectroscopy of IRN-preloaded aerogels.....	112
4.3.4 IRN HPLC analysis.....	115
4.3.5 IRN content distribution in the agar hydrogel formulations	116
4.3.6 In vitro release of IRN from the agar hydrogels, pre- and post-loaded aerogels.....	117
4.3.7 Cytotoxicity of the IRN-preloaded agar aerogels against MIA PaCa-2 and Panc-1 cells	120
4.3.8 Cytotoxicity of the IRN post-loaded agar aerogels against MIA PaCa-2 and Panc-1 cells	121
4.4 Discussion.....	125
4.5 Conclusion	133
Chapter 5: Development of HEC and HPMC Hydrogels for Intravesical Delivery of Infigratinib for The Localised Treatment of Non-Muscle Invasive Bladder Cancer.....	135
5.1 Introduction.....	135
5.2 Materials and methods	137
5.2.1 Materials	137

5.2.2	Preparation of the INF-loaded HEC and HPMC hydrogels.....	137
5.2.3	Characterization of the INF-loaded HEC and HPMC hydrogels.....	139
5.2.3.1	Injectability of INF-loaded HEC and HPMC hydrogels through a syringe....	139
5.2.3.2	Injectability of INF-loaded HEC and HPMC hydrogels through a catheter...	140
5.2.3.3	Rheological evaluation of INF-loaded HEC and HPMC hydrogels.....	140
5.2.3.4	Mucoadhesive Properties of the INF-loaded HEC and HPMC hydrogels.....	141
5.2.3.5	INF Content of the HEC and HPMC hydrogels	141
5.2.4	In vitro release of the INF from HEC and HPMC hydrogels	141
5.2.5	HPLC analysis	142
5.2.5.1	INF chromatographic conditions	142
5.2.5.2	Stock solution and calibration curve.....	142
5.2.6	Cell lines	143
5.2.7	Cell viability.....	143
5.2.8	Statistical analysis.....	143
5.3	Results.....	144
5.3.1	Evaluation of the INF-loaded HEC and HPMC hydrogels injectability.....	144
5.3.2	Injectability of the INF-loaded HEC and HPMC hydrogels through catheter.....	144
5.3.3	Rheological evaluation of the INF-loaded HEC and HPMC hydrogels.....	146
5.3.4	Mucoadhesive properties of the INF-loaded HEC and HPMC hydrogels.....	151
5.3.5	HPLC analysis of INF.....	151
5.3.6	INF content of the HEC and HPMC hydrogels	153
5.3.7	In vitro release of INF from the HEC and HPMC hydrogels	156
5.3.8	Dose titration on bladder cancer cell lines	160

5.3.9 Evaluation of INF-loaded HEC hydrogel formulation on FGFR mutant cell lines ...	160
5.3.10 Discussion	163
5.4 Conclusion	172
Chapter 6: General discussion and future work.....	173
6.1 General discussion	173
6.1.1 Pancreatic cancer.....	173
6.1.1.1 The IRN-loaded agar hydrogels.....	174
6.1.1.2 The IRN pre- and post-loaded agar aerogels	175
6.1.2 Bladder cancer.....	178
6.1.2.1 INF-loaded HEC and HPMC hydrogels	178
6.2 Future work.....	180
References.....	182

List of tables

Table 1-1: The capability of surgical intervention based on pancreatic cancer staging	2
Table 1-2: Pathologic staging of muscle-invasive bladder cancer.....	11
Table 1-3: Summary of some developed nanocarriers for bladder cancer treatment	19
Table 1-4: Summary of some developed aerogels as controlled drug delivery systems	38
Table 2-1: Formulations of prepared caffeine loaded hydrogels	47
Table 3-1: Formulations of prepared caffeine loaded hydrogels	73
Table 3-2: Formulations of prepared caffeine post-loaded aerogels.....	74
Table 4-1: Formulations of prepared IRN-loaded hydrogels.....	104
Table 4-2: Formulations of prepared IRN-preloaded aerogels	105
Table 4-3: Formulations of prepared IRN post-loaded aerogels.....	105
Table 5-1: Formulations of INF-loaded HEC hydrogels	138
Table 5-2: Formulations of INF-loaded HPMC hydrogels	139

List of figures

Figure 1-1: schematic presentation of on pancreatic cancer staging	3
Figure 1-2: Pancreatic cancer treatment based on patient prognosis.....	4
Figure 1-3: Schematic illustration of bladder cancer staging ... Error! Bookmark not defined.	
Figure 2-1: Effect of different agar concentrations (2, 2.5, 3, and 3.5%) and caffeine loadings (1, 5, and 10%) on 2 and 2.5% hydrogels mechanical strength (A), and adhesion (B).....	53
Figure 2-2: Amplitude sweep for different formulations, (A) different concentrations of unloaded agar hydrogels, (B) 1, 5, and 10% caffeine loaded 2% agar hydrogels, (C) 1, 5, and 10% caffeine loaded 2.5% agar hydrogels.....	55
Figure 2-3: Amplitude sweep for different formulations, (A) 1, 5, and 10% caffeine loaded 3% agar hydrogels, (B) 1, 5, 10% caffeine loaded 3.5% agar hydrogels.....	56
Figure 2-4: Frequency sweep for different formulations, (A) different concentrations of unloaded agar hydrogels, (B) 1, 5, and 10% caffeine loaded 2% agar hydrogels, (C) 1, 5, 10% caffeine loaded 2.5% agar hydrogels, (D) 1, 5, 10% caffeine loaded 3% agar hydrogels, and (E) 1, 5, 10 % caffeine loaded 3.5% agar hydrogels.....	57
Figure 2-5: Standard curve for caffeine using HPLC (n=3).....	58
Figure 2-6: The HPLC chromatogram depicting the peak of caffeine at 273 nm wavelength.	59
Figure 2-7: Drug content distribution of caffeine (1, 5, 10%) in four different hydrogels (2, 2.5, 3, and 3.5%).....	60
Figure 2-8: In vitro cumulative release profiles of caffeine (1, 5, 10%) from four different hydrogels (2, 2.5, 3, and 3.5%) in the PBS at normal pH over 48 hours in the shaking incubator at 60 rpm and 37°C.	62

Figure 3-1: Effect of different agar concentrations (2, 2.5, 3, and 3.5%) and caffeine loading concentrations (1 and 5%) aerogels mechanical strength.	79
Figure 3-2: Effect of post loading volumes (1, 2, and 3 ml) on 2, 2.5, 3, and 3.5% agar aerogels mechanical strength	79
Figure 3-3: Effect of varying agar concentrations (2, 2.5, 3, and 3.5%) on aerogels porosity (A), and swelling (B).....	80
Figure 3-4: The distribution maps of agar aerogels 2 and 2.5% loaded with 1ml of different caffeine concentrations (1, 5, and 10%).....	82
Figure 3-5: The reference Raman spectra of the pure caffeine.....	83
Figure 3-6: Standard curve for caffeine using HPLC (n=3).....	83
Figure 3-7: The HPLC chromatogram depicting the peak of caffeine at 273 nm wavelength.	84
Figure 3-8: Caffeine content distribution (1, 5, and 10%) in four preloaded aerogels (2, 2.5, 3, and 3.5%).....	85
Figure 3-9: <i>In vitro</i> cumulative release profiles of caffeine (1, 5, and 10%) from four different preloaded aerogels (2, 2.5, 3, and 3.5%) in the PBS at normal pH over 48 hours in the shaking incubator at 60 rpm and 37 °C	87
Figure 3-10: <i>In vitro</i> cumulative release profiles of different volumes (1, 2, and 3 ml) of 1% caffeine from four different post-loaded aerogels (2, 2.5, 3, and 3.5 %) in the PBS at normal pH over 48 hours in the shaking incubator at 60 rpm and 37 °C.....	90
Figure 3-11: <i>In vitro</i> cumulative release profiles of different volumes (1, 2, and 3 ml) of 5% caffeine from four different post loaded aerogels (2, 2.5, 3, and 3.5 %) in the PBS at normal pH over 48 hours in the shaking incubator at 60 rpm and 37 °C.....	91

Figure 3-12: *In vitro* cumulative release profiles of different volumes (1, 2, and 3 ml) of 10% caffeine from four different post loaded aerogels (2, 2.5, 3, and 3.5 %) in the PBS at normal pH over 48 hours in the shaking incubator at 60 rpm and 37 °C..... 92

Figure 4-1: Effect of different agar concentrations (2 and 2.5%) and IRN loading (5%) on hydrogels and aerogels mechanical strength..... 110

Figure 4-2: Effect of different agar concentrations (2, 2.5, 3, and 3.5%) and IRN loading (5%) on hydrogels adhesive properties..... 110

Figure 4-3: (A) Amplitude sweep, (B) Frequency sweep of different agar hydrogel concentrations (2, 2.5, 3, and 3.5%) with 5% IRN loading. 113

Figure 4-4: The distribution maps of agar aerogels 2, 2.5, 3, and 3.5% loaded with 5% IRN 114

Figure 4-5: The reference Raman spectra of the pure IRN..... 115

Figure 4-6: Standard curve for IRN using HPLC (n=3). 115

Figure 4-8: IRN content distribution in four different hydrogels 2, 2.5, 3, and 3.5% loaded with 5% IRN. 117

Figure 4-9: *In vitro* cumulative release profiles of 5% IRN from four hydrogels 2, 2.5, 3, and 3.5% (A), and four aerogels 2, 2.5, 3, and 3.5% (B) in water at pH 6.5 over 96 hours in the shaking incubator at 60 rpm and 37°C..... 119

Figure 4-10: *In vitro* cumulative release profiles of different volumes (1, 2, and 3 ml) of 1% IRN from four different post-loaded agar aerogels (2, 2.5, 3, and 3.5%) in water at pH 6.5 over 96 hours in the shaking incubator at 60 rpm and 37°C..... 120

Figure 4-11: Viability of MIA PaCa-2 cells cultured with 5% IRN-preloaded aerogels using different agar concentrations (2, 2.5, 3, and 3.5%) (A). Viability of Panc-1 cells cultured with 5% IRN-preloaded aerogels using different agar concentrations (2, 2.5, 3, and 3.5%) (B) ... 123

Figure 4-12: Viability of MIA PaCa-2 cells cultured with four different agar aerogels (2, 2.5, 3, and 3.5%) post-loaded with different volumes (1, 2, and 3 ml) of 1% IRN using over 96 hours 124

Figure 4-13: Viability of Panc-1 cells cultured with four different agar aerogels (2, 2.5, 3, and 3.5%) post-loaded with different volumes (1, 2, and 3 ml) of 1% IRN using over 96 hours. 125

Figure 5-1: Effect of HEC and HPMC concentrations (1, 1.5, 2, and 2.5%) and INF loadings (1, 2.5, and 5%) on the injectability of HEC hydrogels (A), and HPMC hydrogels (B)..... 145

Figure 5-2: The percentage of unloaded HEC and HPMC hydrogels (1, 1.5, 2, and 2.5%) and 1% INF-loaded HEC hydrogels (A), and HPMC hydrogels (B) pushed through the urinary catheter..... 146

Figure 5-3: Shear stress ramps for different formulations, (A) different concentrations of unloaded HEC hydrogels (1, 1.5, 2, and 2.5%). (B) different concentrations of unloaded HPMC hydrogels (1, 1.5, 2, and 2.5%). Solid and empty points represent the effect of first and second ramp runs respectively. 148

Figure 5-4: Shear stress ramps for different formulations, (A) 1% INF-loaded HEC hydrogels (1, 1.5, 2, and 2.5%). (B) 2.5% INF-loaded HEC hydrogels (1, 1.5, 2, and 2.5%). (C) 5% INF-loaded HEC hydrogels (1, 1.5, 2, and 2.5%). 149

Figure 5-5: Shear stress ramps for different formulations, (A) 1% INF-loaded HPMC hydrogels (1, 1.5, 2, and 2.5%). (B) 2.5% INF-loaded HPMC hydrogels (1, 1.5, 2, and 2.5%). (C) 5% INF-loaded HPMC hydrogels (1, 1.5, 2, and 2.5%)..... 150

Figure 5-6: Mucoadhesion evaluation of HEC hydrogels (A) and HPMC hydrogels (B), based on different polymeric concentrations (1, 1.5, 2, and 2.5%) and INF loadings (1, 2.5, and 5%) for both hydrogels 152

Figure 5-7: Standard curve for INF using HPLC (n=3). 153

Figure 5-8: The HPLC chromatogram depicting the peak of INF at 230 nm wavelength. ... 153

Figure 5-9: The content of different INF loadings (1, 2.5, and 5%) in four different HEC hydrogels (1, 1.5, 2, and 2.5%) (A), and four different HPMC hydrogels (1, 1.5, 2, and 2.5%) (B). 155

Figure 5-10: *In vitro* cumulative release profiles of 1% INF (A), 2.5% INF (B), and 5% INF (C) from four different HEC hydrogels (1, 1.5, 2, and 2.5%) in (80:20) DMSO:methanol over 24 hours in the shaking incubator at 60 rpm and 37 °C..... 158

Figure 5-11: *In vitro* cumulative release profiles of 1% INF (A), 2.5% INF (B), and 5% INF (C) from four different HPMC hydrogels (1, 1.5, 2, and 2.5%) in (80:20) DMSO:methanol over 24 hours in the shaking incubator at 60 rpm and 37 °C..... 159

Figure 5-12: INF dose titration on VM-CUB1, SW780 and T24 cells for continues exposure of 72 hours. Cells viability was tested by Cell Titre Blue assay 161

Figure 5-13: INF dose titration on RT4 and MGH-U3 cells for continues exposure of 72 hours (CE) or 2-hour pulse (2HP). Cell viabilities were tested by Cell Titre Blur assay 162

Figure 5-14: RT4 and MGH-U3 cells were treated with the INF, INF-loaded HEC hydrogel formulation (INF GEL) or the INF-free gel (HEC hydrogel) for continuous exposure of 72 hours (CE) or the 2 hour pulse (2HP). Cell viability was tested by Cell Titre Blue assay..... 163

List of abbreviations

NMIBC: Non-muscle invasive bladder cancer

MIBC: Muscle invasive bladder cancer

TNM: Tumour–node–metastasis

TURBT: Transurethral resection of bladder tumour

BPB: Bladder permeability barrier

GAGs: Glycosaminoglycans

CAR: Chimeric antigen receptor

STING: Stimulator of interferon genes

FGFR : Fibroblast growth factor receptor

RTK : Receptor tyrosine kinases

FOLFIRINOX: Fluorouracil, leucovorin, irinotecan, and oxaliplatin

5-FU: Fluorouracil

IRN: Irinotecan

INF: Infigratinib

DOX: Doxorubicin

MVAC: Methotrexate, vinblastine, doxorubicin, and cisplatin

CMV: Cisplatin, methotrexate, and vinblastine

BCG: Bacillus Calmette–Guérin

PLA: Poly (lactic acid)

PLG: Poly lactide-co-glycolide

PEG: Polyethylene glycol

PAA: Poly (acrylic acid)

MMA: Methyl methacrylate

DMAEM: N, N'-dimethyl amino ethyl methacrylate

PDMAEM: Poly (N, N'-diethylamino ethyl methacrylate)

PDEA: Poly (N, N-diethyl acrylamide)

PNIPAM: Poly (N-isopropylacrylamide)

(PNIPAM-co-IA): Poly (*N*-isopropylacrylamide-co-itaconic acid)

PEO: Poly (ethylene oxide)

PPO: Poly (propylene oxide)

ROS: Reactive oxygen species

HEC: Hydroxyethyl cellulose

HPMC: Hydroxypropyl methylcellulose

DMSO: Dimethyl sulfoxide

PS: Protamine sulphate

Chapter 1: Introduction

1. Hydrogels and aerogels: opportunities for localised treatment of cancer

1.1 Pancreatic cancer

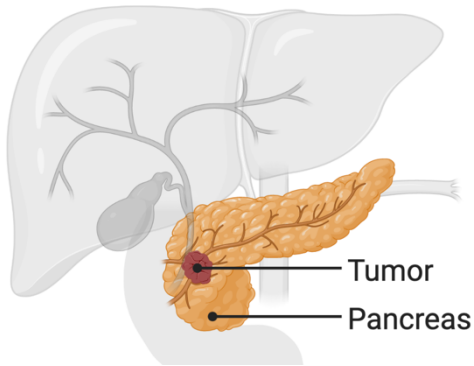
Every year almost 9600 cases of pancreatic cancer are registered, which is expected to increase leading it to be the fifth cause of death in the UK (O'Reilly, Fou et al. 2018). Also, several reports have shown that there are increased mortality and lower survival rates in UK and other European countries related to the pancreatic cancer. The average life expectancy upon diagnosis is approximately six months, while around 20% of patients have a survival rate of one year while the five-year survival remains as low at only 3% (Ferlay, Steliarova-Foucher et al. 2013, Malvezzi, Bertuccio et al. 2014, Collaboration 2017). Such low survival rates are mainly due to late diagnosis since most pancreatic cancer patients are asymptomatic until they reach late stage. Family history of pancreatic cancer, cigarette smoking, pancreatitis, and diabetes mellitus are considered to be common risk factors as well (Iodice, Gandini et al. 2008, Hruban, Canto et al. 2010, Raimondi, Lowenfels et al. 2010, Bosetti, Rosato et al. 2014, Kamisawa, Wood et al. 2016).

Most pancreatic cancers occur due to microscopic epithelial proliferations within the pancreatic ducts, which are known medically as pancreatic intraepithelial neoplasias. This proliferation is mostly driven by the mutations in four different genes, KRAS, CDKN2A, TP53, and SMAD4 (Pelosi, Castelli et al. 2017).

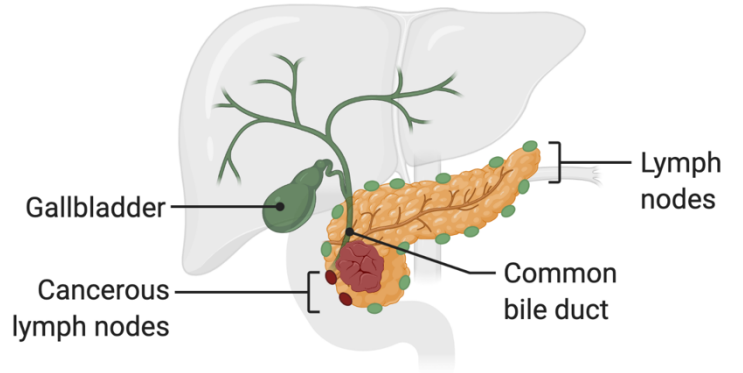
According to the American Joint Committee on Cancer, pancreatic cancer diagnosis and staging is based on tumour–node–metastasis (TNM) classification that describes capability of surgical intervention to resect the tumour. Tumours classified as T1, T2, and T3 are considered resectable, while T4 tumours are not resectable due to celiac axis and/or mesenteric artery involvement as described in figure 1-1 and table 1-1 (Edge and Compton 2010).

Table 1-1: The capability of surgical intervention based on pancreatic cancer staging (Bilimoria, Bentrem et al. 2007)

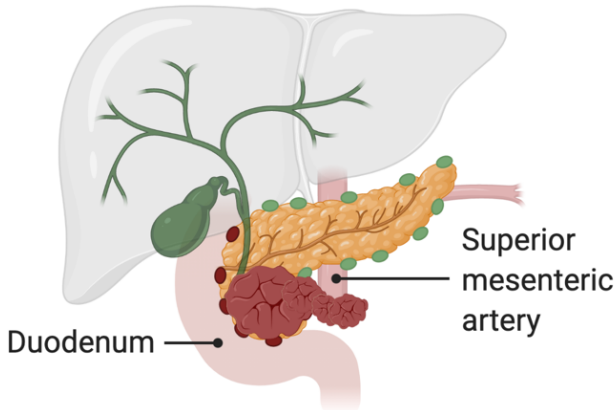
Stage	Tumour Grade	Nodal status	Distant Metastases	Median Survival (Months)	Characteristics
IA	T1	N0	M0	24.1	Tumour limited to the pancreas, ≤ 2 cm
IB	T2	N0	M0	20.6	Tumour limited to the pancreas, > 2 cm
IIA	T3	N0	M0	15.4	Tumour does not involve celiac axis or superior mesenteric artery
IIB	T1, T2, or T3	N1	M0	12.7	Regional lymph node metastasis
III	T4	N0 or N1	M0	10.6	Tumour involves celiac axis or superior mesenteric artery
IV	T1, T2, T3, or T4	N0 or N1	M1	4.5	Distant metastasis.



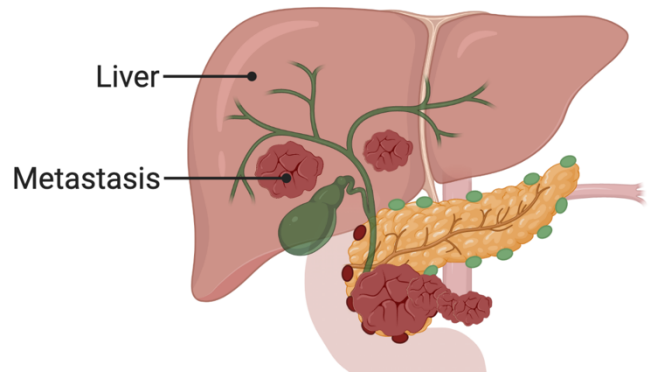
Stage I: Tumour is limited to pancreas.



Stage II: Tumour involves lymph nodes and outside pancreas.



Stage III: Tumour involves celiac axis or superior mesenteric artery



Stage IV: Distant metastasis.

Figure 1-1: schematic presentation of on pancreatic cancer staging

1.1.1. Treatment of pancreatic cancer

Pancreatic cancer treatment is dependent on the tumour stage and prognosis. Typically, the treatment includes surgery, adjuvant chemotherapy, radiotherapy and palliative care for cases that have very narrow survival rates (Figure 1-2) (Pawlik, Laheru et al. 2008, Gall, Tsakok et al. 2015).

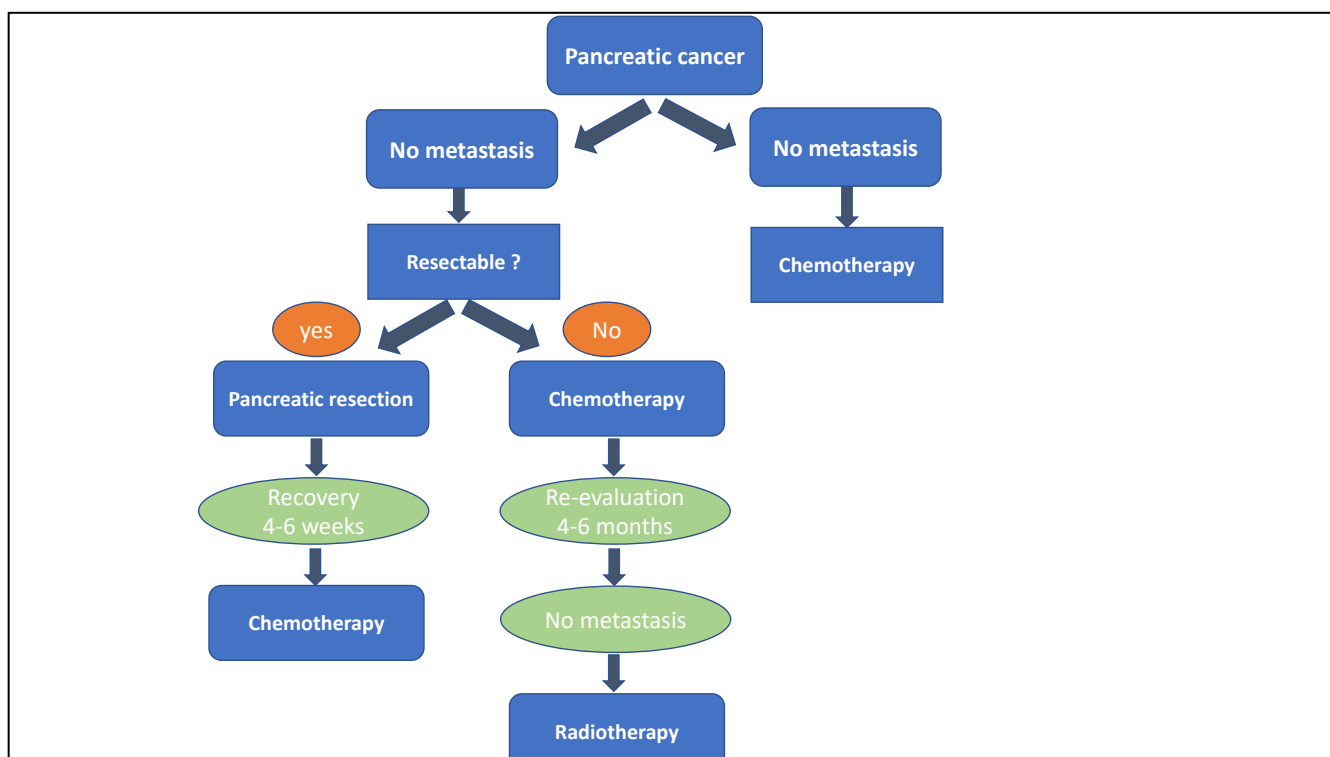


Figure 1-2: Pancreatic cancer treatment based on patient prognosis (Gall, Tsakok et al. 2015).

1.1.1.1. Surgical treatment of pancreatic cancer

Surgery is known to be the optimal treatment for patients diagnosed with a resectable pancreatic tumour. Various surgical procedures are available depending on the tumour site. Pancreatoduodenectomy or the Whipple procedure will be performed when tumours are located on the head of the pancreas and involves the resection of the pancreatic head, duodenum, proximal jejunum, bile duct, gall bladder, and a part of the stomach (Mizrahi, Surana et al. 2020). However, if the tumour is located in the body or tail of the pancreas a distal pancreatectomy, or total pancreatectomy will be performed (Kuhlmann, de Castro et al. 2004, Hidalgo 2010). Nodal disease, lympho-vascular and peritoneal invasion, histologic grade, and margin status all have significant impact on the outcome of surgery (Kooby, Lad et al. 2014, Ethun and Kooby 2016).

Despite recent advances in surgical procedures, only 20% of patients who undergo surgical resection have a 5-year complete remission with a median survival of 18 months (Richter, Niedergethmann et al. 2003, Wagner, Redaelli et al. 2004). In the majority of patients, the low level of survival is a result of local or distant recurrences, which suggests the presence of microscopic residual malignant cells at the time and site of resection (Kayahara, Nagakawa et al. 1993, Kleeff, Reiser et al. 2007, Kurahara, Takao et al. 2007). Therefore, adjuvant medical chemotherapy following any surgical procedure is required to eradicate any remaining malignant cells to minimize the chance of metastasis and recurrence. Alternatively, reports showed that preoperative therapy through the delivery of chemotherapeutic agents prior to surgery showed better efficacy compared to postoperative chemotherapy. These results are due to poor drug delivery to the tumour bed site following surgery (He, Page et al. 2014, Kamisawa, Wood et al. 2016).

1.1.1.2. Chemotherapeutic treatment of pancreatic cancer

In order to achieve advanced localised tumour control to enhance patients' survival, post-operative chemo and/or radio therapy has been studied extensively in many clinical trials. A clinical trial was performed on group of pancreatic cancer patients who received adjuvant chemotherapy of leucovorin and fluorouracil following tumour resection surgery. Results showed a significant survival rate in comparison to those who received chemotherapy only (Neoptolemos, Stocken et al. 2004). A different clinical trial discovered that patients who received six cycles of adjuvant chemotherapy using gemcitabine have shown an improved cancer free survival following surgery comparing to patients who did not receive adjuvant chemotherapy (Oettle, Neuhaus et al. 2013). Over the years, the role of adjuvant chemotherapy in pancreatic cancer has developed. This development led to a new adjuvant therapeutic strategy using combination chemotherapy regimens such as FOLFIRINOX (fluorouracil [5-FU], leucovorin, irinotecan, and oxaliplatin) and gemcitabine in replace of a single chemotherapeutic agent (Conroy, Desseigne et al. 2011, Petrelli, Coinu et al. 2015).

Nowadays, the standard first-line chemotherapy regimen for metastatic pancreatic cancer is FOLFIRINOX due to the significant improvement of overall survival rates. A clinical trial demonstrated that patients treated with FOLFIRINOX had an overall survival of 11.1 months compared to 6.8 months with gemcitabine only (Conroy, Desseigne et al. 2011, Yoo, Kang et al. 2017).

Fluorouracil [5-FU]

5-FU is a fluoropyrimidine antimetabolite drug that provides antitumoral effects by inhibiting the thymidylate synthase enzyme, resulting in impairment of the synthesis of the pyrimidine thymine that has an important role in genetic material synthesis. Consequently, the inhibits fluoronucleotides from incorporation into RNA and DNA strands resulting in cell death (Longley, Harkin et al. 2003, Pereira and Corrêa 2018).

Leucovorin

Leucovorin also known as 5-formyltetrahydrofolic acid, is a metabolite of folinic acid. In combination with 5-FU, it enhances the effect of 5-FU through stabilizing the bond between the 5-FU metabolites and the thymidylate synthase enzyme, which can improve the survival rate in advanced pancreatic cancer patients (Porcelli, Assaraf et al. 2011, Danenberg, Gustavsson et al. 2016).

Irinotecan hydrochloride [IRN]

IRN is a camptothecin-derived drug whose cytotoxic action specifically targets DNA topoisomerase I via an IRN - topoisomerase I – DNA complex. This complex prevents DNA strand ligation and leads to double-stranded DNA breakage and cell death (Creemers, Lund et al. 1994).

Oxaliplatin

Oxaliplatin is a platinum anticancer drug like cisplatin, which exerts its cytotoxic activity by inhibiting DNA synthesis and transcription via crosslinking of the drug's active derivatives

to guanine and cytosine moieties of DNA (Faivre, Chan et al. 2003, Arango, Wilson et al. 2004, Tyagi, Gahlot et al. 2008).

Gemcitabine

Gemcitabine is a deoxycytidine analogue that provides an antitumor effect by inhibition of DNA synthesis. This inhibition occurs due to DNA polymerase enzyme masking by gemcitabine that accordingly inhibits DNA chain elongation, and gemcitabine eradication by DNA repair enzymes (Huang, Chubb et al. 1991, Gandhi, Legha et al. 1996, de Sousa Cavalcante and Monteiro 2014).

1.1.2. Limitations of systemic chemotherapy in the treatment of pancreatic cancer

Although the systemic FOLFIRINOX regimen showed an improvement in survival rate and no treatment related mortality in a clinical trial, common serious adverse reactions were linked to FOLFIRINOX systemic administration. Side effects included neutropenia in the majority of the cases, febrile neutropenia, nausea and vomiting (Yoo, Kang et al. 2017). These adverse effects in some cases outweighed the benefits of the treatment, and accordingly chemotherapy was discontinued. As a result, FOLFIRINOX became limited to patients who are 76 years old or younger and described with “good performance status” (ECOG 0 or 1) (Conroy, Desseigne et al. 2011, Tong, Fan et al. 2018). Due to the severe side effects associated with systemic administration of chemotherapeutic agents, development of alternative controlled drug delivery methods for FOLFIRINOX could minimize such adverse events. Advances in drug delivery systems has led to further improvements in pharmacological activity of different

anticancer drugs that previously had limited pharmacokinetic, bio-distribution properties and higher toxicity (Avramis, Sencer et al. 2002, Molineux 2004, Li, Wang et al. 2019, Hu, Lu et al. 2021, Prasher, Sharma et al. 2021). Therefore, one of the aims of this thesis is to design a localised drug delivery system capable of improving the delivery of FOLFIRINOX to target tissues, while minimizing its systemic toxicity.

1.2. Bladder cancer

Bladder cancer is a complicated disease and related to a substantial rate of morbidity and mortality if not managed and treated properly. Globally, bladder cancer ranks as 10th common type of cancers with more than 430 000 patients diagnosed annually and considered to be the 13th cause of death among cancer patients. In UK, 10,171 new patients were diagnosed with bladder cancer in 2015 (Cox, Saramago et al. 2020, Wen 2021).

The most common risk factors associated with bladder cancer are mainly related to direct occupational exposures to carcinogens and cigarette smoking. Visible haematuria is the major symptom presented in bladder cancer patients during diagnosis in addition to recurrent infections and a small lesion (Månsson, Anderson et al. 1993, Jones, Latinovic et al. 2007, Jancke, Rosell et al. 2011).

Bladder cancer diagnostic assessment involves CT urography for the upper urinary tract, while cystoscopy is used to assess the lower urinary tract. The diagnosis is more likely to be confirmed following to transurethral resection of bladder tumour (TURBT), which is both a diagnostic and treatment procedure (Helenius, Brekkan et al. 2015, Sanli, Dobruch et al. 2017).

Most bladder cancers are identified as urothelial carcinomas (UC). Approximately, 70 – 80 % of patients are diagnosed with non-muscle invasive bladder cancer (NMIBC), while the remaining 20 - 30 % are diagnosed with muscle-invasive bladder cancer (MIBC) (Ferlay, Soerjomataram et al. 2015, Kamat, Hahn et al. 2016). Nearly, half of NMIBC cases are recognized as low grade, unlike most of the MIBC cases which are known to be high grade (Moch, Humphrey et al. 2016).

Grading is the most critical prognostic factor for NMIBC according to world health organization (WHO). WHO 1973 numerical grading system categorised UC based on cellular anaplasia into Grade 1, 2, 3 (Mostofi, Davis et al. 2012). Alternatively, based on the cytological atypia, WHO in 2004 provided another grading system classifies UC into high or low grade and papillary urothelial neoplasm of low malignant potential (PUNLMP) (Murphy, Takezawa et al. 2002, Tuna, Yörükoglu et al. 2011, Cheng, MacLennan et al. 2012). However, based on pathological and clinical assessments staging is the most significant prognostic factor for MIBC. Staging depends on two main factors including tumour invasion and metastasis as illustrated in Table 1-2 and Figure 1-3 (Edge, Byrd et al. 2010, Compton, Byrd et al. 2012).

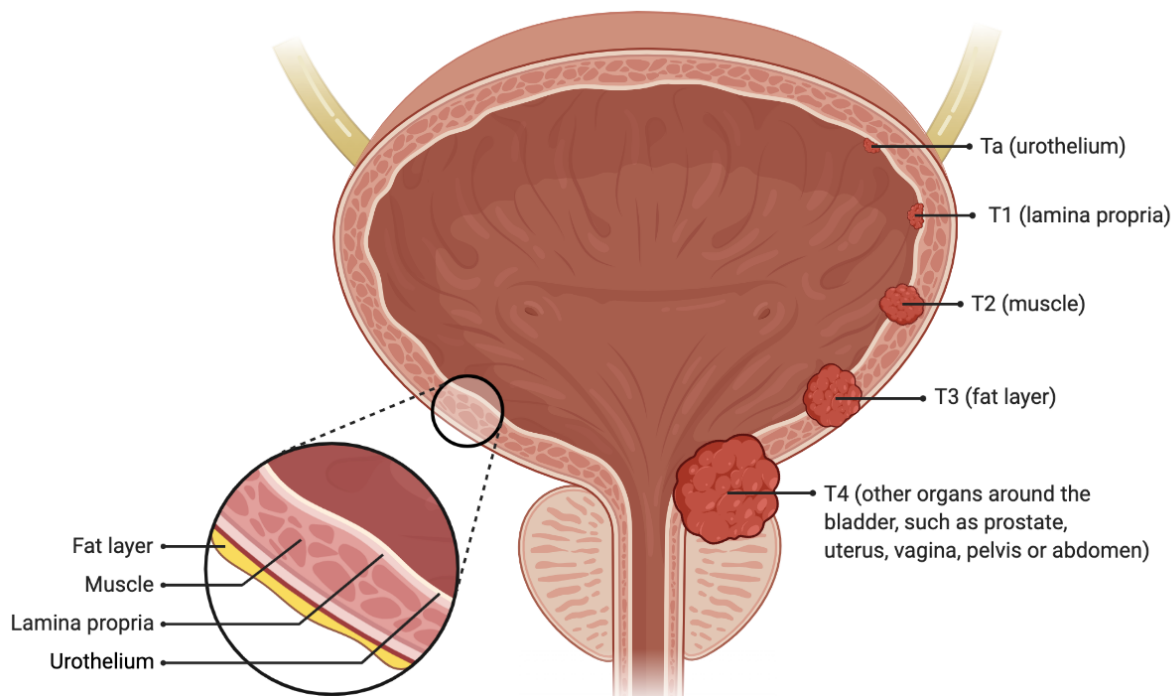


Figure 1-3: Schematic illustration of bladder cancer staging

Table 1-2: Pathologic staging of muscle-invasive bladder cancer

Stage	Tumour Grade	Nodal status	Distant Metastases	Characteristics
0	Ta or Ti	N0	M0	Non-invasive papillary urothelial carcinoma or urothelial carcinoma in situ.
I	T1	N0	M0	Tumour invades lamina propria
II	T2	N0	M0	Tumour invades superficial (2a) or deep (2b) muscularis propria
III	T3 or T4a	N0	M0	Tumour invades microscopically (3a), macroscopically (3b) perivesical tissue, adjacent organs (4a)
IV	T4b	N0, 1, 2, 3	M1	Tumour invades abdominal wall (4b) with single or multiple true pelvis lymph nodes and distant metastasis.

1.2.1. Treatment of muscle invasive bladder cancer MIBC

1.2.1.1. Surgical resection

The optimal surgical treatment for MIBC after the neoadjuvant cisplatin chemotherapy, is radical cystectomy as well as bilateral pelvic lymphadenectomy due to common tumour metastasis to the contralateral side (Gakis, Efstathiou et al. 2013, Witjes, Comp erat et al. 2014). However, it was reported that about 50% of the patients eventually develop distant micrometastasis (Stein, Lieskovsky et al. 2001, Yafi, Aprikian et al. 2011, Patel, Oh et al. 2020). Therefore, several systemic chemotherapy regimens were developed and studied to be used in conjunction with the surgical procedures to minimize the recurrence rates (Malmstrom, Rintala et al. 1996, Finnbladder, de Tratamiento Oncologico et al. 1999, Sherif, Rintala et al. 2002, Grossman, Natale et al. 2003, Choueiri, Jacobus et al. 2014, Plimack, Hoffman-Censits et al. 2014).

1.2.1.2. Systemic chemotherapy

The neoadjuvant chemotherapy has been found to be more advantageous in improving the survival rates in MIBC compared to adjuvant chemotherapy (Sonpavde, Goldman et al. 2009, Kamat, Hahn et al. 2016). The neoadjuvant chemotherapy regimens based on cisplatin such as methotrexate, vinblastine, doxorubicin, and cisplatin (MVAC), as well as cisplatin, methotrexate, and vinblastine (CMV) have demonstrated improved survival rates as reported in clinical and meta-analysis studies (Grossman, Natale et al. 2003, Vale 2005, of Trialists 2011). According to different clinical studies, establishing a neoadjuvant chemotherapy based on dose-dense MVAC (dd-MVAC) has demonstrated good safety and better pathological response rates in the range of (26–38%) (Choueiri, Jacobus et al. 2014, Plimack, Hoffman-Censits et al. 2014).

For adjuvant chemotherapy, a clinical trial was conducted to compare between immediate and deferred treatment using platinum-based chemotherapeutic drugs. Results showed that a significant improvement in 5 year progression-free survival with the immediate chemotherapy, while non-significant improvement in 5 year overall survival compared to deferred chemotherapy (Sternberg, Skoneczna et al. 2015).

1.2.2. Treatment of non-muscle invasive bladder cancer NMIBC

The rate of NMIBC recurrence within five years following treatment is between 50 – 70%, while the progression rate is around 10 – 30 %. NMIBC can be subclassified into low risk, intermediate risk, and/or high risk of recurrence and progression based on cases concomitant factors of advanced grade and stage or tumour size extent (Sylvester, Van Der Meijden et al. 2006, Gontero, Sylvester et al. 2015, Martin-Doyle, Leow et al. 2015, Cambier, Sylvester et al. 2016). Also, deep tumour invasion as well as lympho-vascular involvement are considerable negative prognostic factors that impact NMIBC subclassification, and therefore the treatment plan (Martin-Doyle, Leow et al. 2015, Willis, Fernandez et al. 2015).

1.2.2.1. Surgical resection

In NMIBC, surgical TURBT with adequate surgical margins is the primary treatment to eliminate macroscopic tumours and surrounding tissues of muscularis propria to ensure cancerous cells eradication. This procedure also provides an accurate diagnostic assessment of grading and staging, especially if TURBT was repeated following 4 to 6 weeks of adjuvant intravesical treatments according to many reports (Divrik, Yildirim et al. 2006,

Guevara, Salomon et al. 2010, Sfakianos, Kim et al. 2014). Alternatively, for patients with high risk NMIBC radical cystectomy is the procedure of choice to achieve an improved survival rate (Segal, Yafi et al. 2012, Gontero, Sylvester et al. 2015, Martin-Doyle, Leow et al. 2015).

1.2.2.2. Intravesical treatment

Intravesical chemotherapeutic treatment in low-risk NMIBC should be within six hours after TURBT using a single instillation of chemotherapy including mitomycin, epirubicin, or gemcitabine directly to the bladder in order to achieve the best efficacy. Reports found that intravesical chemotherapy administered after more than 24 hours showed lower efficacy rate (Kaasinen, Rintala et al. 2002, Sylvester, Oosterlinck et al. 2016). Similarly, in intermediate-risk NMIBC single instillation of chemotherapy after surgery, then maintenance intravesical chemotherapy one year after the initial treatment showed promising results according to researchers (Huncharek, Geschwind et al. 2000). However, there are no significant reports discussing the impact of intravesical chemotherapy on minimizing the progression rates in intermediate-risk NMIBC. Many studies have concluded that intravesical Bacillus Calmette–Guérin (BCG) immunotherapy is the most effective treatment for high-risk NMIBC in comparison to intravesical chemotherapy (Malmström, Sylvester et al. 2009, Kamat and Orten 2014, Kamat, Flaig et al. 2015). A study found that one year maintenance intravesical BCG treatment led to improved recurrence-free survival rate. Additionally, co-administration of BCG vaccine and hyperthermic mitomycin demonstrated a relapse-free survival rate of 24 month (Brausi, Oddens et al. 2014, Arends, Nativ et al. 2016).

1.2.3. Challenges of intravesical drug delivery for bladder cancer treatment

Intravesical delivery of chemotherapeutic agents through a catheter, has proved to be an effective way to ensure their maximal delivery at the tumour site, while reducing their side effects. The efficacy of this method relies on its capability to prolong the retention of chemotherapeutic drugs within the bladder and hence the drugs' ability to reach as well as penetrate into the bladder wall. One of the biggest challenges associated with intravesical treatment is reduced retention time of the drugs due to frequent urination which decreases its concentration in the bladder, with repeated interval doses being required. Additionally, when the bladder fills up with urine the concentration of the instilled chemotherapeutic agents is diluted.

1.2.3.1. Bladder permeability barrier (BPB)

The reduced retention time of instilled drugs is also directly related to the urothelium in the urinary bladder wall (Figure 1-3) that acts as the impenetrable barrier between the blood and the urine or drug solutes. The epithelial tissues of the urothelium consist of three layers of cells that influence BPB and include germinal basal layer with cells of diameter 5–10 μm , the intermediate layer with cells size of 20 μm and the superficial layer with stretching cells commonly identified as umbrella cells. These cells can stretch from 50–120 μm based on the bladder expansion (Lewis 1986, Lewis 2000, Birder 2005). The presence of a mucin layer adjacent to the luminal side, which located on top of umbrella cells and known as glycosaminoglycans (GAGs) play further role in enhancing BPB. This layer significantly prevents drug solutes from penetrating the cell layers by blocking their adhesion to the bladder wall (Poggi, Johnstone et al. 2000, Soler, Bruschini et al. 2008).

1.2.4. Strategies for drug delivery to the urinary bladder

Several primitive techniques were developed to solve obstacles related to reduced drug residence time upon intravesical drug delivery, such as voiding urine from bladder prior to drug instillation or controlling urine production by limiting fluid intake in advance before and after intravesical delivery (Au, Jang et al. 2002, Tyagi, Wu et al. 2006).

1.2.4.1. Physical improvement of bladder wall permeability

Most drugs particles pass through the bladder wall by passive diffusion. However, several factors control their penetration into the urothelium including their molecular weight, chemical structure, degree of ionization within the bladder pH, retention time on the tissue, concentration gradients and periodical urination (Negrete, Lavelle et al. 1996).

One of the suggested physical methods to assist drug molecules to counteract the urothelium resistance and increase their rate of diffusion into the tissues is based on electrophoresis. This method causes short-term disruption in the electrochemical gradient of the urothelium. A minimal invasive technique termed electromotive drug administration uses one electrode inserted into the bladder via a catheter while another electrode is placed on top of the abdominal skin. In this technique, a monitored electric current is applied on the urinary bladder wall and therefore, drug solution diffusion through the wall is improved without causing significant damage to the tissues. The efficacy of electromotive drug administration technique in reducing BPB was reported in many studies using mitomycin C, lidocaine, RTX, oxybutynin,

dexamethasone and showed a great improvement in drugs diffusion through the urothelium (Negrete, Lavelle et al. 1996, Giannantoni, Di Stasi et al. 2006).

1.2.4.2. Chemical improvement of bladder wall permeability

The role of the antiadherent mucin GAG layer, that blocks drugs adhesion to the bladder wall, could be modified via chemical agents that can reduce BPB and consequently improve drug penetration through the wall. Dimethyl sulfoxide (DMSO) is one of the chemical substances that has been used with many chemotherapeutic drugs like cisplatin, doxorubicin and pirarubicin to improve the bladder wall permeability without causing harm to the tissue (Giannantoni, Di Stasi et al. 2006). Another reported chemical technique focuses on damaging the GAG layer using protamine sulfate (PS). Following one hour of PS installation, a complete disruption of BPB occurs and thus enhance drugs penetration through the wall after their co-administration with hyaluronidase that provides further improvement. Usually, the damage is temporary with recovery within 3-5 days (Lavelle, Meyers et al. 2002, Vemulakonda, Somogyi et al. 2005, Di Stasi, Giannantoni et al. 2006). The chemical agents acting by disruption of BPB might lead to significant damage to the urinary bladder tissues if protective precautions and measures were not taken. This could lead to a leakage of toxic substances into the bladder wall, and thereby unwanted side effects like pain during urination or worsening patient symptoms may occur (GuhaSarkar and Banerjee 2010).

1.2.4.3. Nanocarriers

Significant advances in nanotechnology and drug delivery have led to the development of nanoscale carriers with different physical and chemical properties that developed a great interest

for therapeutic purposes (Wang, Gu et al. 2008). Nanocarriers have been proven to be advantageous in improving the controlled delivery of many drugs (Wagner, Dullaart et al. 2006). Furthermore, they enhance the bioavailability of drugs via altering their pharmacokinetic properties and biodistribution. They can be used as reservoirs for prolonged sustained release, increasing the retention time while decreasing the systematic toxicity of many chemotherapeutic agents (Allen and Cullis 2004). Many nanocarriers composed of different materials like polymers, lipids (liposomes or micelles), and dendrimers have shown good efficacy in preclinical and clinical studies (Liu, Kono et al. 2000, Moghimi, Hunter et al. 2001, Lavan, McGuire et al. 2003). Nevertheless, choosing the appropriate nanocarrier for a specific drug depends on the properties of the drug itself, such as potency, solubility, chemical charge, and molecular weight (De Jong and Borm 2008). Several nanocarriers that have been developed to improve the efficacy of intravesical delivery of chemotherapeutic agents for bladder cancer are summarized in table 1-3

Table 1-3: Summary of some developed nanocarriers for bladder cancer treatment

Nanocarrier	Material	Drug	Characteristics	Ref
Liposomes	Lipid bilayers vesicles	Interferon alfa	High cellular uptake, can encapsulate both hydrophobic and hydrophilic drugs.	(Frangos, Killion et al. 1990)
		Doxorubicin	Improve targeting and controlled release	(van Valenberg, Brummelhuis et al. 2021)
Polymeric nanoparticles	PLGA	Epirubicin	Biodegradable, variable drug loading and release.	(Chang, Wu et al. 2009)
Protein nanoparticles	Gelatine	Paclitaxel	Controlled drug loading, surface modification.	(Lu, Yeh et al. 2004)
Biopolymeric nanoparticles	Chitosan	Mitomycin C	Mucoadhesive, improves drug penetration into bladder wall.	(Bilensoy, Sarisozen et al. 2009)
	Chitosan	Gemcitabine	Improved drug targeting and controlled release.	(Xia, Li et al. 2015)
	Chitosan	Indole-3-carbinol	Improved drug targeting	(Melo, Pereira et al. 2021)
Magnetic nanoparticles	Iron oxide	Doxorubicin	Contrast material for imaging, controlled by magnetic field.	(Leakakos, Ji et al. 2003)
Mesoporous nanoparticles	Silica	Doxorubicin	Improved mucoadhesion and surface modification.	(Wang, Zhang et al. 2020)

1.3. Hydrogels as a controlled drug delivery system

Hydrogels have taken on several definitions since their discovery in 1960 by Wichterle and Limwre (Kopecek 2009). The most commonly used definition describes hydrogels as either a single or several component system composed of polymeric chain networks containing water that fills hydrogel gaps while remaining insoluble in aqueous media (Ahmed 2013). Classification of hydrogels is based on different factors such as polymeric component (mono-polymer or co-polymer) (Iizawa, Taketa et al. 2007, Karoyo and Wilson 2021, Zheng and Du

2021), cross-linking method (Chen, Kohane et al. 2004, Chen, Park et al. 2004, Kurisawa, Chung et al. 2005, Jin, Hiemstra et al. 2007, Hoare and Kohane 2008, RAO and CHVS 2021), reactivity towards external and physiological stimuli (temperature, pH, magnetic field)(Rafael, Melendres et al. 2021, Chang, Wang et al. 2022, Ma, Wang et al. 2022) and source (natural or synthetic) of the polymers (Hoffman 2012, Zhao, Jin et al. 2013, Mishra and Singh 2021). Developments in hydrogel technology has led to an increase in their use in the pharmaceutical application (Kashyap, Kumar et al. 2005, Ma, Wang et al. 2022).

The hydrogels developed from naturally sourced polymers have several advantages, such as better biocompatibility and biodegradability that make them more suitable for pharmaceutical applications compared to synthetic polymers, which could alter the immune system and cause an inflammatory reaction from pathogens inadvertently embedded in the polymer moieties (Lin and Metters 2006, Mano, Silva et al. 2007, Safarzadeh Kozani, Safarzadeh Kozani et al. 2021). However, some natural based hydrogels do not offer the appropriate mechanical properties such as poor physical strength and elasticity as well as limited stability at physiological environment, which require further improvement to be used as drug delivery system (Dash, Foston et al. 2013, Xing, Yates et al. 2014).

1.3.1. Biomimetic hydrogels

Hydrogels has been developed and used as an extra-cellular matrix to mimic physiological tissues for enhancing the sustained delivery of drugs and biomolecules (Caló and Khutoryanskiy 2015, Sheikhpour, Barani et al. 2017). Different synthesis methods were developed to formulate such hydrogels (Hutmacher, Goh et al. 2001, Nguyen and West 2002,

Pham, Sharma et al. 2006, Fatimi, Okoro et al. 2022). One of the techniques was based on creating a molecular concentration gradient in the extra-cellular matrix encapsulating drugs and other therapeutic agents like proteins, and growth factors (Hanauer, Latreille et al. 2015). Three-dimensional hydrogel scaffolds have also been developed for sustained drug delivery (Lee, Cuddihy et al. 2008, Nicodemus and Bryant 2008, Atma 2021, Sordi, Cruz et al. 2021).

Different techniques were explored for loading therapeutic substances or active cells within a hydrogel. For example, a method was developed based on loading the cells within the hydrogel during the gelation process. A study using corneal epithelial cells to evaluate the cells ability to survive in a calcium alginate-hydroxyethyl cellulose hydrogel revealed that the introduction of the cells during the gelation process had no impact on their activity and survival (Wright, Cave et al. 2012).

Another method used an in situ loading of vancomycin into biomimetic hydrogel based on chitosan crosslinked with maleic acid-grafted dextran was developed and characterized by improved swelling behaviour and biocompatibility (Zhao, Zhang et al. 2014). Results demonstrated that the biomimetic hydrogel provided an improved sustained release of vancomycin and was able to kill both Gram-positive as well as Gram-negative bacteria. They suggested that this hydrogel has a great potential for wound healing purposes.

1.3.2. Biodegradable hydrogels

Biodegradable hydrogels are some of the most investigated hydrogels for drug delivery, due to their preference over non-degradable hydrogels due to the optimisation of their degradation rate. As a result, biodegradable hydrogels minimize the need for surgical extraction after implantation (Park, Park et al. 2011, Freedman, Uzun et al. 2021, Kang, Turabee et al. 2021). Nevertheless, several parameters and methods during hydrogel synthesis are required to optimize the degradation rate. For example, the type and molecular weight of the polymers (Kharkar, Kiick et al. 2013), the use of polymer blends (Martens, Bryant et al. 2003), polymer concentrations as well as crosslinking rate (Kharkar, Kiick et al. 2015, Jahanmir and Chau 2019). These parameters and process techniques need to be optimised in order to achieve the desired biodegradation and drug release properties of the gels.

For example, degradable hydrogels of poly(lactic acid)-b-polyethylene glycol-b- poly(lactic acid) (PLA-b-PEG-b-PLA) were designed using block copolymers of PLA and PEG for protein delivery. Based on specific parameters like compressive strength and swelling ratio, the degradation rate of the hydrogels was examined to evaluate protein release and diffusion (Metters, Bowman et al. 2000, Mason, Metters et al. 2001, Metters, Anseth et al. 2001, Wei, Hsu et al. 2021, Zhang, Wang et al. 2021). In addition, biological molecular moieties were involved in designing hydrogels that allow them to be degradable by certain enzymes. Peptides were efficiently used not only to develop biodegradable hydrogels, but also to control the level of degradation and release of drugs (Hu and Messersmith 2003, Zargarzadeh, Silva et al. 2022). In a study, a system was created to simulate extra-cellular matrix, binding receptors were

designed using integrin and peptide molecules to be broken down by metalloprotease enzyme (Lutolf, Lauer-Fields et al. 2003, Lutolf, Raeber et al. 2003, Sobczak 2022).

Another study discussed the development of injectable near-infrared light-triggered reactive oxygen species (ROS) degradable hyaluronic acid hydrogel co-loaded with photosensitizer protoporphyrin IX and doxorubicin (DOX) as a localized delivery system for combined chemo-photodynamic therapy regimen (Xu, Zeng et al. 2020). The degradable hydrogel offers light-tuneable controlled drug release rate. This is achieved by applying near-infrared radiation on the loaded hydrogel, which generates ROS that break the ROS-breakable crosslinker molecules and accordingly initiate the degradation process and hence controlled release of DOX. Moreover, the hyaluronic acid hydrogel has demonstrated great biocompatibility, biodegradability and showed excellent therapeutic outcomes following *in vitro* cytotoxicity studies and *in vivo* antitumor investigations.

1.3.3. Smart hydrogels

Smart hydrogels are designed to be an improvement in comparison to other conventional hydrogels due to their sensitivity to certain parameters such as temperature and pH that influence their biodegradation, rate of swelling and drug release (Akala, Kopečková et al. 1998, Cao, Duan et al. 2021). The ability to modify the stimuli response of such hydrogels makes them an effective controlled drug delivery system, as their release rate of drugs is controllable via adjusting external parameters (Bromberg and Ron 1998, Kost and Langer 2012, Qiu and Park 2012, Ali, Nagumantri et al. 2021, Liang, Li et al. 2022).

For example, pH-sensitive polymers used to formulate pH sensitive hydrogels are commonly identified as polyelectrolytes. Polymers used for such purpose include poly (acrylic acid) (PAA) and poly (N, N'-diethylamino ethyl methacrylate) (PDMAEM), which are sensitive to pH (Huang, Yu et al. 2007, Plamper, Ruppel et al. 2007, Wu, Liu et al. 2011, Liu, Xu et al. 2021, de Moraes Zanata and Felisberti 2022). Thus, they express different swelling rates when formulated in medias of different pH levels. However, neutral co-monomers like 2-hydroxyethyl methacrylate and methyl methacrylate when introduced during polyelectrolyte hydrogels preparation can alter and control their pH sensitivity, swelling behaviour, and hence the rate of drug release (Brannon-Peppas and Peppas 1990, Khare and Peppas 1993, Falamarzian and Varshosaz 1998, Andrade, Roca-Melendres et al. 2021, Guven, Balaban et al. 2021). pH sensitive hydrogels are used frequently in oral dosage forms for controlling drug release due to the variation of pH in the gastrointestinal tract (Siegel, Falamarzian et al. 1988, Brannon-Peppas and Peppas 1990). A study involving the loading of caffeine into a hydrogel produced from N,N'-dimethylamino ethyl methacrylate (DMAEM) copolymers and methyl methacrylate (MMA) demonstrated that the release of caffeine from the hydrogel was only triggered at acidic pH (Siegel, Falamarzian et al. 1988).

An *in vitro* study developed and investigated a pH sensitive injectable hydrogel based on PEG and α,β -polyaspartylhydrazide loaded with DOX as a drug delivery system for localised chemotherapy (Li, Gu et al. 2015). This hydrogel was developed to respond to pH variation in term of sol-gel phase transition, as it maintains its fluid form prior to their injection. However, following their direct intertumoral injection into mice with human fibrosarcoma the hydrogel

changed its conformation into semisolid structure. Results demonstrated that this pH sensitive hydrogel offered good biocompatibility, syringeability and degradation rate. Moreover, the loaded hydrogel offered variable release rates of DOX according to the pH levels, as it demonstrated accelerated release rates at low pH and better sustained release the pH increases to a neutral level. In addition, better tumoral growth inhibition was reported mice injected with doxorubicin-loaded hydrogels compared to those who receive free doxorubicin.

Thermo-sensitive hydrogels are formulated from polymers like poly(N-isopropylacrylamide) (PNIPAM) and Poly (N, N-diethylacrylamide) (PDEA) (Vihola, Laukkanen et al. 2005, Zhang, Chu et al. 2007, Ngadaonye, Geever et al. 2012, Carreño, Pereira et al. 2021, Zhang, Xue et al. 2021). The low critical solution temperature property of PDEA, which is relatively similar to body temperature made it the polymer of choice in many studies (Liu and Zhu 1999, Chen, Liu et al. 2009, Cook, Haddow et al. 2021). Apart from other polymeric materials, the water solubility of polymers similar to PDEA decreases at higher temperatures that results in hydrogel shrinking (Shibanuma, Aoki et al. 2000). The change in hydrogels swelling rate at higher temperature is due to the structure of the polymer chains components, which have either hydrophobic groups or combination of alternating hydrophobic and hydrophilic segments. At low temperature, Hydrogen bonds between hydrophilic groups and aqueous solution molecules are enhanced and hence increases polymers dissolution and swelling. Contrarily, hydrogen bonds dissociate at high temperature while hydrophobic interactions dominate between hydrophobic segments and thereby hydrogel shrinking occurs (Qiu and Park 2012, Smith, Maikawa et al. 2021).

In order to obtain better control over the swelling behaviour of the hydrogels, a method was created based on modifying the ratios of polymers hydrophilic and hydrophobic segments by developing copolymers using NIPAM, which consists of acrylic acid as hydrophobic and hydrophilic monomers (Feil, Bae et al. 1992, Schild 1992, Hirotsu 1993, Abdelaty 2022). Additionally, further types of copolymers of poly (ethylene oxide) (PEO) and poly (propylene oxide) (PPO) have similar features as PDEA polymer of having a lower critical solution temperature that can be used for controlled drug delivery. Pluronic® (or Poloxamers) is an example of applicable in-situ thermo-sensitive hydrogel using PEO–PPO copolymers (Bromberg and Ron 1998, Edsman, Carlfors et al. 1998).

A recent study reported a development of a smart DOX-loaded hydrogel with dual pH and thermal responsiveness using polymeric mixtures of poly(*N*-isopropylacrylamide-co-itaconic acid) (PNIPAM-co-IA) with chitosan ionically crosslinked via glycerophosphate for local breast cancer treatment (Fathi, Alami-Milani et al. 2019). The investigations showed that the dually responsive hydrogel provided better DOX controlled release at higher temperature and neutral pH, while faster release rate was reported at lower pH and temperature.

There are some concerns associated with smart hydrogels that use NIPAM for therapeutic purposes because of problems related to their rate of biodegradability and metabolism (Bromberg and Ron 1998). Also, it was reported that hydrogel polymers based on acrylamide have the ability to activate platelets once it reaches to blood stream (Peppas 1986, Merrill and Pekala 1987, Hina, Bashir et al. 2021).

1.3.4. Hydrogel technologies for localised cancer chemotherapy

Although systemic chemotherapy has been shown to be efficacious, the use of some anticancer drugs is restricted due to severe side effects, narrow therapeutic index, and off-target toxicity (Wheate, Walker et al. 2010). Numerous strategies have been developed to improve the efficacy of chemotherapy while minimising their side-effects. One of these strategies is using nanocarriers, which have successfully achieved improvement in the efficacy of chemotherapy via targeting them to the tumour site either by passive or active targeting (Wang and Guo 2013, Gurunathan, Kang et al. 2018). However, some limitations were reported with the use of nanocarriers such as aggregation, rapid drug release, rapid elimination from the blood, toxicity, and variations in the physicochemical properties may from batch to batch (Sercombe, Veerati et al. 2015, ud Din, Aman et al. 2017, Gurunathan, Kang et al. 2018, Hossen, Hossain et al. 2019, Navya, Kaphle et al. 2019). Hydrogels offer an alternative drug delivery strategy with excellent biocompatibility, negligible cytotoxicity, and notable drug loading capacity and therefore have been widely studied for localized cancer treatment (Ta, Dass et al. 2008, Wang, Adrianus et al. 2009, Ma, He et al. 2015, Norouzi, Nazari et al. 2016, Cacicedo, Islan et al. 2018, Rossi, Ryan et al. 2020).

1.3.4.1. Injectable hydrogels for localised cancer treatment

Direct administration of anti-cancer drugs into tumours will result in their rapid clearance. However, loading chemotherapeutic drugs within hydrogels and injecting them into the tumour tissue (*in situ* delivery) could provide controlled delivery and release due to the adhesion properties of the hydrogels (Li, Rodrigues et al. 2012, Wang, Liu et al. 2015). The hydrogel serve as drugs reservoir and have the ability to act as a carrier for the drugs offer the

possibility of co-loading multiple chemotherapeutic agents into a single gel, which would be beneficial in reducing the dose for every drug and thus decrease the toxicity of treatment (Takimoto and Awada 2008, Zhu, Zheng et al. 2021).

An *in vitro* study discussed the dual formulation of 5-FU and DOX-loaded microcapsules into a Pluronic hydrogel and a di-block copolymer hydrogel. Both hydrogels demonstrated sufficient fluid texture to be injected into tumour tissues and form gels *in situ* at physiological temperature. The results revealed that the microcapsules loaded into the hydrogel exhibited further controlled delivery and release up to 18 days when compared to the microcapsules only (Kwon, Kwon et al. 2016).

An injectable hydrogel used in photodynamic therapy for localized cancer treatment was investigated in an *in vivo* study. In this study, a dipeptide fibrous injectable hydrogel embedding a photosensitive drug known as Chlorin e6 was injected to the tumour sites in mice. The injectable hydrogels showed no toxicity to normal tissues as well as providing controlled delivery at the tumour site over 4 days and efficiently inhibited tumour growth (Abbas, Xing et al. 2017).

Another method based on combining doxorubicin chemotherapy and photodynamic therapy using zinc phthalocyanine encapsulated within injectable thermosensitive hydrogels for localized bladder cancer treatment was studied. This approach improved treatment by significantly inhibiting 5637 cells and the fluorescence intensity was higher in comparison to a control group who received the treatment without hydrogels (Huang, Xiao et al. 2018).

Certain tumours might require dual treatment of chemotherapy and gene therapy to overcome tumour angiogenesis and tumour resistance to chemotherapy alone. As a result, hydrogels can be designed in a specific way to ensure an efficient gene delivery to the tumour tissues (El-Aneed 2004, Dai and Tan 2015). This can be achieved by tailoring a hydrogel from a positively charged polymer to bond with negatively charged nucleic acids. For example, an injectable hydrogel mainly consisting of the positively charged amphiphilic copolymer (methoxy-poly(ethylene glycol)-b-poly(ϵ -caprolactone)-b-poly(ethylene imine) with a folic acid targeted group and α -cyclodextrin co-loaded with paclitaxel and B-cell lymphoma 2-transformed gene Nur77 was developed. Following hydrogel injection into the tumour, the electrostatic interaction between the polymers and gene led to the controlled codelivery of paclitaxel and Nur77 for 7 days and successfully prohibited drug-resistant tumour cell growth (Liu, Li et al. 2019).

1.3.4.2. Hydrogel niches for localised cancer treatment

Immunotherapeutic based cancer treatment has proved its importance and efficacy over the years in minimizing cancer recurrence (Fuge, Vasdev et al. 2015, Jo, Nam et al. 2017). Cytokines, antitumour vaccines, and immune-cellular engineering are examples of efficient immunotherapy but can have negative impacts in terms of toxicity and limited efficacy if administered systemically (Weiden, Tel et al. 2018). The resemblance between the texture of the hydrogel matrix and the extracellular matrix has made hydrogels a suitable carrier for localized delivery of many immunotherapeutic agents like immune cells, proteins, and cytokines while also maintaining their structural integrity. Thus, an improved specificity, better efficacy, and limited toxicity will be achieved (Fransen, Arens et al. 2013).

For this purpose, an *in vitro* study was conducted by designing a chitosan hydrogel for T lymphocyte encapsulation and proliferation that expressed cytotoxic biomarkers, released interferon- γ and induced annexin V expression upon their embedment within the hydrogel along with melanoma cells. Results also revealed the ability of T cells to diffuse out from the hydrogels scaffolds which suggests that hydrogels are a promising delivery device for living cells (Lerouge, Monette et al. 2018).

A promising strategy to treat solid tumours is chimeric antigen receptor (CAR) T cell therapy. However, its systemic infusion provides poor targeting at the tumour site due to the tumour's immunosuppressive environment as well as heterogeneous properties. Thereby, authors developed an implantable alginate hydrogel encapsulating CAR T cells that allow their long adhesion and controlled delivery directly to the solid tumour tissues. They discovered that not only the tumours were effectively eradicated by CAR T cells, but also co-loading and delivery of stimulator of interferon genes (STING) agonists enhanced the tumour elimination (Smith, Moffett et al. 2017). Hydrogels have been studied as a vaccine carrier and proven to maintain their accompanying antigen stability, which is required for dendritic cells activation and proliferation *in vivo* (Ali, Huebsch et al. 2009, Zhang, Guo et al. 2021). An implantable hydrogel based on macroporous poly lactide-co-glycolide (PLG) polymer encapsulating granulocyte-macrophage colony-stimulating factor was developed to activate dendritic cells inside mice. The results demonstrated a 90% survival rate compared to the control group who all died after 25 days (Ali, Huebsch et al. 2009).

1.3.4.3. Sprayable hydrogel for localised cancer treatment

Despite tumoral surgical resection and accompanying chemotherapy for cancer treatment, there is a chance for cancer recurrence. Therefore, one of the developed technologies to eliminate the residual tumour tissues and promoting the post-surgical wound healing locally is sprayable hydrogels. A recent study reported the development of sprayable bio-adhesive hydrogel based on pectin loaded with etoposide and olaparib nanocrystals coated with PLA-PEG (NCP) stabilised by Pluronic F127 to facilitate the spraying for localised post-surgical treatment of brain tumour (McCrorie, Mistry et al. 2020). Results demonstrated that pectin offered good *in vivo* and *in vitro* biocompatibility. Also, highly loaded NCP provided sustained release of chemotherapeutic drugs up to 5 days.

For the same purpose, a thermosensitive sprayable hydrogel based on [poly(d,l-lactide)-poly(ethylene glycol)-poly(d,l-lactide)] loaded with black phosphorus nanosheets was developed and investigated for post-surgical photothermal therapy (Shao, Ruan et al. 2018). They reported that this hydrogel offered very good biocompatibility and biodegradability. Furthermore, due to hydrogel's outstanding photothermal performance, the sprayed black phosphorus-loaded hydrogel exhibited fast gelation process under near infrared irradiation leading to formation of a membrane on the surgical site and provided excellent photothermal treatment outcome in eliminating the residual cancer cells.

In a different study, they explored a thermoelectric material called β -FeSi₂ as a bioactive compound, and they discovered that it has a potential to be used anti-tumour agent due to its great photothermal properties. As a result, they developed sprayable β -FeSi₂-loaded

sodium alginate hydrogel for local treatment of skin tumours that exerts its tumour suppression as photothermal and chemodynamic therapy by releasing the loaded Fe ions from the loaded hydrogels (Ma, Ma et al. 2021). Moreover, results from *in vivo* investigations showed that tumour suppression was successfully achieved.

1.4. Aerogels as a controlled delivery system

Aerogels were discovered in 1931 by Samuel Kistler. They are materials that maintain their porous and network structure while exchanging their liquid component with gas within their pores. Aerogels are characterized by a highly open porous structure with high surface areas due to their non-uniform solid design (Kistler 1931, Horvat, Pantić et al. 2022). The use of aerogels in biomedical applications such as regenerative medicine and drug delivery has generated a great interest. As a result, different types of inorganic or organic aerogels have been developed for biomedical applications (Ulker and Erkey 2014, Okutucu 2021).

Aerogels as porous formulations are suitable as drug delivery carriers for the encapsulation of many drug molecules because of their large inner surface areas, high surface to volume ratios, and regular pore sizes (Sher, Ingavle et al. 2007, Ahuja and Pathak 2009, Arruebo 2012, Horvat, Pantić et al. 2022). According to the International Union of Pure and Applied Chemistry (IUPAC) classification system, solid structure pores are classified based on their size with pore sizes less than 2 nm known as micropores, while those in the range of 2 nm to 50 nm are known as mesopores with pores over 50 nm called macropores (Davis 2002, Zou and Budtova 2021). Many studies have investigated the impact of pore size and surface area on drug loading, drug

release, as well as drug-matrix interactions in several potential micro- and mesoporous controlled drug delivery systems (Andersson, Rosenholm et al. 2004, Song, Hidajat et al. 2005, Sher, Ingavle et al. 2007, Arruebo 2012).

Aerogels as drug delivery system are prepared through several steps: sol-gel transition (gelation process), followed by the network formation (polymerization), then the gel-aerogel transition (drying process). Upon choosing the appropriate polymer for aerogel synthesis, the polymer is dispersed in aqueous media and the gelling process takes place. The polymerization process subsequently occurs and polymeric networks interconnect and form the hydrogel. Some polymers may require a crosslinking material to facilitate the gelling process and enhance the interaction between polymeric chains and form a strong network. Once the hydrogel is formed, the drying process to form the aerogel takes place using different methods like supercritical fluid extraction using supercritical carbon dioxide or freeze-drying (lyophilization).

Generally, aerogels have specific properties that make them suitable for use in controlled drug delivery systems such as high porosity, high surface area, improved stability, and higher drug loading capacity. Such features can be adjusted by modifying the aerogel preparation methodologies. Polysaccharide based aerogels are considered to be the optimal type of materials for designing controlled drug delivery systems over synthetic polymers due to their biocompatibility and biodegradability (Maleki, Durães et al. 2016, Stergar and Maver 2016). However, aerogels based on silica have been studied previously but their poor biodegradation rate limited their use in pharmaceutical applications although they did have improved stability and adhesiveness properties (Stergar and Maver 2016, Shao, Cao et al. 2018). Similarly to

hydrogels, the porous structure and their design which mimicked an extracellular matrix made aerogels not only able to act as carriers for drugs but also to simulate cell attachment, proliferation, and differentiation.

1.4.1. Aerogels as a wound healing technology

The healing process of wounds is complicated and usually accompanied with several challenges like pH changes and infections that impact and delay the treatment outcomes (Guo and DiPietro 2010). As a result, appropriate aerogel biomaterials are required to improve the healing process by enhancing clotting and limiting the microbial activity throughout absorbing toxic substances (Ashtikar and Wacker 2018, Rodríguez-Cabello, González de Torre et al. 2018, Sheikholeslam, Wright et al. 2018). The aerogel's macroporous and permeable structures allow them to absorb and embed significant amounts of fluids (Zheng, Zhang et al. 2020). Many aerogels were developed and studied for this purpose, and they are mainly derived from natural origins like cellulose, alginate, collagen, and chitosan (Barrios, Fox et al. 2019).

A study reported the development of cellulose nanofibrils aerogels as a wound dressing, which was characterised by limited endotoxin level and significant absorbing capacity. Also, it was reported that this aerogel has an excellent safety similar to commercially approved wound dressing (AquaCel®) (Nordli, Chinga-Carrasco et al. 2016).

Another naturally sourced aerogel based on collagen was discovered and showed better mechanical features in comparison to other aerogels. In addition, a collagen aerogel offered improved properties in terms of cell adhesion and proliferation along with its great water

absorption capability. These properties made this aerogel an excellent candidate for wound treatment and tissue regeneration (Dharunya, Duraipandy et al. 2016).

Advancements in aerogel technology have led to the discovery of chitosan derived aerogels that demonstrated good potential in tissue engineering and wound healing because of its role in preventing infections and its strong adhesive properties (Jayakumar, Prabakaran et al. 2011). Chitosan's antimicrobial activity is attributed to its ability to prevent gram-positive and gram-negative bacterial growth. It was also reported that formulating aerogels loaded with vancomycin provided more significant antibacterial effect and thus improved treatment outcomes (López-Iglesias, Barros et al. 2019).

1.4.2. Aerogels as a regenerative medicine technology

Research on the role of aerogels in tissue engineering and regenerative medicine was majorly focused on scaffolds for bone regeneration (García-González, Concheiro et al. 2015, Berrio, Oñate et al. 2021, Yahya, Amirul et al. 2021). Aerogels consist of a three-dimensional interconnected highly microporous structure simulating cancellous bone structure. Generally, bone tissues are composed of 70% minerals (hydroxyapatite nanocrystals) and organic compositions like collagen and glycoproteins (Palmer, Newcomb et al. 2008, Chen, McKittrick et al. 2012, Wegst, Bai et al. 2015, Tertuliano and Greer 2016). Therefore, it was suggested to develop synthetic hydroxyapatite as an aerogel material so that it mimics biomechanical features of cancellous bone making aerogels potential an excellent carrier for bioactive agents required for bone regeneration (Li, Li et al. 2010). Recently, a new synthetic ultralight aerogel nanowire based on hydroxyapatite biopolymer was fabricated with a similar meshwork design

to cancellous bone. This aerogel nanowire was characterised by a very high porosity and elasticity, which was specifically developed for air filters but also showed interesting potentials for medical purposes in regenerative medicine (Zhang, Zhu et al. 2018). Furthermore, using lyophilization and a chemical crosslinker an aerogel scaffold was prepared based on a combination of hydroxyapatite and collagen biomaterials to enhance mesenchymal stem cells adhesion and proliferation *in vivo*. Results showed that the hydroxyapatite/collagen aerogel phenomenal mechanical features and successfully promoted bone tissues regeneration (Sun, Zhu et al. 2018).

1.4.2.1. Aerogels as a drug delivery system

Significant advancements in the field of pharmaceutical research have provided solutions using aerogels for issues associated with cytotoxic and poorly soluble drugs, mainly limited site targeting and low bioavailability respectively. Aerogels can improve the bioavailability and release behaviour of a drug due to their high surface area, porosity, and biocompatibility as a result of the biomaterials used for aerogel synthesis (García-González and Smirnova 2013, Ulker and Erkey 2014). The employment of aerogels as controlled drug delivery systems was initially assessed using silica material due to its biocompatibility and familiar sol-gel methodology (Hüsing and Schubert 1998). A drug's release kinetics from the loaded silica aerogels is usually rapid due to the fast collapse of the silica's aerogel network upon their exposure to aqueous media (Smirnova, Suttiruengwong et al. 2004, García-González, Alnaief et al. 2011, Murillo-Cremaes, López-Periago et al. 2013, Rajanna, Kumar et al. 2015). However, Different techniques were reported to tune the drug release rate from silica-based aerogels such as aerogel surface modifications to sustain the drug release or altering aerogel porous structure

by incorporating additional polymeric components during silica aerogel preparation to accelerate the drug release rate (Veres, Kéri et al. 2017, Jabbari-Gargari, Moghaddas et al. 2021).

One of the silica aerogel surface modification techniques is via carboxylic functionalization, which was investigated to evaluate the modified aerogel's ability to sustain the release of celecoxib (Jabbari-Gargari, Moghaddas et al. 2021). The carboxylic modification was performed by treating silica aerogel with N-(2-Aminoethyl)-3-aminopropyltrimethoxysilane and succinic anhydride before the drug loading. Results demonstrated that carboxylic modification was successful, and the modified silica aerogel offered better sustained release compared to the original aerogel due to the stronger bonding formed between celecoxib's functional group NH_3^+ and COO^- in the modified aerogel.

In contrast, a drug delivery system was developed using an aerogel composed of silica and gelatine encapsulating ketoprofen and ibuprofen. The results demonstrated that the release kinetics of the drugs were much slower from the silica-based aerogel only compared to silica/gelatine aerogels. This occurred due to the strong hydration of silica/gelatine that promoted fast drug dissolution from the aerogels (Veres, Kéri et al. 2017). On the other hand, polysaccharides from different sources as alternative biomaterials to silica have been investigated thoroughly to improve aerogels as controlled delivery systems and overcome the relatively rapid release kinetics seen with silica-based aerogels. One such aerogel was a starch aerogel, which was characterised by high biocompatibility and biodegradability because of their natural source and porous structure (De Marco, Iannone et al. 2018, Ubeyitogullari, Brahma et

al. 2018, De Marco, Riemma et al. 2019). A study was performed to evaluate the ability of starch aerogels to improve the dissolution the poorly water-soluble antifungal drug Itraconazole. The results showed that starch aerogels significantly enhanced the dissolution and bioavailability of the drug (Jaywant, Meer Tarique et al. 2017). Additionally, using a thermal inkjet printing technique aerogel alginate microspheres loaded with salbutamol sulphate were formulated (López-Iglesias, Casielles et al. 2019). The alginate aerogel microspheres demonstrated promising results as a controlled drug delivery system for pulmonary administration. Table 1-4 summarises more aerogels developed as controlled drug delivery systems.

Table 1-4: Summary of some developed aerogels as controlled drug delivery systems

Aerogel type	Drug loaded	Reference
Starch aerogel, alginate aerogel	Ibuprofen	(Mehling, Smirnova et al. 2009)
PEG hydrogel coated silica aerogel	Ketoprofen	(Giray, Bal et al. 2012)
Polymer coated silica aerogel	Ibuprofen	(Alnaief, Antonyuk et al. 2012)
Whey protein-based aerogel	Ketoprofen	(Betz, García-González et al. 2012)
Amine modified silica aerogel	Ketoprofen	(Alnaief and Smirnova 2010)
Alginate aerogel	Nicotinic acid	(Veronovski, Novak et al. 2012)
Multi membrane alginate aerogel	Nicotinic acid	(Veronovski, Knez et al. 2013)
Bacterial cellulose aerogels	Dexpanthenol, L ascorbic acid	(Haimer, Wendland et al. 2010)
Starch aerogel	Paracetamol	(Mehling, Smirnova et al. 2009)

1.4.3. Aerogels for localised cancer treatment

Recently, aerogels have attracted attention as a technology to improve the efficacy of chemotherapeutic agents' via local delivery to the tumour sites while minimizing their systemic toxicities (Ahmad, Ahmad et al. 2021). Aerogels have the potentials as drug delivery system to be used for co-adjuvant chemotherapy post tumoral surgical resection or in local treatment of inoperable tumours. For example, *in vitro* experiments on different human and animal cancer cells have explored a silica and gelatin composite aerogel loaded with the chemotherapeutic drug methotrexate. The controlled delivery and release was promoted through hydrolysis by the collagenase enzyme from cancerous cells that allowed the methotrexate to be selectively released from aerogels when in contact with tumour tissue (Nagy, Király et al. 2019).

Another aerogel formulation using chitosan, carboxymethyl cellulose, graphene oxide, and crosslinked by calcium ion was investigated as a smart pH responsive controlled delivery system loaded with 5-FU. The study concluded that the release kinetics of 5-FU from the aerogels was controlled via altering the pH level due to chitosan and carboxymethyl cellulose being pH responsive. The authors suggested that this hybrid aerogel has great potential and could be further improved to be employed as a carrier for targeted chemotherapy (Wang, Shou et al. 2017).

1.5. Limitations of available hydrogels and aerogels as controlled drug delivery systems

Hydrogel and aerogel formulations as drug carriers have expressed different biocompatibility levels based on their polymeric monomers and cross-linkers (Lee and Mooney 2001). Many limitations exist, including rapid burst release of drugs from hydrogels as a result of their high water content and large network of pores (Huang and Brazel 2001) Also, poor mechanical strength, which is dependent on choice of polymer used, can result in poor drug encapsulation (Hutmacher 2001). For example, during the early stages of our research, we aimed to produce hydrogel and aerogel formulations of natural biocompatible source with improved mechanical properties and able to provide controlled delivery of chemotherapeutic agents for the localised treatment of pancreatic and bladder cancer. Therefore, several polymers were initially investigated for both cancer types, including Carboxymethyl cellulose CMC, hydroxyethyl cellulose (HEC) and hydroxypropyl methylcellulose (HPMC). These polymers were initially used to prepare several drug free hydrogels and aerogels using different concentrations, ratios, and molecular weights in order to evaluate their capability and stability to be implanted at the tumour resection site for pancreatic cancer. However, the HEC, HPMC, and CMC aerogels and hydrogels do not offer the sufficient mechanical properties be designed as surgically implantable drug delivery system for the post-surgical localised treatment of pancreatic cancer at resection margin. They demonstrated rapid collapse and dissolved within less than 24 hours after placing them in water at 37°C, while longer contact, release time, as well as ease of implantations at the resection margins are required to achieve better drug delivery of chemotherapeutic drugs. Consequently, using chemical crosslinkers or additional polymeric

blends are required to improve their physical features, which could lead to undesired adverse effects especially upon their direct contact with wounded resection site. Nevertheless, these polymers demonstrated potentials to be considered as good candidates to develop injectable hydrogels for the localised bladder cancer treatment.

In addition, the sterilization process of hydrogels and aerogels is a considerable challenge (Hoffman 2012). These drawbacks are limiting the potentials of hydrogels and aerogels as controlled drug delivery systems. Therefore, there is an increasing need to develop formulations using alternative polymers to allow these promising delivery systems to be used for biomedical and pharmaceutical applications. This is especially true for aerogels that have not been as extensively investigated for localised cancer treatment in comparison to hydrogels. Developing systems based on natural monomeric hydrogels and aerogels without additional synthetic polymers or reactive cross linkers could overcome some of the limitations associated with the current formulations, especially those influencing their release and biocompatibility.

1.6. Hypothesis and objectives

Due to the side effects associated with systemic administration of anti-cancer drugs, development of alternative controlled drug delivery systems could minimize such adverse events. Advances in the drug delivery systems has led to further improvements in efficacy of current anti-cancer drugs that had limited pharmacokinetic, bio-distribution properties and higher toxicity. Therefore, one of the main aims is to design a system capable of improving the efficacy of chemotherapy at target tissues, while minimizing its systemic toxicity.

Previously, hydrogels have been widely used as drug delivery systems, but in some cases, hydrogels suffer from rapid burst release of drugs, limited biocompatibility. However, by developing hydrogels and reversible aerogels based on totally natural materials without any reactive substances or crosslinkers could overcome such limitations. This could improve the safety of the formulation and the stability of drugs and improve their release profiles.

The main aim of this project is to develop natural hydrogels and aerogels as safe drug delivery systems in order to counteract the anti-cancer systemic toxicity, and the deficiencies observed in the previously developed formulations that would lead to an enhanced controlled release delivery system. More specifically, the goal is to develop a structured hydrogel and aerogel embedding anti-cancer drugs that would be released in a controlled fashion for the treatment of post-operative pancreatic cancer and non-invasive urinary bladder cancer patients.

The first objective is to prepare and characterize multiple hydrogel and aerogel formulations using several agar concentrations loaded with different concentrations of caffeine as a model drug. Following that, the effects of varying agar concentrations, drug loading rates, and loading method on the formulations mechanical properties as well as drug release will be evaluated.

The second objective is to study the optimized agar hydrogel and aerogel formulations loaded with the anti-cancer drug irinotecan hydrochloride (IRN) for pancreatic cancer. Then, the effect of varying agar ratios on the formulations mechanical properties and drug release will be studied.

The third objective is to establish cytotoxicity study against different pancreatic cancer cell lines using the optimised IRN pre- and post-loaded agar formulations.

The fourth objective is to synthesize and characterize multiple hydrogel formulations using hydroxyethyl cellulose (HEC) and hydroxypropyl methylcellulose (HPMC) of different concentrations loaded with multiple concentrations of infigratinib (INF) anti-cancer drug for urinary bladder cancer. Then, determine the impact of different HEC and HPMC concentrations, as well as the INF loadings on the hydrogels physical properties and drug release profiles.

The fifth objective is to conduct a cytotoxicity study against different bladder cancer cell lines using the optimised INF-loaded hydrogel formulation.

Chapter 2: Development and Optimization of Implantable Agar Hydrogels as a Localised Drug Delivery System

2.1 Introduction

The main goal of drug encapsulation and loading within implantable devices is to improve their controlled delivery to, or uptake by, target tissues and to decrease the toxicity of the free drug in non-target tissues (Uhrich, Cannizzaro et al. 1999, Osorno, Brandley et al. 2021). An improvement in either of the previous properties would lead to an enhanced therapeutic index. Thus, developing a formulation for controlled drug delivery is of interest (Senapati, Mahanta et al. 2018). Nevertheless, the criteria for choosing the appropriate formulation depends on maintaining or improving the drug's pharmacological, physical, and chemical properties (Chen, Wu et al. 2004, Shi, Li et al. 2021). Also, such a proposed drug delivery system should be comprised of biocompatible materials that offer excellent drug-encapsulating capability (Li and Mooney 2016). Generally, finely designed formulations, such as hydrogels meet such required properties, and are able to encapsulate a large amount as well as multiple drug molecules compared to other formulations (Sun, Song et al. 2020).

Natural hydrogels with a high water content and a highly porous network structure were designed to represent biocompatible or tissue mimicking synthetic matrices for embedding drug molecules (Kesharwani, Bisht et al. 2021). Agar, is a naturally sourced polysaccharide extracted from seaweed of Phaeophyceae (Silberfeld, Rousseau et al. 2014). It was discovered in 1658 by

Tarazaemon Minoya and has been used as a natural food additive and categorized by Food and Drug Administration FDA as Generally Recognized as Safe (GRAS) (Armisen and Galatas 1987, Nussinovitch 2019). Agar composed of two main polysaccharides known as agarose, which is gelling component of agar and the second component is agaropectin that has very limited gelling capacity (Araki 1956, Armisen and Gaiatas 2009). Agar is soluble in water at near boiling temperature, and upon the solution cooling below the gelation temperature of around 30°C forms a physically crosslinked hydrogel with excellent physical properties directly related to amount of agar is produced (Guiseley 1970, San Biagio, Madonia et al. 1984, Piazza and Benedetti 2010).

Caffeine is a water soluble solid white powder with a molecular weight of 194.1906 g/mol, molecular formulation of $C_8H_{10}N_4O_2$. and stable at temperatures ranging from 155 to 237°C (Zabot 2020). The caffeine is featured by its hydrophilicity and improved thermal stability at temperatures higher than the boiling point that is required during the agar hydrogel preparation. The cost efficiency of caffeine and its hydrophilic nature as a small molecule drug makes it an acceptable candidate as a preliminary drug for the development and optimization of considerable quantities of agar hydrogel formulations to evaluate their potentials and behaviour as implantable drug delivery systems loaded with a hydrophilic drug.

In this chapter, the capability of agar polymeric hydrogel matrix as an implantable drug delivery system embedding a model drug was investigated. The objectives were to evaluate its potentials in controlling the release of the model drug caffeine from a three-dimensional matrix of hydrogels and assessing the impact of polymer concentration (2, 2.5, 3, and 3.5 %) and drug

loading concentration (1, 5, and 10%). The comparison investigations between different free unloaded and caffeine loaded hydrogel formulations should help elucidate the different physical properties and how the variations in the agar hydrogel compositions influence the release profile of each formulation.

2.2 Materials and method

2.2.1 Materials

A polysaccharide complex Agar composed of 70% agarose and 30% agarpectin and porcine gastric mucin was purchased from Sigma (UK) for hydrogel preparation. Caffeine was purchased from Alfa Aesar, while Methanol 99% was purchased from Fisher Scientific. Phosphate buffered saline (PBS) tablets was purchased from VWR (UK).

2.2.2 Preparation of caffeine-loaded agar hydrogels

The agar hydrogels were prepared using the sol-gel method by dissolving predetermined amounts (Table 2-1) of agar in distilled water (100 ml) separately, to prepare four different hydrogels with agar concentrations of 2, 2.5, 3 and 3.5% w/v. The mixtures were placed under high pressure at 126°C using Prestige medical 2100 Classic portable autoclave sterilizer for 20 minutes. Following that, the agar hydrogel solutions were collected, and fixed amount of every hydrogel solution (10 ml) poured into cylindrical mould and mixed with predetermined amounts of caffeine (Table 2-1) under stirring for 15-20 minutes to achieve complete dispersion. The different agar hydrogel formulation batches contained either 1, 5, and 10% w/v of caffeine.

Table 2-1: Formulations of prepared caffeine loaded hydrogels

Formulations	Agar % w/v	Caffeine % w/v	hydrogel solution volume ml
1	2	1	10
2	2	5	10
3	2	10	10
4	2.5	1	10
5	2.5	5	10
6	2.5	10	10
7	3	1	10
8	3	5	10
9	3	10	10
10	3.5	1	10
11	3.5	5	10
12	3.5	10	10

2.2.3 Characterization of the agar hydrogel formulations

2.2.3.1 Hydrogel mechanical strength

In order to study the impact of agar concentration and caffeine loading on the hydrogels mechanical strength, tests were carried out on different agar hydrogel concentrations of 2, 2.5, 3, and 3.5% as well as 2 and 2.5% agar hydrogels loaded with 1, 5, and 10% caffeine. The mechanical strength was determined using a texture analyser (TA.XT. Plus C) equipped with a 20 mm cylindrical probe, and oven to control the temperature at 37°C. The hydrogels were

placed under the probe and a maximum force of 5 Kg was applied at a fixed speed of 1 mm/s and a 10 mm depth. The mechanical properties tests were performed in triplicate using separate formulation batches and drug free hydrogels as control

2.2.3.2 Hydrogel mucoadhesive properties

The mucoadhesive properties of the unloaded and caffeine-loaded agar hydrogels were evaluated using a texture analyser (TA.XT. Plus C) equipped with 10 mm cylindrical probe, and oven to control the temperature at 37°C. Mucin discs were prepared by compression of 250 mg of mucin powder using a ring press with a 10 mm die and a compression force of 5 tonnes, applied for 40 seconds. The mucin discs were attached to the lower end of the TA probe using double sided adhesive tape. The agar hydrogels were placed into a cylindrical mould below the probe holding the mucin disc. The probe was lowered onto the surface of each hydrogel at a constant speed of 0.5 mm/s with a force of 0.1 N applied for 30 seconds to ensure good contact between the mucin disc and the hydrogels. The probe was then moved upwards at a constant speed of 0.5 mm/s and the force required to detach the mucin disc from the surface was determined from the resulting force-distance plot. All measurements were conducted in triplicate using separate formulation batches and drug free hydrogels as control.

2.2.3.3 Hydrogels rheology

Rheological characterisation of the agar hydrogels was performed to investigate the impact of polymer concentration and drug loading on their viscoelastic behaviour. The experiments were performed on the hydrogel formulations of 2, 2.5, 3, and 3.5% without drug as controls, as well as the hydrogels with 1, 5, and 10% caffeine. Rheological analysis was

performed using a discovery HR10 TA rotational rheometer equipped with a Peltier heating system. All tests were conducted at a temperature of 37°C. A plate-plate geometry with a diameter of 40 mm (PP40) was used and a fixed normal force of 0.15 N was applied to avoid the sample slipping and the gap was approximately 3 mm depending on the hydrogel sample height. Amplitude sweep tests were performed on every loaded and unloaded hydrogel to determine the linear viscoelastic region (LVER) at a frequency of 1 Hz and a strain between 0.005 to 1%. Also, frequency-dependent response of the hydrogels was studied based on the average of frequency sweep tests performed in the frequency range between 0.1 – 80 Hz with a deformation among the LVER (0.05 – 0.1%).

2.2.3.4 Caffeine content distribution in hydrogels

The caffeine-loaded agar hydrogels cut into three equal parts and placed in glass bottles containing 100 ml of 50:50 methanol:deionized water under vigorous stirring overnight and then subsequently vortexed to ensure complete extraction of the caffeine. 1 ml of each extraction solution was centrifuged at $2100 \times g$ for 15 minutes and filtered using a 0.45 μm membrane filter and analysed by HPLC.

2.2.4 In vitro release of caffeine from the hydrogel formulations

10.5 to 11.5 g of (dependent on their agar and caffeine content) loaded agar hydrogel were placed into a glass bottle containing 100 ml of pre-prepared PBS buffer (pH 7.4) and placed in an orbital shaking incubator at 37°C and 60 rpm. At time intervals of 0, 1, 3, 6, 24, and 48 hours a 1 ml sample was collected, replaced with 1 ml of fresh PBS buffer, and subsequently

stored at 4°C until analysed by HPLC. The release study was conducted in triplicate and the percentage of cumulative released caffeine calculated relative to the maximum loaded caffeine concentration of the hydrogels.

2.2.5 HPLC analysis

2.2.5.1 HPLC chromatographic conditions

The caffeine was analysed using an Agilent HPLC System (Agilent Technologies 1260 infinity II, Santa Clara, California, United States) equipped with a quadratic pump and autosampler. The separation was performed using a Thermo Scientific® 5 µm, C18 analytical HPLC column (150 mm *4.6 cm) at 25°C with a mobile phase composed of methanol and deionized water in 50: 50 ratios at a flow rate of 1ml/ min. An injection volume of 10 µl and run time of 10 minutes was used, and UV detection was conducted at 273 nm.

2.2.5.2 Stock solution and calibration curve

10 mg of caffeine was transferred into a 10 ml volumetric flask and dissolved in 50:50 methanol and deionized water to produce a stock solution with a final concentration of 1 mg/ml. The stock solution was then used to prepare working standard solutions with concentrations of 0.001, 0.005, 0.01, 0.1, 0.5, and 1 mg/ml. The calibration curve was prepared by plotting the area under the curve versus concentration. All measurements were conducted in triplicate.

2.2.6 Statistical analysis

Statistical analysis was performed using a two-ways analysis of variance dependent on the presence of two independent variables, including increased agar hydrogel concentrations and caffeine drug loadings (ANOVA) (GraphPad Prism version 9.0.2 for MacOS, GraphPad Software, San Diego, CA). Post-hoc comparisons of the means were performed using Tukey's Honestly Significance Difference test. A significance level of $p < 0.05$ was accepted to denote significance in all cases.

2.3 Results

2.3.1 Hydrogel mechanical and mucoadhesive properties

The mechanical characterization of the hydrogels showed varied mechanical properties based on their agar concentrations and caffeine loadings. The higher agar composition in the unloaded hydrogels significantly ($p < 0.05$) increased their mechanical strength, and resistance to rupture upon the application of a compression force, which are further significantly ($p < 0.05$) increased upon increasing caffeine loading 1, 5, and 10% in 2 and 2.5% agar hydrogels (Figure 2-1). Results in Figure 2-1 A report that the mechanical strength levels recorded were increased significantly ($p < 0.05$) from 1260 ± 61 g/cm² in 2% agar unloaded hydrogel to 2930 ± 161 g/cm² in 2.5% agar unloaded hydrogel. Comparably, the 3% agar hydrogel had a non-significant ($p > 0.05$) increase in its physical strength compared to the 2.5% hydrogels by recording 3315 ± 242 g/cm². However, the 3.5% agar hydrogel demonstrated significantly ($p < 0.05$) improved mechanical properties with a strength of 4460 ± 205 g/cm². Nevertheless, the agar hydrogel formulations of 2 and 2.5% agar loaded with either 1, 5, and 10% caffeine demonstrated

improved mechanical properties compared to drug free hydrogels. Furthermore, increased drug loading provided further significant ($p < 0.05$) increase in the mechanical strength. The caffeine loaded hydrogels with 3 and 3.5% agar expressed greater mechanical stability and resistance upon applying the maximum compression force of 5 Kg which was not sufficient to rupture them. Additionally, the unloaded hydrogels demonstrated mild mucoadhesive properties, which were decreased significantly ($p < 0.05$) as the agar increased and further reduced upon caffeine loadings (Figure 2-1 B).

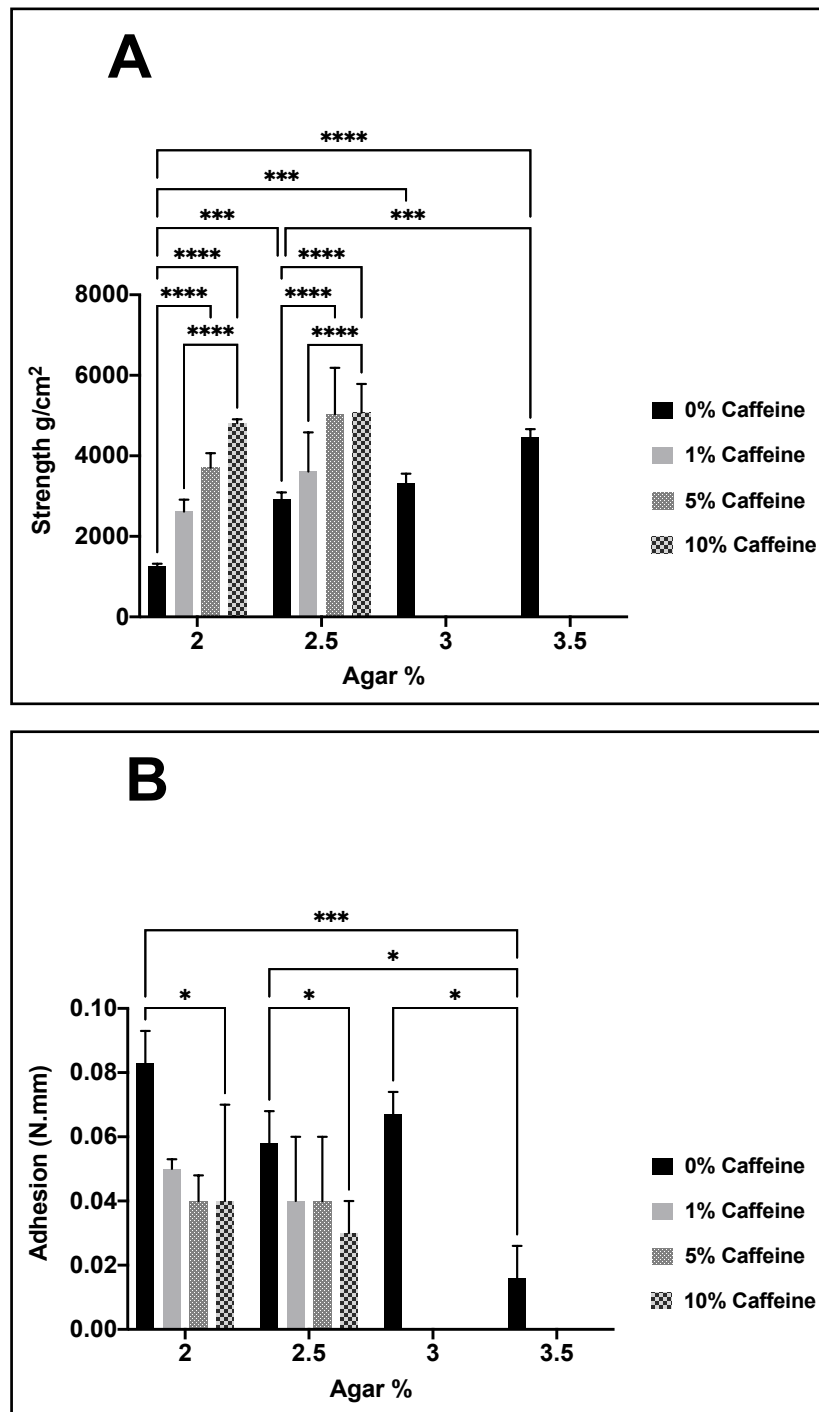


Figure 2-1: Effect of different agar concentrations (2, 2.5, 3, and 3.5%) and caffeine loadings (1, 5, and 10%) on 2 and 2.5% hydrogels mechanical strength (A), and adhesion (B). Results shown as mean \pm SD, n=3, significance found using a two-way ANOVA with a Tukey's post-hoc test, * = P<0.05 ** = P<0.01, *** = P<0.001, **** = P<0.0001.

2.3.2 Hydrogel rheology

The rheological behaviour of the agar hydrogels with different polymer concentrations and drug loadings is presented in Figures 2-2 and 2-3. The effect of agar concentration on the viscoelastic moduli (storage or elastic modulus G' and loss or viscous modulus G'') of unloaded agar hydrogels of 2, 2.5, 3, and 3.5% under shear strain is represented in Figure 2-2 A. The region in which the moduli are strain-independent and parallel corresponds to the linear viscoelastic region (LVER). As demonstrated, a higher agar concentration corresponds to higher moduli, as well as to a reduction of the LVER and to the decrease of the yield strain (critical strain value at which the moduli crossover occurs), capable of holding during lower stress before being subjected to deconstruction behaviour at higher stresses. The amplitude sweep results for 2 and 2.5% agar hydrogels with 1, 5, and 10% caffeine loadings are shown in Figures 2-2 B and C, while 3 and 3.5% agar hydrogels with 1, 5, and 10% caffeine loadings respectively are illustrated in Figures 2-3 A and B, respectively. The caffeine-loaded hydrogels are characterized by greater viscoelastic properties which increase with caffeine loading especially at 10% caffeine. Similarly, Figure 2-4 A to E reports the dynamical rheological properties based on the frequency sweep of the unloaded agar gels across whole frequency range. The caffeine loaded hydrogels demonstrated a predominance of the storage modulus G' above the loss modulus G'' with higher caffeine loadings and agar content in comparison to the unloaded agar hydrogels, therefore indicating stronger hydrogel behaviour.

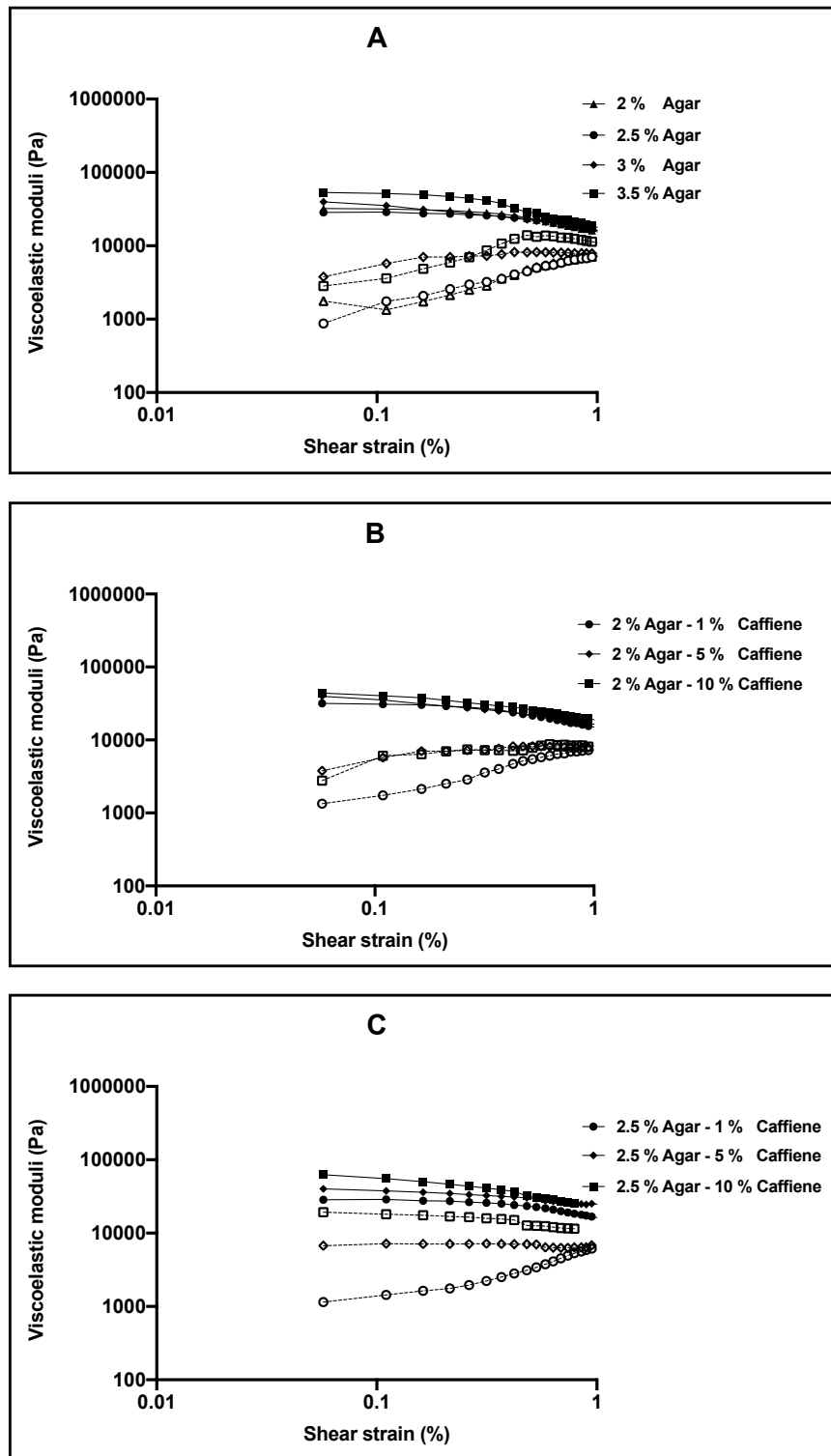


Figure 2-2: Amplitude sweep for different formulations, (A) different concentrations of unloaded agar hydrogels, (B) 1, 5, and 10% caffeine loaded 2% agar hydrogels, (C) 1, 5, and 10% caffeine loaded 2.5% agar hydrogels. Solid and empty points represent the storage (elastic) modulus G' and the loss (viscous) modulus G'' , respectively.

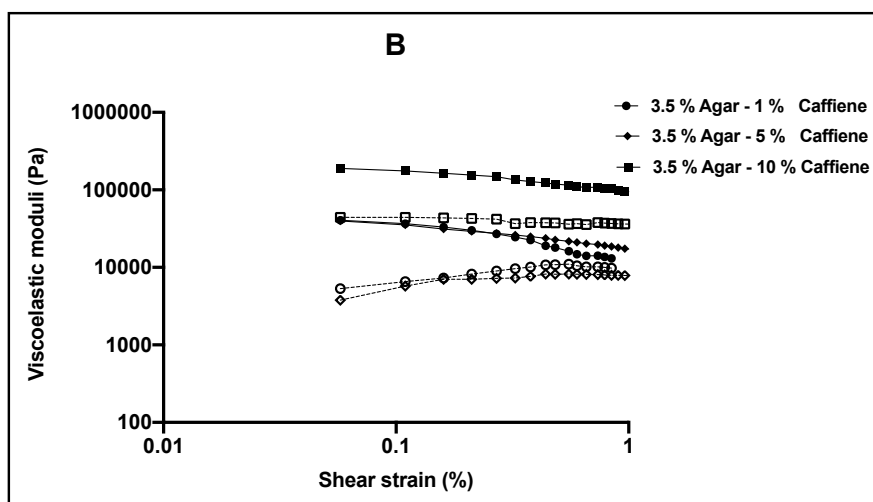
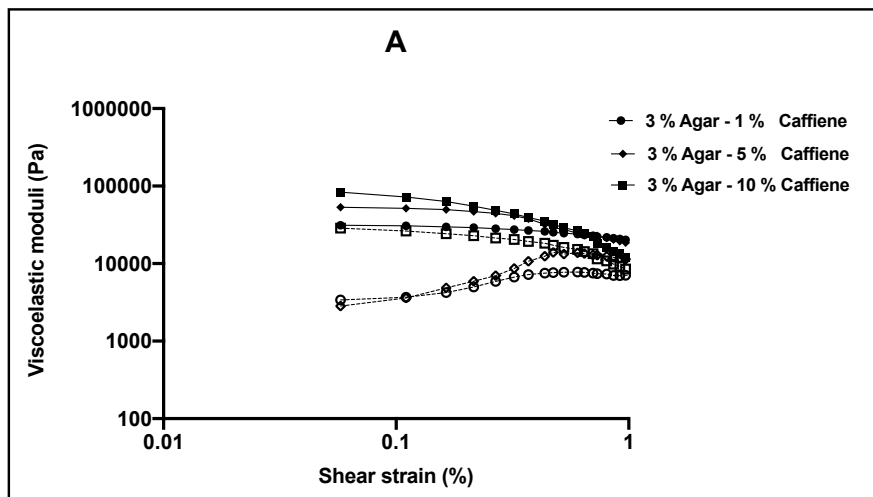


Figure 2-3: Amplitude sweep for different formulations, (A) 1, 5, and 10% caffeine loaded 3% agar hydrogels, (B) 1, 5, 10% caffeine loaded 3.5% agar hydrogels. Solid and empty points represent the storage (elastic) modulus G' and the loss (viscous) modulus G'' , respectively.

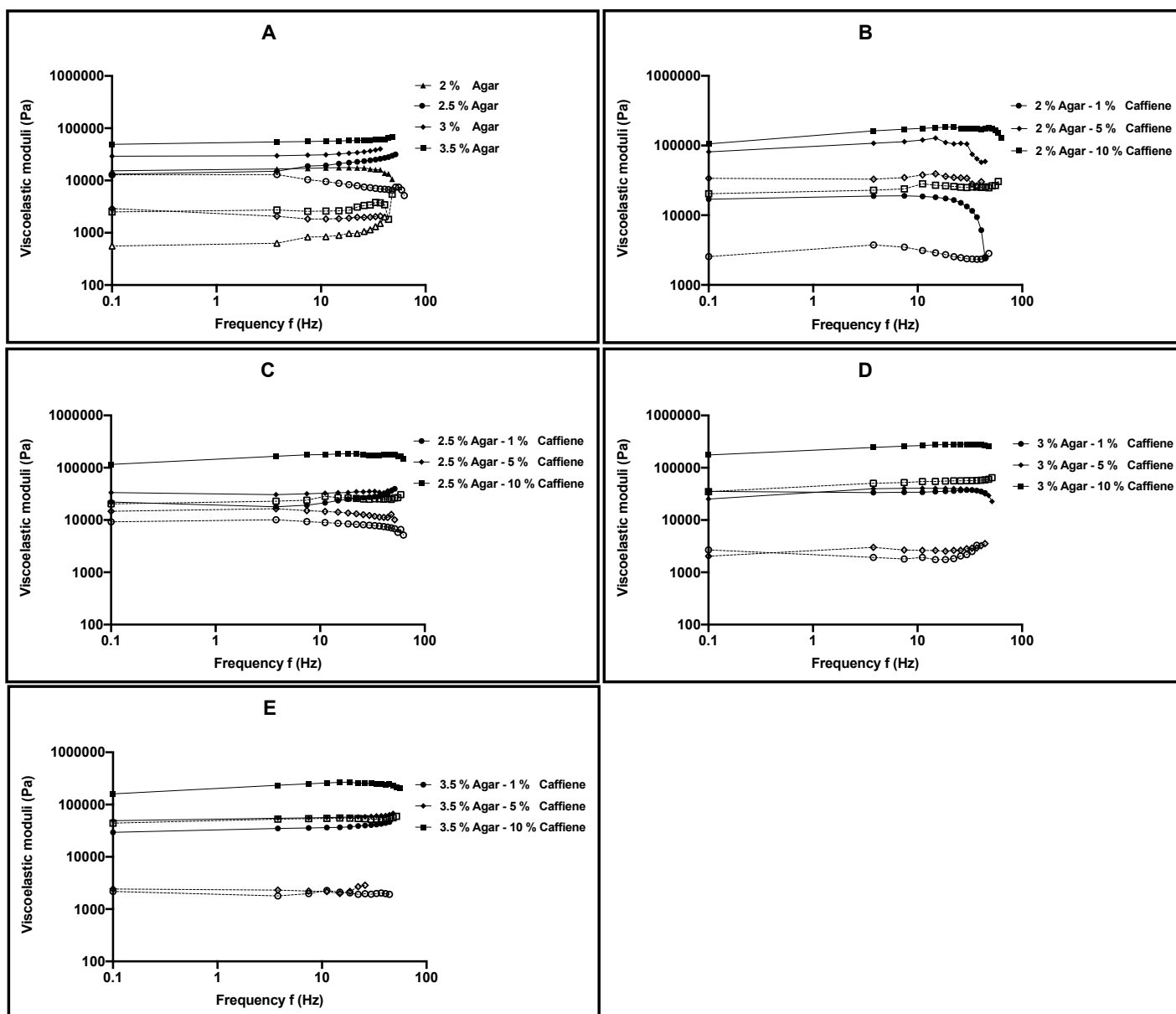


Figure 2-4: Frequency sweep for different formulations, (A) different concentrations of unloaded agar hydrogels, (B) 1, 5, and 10% caffeine loaded 2% agar hydrogels, (C) 1, 5, 10% caffeine loaded 2.5% agar hydrogels, (D) 1, 5, 10% caffeine loaded 3% agar hydrogels, and (E) 1, 5, 10% caffeine loaded 3.5% agar hydrogels. Solid and empty points represent the storage (elastic) modulus G' and the loss (viscous) modulus G'' , respectively.

2.3.3 HPLC analysis of caffeine

Figure 2-5 shows the caffeine standard curve at 6 different concentrations of caffeine quantified by HPLC. The correlation between the caffeine concentrations and the HPLC area under the curve AUC was excellent with the R value at 0.9989 from 0.001 to 1 mg/ml. The retention time was approximately 2.9 minutes (Figure 2-6).

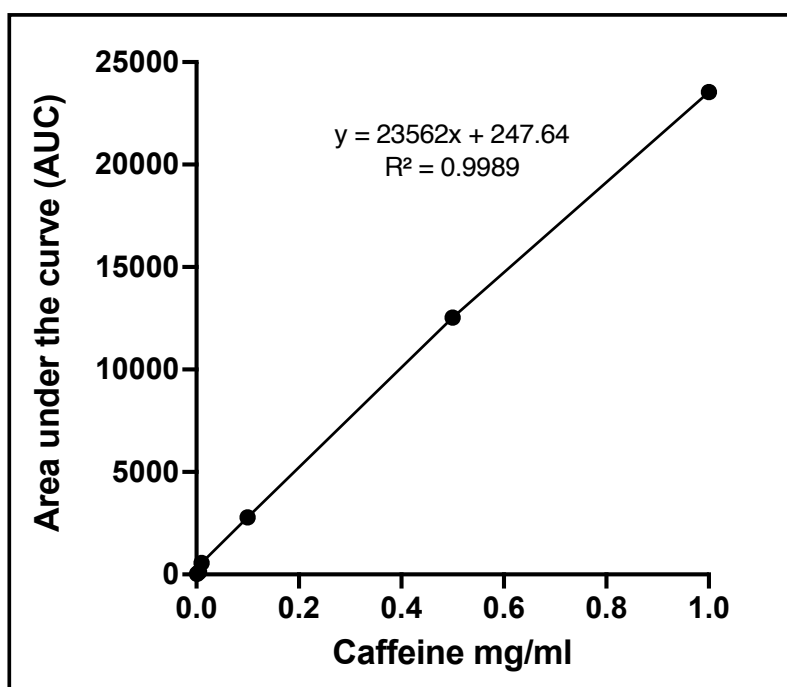


Figure 2-5: Standard curve for caffeine using HPLC (n=3).

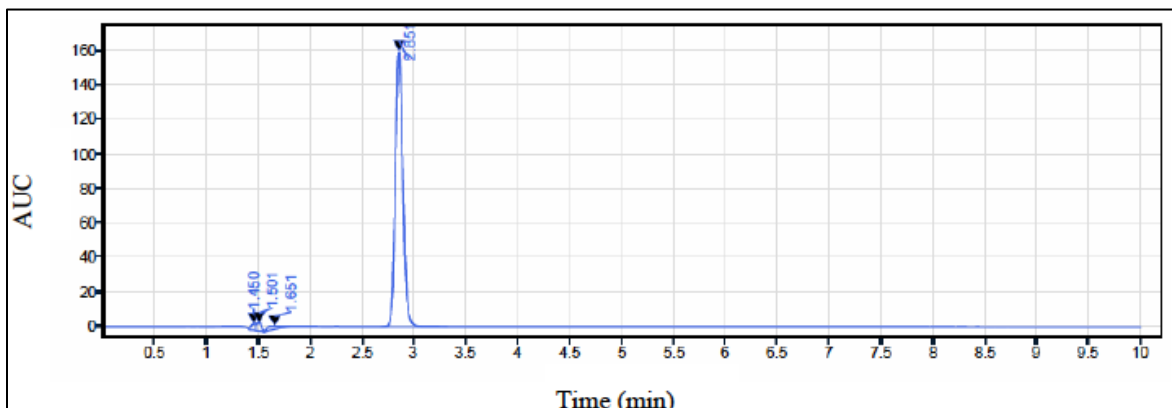


Figure 2-6: The HPLC chromatogram depicting the peak of caffeine at 273 nm wavelength.

2.3.4 Caffeine content distribution in hydrogels

The drug content distribution in all agar hydrogel formulations (2, 2.5, 3, and 3.5%) loaded with caffeine (1, 5, 10%) for every formulation was determined (Figure 2-7). As illustrated, the 2% agar loaded hydrogel caffeine contents varied from 83.3 ± 13 to $92.8 \pm 31.3\%$ between the different portions of the hydrogels. Comparably, the 2.5 and 3% agar hydrogels caffeine contents were found to be vary with higher caffeine loadings. For example, the 2.5% hydrogels had caffeine contents of 105.6 ± 16.6 , 99.3 ± 24.6 , and $79.4 \pm 17.5\%$ for 1, 5, and 10% caffeine loading respectively. The 3% hydrogels demonstrated significant ($p < 0.05$) reduction in their content upon increasing the loading from 1 up to 10% caffeine. With contents of 104.8 ± 8.8 , 87.2 ± 3.4 , and $60.2 \pm 16.6\%$ respectively, for the same increased caffeine loading order. Additionally, the caffeine contents within 3.5% hydrogels varied from 86.7 ± 7.5 to $98.2 \pm 22\%$.

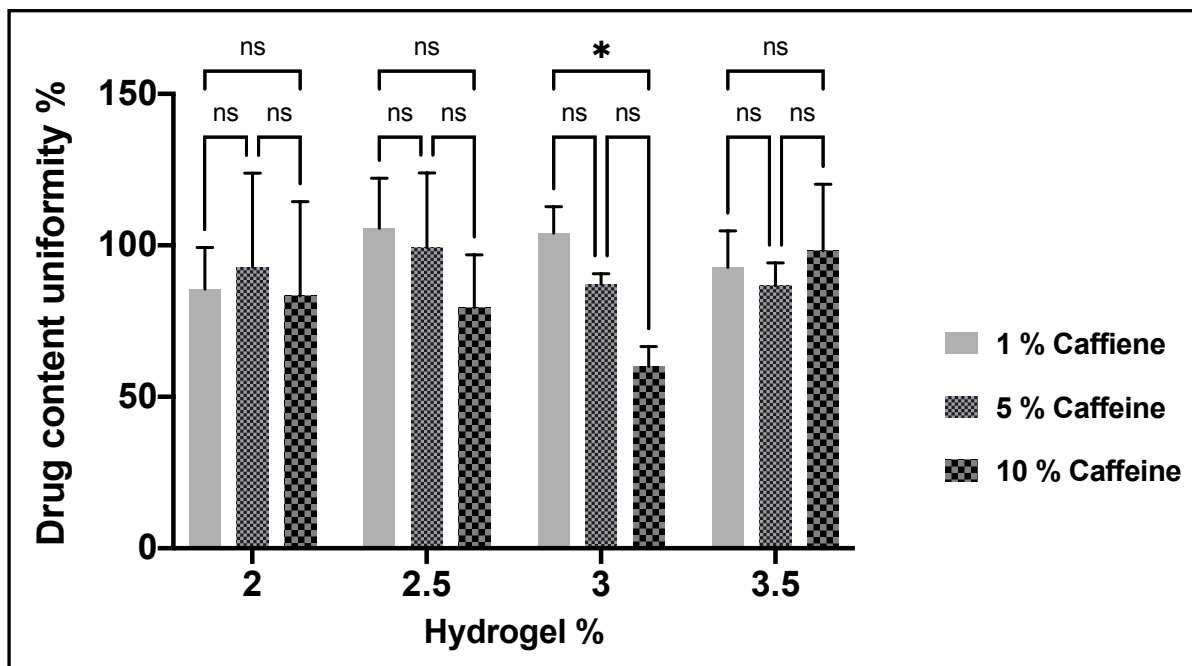


Figure 2-7: Drug content distribution of caffeine (1, 5, 10%) in four different hydrogels (2, 2.5, 3, and 3.5%). Results shown as mean \pm SD, n= 3, significance found using a two-way ANOVA with a Tukey's post-hoc test, * = P<0.05 ** = P<0.01, *** = P<0.001, **** = P<0.0001.

2.3.5 In vitro release of caffeine from the agar hydrogel formulations

The release of caffeine from all hydrogel formulations was performed in PBS (pH 7.4) at 37°C. The percentage cumulative release profiles for caffeine loaded hydrogels are presented in Figure 2-8. The release of caffeine from all hydrogels is varied based on two factors, including the agar concentration (2, 2.5, 3, and 3.5%) of hydrogel formulations and the caffeine loadings (1, 5, and 10%) in every agar hydrogel concentration. As seen in Figure 2-8, the caffeine displayed a biphasic release profile over 48 hours from all hydrogels. First, a rapid 'burst' release was observed, followed by the second phase of release that yielded a slower release after 6 hours as the caffeine loading, and agar component increased. The 2% agar hydrogel encapsulating 1%

caffeine showed faster release behaviour in comparison to the same hydrogels loaded with 5 and 10% caffeine mainly within six hours (Figure 2-8 A). Within six hours, the 2% hydrogel released $73.5 \pm 2.4\%$ of its 1% loaded caffeine, while for 5 and 10% loaded caffeine hydrogels exhibited slower release of 54.8 ± 2.5 and $57.8 \pm 2.8\%$ respectively compared to 1% caffeine loading. Most of the caffeine content in the 2% hydrogels were released after 48 hours significantly ($p < 0.05$) faster compared to 5 and 10% loaded caffeine hydrogels. Additionally, the higher agar component in the 2.5% loaded hydrogels resulted in similar release profiles for 1% loaded caffeine when compared to the 2% hydrogels, while the 5 and 10% caffeine loaded hydrogels had a reduction in their release at 3 and 6 hours compared to 1% caffeine loading within the same formulation (Figure 2-8 B). The release profiles represented in Figure 2-8 C from the 3% agar loaded hydrogels demonstrated a fast release initially for all the caffeine loadings, then a slower release for 1% caffeine hydrogel compared to the same drug loading in previous formulations as well as to the 5 and 10% caffeine loadings within the same 3% agar hydrogel. By 3 hours, $64.6 \pm 2.4\%$ of the 1% caffeine loading was released, followed by a constant sustained release up to $83.3 \pm 7.3\%$ at 48 hours. In contrast, the 5 and 10% caffeine loaded 3% agar hydrogels had a slower release at 3 hours, releasing 45.6 ± 4.4 and $53.2 \pm 4.5\%$ of their caffeine content respectively and they maintained this slow release until 6 hours, when they exhibited a faster release of caffeine compared to the 1% caffeine hydrogel at 24 hours until achieving nearly complete release at 48 hours with no statistical significance ($p > 0.05$) between different caffeine loadings. Moreover, the impact of the higher agar component of the hydrogels as well as caffeine loading on the release profiles from the 3.5% agar hydrogels is shown in Figure 2-8 D. The 3.5% hydrogel loaded with 1% caffeine expressed significantly ($p < 0.05$) faster release behaviour compared to 5 and 10% caffeine loadings and released most of its

caffeine content within 6 hours. However, with higher caffeine loading the 3.5% agar hydrogels presented more of a sustained release following the initial ‘burst’ release. For the 5% caffeine loaded gels, $69.4 \pm 3.7\%$ of the caffeine was released after 6 hours compared to $55 \pm 10.8\%$ for the 10% caffeine loaded hydrogels. Then, both hydrogels provide sustained release up to 48 hours releasing a total of 81.9 ± 4.2 and $82.6 \pm 15.8\%$ of their caffeine content respectively.

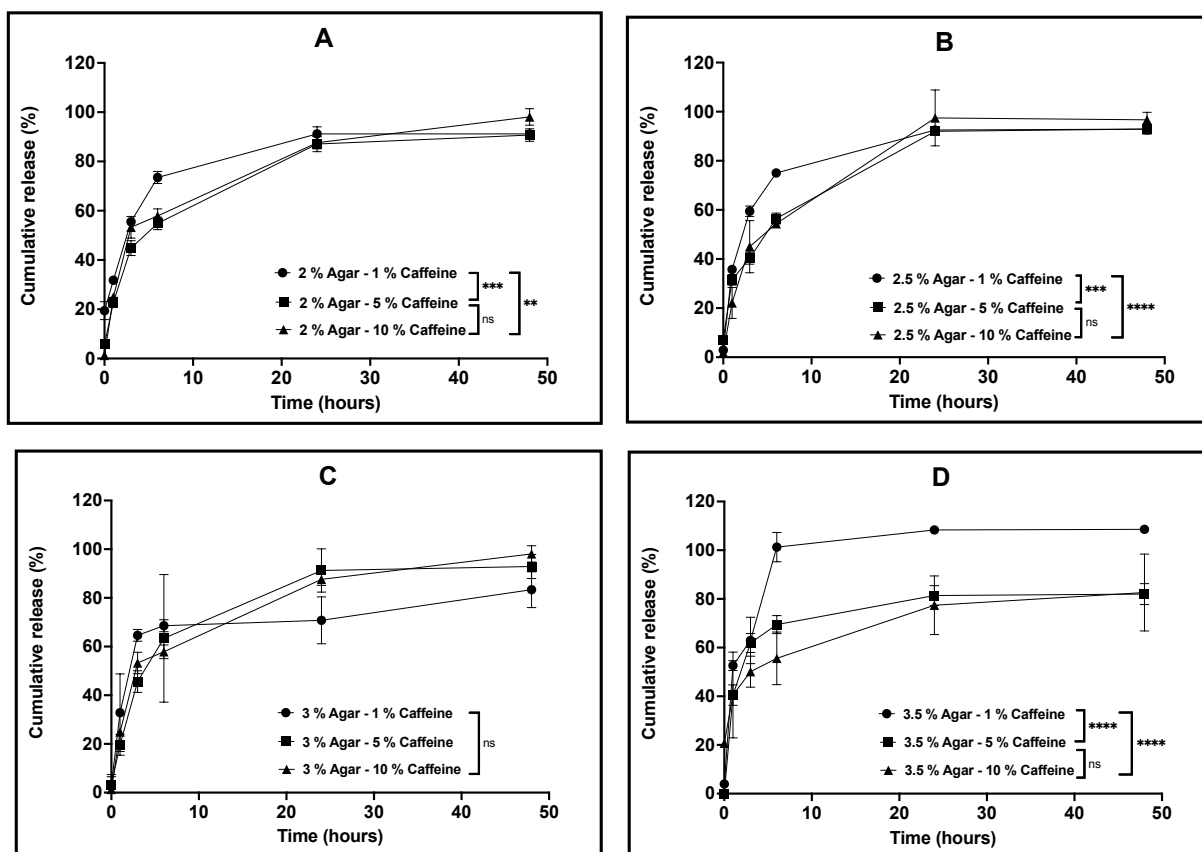


Figure 2-8: In vitro cumulative release profiles of caffeine (1, 5, 10%) from four different hydrogels (2, 2.5, 3, and 3.5%) in the PBS at normal pH over 48 hours in the shaking incubator at 60 rpm and 37°C. Results shown as mean \pm SD, n= 3, significance found using a two-way ANOVA with a Tukey’s post-hoc test, * = P<0.05 ** = P<0.01, *** = P<0.001, **** = P<0.0001.

2.4 Discussion

In this study, the agar hydrogels were investigated as a potential implantable drug delivery system for post-surgical localised treatment of pancreatic cancer. The agar hydrogels were loaded with caffeine during the conventional gelation process which is commonly known as the sol-gel method. Several formulations were prepared with increased agar (2, 2.5, 3, and 3.5% w/v) and caffeine (1, 5 and 10% w/v) loadings. The hydrogels were characterised for strength, adhesion, rheology, content distribution, as well as *in vitro* drug release.

The development of hydrogels as a drug delivery system with improved mechanical properties is essential for their role in biomedical and drug delivery applications to ensure that the hydrogels can be prepared and designed into different shapes and sizes in order to meet the required therapeutic goals (Wu, Dong et al. 2017). The mechanical strength investigations performed on agar hydrogels demonstrated a direct relationship between the agar concentration and their increased mechanical strength. As a result, the hydrogels prepared using a low agar concentration (2%) yielded hydrogels with reduced mechanical features, while those hydrogels with a greater physical strength were associated with an increased agar concentration (3.5%). The improved mechanical properties associated with the higher agar concentrations is mainly attributed to the increased number of intermolecular hydrogen bonds formed between agarose (gelling component of agar) chains that are responsible of for the formation of the hydrogel network, which results in double helical structures that accumulate into thick bundles and consequently stronger hydrogels (Aymard, Martin et al. 2001, Xiong, Narayanan et al. 2005). Loading caffeine into the hydrogels significantly increased the physical strength, especially at higher loadings. This is due to the increased caffeine agglomeration associated with higher

caffeine loadings within the hydrogel network, which could promote higher hydrogel density compared to the unloaded hydrogels resulting in a stronger mechanical behaviour (Buckley, Thorpe et al. 2009). Moreover, the predominance of the elastic properties of agar hydrogels over the viscous properties was also found to be related to an increase in agar concentration as well as their caffeine loading, which can be explained by the presence of higher amounts of anhydrous units (3,6-*anhydrous*-l-galactose and d-galactose) of agar that improve the elastic behaviour by increasing the number of crosslinking points within the hydrogel network and potential drug polymer interaction (François, Rojas et al. 2005, de Vries, Wesseling et al. 2017, Bertasa, Dodero et al. 2020). These findings suggest that agar hydrogel offers sufficient and adjustable mechanical properties based on the agar concentration and drug loading used for the hydrogel preparation. Such improved and controlled mechanical features are beneficial for the development of implantable hydrogels as localised drug delivery systems that will provide support against deconstruction upon implantation. Also, these features are helpful to produce implants of desired shapes and sizes while maintaining their physical integrities.

The evaluation of unloaded and caffeine loaded agar hydrogels adhesive properties demonstrated that they offer mild adhesion characteristics, which were reduced with increasing the agar concentrations as well as caffeine loadings used in hydrogel synthesis. This can be attributed to many reasons including the absence of liquid like properties in the highly crosslinked solid agar hydrogel, which is required to form good molecular contact under an applied pressure. Also, the higher elastic properties associated with increased agar concentrations of the hydrogels and caffeine loadings are directly related to their lower adhesive properties due to the difficulty to deform in order to make sufficient contact with the hydrogel

surface (Zosel 1989, Grillet, Wyatt et al. 2012). Moreover, the hydrogels mild adhesion characteristics can be related to the increased surface roughness caused by coil-like helical structures that build up the hydrogels network with the higher agar composition, which were also increased with the presence of higher caffeine on the gel surface with increased loadings (Rudge, Scholten et al. 2020). As a result, an improvement in the mucoadhesive properties of agar hydrogels is required to be used as an implantable drug delivery system for post-surgical localised treatment of cancer. Therefore, more investigations are required to develop agar hydrogels with better adhesive properties.

The investigations of the caffeine content distribution were performed on the agar hydrogels 2, 2.5, 3, and 3.5% with caffeine loadings of 1, 5, and 10%. Results demonstrated that the low agar hydrogel (2%) caffeine content distribution of increased loadings were found to be varied with higher caffeine loadings (5 and 10%). The caffeine content in 2.5% agar hydrogel relatively reduced as the caffeine loading increased to 10%, and the variations in the content distribution were found to be associated with higher caffeine loadings. The 3% agar hydrogel caffeine content reduction was significant ($p < 0.05$) as the drug loading increased to 10%, while the 3.5% hydrogels showed variations in their caffeine content with lower levels of homogenous distribution within the hydrogel as the caffeine loading increased to 10%. The caffeine content reduction in higher agar hydrogels and caffeine loadings simultaneously can be referred to the entrapment of the remaining caffeine within the hydrogels. This is due to the reduced network pores sizes with higher agar concentration that will lead to entrapment and increases the time required for higher caffeine loadings diffusion (Han, Choi et al. 2013). Subsequently, incomplete extraction of higher caffeine contents from the hydrogels. Therefore, longer

extraction time may be required for higher caffeine loaded agar hydrogels to ensure complete caffeine extraction. The differences in the caffeine distributions indicate that higher caffeine loadings can alter the drug homogeneity within the hydrogels, which could be due to the high viscosity of the gel solution. Subsequently, the homogenous dispersion of higher caffeine loadings especially 10% within the hydrogels is difficult to obtain. These findings may suggest that obtaining agar hydrogel as an implantable drug delivery system with lower drug loadings is more efficient for better content and homogeneity. In addition, the alternative drug post-loading technique should be investigated to evaluate its capability in improving the loaded hydrogel content distribution.

The release of caffeine from most hydrogels demonstrated a very rapid ‘burst’ release during the first 6 hours for all drug loadings. As both the caffeine and agar loadings increase the release percentage of caffeine reduces within the first 3-6 hours with sustained release over the remaining 48 hours. The initial ‘burst’ release is associated with the caffeine adsorbed onto the surface of the hydrogels being released, which is mediated by a concentration gradient due to drug’s hydrophilicity (Pekarek, Jacob et al. 1993). The slower sustained release phase can be attributed to several related factors including, increased agar concentrations of the hydrogels that results in a more elastic and compact hydrogel network resulting in reduced porosity (discussed in Chapter 3) and mesh size of hydrogels (Nordqvist and Vilgis 2011, Han, Choi et al. 2013). Consequently, the caffeine molecules would encounter greater resistance, reducing diffusion through those narrowed pores and correspondingly increasing the time required for diffusion of the higher caffeine loadings through the agar polymeric network (Franson and Peppas 1983, Brazel and Peppas 1999, Brazel and Peppas 1999). These results indicate that the

amount and the duration of drug release from agar hydrogels as an implantable drug delivery system can be adjusted based on the required treatment plan. In addition, caffeine-loaded hydrogels with lower agar concentrations (2 and 2.5%) are capable to release sufficient drug amount after 2 days, while loaded hydrogels with higher agar concentrations (3 and 3.5%) can reduce and sustain the release up to 4 or 5 days especially with the simultaneous increased drug loading (5 and 10%).

Generally, our findings indicate that most hydrogel formulations are characterized by improved mechanical strength and elastic properties even at lowest agar concentration (2%), which further increased as the agar and caffeine loadings increased during hydrogel preparation. Such improved mechanical features will provide supported implantable hydrogels against deconstruction upon their surgical implantation. Nevertheless, these hydrogel formulations offered limited adhesive properties regardless the agar or drug loadings due to the difficulty of hydrogel deformation, which is essential for adhesion to the tissues. Therefore, an improved adhesive feature is still a demand in order to facilitate hydrogels adherence to the target tissue through molecular interaction between the hydrogel surface and the resection site mucosal tissues upon surgical implantation for improved drug delivery. However, due to the solid nature and strongly crosslinked agar hydrogels, the adhesive molecular interactions as well as hydrogel biodegradation are difficult to obtain. Accordingly, further investigations are required to modify the agar hydrogel structural components chemically by using polymeric blend that could overcome the problems related to their limited adhesion and biodegradation (Zhang, Ren et al. 2019, Chaudhary, Thakur et al. 2020). Also, casting the agar hydrogel within biocompatible adhesive polymeric patch to facilitate its adhesion to the tissue upon implantation, while using

a surgical technique managing simple extraction of the implantation due to the insufficient degradation rate. Ideally, developing hydrogel formulations for localised controlled drug delivery should provide an acceptable homogenous drug content and sustained release for extended duration between 3-5 days with reduced burst release effect. As a result, 2 and 2.5% agar hydrogels with 5% loading were chosen for further investigations using chemotherapeutic agent Irinotecan (IRN) (Chapter 4) based on their slower rapid burst drug release compared to lower drug loading (1%), to evaluate their release profiles using 5% IRN. They were also selected for their appropriate physical properties, better drug homogeneity than higher drug loading (10%), Furthermore, 3 and 3.5% agar hydrogels with 5% loaded were also selected using chemotherapeutic agent Irinotecan (IRN) (Chapter 4) due to their great mechanical stability as well as their extended-release profiles compared to 2 and 2.5% formulations with the same drug loading.

2.5 Conclusion

The caffeine-loaded agar hydrogels were developed using sol-gel method. During the development and optimization, two main parameters were studied including the amount of agar used in hydrogel synthesis and caffeine loading rate. 12 caffeine loaded hydrogel formulations were prepared and characterized in terms of hydrogels mechanical features including their strength, elasticity, adhesion, and rheology. Also, the content and distribution of caffeine-loaded agar hydrogels were investigated. The influence of both agar concentration and caffeine loadings on the release profiles from hydrogel formulations were evaluated. The release profiles of caffeine from hydrogels showed initial fast 'burst' release followed by sustained release. The

mechanical properties and the release profiles were affected by the agar concentrations of the hydrogel and caffeine loading rates. Four agar hydrogels 2, 2.5, 3 and 3.5% with caffeine loadings of 5% were determined as the optimized hydrogel formulations for further studies based on their physical features, content distribution, as well as in vitro release profiles. Therefore, we propose that these optimized agar hydrogels and drug loading should be considered as implantable drug delivery system for the localised post-surgical treatment of cancer.

Chapter 3: Development and Optimization of Implantable Agar Aerogels as a Localised Drug Delivery System

3.1 Introduction

Aerogels are defined as a highly porous structured matrix system with interesting features making them attractive to be investigated as a potential drug delivery system. These features include significant low density, high surface area, and high porosity (Du, Zhou et al. 2013). Also, the varieties of the biomaterials that can be used for aerogels development comprise, the uncomplicated conditions required for their preparations. Furthermore, the versatility of tuning aerogels mesh size, interconnected pores, and shapes are promising properties to explore aerogels capabilities as pharmaceutical formulations (Barrios, Fox et al. 2019, Liu, Ran et al. 2020). In comparison to common hydrogels, their freeze-dried aerogels may demonstrate faster loading of drug molecules, easier access to core region of the matrix, and more efficient interactions with the aerogel matrix. Nevertheless, adjusting the aerogels polymeric components and the rate of crosslinking, could influence aerogels ability to control drug release or, in contrast, their ability as drug diffusing enhancers (Alnaief, Antonyuk et al. 2012, Valo, Arola et al. 2013, Veronovski, Knez et al. 2013, Ulker and Erkey 2014).

In addition, the adjustable porous flexible mechanical structure of aerogels could make them capable to be designed into different shapes and sizes, which is helpful to develop the aerogels as a local drug delivery system. For example, aerogels could be moulded into the cancer resection cavities based on the required implantation site to ensure good contact with the margin

tissue. Also, aerogels could offer the option for drug loading method to be either preloaded during the formulation preparation or post-loaded after obtaining the formulation. The post loading method may offer better flexibility for the surgical team to load the required chemotherapeutic agent and dose upon implantation based on the histopathological evaluation following tumour resection.

Several naturally sourced polysaccharide biopolymers for the development of aerogel formulations have been shown to be superior in terms of mechanical properties, sustainability, and biocompatibility (Nita, Ghilan et al. 2020, Wei, Ching et al. 2020). This chapter will focus on the assessment of highly porous agar matrices as aerogels encapsulating caffeine as a model drug. The main goals are to investigate the effect of varying the agar concentration (2, 2.5, 3 and 3.5%), caffeine loading (1, 5 and 10%), loading method on the mechanical properties of the aerogels, as well as the distribution of caffeine within the aerogels and its subsequent release.

3.2 Materials and methods

3.2.1 Materials

A polysaccharide complex Agar composed of about 70% agarose and 30% agarpectin was purchased from Sigma (UK) for hydrogel preparation. Caffeine was purchased from Alfa Aesar, while Methanol 99% was purchased from Fisher Scientific. Phosphate buffered saline (PBS) tablets were purchased from VWR (UK).

3.2.2 Preparation of caffeine preloaded and post-loaded agar aerogels

The agar aerogels were prepared using the same method described before (Chapter 2, section 2.2.2). Shortly, predetermined amounts (Table 3-1) of agar in distilled water to prepare four different hydrogel formulations with agar concentrations of 2, 2.5, 3 and 3.5% w/v. predetermined amounts of caffeine were added to the mixtures. The final agar hydrogel formulation batches contained either 1, 5, and 10% w/v of caffeine. The obtained hydrogels were placed in -80°C freezer for 48 hours. Next, the caffeine loaded hydrogels undergo lyophilization process using freeze-dryer for 48 hours to remove all the water content within the hydrogels to obtain the caffeine preloaded aerogels. Alternatively, post-loaded aerogels were prepared using the same method without prior loading of caffeine as blank aerogels only. The caffeine post loading was performed by injecting different volumes (1, 2, and 3 ml) from different caffeine concentrations stock solutions (1, 5, and 10% w/v) (Table 3-2) to evaluate the effect of volume, concentration, and loading method.

Table 3-1: Formulations of prepared caffeine loaded hydrogels

Formulations	Agar	Caffeine	hydrogel solution volume
	% w/v	% w/v	ml
1	2	1	10
2	2	5	10
3	2	10	10
4	2.5	1	10
5	2.5	5	10
6	2.5	10	10
7	3	1	10
8	3	5	10
9	3	10	10
10	3.5	1	10
11	3.5	5	10
12	3.5	10	10

Table 3-2: Formulations of prepared caffeine post-loaded aerogels

Agar aerogel	Caffeine solution	Loading volume
% w/v	% w/v	ml
2	1	1, 2, 3
	5	1, 2, 3
	10	1, 2, 3
2.5	1	1, 2, 3
	5	1, 2, 3
	10	1, 2, 3
3	1	1, 2, 3
	5	1, 2, 3
	10	1, 2, 3
3.5	1	1, 2, 3
	5	1, 2, 3
	10	1, 2, 3

3.2.3 Characterization of the agar aerogel formulations

3.2.3.1 Aerogels mechanical strength

The effects of agar concentration and loading methods on the strength of the aerogels was evaluated. Experiments were performed on different agar aerogels concentrations of 2, 2.5, 3, and 3.5% without drug loading as well as 2 and 2.5% agar hydrogels preloaded with 1 and 5% caffeine, while 3 and 3.5% agar hydrogels preloaded with 1% caffeine. Also, the impact of

post-loading method was investigated by injecting different volumes of 1, 2, and 3 ml of deionized water into each formulation. The mechanical strength was determined in triplicate using separate formulation batches and drug free aerogels as controls using the same method described earlier (Chapter 2, section 2.2.3.1).

3.2.3.2 Aerogels porosity and swelling ratios

The porosity and swelling ratios of the aerogels were evaluated using different agar aerogel concentrations of 2, 2.5, 3, and 3.5%. First, the porosity tests were performed using liquid the displacement method. Every aerogel was placed into 30 ml of ethanol (V_1) inside a 50 ml centrifuge tube. The volume of ethanol with the aerogel was recorded (V_2). Then, the aerogel was removed from the centrifuge tube and the remaining volume was recorded (V_3). The porosity ratio (ϵ_1) was calculated using equation 1 (Kanokpanont, Damrongsakkul et al. 2012). The aerogel swelling ratio was determined by measuring the weight of each dry aerogel (W_0). Every aerogel was submerged into a bath of deionized water for 1 hour at room temperature. After that, aerogels were removed from the water bath and excess water on the surface was removed via filter paper. The aerogels weight was then measured again (W_1). Equation 2 was used to determine the swelling ratio (ϵ_2) (Yang, Xiao et al. 2018). The porosity and swelling ratios of the aerogels were performed in triplicate using separate formulation batches.

$$\epsilon_1 (\%) = (V_1 - V_3) / (V_2 - V_3) \times 100$$

$$\epsilon_2 (\%) = (W_1 - W_0) / W_0 \times 100$$

3.2.3.3 Raman mapping of caffeine post-loaded aerogels

The aim of this test is to determine the spatial distribution of caffeine post-loaded agar aerogels. The aerogels were investigated by collecting approximately 5 X 3 mm dried samples from the 2 and 2.5% aerogels post-loaded with 1 ml of different caffeine concentrations 1, 5, and 10%. The samples were placed and fixed on microscopic glass slides using double sided tape. Raman mapping tests were performed using a Thermo Scientific™ DXR system fitted with an external DXR 720 nm frequency laser source and an Olympus TH4-200 optical microscope. A 10X objective was used for optical imaging and spectrum acquisition. All spectra were obtained in the spectral range of 200 - 3413 cm^{-1} with a resolution range 2.4 - 4.4 cm^{-1} provided by a grating monochromator of 400 lines/mm. Raman maps and reference spectra of the samples were collected using laser spot size 3.1 μm and 30 μm step size. The reference Raman spectra of the pure caffeine was collected in a powder form. The measured area for every sample was 0.4 mm \times 0.4 mm.

3.2.3.4 Caffeine content distribution of the preloaded aerogel formulations

The caffeine preloaded agar aerogels contents distribution was determined similarly to the previous method in hydrogels (Chapter 2, section 2.2.3.4).

3.2.4 In vitro release of caffeine from pre- and post-loaded aerogels

0.4 to 1.5 g (dependent on their agar and caffeine content) of the preloaded agar aerogels were placed into a glass bottle containing 100 ml of pre-prepared PBS buffer (pH 7.4). The post-loaded aerogels were fixed one side so that they remained in floating position in plastic tubes

containing 50 ml of pre-prepared PBS buffer (pH 7.4) and placed in an orbital shaking incubator at 37°C and 60 rpm. The aerogels were fixed by pushing a needle through the plastic cap of the tube and into the aerogel. At time intervals of 0, 1, 3, 6, 24, and 48 hours a 1 ml sample was collected, replaced with 1 ml of fresh PBS buffer, and subsequently stored at 4°C until analysed by HPLC. The release study was conducted in triplicate and the percentage of caffeine released calculated relative to the caffeine content of the aerogels.

3.2.5 HPLC analysis

3.2.5.1 HPLC chromatographic conditions, stock solution and calibration curve

The caffeine was analysed using the technique described previously (Chapter 2, sections 2.2.5.1 and 2.2.5.2).

3.2.6 Statistical analysis

Statistical analysis was performed using a one-way or two-ways analysis of variance dependent on the presence of one variable or two independent variables respectively (ANOVA) (GraphPad Prism version 9.0.2 for MacOS, GraphPad Software, San Diego, CA). Post-hoc comparisons of the means were performed using Tukey's Honestly Significance Difference test. A significance level of $p < 0.05$ was accepted to denote significance in all cases.

3.3 Results

3.3.1 Aerogels mechanical properties

The mechanical tests performed on the agar aerogels demonstrated that the higher agar concentration in the unloaded aerogels significantly increased their mechanical strength (Figure 3-1). Results in Figure 3-1 report that the mechanical strength levels recorded were significantly ($p < 0.05$) increased from $305.5 \pm 31 \text{ g/cm}^2$ for the 2% agar aerogel to $375.8 \pm 30 \text{ g/cm}^2$ with the 2.5% agar aerogel, while the 3 and 3.5% agar aerogels showed a significant increase in their physical strength increasing to 486.8 ± 54 and $822.1 \pm 64 \text{ g/cm}^2$, respectively. Nevertheless, the agar aerogel formulations preloaded with either 1 or 5% caffeine demonstrated improved mechanical properties compared to the unloaded aerogels. Moreover, increasing the caffeine loading provided a further significant increase in their mechanical strength. However, the post-loaded agar aerogels demonstrated a significant reduction in their measured strength levels upon post loading, which further reduced with increasing injection volume (Figure 3-2)

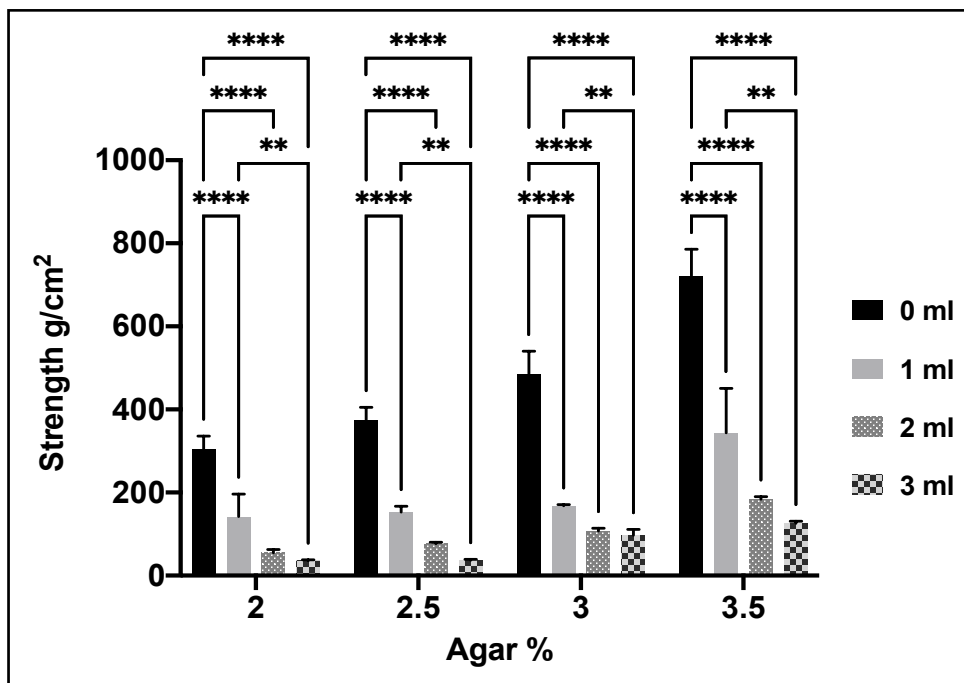


Figure 3-1: Effect of different agar concentrations (2, 2.5, 3, and 3.5%) and caffeine loading concentrations (1 and 5%) aerogels mechanical strength. Results shown as mean \pm SD, $n=3$, significance found using a two-way ANOVA with a Tukey's post-hoc test, * = $P<0.05$ ** = $P<0.01$, *** = $P<0.001$, **** = $P<0.0001$.

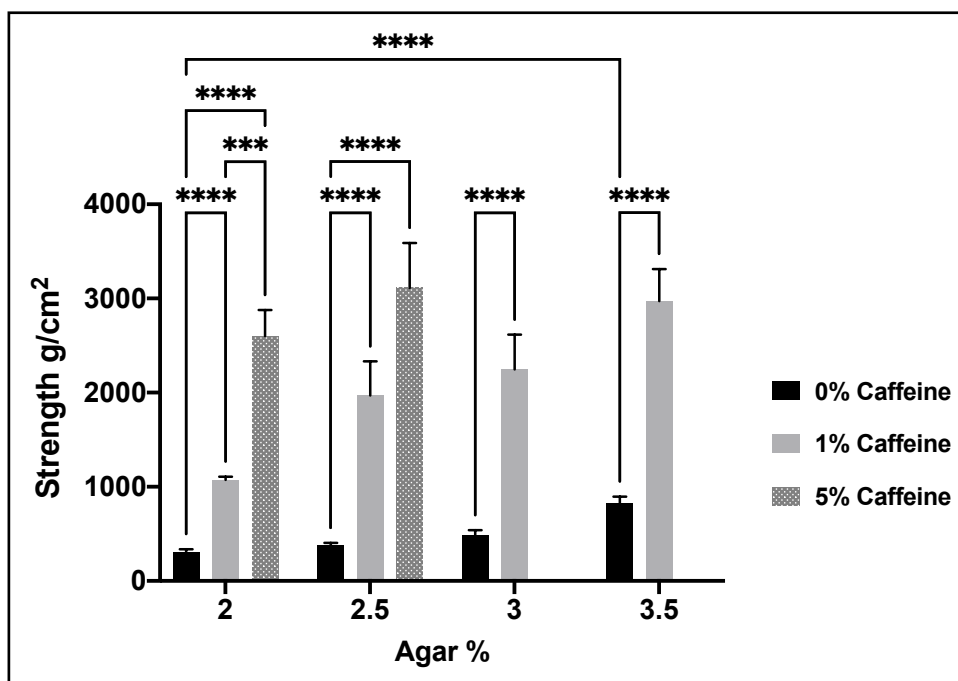


Figure 3-2: Effect of post loading volumes (1, 2, and 3 ml) on 2, 2.5, 3, and 3.5% agar aerogels mechanical strength. Results shown as mean \pm SD, $n=3$, significance found using a two-way ANOVA with a Tukey's post-hoc test, * = $P<0.05$ ** = $P<0.01$, *** = $P<0.001$, **** = $P<0.0001$.

3.3.2 Aerogel porosity and swelling ratios

The mean porosity and swelling ratios for the agar aerogels demonstrated a significant decrease in both porosity and swelling as the agar concentration increased (Figure 3-3). The porosity ratios of agar aerogels showed a non-significant reduction from 73.1 ± 5.7 to $65.2 \pm 3.2\%$ as the agar aerogel concentration increased from 2 to 2.5% (Figure 3-3 A). However, the porosity ratio of both 3 and 3.5% agar aerogels demonstrated a significant reduction (55.2 ± 4.3 and $54.3 \pm 2.1\%$, respectively) compared to 2 and 2.5% aerogels. Their swelling ratios demonstrated a non-significant reduction from 2681.9 ± 291.9 to $2322.9 \pm 169.9\%$ for 2 and 2.5% aerogels, respectively. However, a significant reduction in the swelling ratios was observed with the 3 and 3.5% aerogels at $1922.7 \pm 383.8\%$, and $1568.6 \pm 265\%$ respectively.

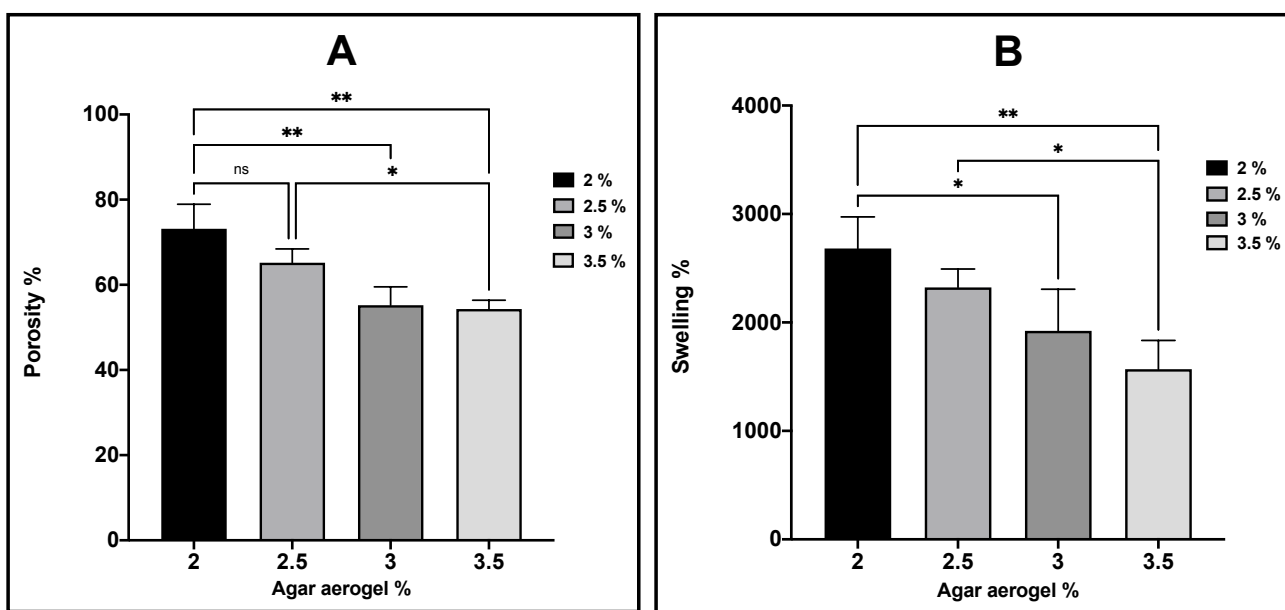


Figure 3-3: Effect of varying agar concentrations (2, 2.5, 3, and 3.5%) on aerogels porosity (A), and swelling (B). Results shown as mean \pm SD, n = 3, significance found using a one-way ANOVA with a Tukey's post-hoc test, * = P<0.05 ** = P<0.01, *** = P<0.001, **** = P<0.0001.

3.3.3 Raman mapping of the caffeine post-loaded aerogels

The distribution Raman maps of the 2 and 2.5% agar aerogels post-loaded with caffeine (1, 5, and 10%) are presented in figure 3-4, with the reference Raman spectra of the pure caffeine presented in figure 3-5. Caffeine distribution is highlighted using the following colour scheme; no caffeine (Blue), low caffeine distribution (Green), medium caffeine distribution (Yellow) and high caffeine distribution (Red). Results showed that the aerogels caffeine content distribution within the aerogel samples was varied based on the agar concentration and the caffeine loading rate. The higher the agar concentration and the lower the caffeine concentration of the solution are related to the lower distribution of the caffeine in the aerogels. However, with the higher concentration caffeine solutions the distribution is significantly improved. This is demonstrated by the significant levels of blue (no caffeine) in both the 2 and 2.5% agar aerogels with the 1% caffeine solutions, while for the 5 and 10% caffeine solution the blue disappears and there is an increase in green (low caffeine distribution), yellow (medium caffeine distribution) and red (high caffeine distribution).

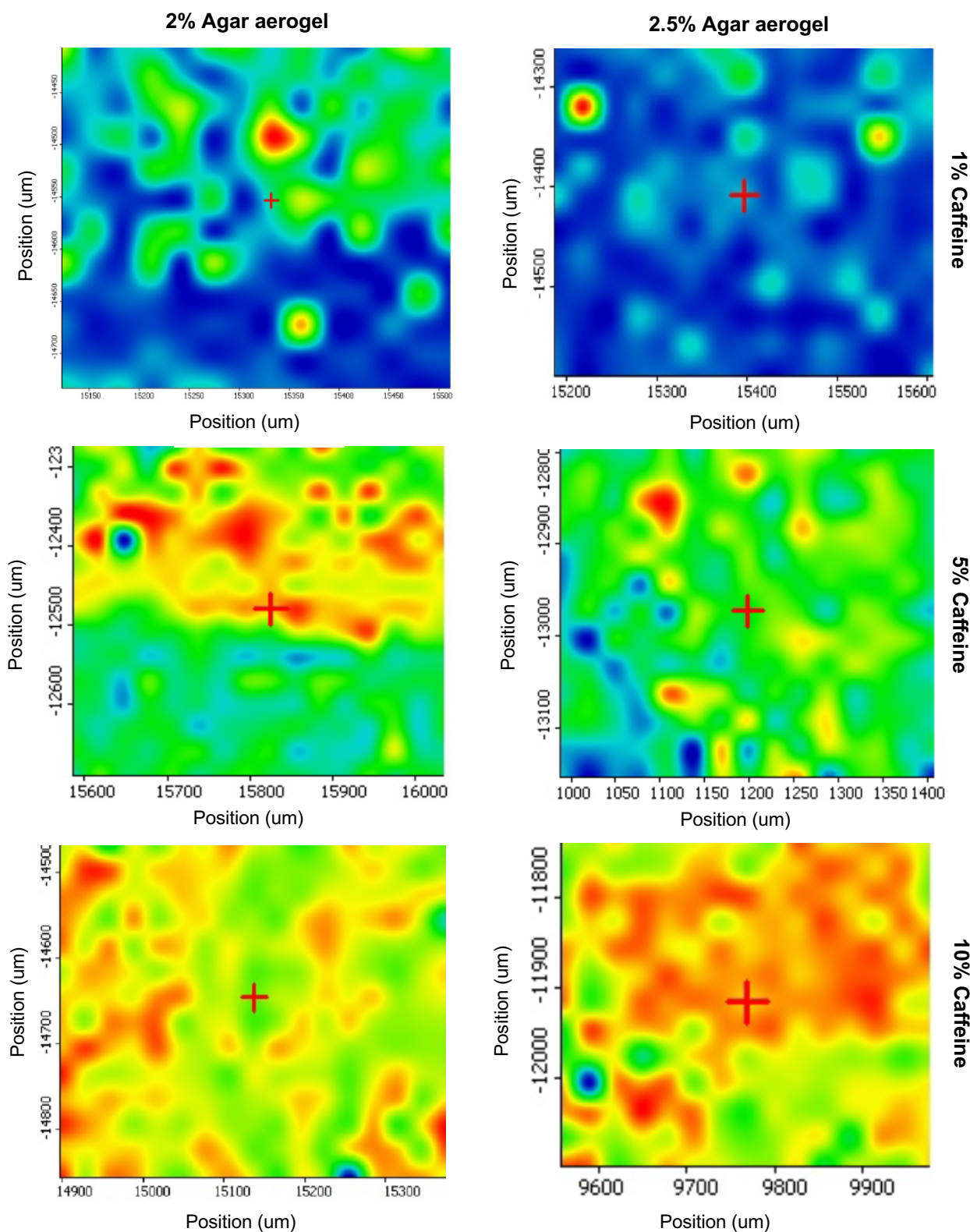


Figure 3-4: The distribution maps of agar aerogels 2 and 2.5% loaded with 1ml of different caffeine concentrations (1, 5, and 10%).

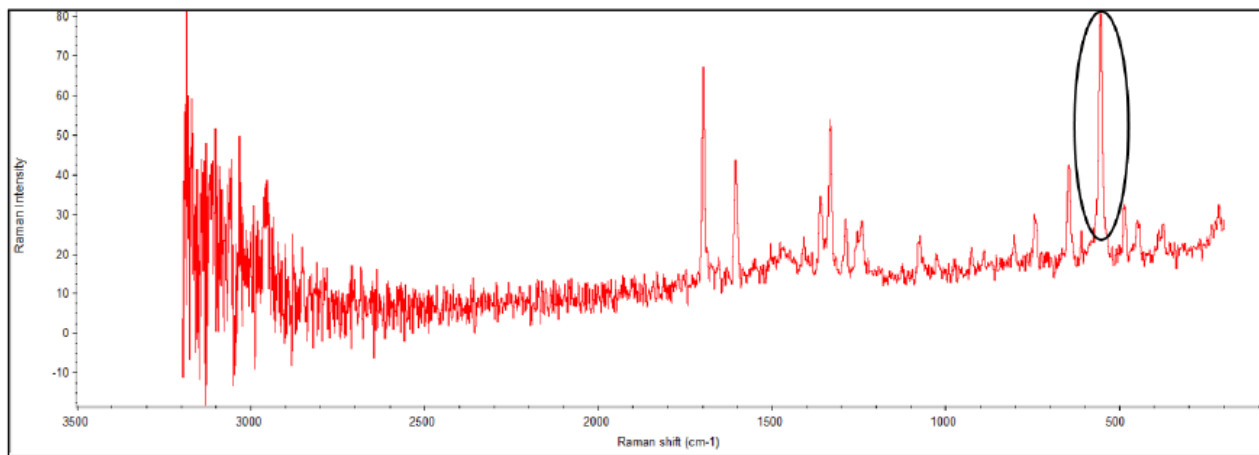


Figure 3-5: The reference Raman spectra of the pure caffeine

3.3.4 HPLC analysis of caffeine

Figure 3-6 shows the caffeine standard curve at 6 different concentrations of caffeine quantified by HPLC. The correlation between the caffeine concentrations and the HPLC area under the curve AUC was excellent with the R value at 0.9989 from 0.001 to 1 mg/ml. The retention time was approximately 2.9 minutes (Figure 3-7).

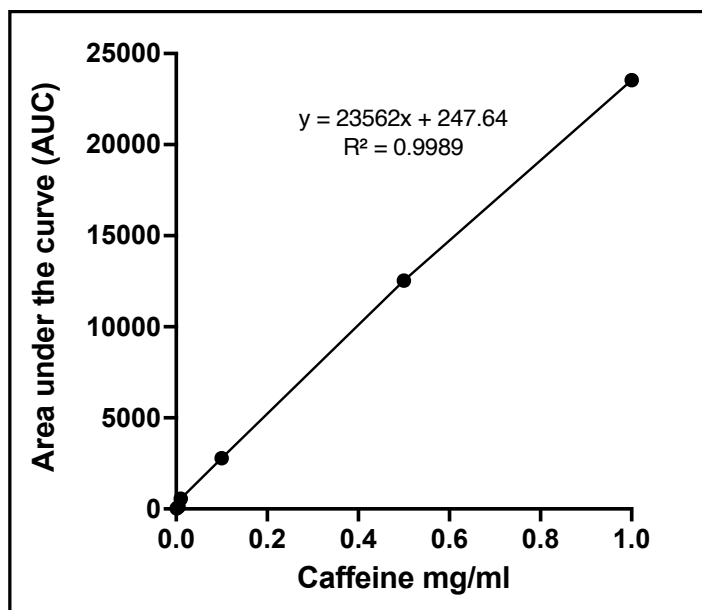


Figure 3-6: Standard curve for caffeine using HPLC (n=3).

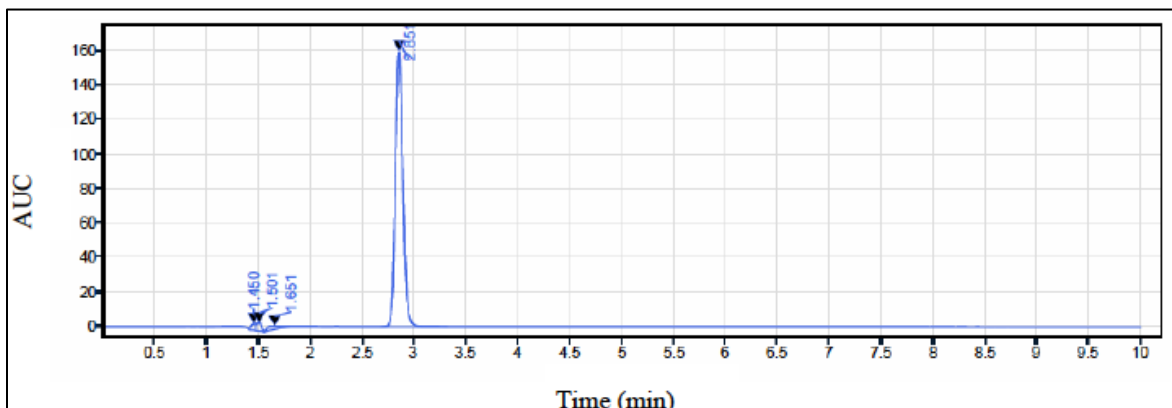


Figure 3-7: The HPLC chromatogram depicting the peak of caffeine at 273 nm wavelength.

3.3.5 Caffeine content distribution of preloaded agar aerogel formulations

The caffeine content distribution in agar aerogels (2, 2.5, 3, and 3.5%) preloaded with caffeine (1, 5, and 10%) was investigated. The caffeine contents distribution in preloaded aerogels were varied based on the increased agar concentration and the caffeine loadings within every aerogel. As demonstrated by Figure 3-8, the caffeine content distribution varied with an increase in drug loading and agar concentration. The lower agar aerogels (2 and 2.5%) preloaded with 1 and 5% caffeine expressed relatively better distribution of caffeine within the aerogels compared to those with an increased agar concentration (3 and 3.5%). In addition, a reduced homogeneity was observed with an increase in caffeine loading to 10%. The 2% agar aerogel caffeine contents varied from 101.1 ± 5.5 to $87.7 \pm 16.8\%$, while the 2.5% aerogels had caffeine contents of 104.4 ± 4.9 , 93.6 ± 4.7 , and $88.03 \pm 20.5\%$ for 1, 5, and 10% caffeine loading respectively. The 3% aerogels showed contents of 94.7 ± 9.8 , 89.7 ± 3.8 , and $82.08 \pm 17.5\%$ respectively, for the 1, 5, and 10% caffeine loadings, while the caffeine contents within 3.5% aerogels varied from 100.6 ± 13.9 to $84.9 \pm 32.3\%$ across the same caffeine loadings.

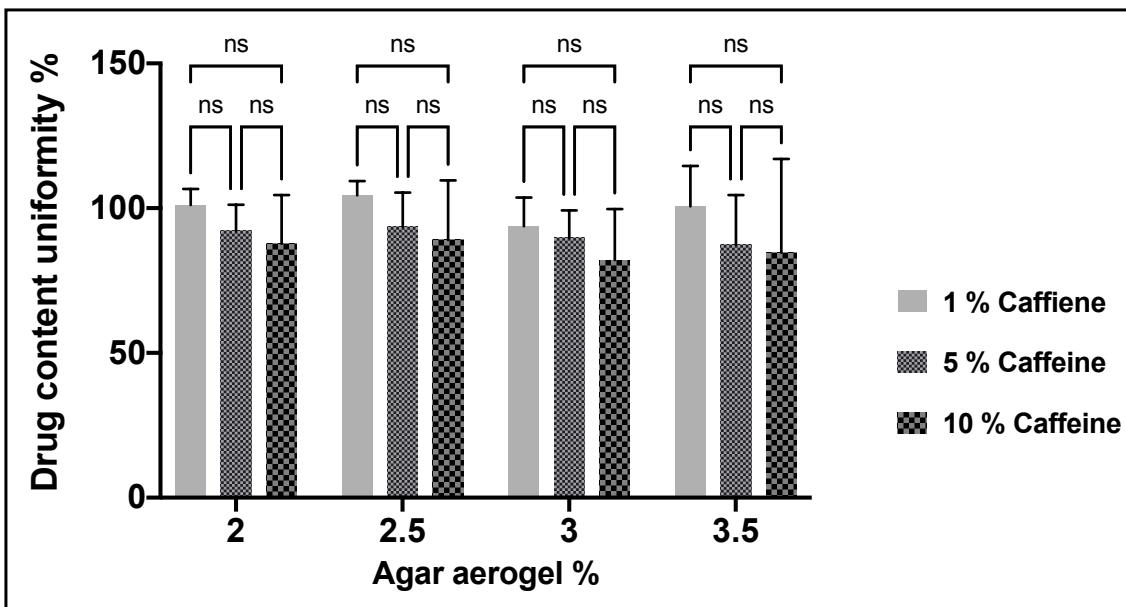


Figure 3-8: Caffeine content distribution (1, 5, and 10%) in four preloaded aerogels (2, 2.5, 3, and 3.5%). Results shown as mean \pm SD, significance found using a two-way ANOVA with a Tukey's post-hoc test, * = $P < 0.05$ ** = $P < 0.01$, *** = $P < 0.001$, **** = $P < 0.0001$.

3.3.6 In vitro release of caffeine from preloaded agar aerogels

The release of caffeine from preloaded agar aerogels was performed in PBS (pH 7.4) at 37°C. The percentage cumulative release profiles are presented in Figure 3-9. The release profiles of caffeine from the preloaded aerogels were varying based on two factors, including the increased agar concentration of the aerogels and the varying caffeine loadings within every aerogel. As seen in Figure 3-9, the caffeine displayed a biphasic release profile over 48 hours from aerogels. First, a rapid 'burst' release was observed, followed by the second phase of release that yielded a slower release after 6 hours as the caffeine loading, and agar concentration increased. The 2% agar preloaded aerogel loaded with 1% caffeine showed the fastest release behaviour in comparison to the same aerogels loaded with 5 and 10% caffeine (Figure 3-9 A).

Within six hours, the 2% aerogels released $96.3 \pm 0.5\%$ of its caffeine, while for both 5 and 10% loaded caffeine aerogels demonstrated slower release of 79.3 ± 4.7 and $38.1 \pm 2.9\%$ respectively. Most of the caffeine in the 2% aerogels were released after 48 hours. Moreover, the higher agar concentration in the 2.5% aerogels resulted in slower release for 1 and 5% loaded caffeine at 3 hours. The 10% caffeine preloaded aerogel showed a further significant ($p < 0.05$) reduction in its release compared to the 1 and 5% caffeine loadings within the same 2.5% agar aerogel (Figure 3-9 B). In addition, both 3 and 3.5% aerogels reduced the initial burst release of their 1 and 5% caffeine compared previous aerogels within 3 and 6 hours for 3 and 3.5% aerogels respectively. This is followed by releasing most of their contents after 48 hours. Nevertheless, 10% caffeine preloaded 3 and 3.5% aerogels provided significant ($p < 0.05$) slower sustained release up to 48 hours releasing a total of 67.5 ± 12.1 and $73.2 \pm 3\%$ of their caffeine content respectively as illustrated in Figures 3-9 C and D.

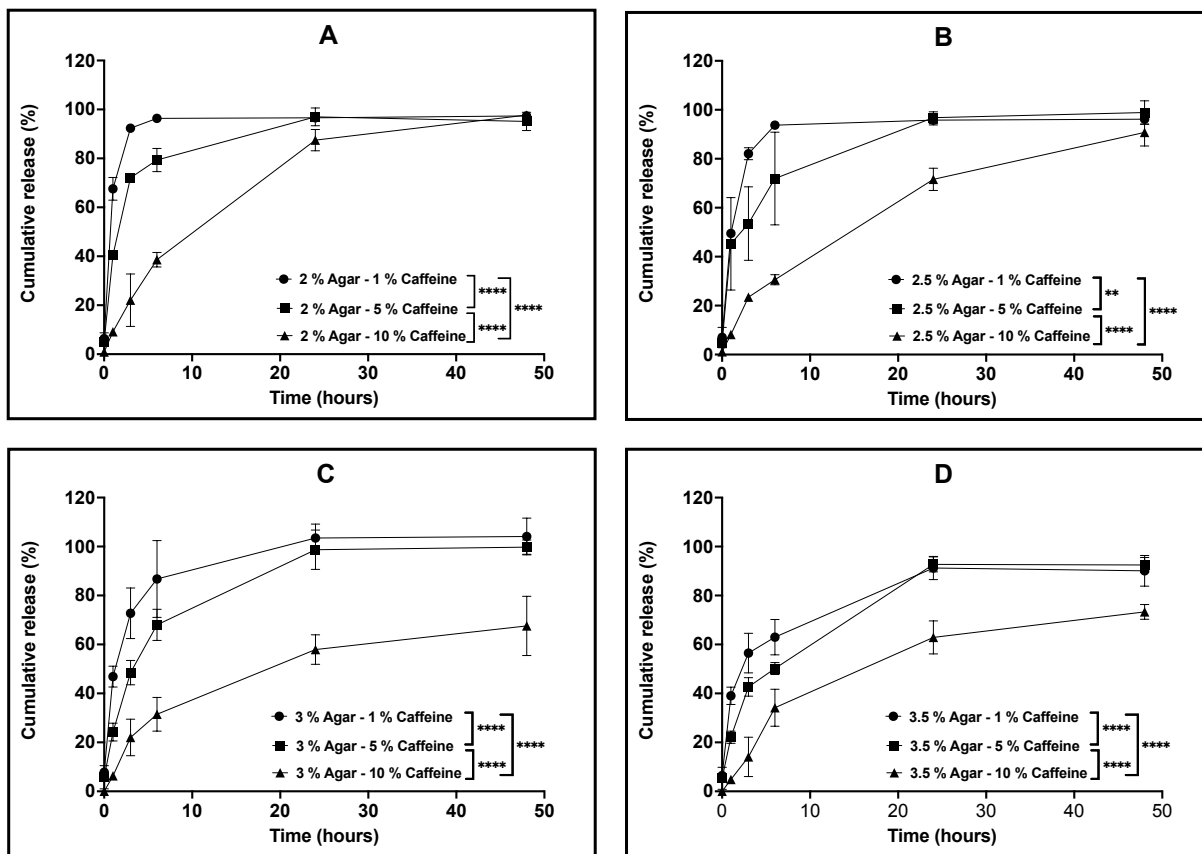


Figure 3-9: *In vitro* cumulative release profiles of caffeine (1, 5, and 10%) from four different preloaded aerogels (2, 2.5, 3, and 3.5%) in the PBS at normal pH over 48 hours in the shaking incubator at 60 rpm and 37 °C. Results shown as mean ± SD, n= 3, significance found using a two-way ANOVA with a Tukey’s post-hoc test, * = P<0.05 ** = P<0.01, *** = P<0.001, **** = P<0.0001.

3.3.7 *In vitro* release of caffeine from post-loaded aerogels

The percentage cumulative release profiles for caffeine post-loaded aerogels are shown in Figures 3-10, 11, and 12. The release of caffeine from the post-loaded aerogels is controlled by three factors, including the agar concentration of the aerogels, the caffeine loading concentration, and post loading volume. Similarly, the caffeine displayed a biphasic release profile over 48 hours from post-loaded aerogels. First, a rapid ‘burst’ release, then the second

phase of release that yielded a slower release after 3-6 hours as the caffeine loading, and agar concentration increased. First, the effect of post-loading volume (1, 2, and 3 ml) of 1% caffeine into all aerogels on the release profiles are illustrated in Figure 3-10. Results demonstrated that the release profiles from post-loaded aerogels were relatively similar, and the caffeine was released rapidly during 6 hours from aerogels until approaching complete release after 48 hours for 1 and 2ml post-loaded caffeine. However, aerogels post-loaded with 3 ml of 1% caffeine had a statistically significant ($p < 0.05$) slower release profile compared to 1 and 2 ml within most aerogel formulations, as well as with increasing the aerogels agar concentrations in 2, 3, and 3.5 % aerogels mainly at 24 and 48 hours. The release profiles of different post-loadings (1, 2, 3 ml) of 1% caffeine from 2% agar aerogel at different time points were compared. Within six hours, 2% agar aerogel post-loaded with 1 and 3ml caffeine showed relatively similar release profiles, while 2 ml post-loaded caffeine demonstrated faster release mainly at 3 and 6 hours. However, 3 ml post-loaded caffeine showed significantly ($p < 0.05$) slower release compared to 1 and 2 ml (Figure 3-10 A). The release profiles of different post-loadings (1, 2, 3 ml) of 1% caffeine from 2.5% agar aerogel at different time points were compared. Within six hours, 1ml post-loaded caffeine showed lower release compared to 2 and 3 ml, while non-significant ($p > 0.05$) differences in the release profiles between 2 and 3 ml post-loaded caffeine were observed (Figure 3-10 B). The release profiles from 3 % agar aerogel showed statistically non-significant ($p > 0.05$) difference between 1 and 2 ml post-loaded caffeine, while 3 ml post-loaded caffeine demonstrated significant ($p < 0.05$) slower release profile compared to 1 and 2 ml post-loaded caffeine (Figure 3-10 C). The release profiles from 3.5 % agar aerogel showed statistically significant ($p < 0.05$) difference between 1, 2, and 3 ml post-loaded caffeine with slower release profile as the caffeine post-loading increase (Figure 3-10 D). Most of the 1%

caffeine content was released after 48 hours from all post-loaded aerogels. Upon post-loading similar volumes of 5% caffeine into aerogels, they provided different release from different aerogels compared to previous 1% post loaded aerogels as described in Figure 3-11. Results showed that 1 ml of 5% caffeine provided a relatively equal initial burst release profiles until 3 hours followed by extended slow sustained release from all the formulations regardless the increased aerogels agar concentrations. At 48 hours, post-loaded aerogels 2, 2.5, 3, and 3.5 % released a total of 80.7 ± 1.6 , 75.2 ± 6.9 , 79.5 ± 1.5 , and $73.1 \pm 1\%$, respectively of their 1 ml 5% caffeine contents. In contrast, aerogels loaded with 2 ml of 5% caffeine displayed significantly faster release by rapidly releasing the majority of their caffeine within 6 hours except from 3.5 % aerogel that released only $43.2 \pm 2\%$ at 6 hours (Figure 3-11 D). Subsequently, all aerogels released most of their 2 ml 5% caffeine content after 48 hours. The release from aerogels post-loaded with 3 ml of 5% caffeine were varied between the formulations. 2% aerogel exhibited the fastest release of its 3 ml 5% caffeine by releasing $83.3 \pm 5.7\%$ at 6 hours until releasing $97.8 \pm 2.5\%$ after 48 hours (Figure 3-11 A). In contrast, results in Figure 3-11 B presented a slower sustained release of the 3 ml caffeine from 2.5% aerogel ($59.6 \pm 4.2\%$) at 6 hours up to $73.1 \pm 19\%$ after 48 hours. The additional increase in the aerogels agar concentrations (3 and 3.5%) reduced the burst release of 3 ml caffeine contents in both formulations, followed by rapid increase in the release until releasing 92.4 ± 3 and $93.3 \pm 4\%$, respectively after 48 hours (Figures 3-11 C and D). The release of 1m post-loaded 5% caffeine from every aerogel formulation was significantly slower ($p < 0.05$) compared to 2 ml in 2, 2.5, and 3% post-loaded agar aerogels, as well as to 3ml in 2 and 3% post-loaded agar aerogels over 48 hours. The release profiles of 1, 2, and 3 ml 10% caffeine from agar aerogels 2, 2.5, 3, and 3.5% are illustrated in Figure 3-12. Results demonstrate that the effect of different post-loading

volumes is limited, as no significant ($p>0.05$) differences were found in the release profiles of different caffeine volumes in the same aerogel formulation except between 1 and 3ml in 2% post-loaded agar aerogel. However, the increased agar aerogels concentrations have the superior role over the release profiles rates of caffeine. Aerogels with higher agar concentrations improved the sustained release within 6 hours, and subsequently most aerogels released their caffeine contents after 48 hours.

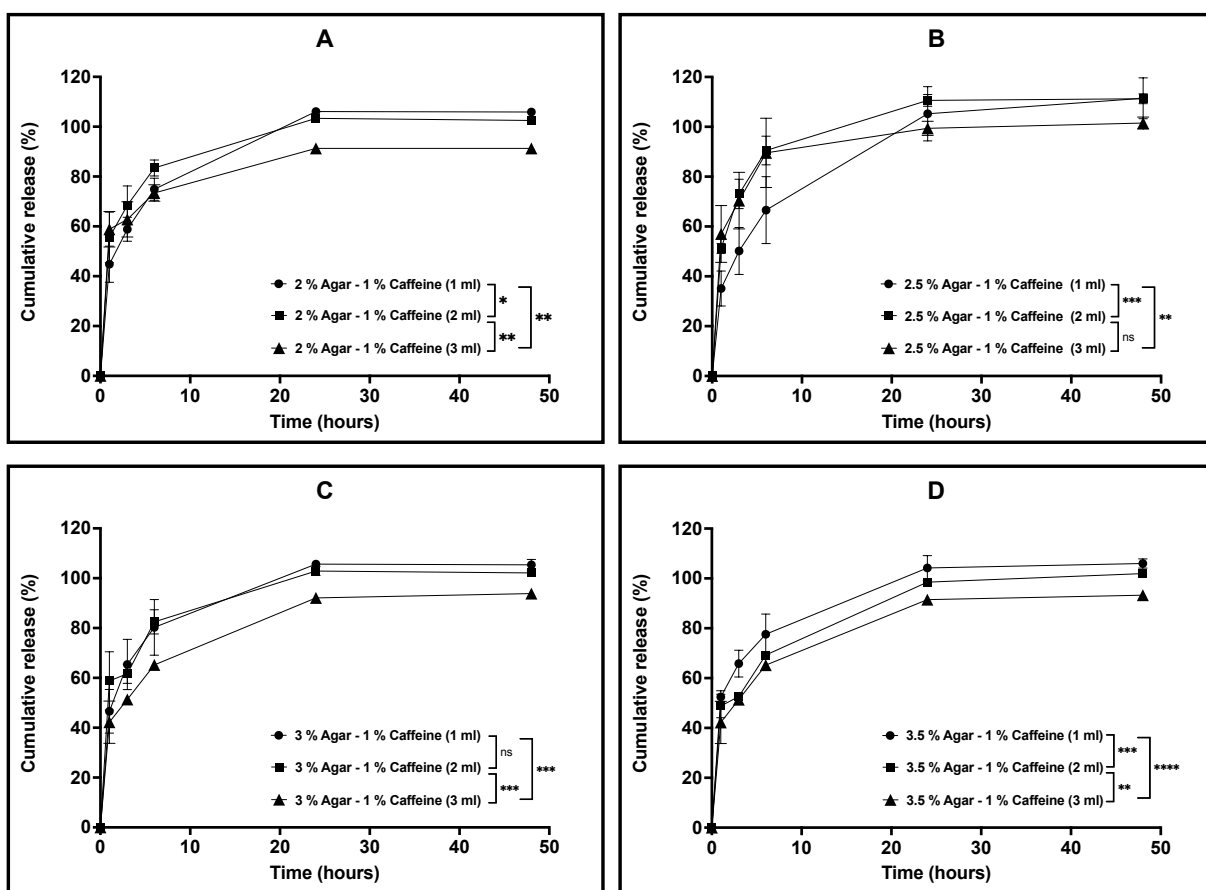


Figure 3-10: *In vitro* cumulative release profiles of different volumes (1, 2, and 3 ml) of 1% caffeine from four different post-loaded aerogels (2, 2.5, 3, and 3.5 %) in the PBS at normal pH over 48 hours in the shaking incubator at 60 rpm and 37 °C. Results shown as mean \pm SD, n= 3, significance found using a two-way ANOVA with a Tukey’s post-hoc test, * = $P<0.05$ ** = $P<0.01$, *** = $P<0.001$, **** = $P<0.0001$.

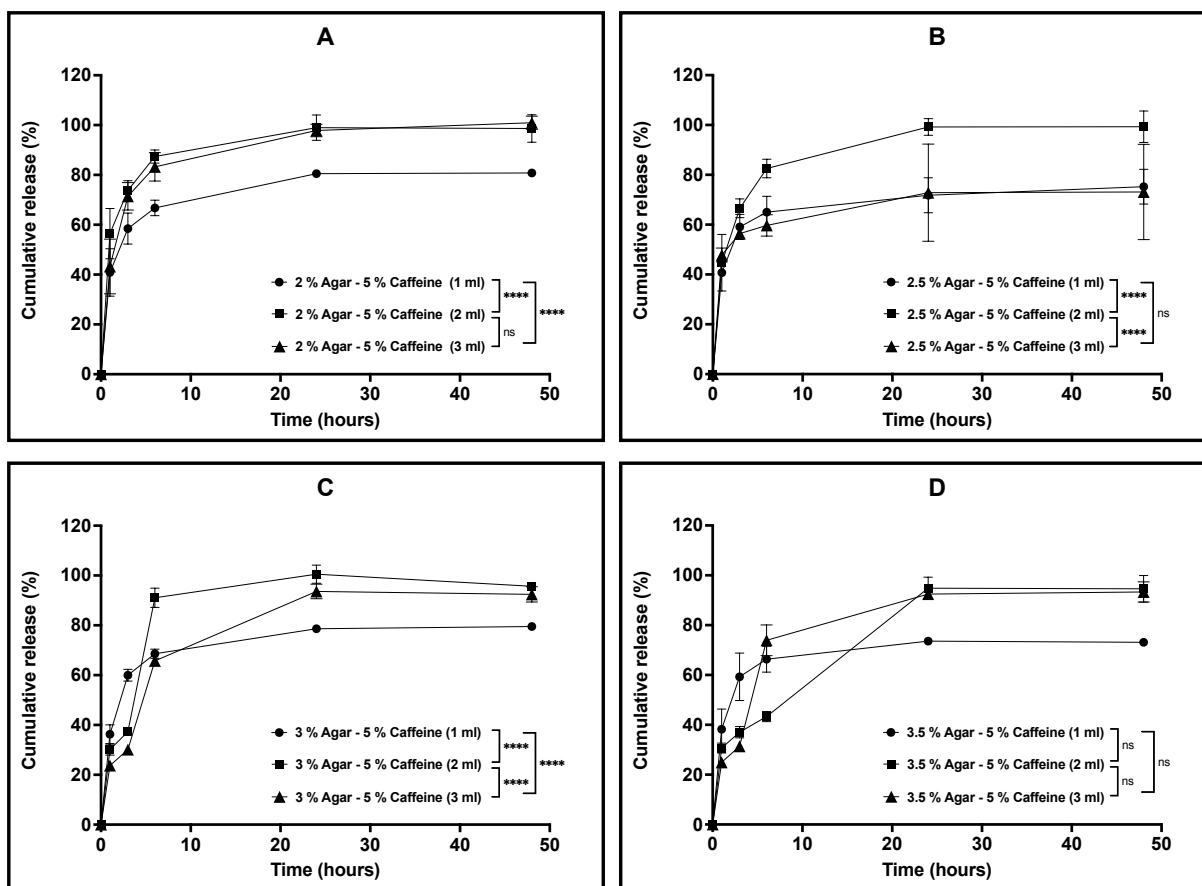


Figure 3-11: *In vitro* cumulative release profiles of different volumes (1, 2, and 3 ml) of 5% caffeine from four different post loaded aerogels (2, 2.5, 3, and 3.5 %) in the PBS at normal pH over 48 hours in the shaking incubator at 60 rpm and 37 °C. Results shown as mean ± SD, n=3, significance found using a two-way ANOVA with a Tukey's post-hoc test, * = P<0.05 ** = P<0.01, *** = P<0.001, **** = P<0.0001.

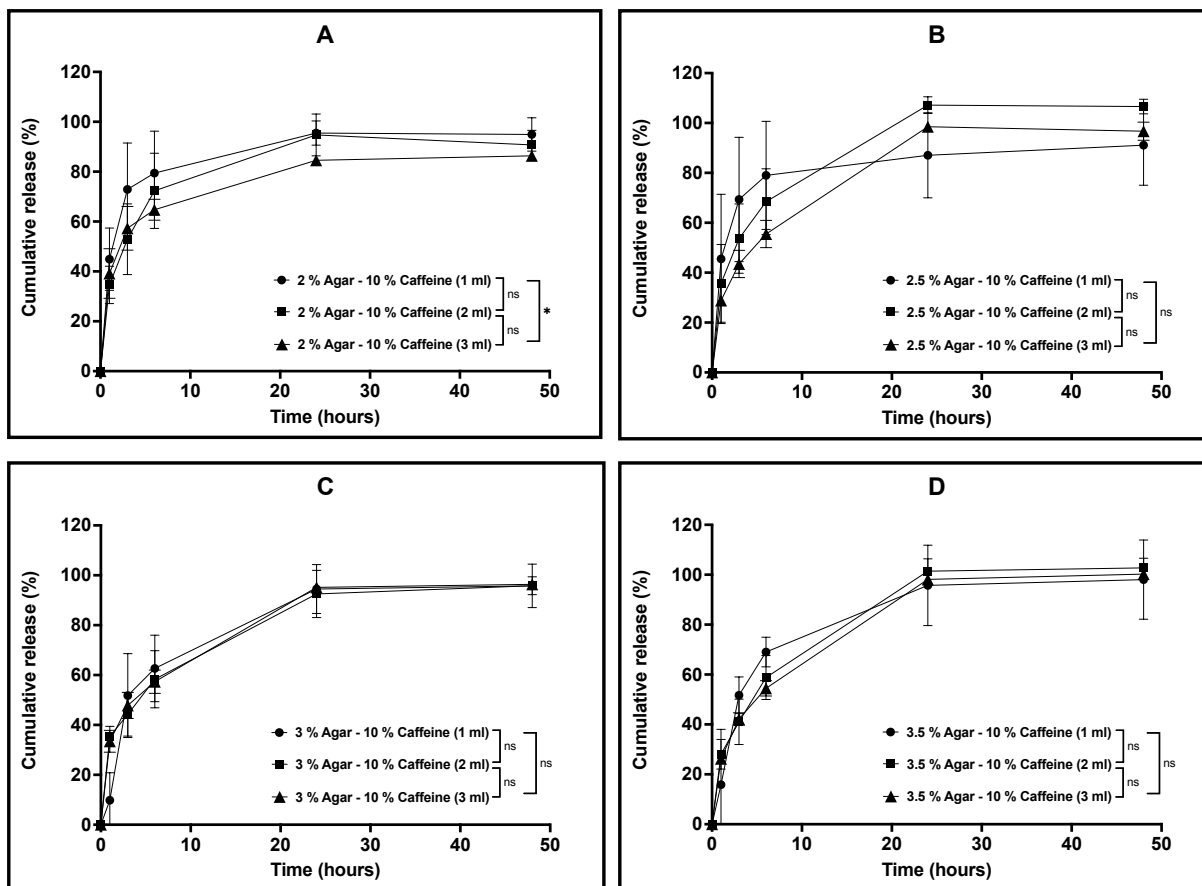


Figure 3-12: *In vitro* cumulative release profiles of different volumes (1, 2, and 3 ml) of 10% caffeine from four different post loaded aerogels (2, 2.5, 3, and 3.5 %) in the PBS at normal pH over 48 hours in the shaking incubator at 60 rpm and 37 °C. Results shown as mean ± SD, n= 3, significance found using a two-way ANOVA with a Tukey’s post-hoc test, * = P<0.05 ** = P<0.01, *** = P<0.001, **** = P<0.0001.

3.4 Discussion

In this chapter, agar aerogels were investigated for their potential as an implantable drug delivery system for post-surgical localised treatment of cancer. Agar aerogels were loaded with caffeine using two different methods. First, the conventional gelation process which is commonly known as the sol-gel method, followed by solvent extraction using freeze-drying or

known as lyophilization technique. Several preloaded aerogel formulations were prepared with increased agar (2, 2.5, 3, and 3.5% w/v) and caffeine (1, 5 and 10% w/v) loadings. Second, aerogels were prepared using the same sol-gel, freeze-drying methods and agar concentrations. Then, aerogels were post-loaded with caffeine. Different post-loaded aerogels were prepared with increased agar (2, 2.5, 3, and 3.5%) and increased caffeine loadings (1, 2, and 3 ml) of every caffeine concentration (1, 5, and 10% w/v). The aerogels were characterised for strength, porosity, swelling, drug content, as well as *in vitro* drug release.

The development of aerogels as a drug delivery system with appropriate mechanical properties and drug release profiles is of importance to achieve the required optimal therapeutic outcomes (Huang, Zuo et al. 2011, Matricardi, Di Meo et al. 2013, Yuan, Wang et al. 2018). In our study, the mechanical strength investigations conducted on agar aerogels showed a direct relationship between the agar concentration and their increased mechanical strength. Accordingly, the aerogels prepared using high agar concentration (3.5%) produced aerogels with improved mechanical properties, while those aerogels with a reduced mechanical strength were associated with a decreased agar concentration (2%). The improved mechanical properties associated with the higher agar concentrations resulted from the higher rates of crosslinking during the gelation process due to the increased hydrogen bonds between the interconnected agar chains. Correspondingly, thicker and stronger network that provided better mechanical features of the aerogel (Kin and Yaphe 1972, Deszczynski, Kasapis et al. 2003). However, the aerogels showed lower strength and more flexibility compared to the hydrogels due to the freeze-drying solvent extraction. The lyophilization phase in agar hydrogel drying eliminates the liquid/vapor interface inside the pores, avoiding the formation of capillary pressure, which collapses the

network. Consequently, without surface tension forces applied on the skeletal framework, hydrogel freeze drying process leaves the geometric dimensions of the water filled gaps unaffected, resulting in low-density aerogel network structure with high porosity and flexibility (Li, Yalcin et al. 2009). The caffeine increased loading into the aerogels significantly increased their physical strength, mainly at higher loadings. This is attributed to the increased caffeine accumulation with higher caffeine loadings within the aerogels network pores, which may results in higher aerogels density compared to the free aerogels and consequently increased mechanical strength (Buckley, Thorpe et al. 2009). In addition, the investigation of post-loading method into aerogels produced aerogels with significantly ($p < 0.05$) lower mechanical properties compared to free aerogels regardless their agar concentrations. Results have shown that the measured strength of the aerogels are significantly deteriorating upon injecting higher volumes into all aerogels. The reduction in the mechanical properties of post-loaded aerogels is mainly attributed to the rehydration of the aerogels network chains that corresponds with the disintegration of network structure and subsequently aerogel collapse (Nweke, Turmaine et al. 2017, Fabra, Talens-Perales et al. 2021). As a result, caffeine preloaded agar aerogels offer good mechanical strength based on the agar concentration and caffeine loading rate. Such improved mechanical properties are beneficial in the development of an implantable preloaded aerogels as a localised drug delivery system that will provide support and resistance to damage upon implantation. However, the post-loaded aerogels lack the increased mechanical features compared to preloaded aerogels under physical stress. In comparison to agar hydrogels, their freeze-dried aerogels may offer better access to core region and more efficient interactions with the aerogel matrix. Nevertheless, adjusting the aerogels polymeric components and the rate of crosslinking, could influence aerogels ability to control drug release or, in contrast, their ability

as drug diffusing enhancers (Alnaief, Antonyuk et al. 2012, Valo, Arola et al. 2013, Veronovski, Knez et al. 2013, Ulker and Erkey 2014). In addition, the adjustable porous flexible mechanical structure of aerogels could make them capable to be moulded into the cancer resection cavities based on the required implantation site to ensure good contact with the margin tissue. Also, aerogels could offer the option for drug loading method to be either preloaded during the formulation preparation or post-loaded after obtaining and implanting the formulation. The post loading method may offer better flexibility for the surgical team to load the required chemotherapeutic agent and dose upon implantation based on the histopathological evaluation following tumour resection.

The porosity and swelling ratios of the agar aerogels were investigated to identify the effect of increased agar concentration on aerogels porous structures and water retaining capabilities, since such features could influence their physical strength and drug release profiles from aerogel formulations (Veres, Kéri et al. 2017, Lázár, Forgács et al. 2020, Pantić, Horvat et al. 2020). Results showed that the aerogel porosity ratios were decreased as the agar concentration increased. The significant ($p < 0.05$) reduction in porosity was recorded between aerogels with increased agar concentration by at least 1%. There was no statistical significance found ($p > 0.05$) between aerogels upon increasing the agar concentrations by 0.5%. The reduction in the aerogels porosity ratios is mainly due to the higher nucleation rate and closer chain packing of the aerogel network associated with increasing the agar concentration (Narayanan, Xiong et al. 2006). Similarly, agar aerogels denoted non-significant ($p > 0.05$) reduction in their swelling rate while increasing agar concentration by 0.5% from 2 to 2.5% and/or 3 to 3.5%, but the significance ($p < 0.05$) was noticed while adjusting the agar concentration by at least 1%. This resulted from

the higher aerogels crosslinking rates as the agar concentration increase. Also, the presence of additional accumulating non-anhydrous moieties of agaropectin (non-gelling component of agar), could prevent the formation of conductive network structure for water absorption at certain crosslinking sites and thus limiting the swelling of aerogels with higher agar concentrations (Pourjavadi, Farhadpour et al. 2009, Bao, Hayashi et al. 2010, Bertasa, Dodero et al. 2020).

The caffeine content and distribution investigations were performed on all agar aerogels (2, 2.5, 3, and 3.5%) preloaded with caffeine (1, 5, and 10%). Results demonstrated that there are non-significant ($p>0.05$) differences between the aerogels caffeine contents as the drug loading and agar concentration increase. Generally, the aerogels with lower agar concentrations (2 and 2.5%) loaded with 1 and 5% caffeine demonstrated improved caffeine distribution between the aerogel different parts compared to higher agar aerogels (3 and 3.5%). However, most aerogels with higher caffeine loading (10%) showed variations in their caffeine content distributions between the different parts of the aerogel. The differences in content distribution can be related to the increased crosslinking density with higher agar concentrations, which will result in formation of more heterogenous network structure and consequently affecting drug homogeneity, especially with higher loadings (Liang, Xu et al. 2006). Also, high drug loading could affect drug homogeneity within aerogel formulations, and probably longer mixing time is required to obtain more homogenous dispersion due to the increased viscosity of the gel solutions. As a result, using lower agar concentrations (2 and 2.5%) and lower drug loadings (1 and 5%) are preferable to obtain preloaded aerogel with more homogenous drug distribution as an implantable drug delivery system.

The distribution of different post-loaded caffeine concentrations (1, 5, and 10%) in agar aerogels (2 and 2.5%) was investigated using Raman spectroscopy. Results illustrated that both agar aerogel samples with low caffeine loading (1%) demonstrated limited drug distribution, while better homogenous distribution was found in those with higher caffeine loadings (5 and 10%). This may suggest that post-loading method can be more efficient to achieve better homogeneity especially for higher drug loading rates. However, in order to develop homogenous agar aerogels as an implantable drug delivery system for post-surgical localised treatment of pancreatic cancer based on post-loading method, further investigations using higher agar aerogel concentrations, several volumes of different drug concentrations, and wider scanning regions are required to confirm these findings.

The release of caffeine from most preloaded aerogels showed a rapid 'burst' release during the first 6 hours for all drug loadings. As the caffeine loadings and agar concentrations increase the release of caffeine reduces within the first 3-6 hours with sustained release over the remaining 48 hours. The influence of increased caffeine loading, and agar concentration on the release profiles from preloaded aerogels was observed. This is referred to the several steps required for the caffeine release following their placement the preloaded aerogels in the release media. First, the hydration phase of the aerogel outer surface and adsorbed caffeine, followed by gradual penetration through the aerogel pores. Then, hydration of the aerogel network and the loaded caffeine within the core of the aerogel leading to caffeine desorption, dissolution and release (García-González, Sosnik et al. 2021). As a result, the release is governed by the rate of release media diffusion into the aerogels, and accordingly the caffeine diffusion through the network pores towards the release media. Therefore, the fast release from the aerogel is mainly referred

to caffeine hydrophilicity in addition to many factors, including the presence of drug molecules on the outer surface of aerogels that will dissolve rapidly. Also, the large open pores of the aerogels with lower agar concentrations will allow faster diffusion of lower caffeine loading (1%) that require shorter time to hydrate and dissolve (Pekarek, Jacob et al. 1993, Brazel and Peppas 1999, Han, Choi et al. 2013). In contrast, the significant slower sustained release profiles from preloaded aerogels were related to the reduced network pore sizes in higher aerogels agar concentrations (3 and 3.5%) and higher caffeine loading (5 and 10%) simultaneously. Consequently, slower hydration rate of the aerogels and the loaded highly concentrated caffeine molecules inside the formulations resulting in slower release profiles. Overall, these findings suggest that the drug release from preloaded aerogels is adjustable based on varying the aerogels agar concentrations and drug loadings. Also, they are able to release sufficient drug amount after 2 days upon using 2 and 2.5% agar aerogels and drug loadings 1 and 5%, while longer time is needed for higher drug loading (10%). However, the extremely fast burst release behaviour of 1% loading from 2 and 2.5% agar aerogels could be associated with unwanted side effects. The 3 and 3.5% agar aerogels relatively reduced the burst release effect of low drug loading, while high drug loading (10%) possibly require longer release time up to 4 or 5 days.

The release profiles from caffeine post-loaded aerogels were assessed and showed different release profiles over 48 hours. First, the increased volume of 1% caffeine post-loaded into the agar aerogels (2, 2.5, 3, and 3.5%) is directly related to the slower release from the aerogels. These results suggest that the release media were able to penetrate the aerogels and facilitate the release of different caffeine loadings successfully from the lower side in contact with the release media. Differently, 5% caffeine post-loaded aerogels expressed slow sustained release of 1 ml

caffeine in all formulation regardless their agar components, which implies that the remaining caffeine could be entrapped inside the networks. Nevertheless, as the aerogels agar concentrations increased, they demonstrated relatively slower release profiles of higher post-loaded volumes (2 and 3 ml) mainly within 6 hours of release. This occurred due to consecutive factors including the narrowed network pore sizes and the higher caffeine loadings that require longer time to be released. Upon loading different volumes of 10% caffeine, post-loaded aerogels (2 and 2.5%) demonstrated release profiles that are controlled by both increased volume loading and agar concentration. However, the increased agar concentrations in 3 and 3.5% post-loaded aerogels apparently have the principal role in reducing the release mainly within the first 6 hours compared to 2 and 2.5% aerogels, since there is no statistical significance ($p > 0.05$) in the release profiles of varied volumes within the same aerogel. Generally, post-loaded agar aerogels demonstrated their capability to reduce the release of increased volumes (1, 2, and 3 ml) of increased caffeine concentrations (1, 5, and 10%) within 6 hours as the agar concentration increased. However, the extended release profiles from the aerogels become less efficient with higher caffeine concentration (5%) and low loading volume (1 ml) which may have resulted from insufficient drug distribution or the reduced mechanical strength of the aerogels. As a result, the post-loaded aerogels with higher agar concentration and increased loading volume are promising for further investigations to be developed as an implantable drug delivery system for localised treatment of cancer.

One of the technologies that should be considered in future investigations during agar aerogel preparation is based on cryoprotection against ice crystals formation within the formulation upon placing agar hydrogel in -80°C freezer prior to the lyophilization process. During the

cooling process, the water molecules start to aggregate and aligned to form hydrogen bonds resulting in ice crystals formation, which could influence the hydrogel/aerogel network in terms of structural design and physical properties that could affect aerogels strength and porosity. Consequently, this might have an impact on the drug distribution and related to the change in the hydrogel and preloaded aerogel formulations drug homogeneity with increased drug loading to 10% and agar concentration (3 and 3.5%). Also, the change in the network structure and porosity design resulting from the ice crystal formation could have an influence on the release profiles behaviour as seen in post-loaded agar aerogels mainly. Therefore, different cryoprotection techniques during hydrogel preparation were developed in order to maintain and improve aerogels mechanical integrity as well as network structural design and porosity. One of the suggested methods is based on developing high-strength and fast self-healing hydrogel with an interpenetrating double network based on polyvinyl alcohol/agar-ethylene glycol (PVA/agar-EG) (Han, Li et al. 2020). The addition of EG during hydrogel preparation as a cryoprotectant agent and as a solvent with water prevents ice crystals formation at extremely low temperatures due to the hydrogen bonds formed between EG and H₂O that bind water molecules, which make it difficult for water molecules to aggregate and bind to each other. As a result, more stable hydrogel properties can be obtained for aerogel development with improved physical and internal structure that may result in enhanced homogenous drug distribution, as well as better controlled release profiles even with increased agar concentration and drug loading to achieve better implantable drug delivery systems for localised treatment of pancreatic cancer. However, further investigations are required to support and confirm that.

3.5 Conclusion

The caffeine loaded agar aerogels were developed using sol-gel and post-loading methods. The development and characterizations focused on several factors including the agar concentration used in aerogel preparation, caffeine loading rate, and loading method. 48 caffeine loaded aerogel formulations were prepared and characterized in terms of mechanical properties including their strength, porosity, and swelling ratio. Also, the content and distribution of caffeine loaded agar aerogels were studied. The effect of both agar concentration and caffeine loadings on the release profiles from pre- and post-loaded aerogels were investigated. The release profiles of caffeine from all aerogels showed an initial fast ‘burst’ release followed by sustained release. The release profiles and the mechanical characteristics were varied based on the agar concentrations of the aerogels, caffeine loading rates, and loading method. Four agar preloaded aerogels 2, 2.5, 3 and 3.5% with caffeine loading of 5% while 12 agar post-loaded aerogels 2, 2.5, 3 and 3.5% with drug loading of 1% of increased volume (1, 2, and 3ml) were chosen as the optimised formulations for additional studies based on their physical features, drug content distribution, as well as *in vitro* release profiles. Thereby, we assume that these optimised pre- and post-loaded agar aerogels should be examined as potential implantable drug delivery system for post-surgical localised treatment of cancer.

Chapter 4: Development and Optimization of Implantable Agar Hydrogels and Aerogels for The Localised Treatment of Pancreatic Cancer

4.1 Introduction

Irinotecan hydrochloride (IRN) is a camptothecin-derived chemotherapeutic drug, which was extracted from Chinese trees called *Camptotheca Acuminata* back in 1983 (Xu and Villalona-Calero 2002). IRN is a water soluble solid pale-yellow powder with a molecular weight of 586.689 g/mol, molecular formulation of $C_{33}H_{38}N_4O_6$ and melting point of 222-223°C. It is a potent DNA topoisomerase I inhibitor that acts by binding to topoisomerase I enzyme, which is an essential enzyme for DNA transcription, and forms IRN-topoisomerase I–DNA complex. This complex prevents the DNA strand ligation that lead to double-stranded DNA breakage and consequently cell death (Creemers, Lund et al. 1994, Bailly 2019).

The IRN is a common chemotherapeutic drug that has been widely used for different types of cancers like colorectal, small cell lung cancers, and glioma (Cunningham, Pyrhönen et al. 1998, Rothenberg 2001, Xu and Villalona-Calero 2002). Also, the IRN has been used as a part of the FOLFIRINOX regimen (IRN, 5-Fluorouracil, Leucovorin, and Oxaliplatin) for pancreatic cancers treatment (Suker, Beumer et al. 2016). However, it has been reported that IRN was associated with many side effects including febrile neutropenia, gastrointestinal toxicities, acute renal failure, as well as cardiovascular complication (Kweekel, Guchelaar et al. 2008, Huisman, de Bruijn et al. 2016). As a result, the development of alternative localized chemotherapy is

required to minimize such adverse reactions associated with systemic administration of chemotherapeutic agents like the IRN.

The improved physical features of agar hydrogels and the flexible aerogels structure may allow them to be prepared into varying designs while maintaining their structural integrity. This can be beneficial for both formulations to be moulded and implanted into the post-surgical tumour resection cavities as a localised chemotherapeutic drug delivery system, which could also be useful to achieve good contact with the tissue margins at the implantation site. Nevertheless, the open porous aerogels matrices provide the ability to preload and post-load the IRN upon formulation preparation or post aerogel preparation, respectively. This offers an ability to personalise or tailor the treatment at the point of implantation.

In this chapter, we will focus on the evaluation of agar hydrogels and aerogels encapsulating IRN. The main goals are to investigate the effect of varying the agar concentration (2, 2.5, 3 and 3.5%) with IRN loading (5%) on the mechanical properties of the agar hydrogels and aerogels, the IRN content distribution within the hydrogels and aerogels and *in vitro* drug release profiles, as well as aerogels cytotoxicity assessment using different pancreatic cancer cell lines.

4.2 Materials and methods

4.2.1 Materials

A polysaccharide complex Agar composed of 70 % agarose and 30 % agarpectin and porcine gastric mucin were purchased from Sigma Aldrich (UK). Irinotecan Hydrochloride was

purchased from LGM Pharma (Georgia, USA). Potassium dihydrogen orthophosphate and methanol 99% were purchased from VWR (Leicestershire, UK). Acetonitrile was purchased from Fisher Scientific (Leicestershire, UK).

4.2.2 Preparation of IRN-loaded agar hydrogels and aerogels

The preparation of the IRN-loaded agar hydrogels was performed using the same method as described earlier (Chapter 2, sections 2.2.2). Briefly, the appropriate amount (Table-4-1) of agar was dissolved in distilled water to prepare four different hydrogels with agar concentrations of 2, 2.5, 3 and 3.5 % (w/v). The final agar hydrogel formulations contained 5% w/v of IRN. IRN-loaded aerogel formulations (Table-4-2) were prepared using the same method described (Chapter 3, section 3.2.2). IRN post-loaded aerogels were prepared by injecting different volumes (1, 2, and 3 ml) using IRN stock solutions (1% w/v) (Table 4-3) to evaluate the effect of volume and loading method.

Table 4-1: Formulations of prepared IRN-loaded hydrogels

Hydrogel	Agar % w/v	IRN % w/v	hydrogel solution volume ml
1	2	5	5
2	2.5	5	5
3	3	5	5
4	3.5	5	5

Table 4-2: Formulations of prepared IRN-preloaded aerogels

Aerogel	Agar % w/v	IRN % w/v	hydrogel solution volume ml
1	2	5	5
2	2.5	5	5
3	3	5	5
4	3.5	5	5

Table 4-3: Formulations of prepared IRN post-loaded aerogels

Agar aerogel % w/v	IRN solution % w/v	Loading volume ml
2	1	1, 2, 3
2.5	1	1, 2, 3
3	1	1, 2, 3
3.5	1	1, 2, 3

4.2.3 Characterization of the IRN-loaded hydrogels and preloaded aerogels

4.2.3.1 IRN-loaded hydrogels and preloaded aerogels mechanical strength

The mechanical strength test was performed on the agar hydrogels and aerogels concentrations of 2 and 2.5% with 5% IRN loading. The mechanical strength was assessed using the methodology illustrated previously (Chapter 2, section 2.2.3.1).

4.2.3.2 IRN-loaded hydrogels mucoadhesive properties

The adhesive properties of unloaded and IRN-loaded agar hydrogels were assessed following the same procedures described earlier (Chapter 2, section 2.2.3.2).

4.2.3.3 IRN-loaded hydrogels rheology

Rheological investigations of IRN-loaded hydrogels to investigate the impact of increased agar concentration on their viscoelastic properties. Experiments were performed on the hydrogel formulations of 2, 2.5, 3, and 3.5% with 5% IRN loading. The rheological analysis was performed by using the same previous parameters (Chapter 2, section 2.2.3.3).

4.2.3.4 Raman mapping spectroscopy of IRN-preloaded aerogels

Raman spectroscopy investigations were performed to determine the spatial distribution of IRN within agar aerogels. The aerogels were investigated by collecting approximately 5 X 3 mm samples from the 2, 2.5, 3, and 3.5% aerogels loaded with 5% IRN. The investigation parameters were described earlier (Chapter 3, section 3.2.3.3). However, the measured areas were between 0.6 mm × 0.6 mm and 0.7 mm × 0.7 mm.

4.2.3.5 IRN content distribution in the agar hydrogel formulations

The IRN-loaded agar hydrogels were cut into three equal parts and placed in glass bottles containing 100 ml solution of 60:20:20 potassium di-hydrogen phosphate (KH_2PO_4), acetonitrile, and methanol under vigorous stirring overnight. Subsequently, vortexed to ensure

complete extraction of the IRN. 1 ml of each extraction solution was centrifuged at $2100 \times g$ for 15 minutes and filtered using a 0.45 μm membrane filter and analysed by HPLC.

4.2.4 In vitro release of the IRN from agar hydrogels, pre- and post-loaded aerogels

5.3 to 5.4 g of the IRN-loaded agar hydrogels and 0.4 to 0.5 g of the IRN-loaded agar aerogels (dependent on their agar and water contents) were placed into a glass bottle containing 200 ml of deionized water (pH 6.5). The IRN post-loaded aerogels were fixed to one side so that they remained in floating position in plastic tubes containing 50 ml of deionized water (pH 6.5) and placed in an orbital shaking incubator at 37°C and 60 rpm. At time intervals of 0, 0.5, 1, 2, 3, 6, 24, 48, 72, and 96 hours, a 1 ml sample was collected, replaced with 1 ml of fresh deionized water, and subsequently stored at 4°C until analysed by HPLC. The release study was conducted in triplicate and the percentage of cumulative released IRN calculated relative to the maximum loaded IRN.

4.2.5 HPLC analysis

4.2.5.1 HPLC chromatographic conditions

IRN was analysed using an Agilent HPLC System (Agilent Technologies 1260 infinity II, Santa Clara, California, United States) equipped with a quadratic pump and autosampler. The separation was performed using a Thermo Scientific® 5 μm , C18 analytical HPLC column (150 mm *4.6 cm) at 25°C with a mobile phase of solution mixture consists of 60:20:20 potassium di-hydrogen phosphate (KH_2PO_4), acetonitrile, and methanol. The mobile phase pH was

adjusted to 3.0 using phosphoric acid and a flow rate of 1 ml/min was used. An injection volume of 10 μ l and run time of 10 min was used, with UV detection conducted at a wavelength of 265nm.

4.2.5.2 Stock solution and calibration curve

5 mg of IRN was transferred into a 10 ml volumetric flask and dissolved in acetonitrile to produce a stock solution with a final concentration of 0.5 mg/ml. The stock solution was then used to prepare standard solutions with concentrations of 0.001, 0.005, 0.01, 0.05, 0.1, and 0.5 mg/ml. The calibration curve was prepared by plotting the area under the curve versus the concentration. All measurements were conducted in triplicate

4.2.6 Cytotoxicity of the IRN pre- and post-loaded agar aerogels against MIA PaCa-2 and Panc-1 cells

The cytotoxicity studies were performed by Bladder Cancer Research Centre at the University of Birmingham. The MIA PaCa-2 and PANC-1 cell lines were maintained under culture with Dulbecco's Modified Eagle's Medium (DMEM) (VWR) supplemented with fetal bovine serum (FBS) (VWR) to a final concentration of 10% (v/v), at 37 °C and in a 5% CO₂ atmosphere. In the case of MIA PaCa-2, horse serum (HS) (VWR) to a final concentration of 2.5% was also added. Every 2–3 days the cells were passaged using trypsinization for cells to detach in order to maintain them in culture. At passage number 20 the cells were plated onto 6-well flat-bottomed plates and cultured in the presence of 3 mL of cell culture media. The 5% IRN pre-loaded aerogels (250 mg) and post-loaded aerogels with increased volume of 1% IRN (1, 2, and 3ml) (16.4, 32.8, and 49.2 mg) were placed into the centre of the 6-well plate. The aerogels were

sprayed with 70% ethanol for sterilization. The study was designed so that MTT assays could be performed on the cells at 0, 1, 3, 6, 24, 48, 72 and 96 hours. 1ml of the MTT solution (0.50 mg/mL) of 3-(4,5-Dimethylthiazol-2-yl)-2,5-Diphenyltetrazolium Bromide per ml of PBS was added to each well and the plates incubated for 3 h. The aerogels were removed before the addition of MTT reagent to the cells. The absorbance of untreated, negative controls (0% IRN aerogels), as well as treated cells was measured at 570 nm. The cell viability was calculated by a percentage of absorbance of the negative control and treated cells to the untreated cells and expressed as percentage of the cell viability. All experiments were performed in triplicate using separate batches of every formulation.

4.2.7 Statistical analysis

Statistical analysis was performed using a one-way or two-ways analysis of variance dependent on the presence of one variable or two independent variables respectively (ANOVA) (GraphPad Prism version 9.0.2 for MacOS, GraphPad Software, San Diego, CA). Post-hoc comparisons of the means were performed using Tukey's Honestly Significance Difference test. A significance level of $p < 0.05$ was accepted to denote significance in all cases.

4.3 Results

4.3.1 IRN-loaded hydrogels and preloaded aerogels mechanical properties.

The mechanical strength analysis demonstrated the effect of the increased agar concentrations in both hydrogels and aerogels with 5% IRN loading on their increased mechanical strength. Results in Figure 4-1 demonstrated that the measured mechanical strength

increased significantly ($p < 0.05$) from $2338.3 \pm 301 \text{ g/cm}^2$ for the 2% agar aerogel to $3055.1 \pm 229 \text{ g/cm}^2$ with the 2.5% agar aerogel, while the 2 and 2.5% agar hydrogels showed a significant increase in their physical strength increasing from 3267.9 ± 339.7 to $4970 \pm 459.3 \text{ g/cm}^2$, respectively. The IRN-loaded agar hydrogel formulations demonstrated stronger mechanical properties compared to the IRN-loaded aerogels. Moreover, the IRN-loaded agar hydrogels expressed weak adhesive properties, which reduced significantly as the agar concentration increased (Figure 4-2).

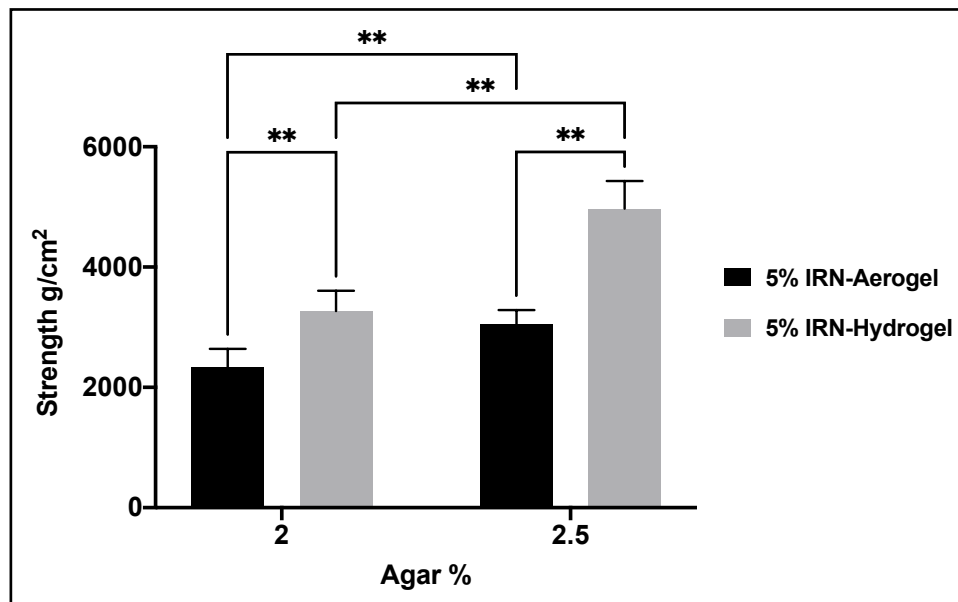


Figure 4-1: Effect of different agar concentrations (2 and 2.5%) and IRN loading (5%) on hydrogels and aerogels mechanical strength. Results shown as mean \pm SD, $n = 3$, significance found using a two-way ANOVA with a Tukey's post-hoc test, * = $P < 0.05$ ** = $P < 0.01$, *** = $P < 0.001$, **** = $P < 0.0001$

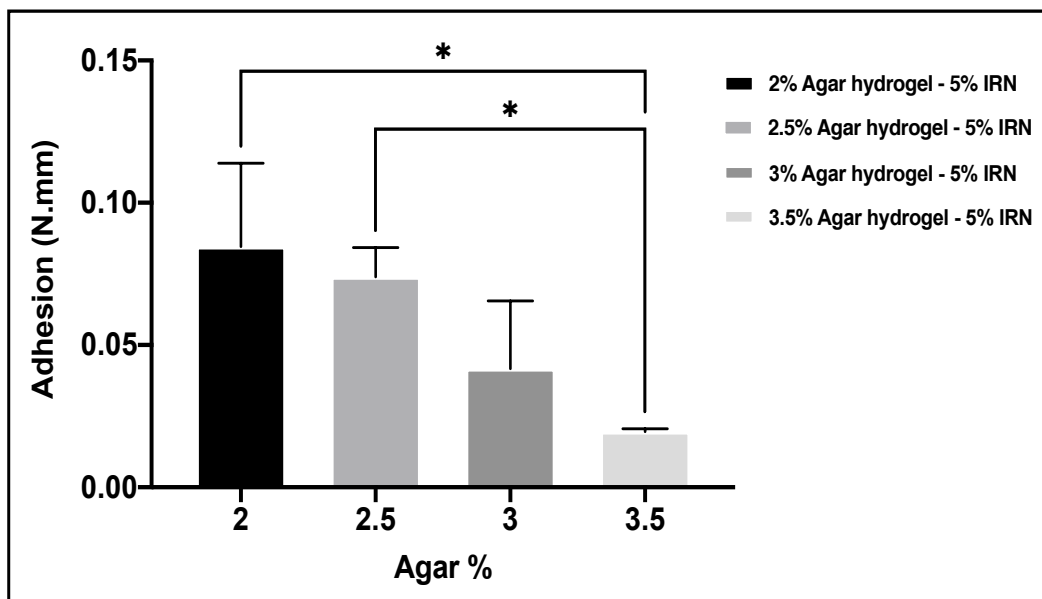


Figure 4-2: Effect of different agar concentrations (2, 2.5, 3, and 3.5%) and IRN loading (5%) on hydrogels adhesive properties. Results shown as mean \pm SD, n= 3, significance found using a one-way ANOVA with a Tukey’s post-hoc test, * = P<0.05 ** = P<0.01, *** = P<0.001, **** = P<0.0001.

4.3.2 IRN-loaded hydrogel rheology

The rheological behaviour of the agar hydrogels with varying agar concentrations and 5% IRN loading is described in Figure 4-3. The influence of the agar concentration in on their elastic modulus G' and viscous modulus G'' upon applying shear strain is demonstrated in Figure 4-3 A. The IRN-loaded hydrogel formulations with higher agar concentration resulted in higher elastic moduli, a reduction of the LVER, and a decrease in their yield strain, which represents their ability to maintain their physical stability at lower shear strain before being deconstructed at higher shear strain. Figure 4-3 B represents the rheological properties based on the frequency sweep of the different IRN-loaded agar hydrogels across the frequency range. The IRN-loaded hydrogels with higher agar concentrations demonstrated a higher G' compared to G'' , thus suggesting improved mechanical properties of the hydrogels.

4.3.3 Raman mapping spectroscopy of IRN-preloaded aerogels

The distribution Raman maps of the agar aerogels (2, 2.5, 3, and 3.5%) preloaded with 5% IRN are presented in figure 4-4. The reference Raman spectra of the pure IRN is illustrated in figure 4-5. The IRN distribution is highlighted using the following colour scheme; no IRN (Blue), low IRN distribution (Green), medium IRN distribution (Yellow) and high IRN distribution (Red). Results showed that the IRN distribution within the aerogel varied based on the agar concentration. The lower agar concentration corresponds to higher distribution of the IRN within aerogels. This is demonstrated by the significant levels of red (high IRN distribution) in both the 2 and 2.5% agar aerogels, while for the 3 and 3.5% aerogel the red disappears and there is an increase in yellow (medium IRN distribution), green (low IRN distribution), and blue (no IRN).

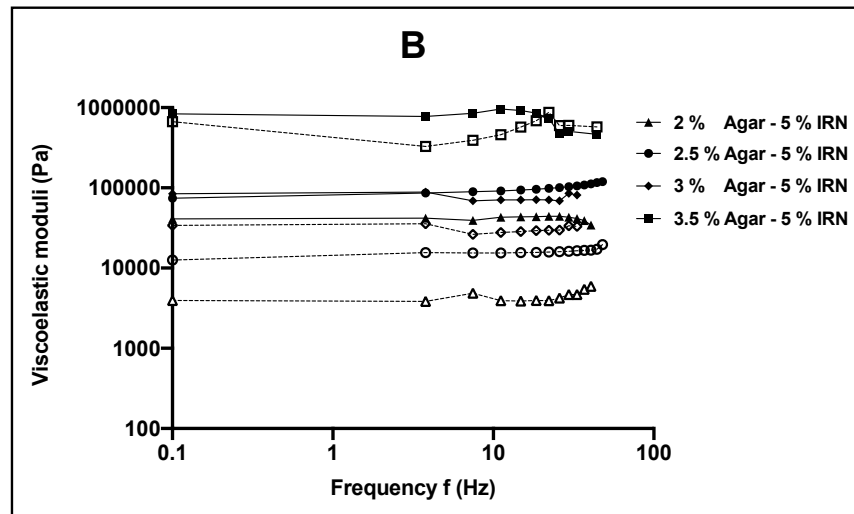
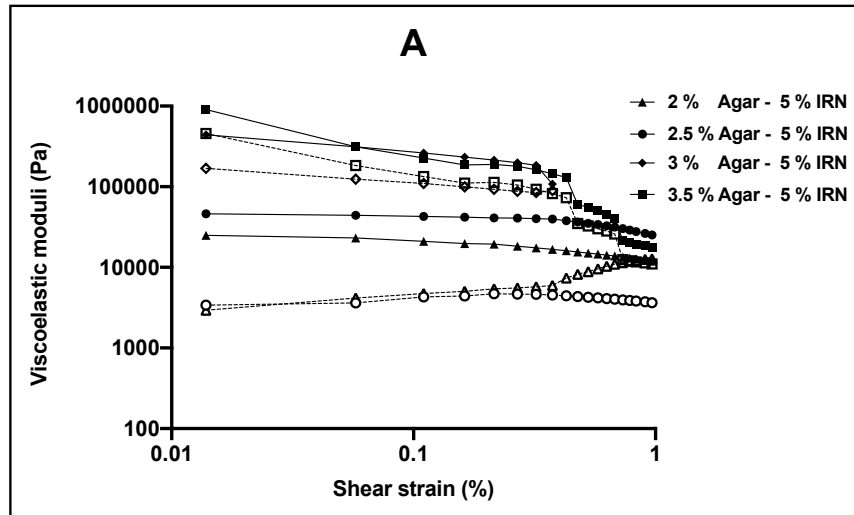


Figure 4-3: (A) Amplitude sweep, (B) Frequency sweep of different agar hydrogel concentrations (2, 2.5, 3, and 3.5%) with 5% IRN loading. Solid and empty points represent the storage (elastic) modulus G' and the loss (viscous) modulus G'' , respectively.

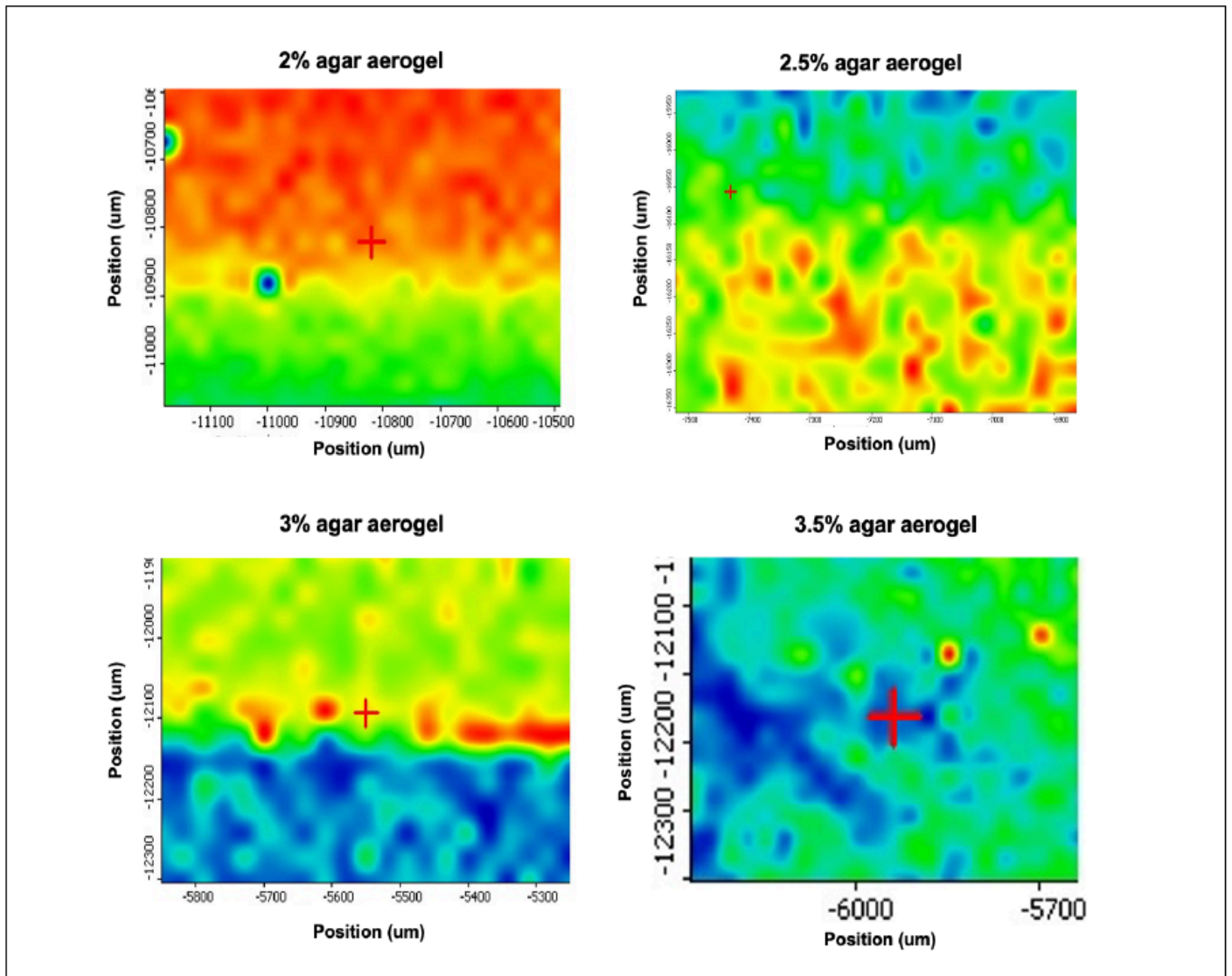


Figure 4-4: The distribution maps of agar aerogels 2, 2.5, 3, and 3.5% loaded with 5% IRN.

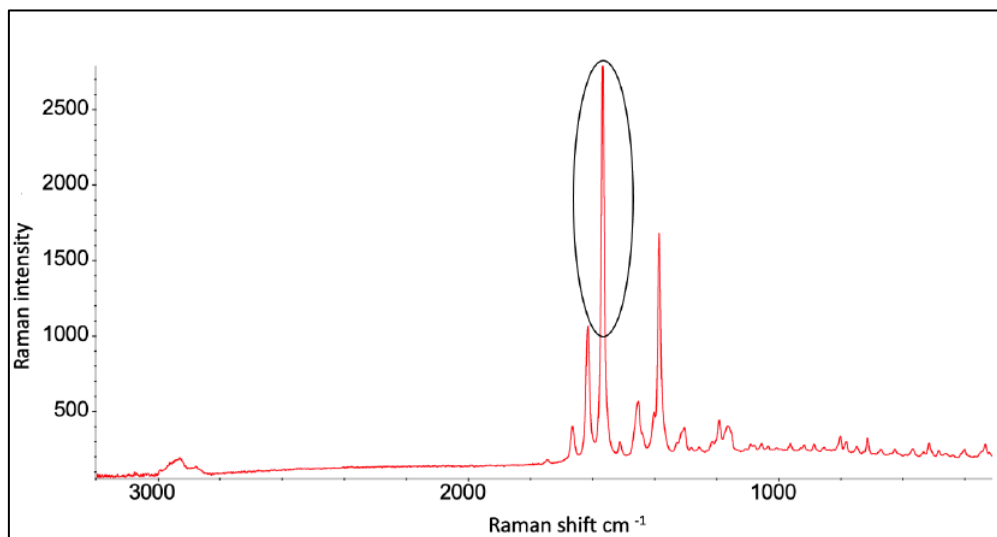


Figure 4-5: The reference Raman spectra of the pure IRN

4.3.4 IRN HPLC analysis

The IRN standard curve is described in Figure 4-6 at 6 different concentrations of IRN quantified by HPLC. The correlation between the IRN concentrations and the HPLC area under the curve AUC was excellent with the R value at 0.99 from 0.001 to 0.5 mg/ml. The retention time was approximately 4.6 minutes (Figure 4-7).

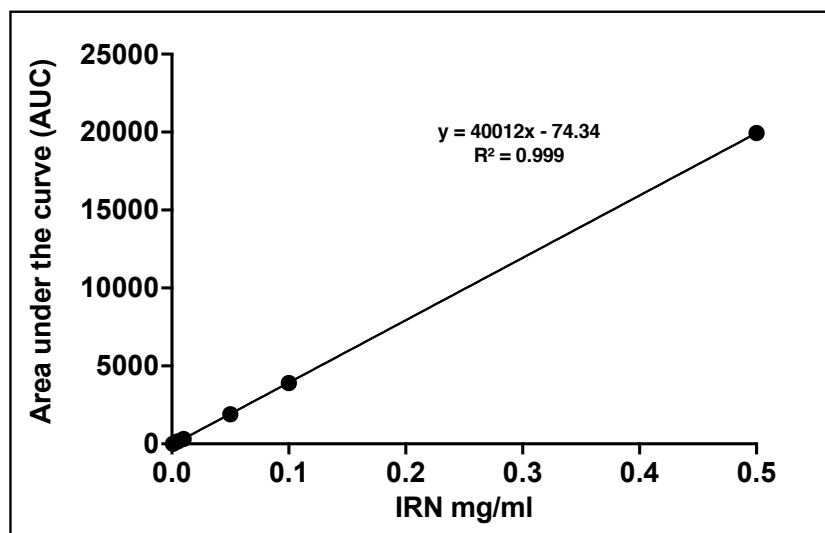


Figure 4-6: Standard curve for IRN using HPLC (n=3).

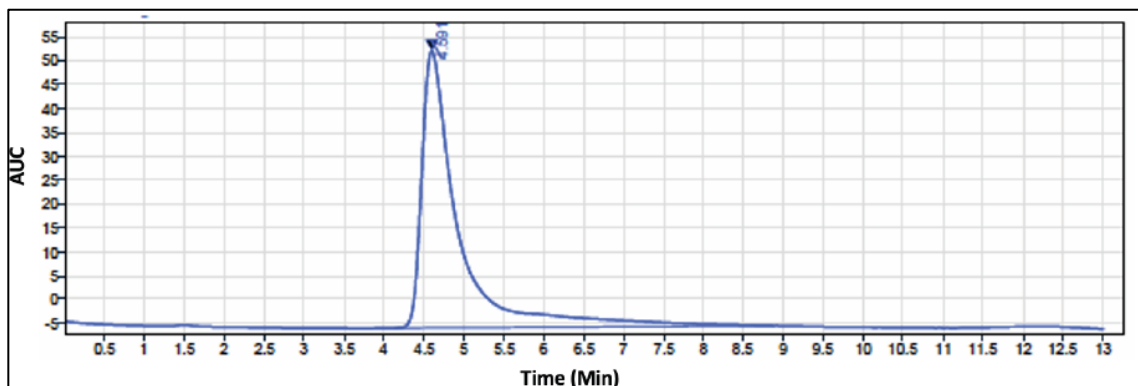


Figure 4-7: The HPLC chromatogram depicting the peak of IRN at 265 nm wavelength.

4.3.5 IRN content distribution in the agar hydrogel formulations

The IRN distribution in agar hydrogels (2, 2.5, 3, and 3.5%) loaded with 5% IRN was investigated. Figure 4-8 demonstrates that the IRN-loaded hydrogels showed a non-significant ($p < 0.05$) difference in their IRN content as the agar concentration of the hydrogels increased. Furthermore, increased variation in the IRN distribution between the different parts of the hydrogels was observed with increasing agar concentration. The 2, 2.5, 3, and 3.5% agar hydrogels demonstrated IRN contents of 96.7 ± 6.2 , 98.3 ± 10.6 , 95.8 ± 16.9 , and $91.6 \pm 20.4\%$ respectively.

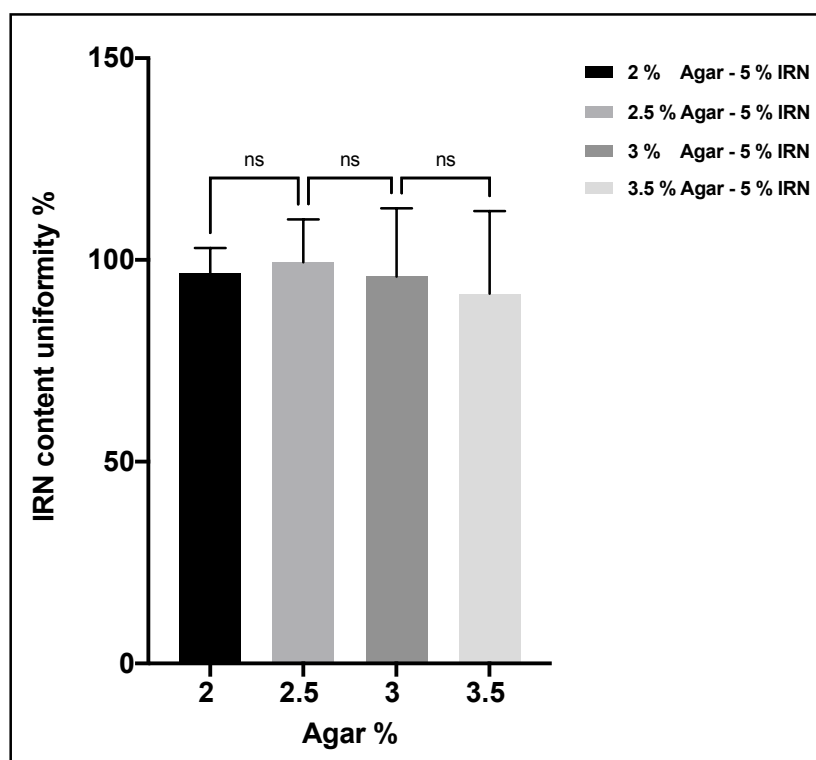


Figure 4-8: IRN content distribution in four different hydrogels 2, 2.5, 3, and 3.5% loaded with 5% IRN. Results shown as mean \pm SD, significance found using a one-way ANOVA with a Tukey's post-hoc test, * = $P < 0.05$ ** = $P < 0.01$, *** = $P < 0.001$, **** = $P < 0.0001$.

4.3.6 In vitro release of IRN from the agar hydrogels, pre- and post-loaded aerogels

The release of IRN from the agar hydrogel and aerogel formulations was performed in H₂O (pH 6.5) at 37°C. The percentage cumulative release profiles for IRN-loaded hydrogels and preloaded aerogels varied based on their increased agar concentration (Figure 4-9). The IRN showed a biphasic release profile over the 96 hours from both hydrogels and aerogels. Initially, a rapid 'burst' release was observed, followed by the second phase of release that provided a slower release after 6 hours as the agar concentration increased in both hydrogels and aerogels, which provided slower sustained release up to 96 hours. Within six hours, all loaded hydrogels

demonstrated relatively similar release profiles (Figure 4-9 A). Subsequently, the 2 and 2.5% agar hydrogels demonstrated faster release profiles by releasing nearly 80% of their loaded IRN after 96 hours with no significant ($p>0.05$) differences between both formulations, while the 3 and 3.5% agar hydrogels provided significantly ($p<0.05$) slower release by releasing 54.7 ± 4.5 and $48.5 \pm 3.9\%$ of their IRN contents, respectively within the same time frame. The 2% agar preloaded aerogel presented similar percentage cumulative release to 2% agar hydrogel at 96 hours, while 2.5% preloaded aerogel demonstrated significantly ($p<0.05$) slower release compared to 2% aerogel and released $72.4 \pm 5.2\%$ of its IRN content after 96 hours (Figure 4-9 B). In contrast, both 3 and 3.5% agar preloaded aerogels demonstrated slower burst release with no statistical significance between both formulations, while after 96 hours they released approximately 75.3 ± 10.6 and $71.4 \pm 9.5\%$ of their IRN content, respectively. The percentage cumulative release profiles for different post-loaded volumes (1, 2, and 3 ml) of 1% IRN from agar aerogels are presented in Figure 4-10. The IRN showed almost similar release profiles over the 96 hours from different post-loaded agar aerogels. Within six hours, a similar slow release behaviour of IRN was observed from all agar aerogels (2, 2.5, 3, and 3.5%), followed by increased sustained release with the increased post-loading volumes (1, 2, and 3 ml) of 1% IRN.

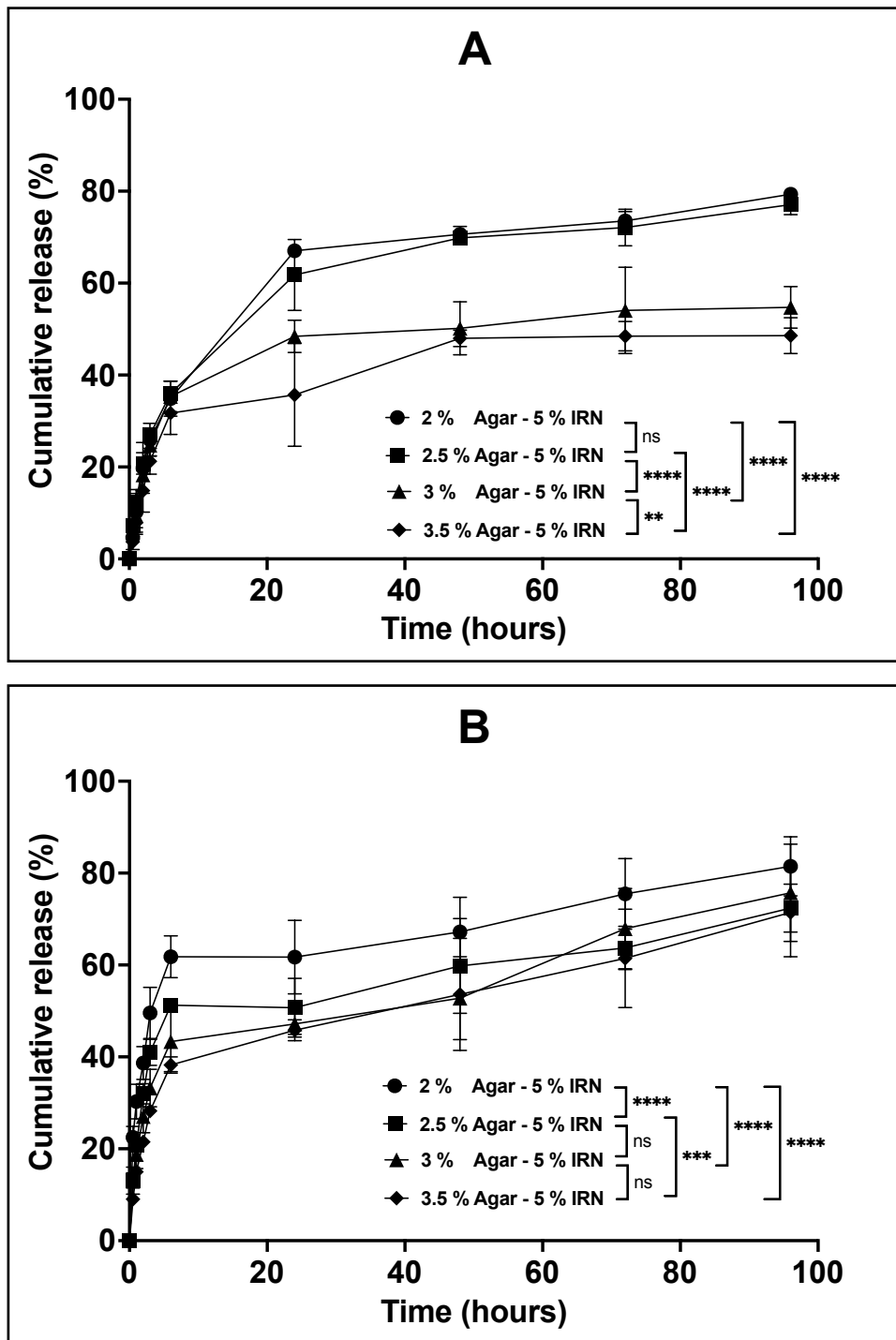


Figure 4-9: *In vitro* cumulative release profiles of 5% IRN from four hydrogels 2, 2.5, 3, and 3.5% (A), and four aerogels 2, 2.5, 3, and 3.5% (B) in water at pH 6.5 over 96 hours in the shaking incubator at 60 rpm and 37°C. Results shown as mean ± SD, n= 3, significance found using a two-way ANOVA with a Tukey's post-hoc test, * = P<0.05 ** = P<0.01, *** = P<0.001, **** = P<0.0001.

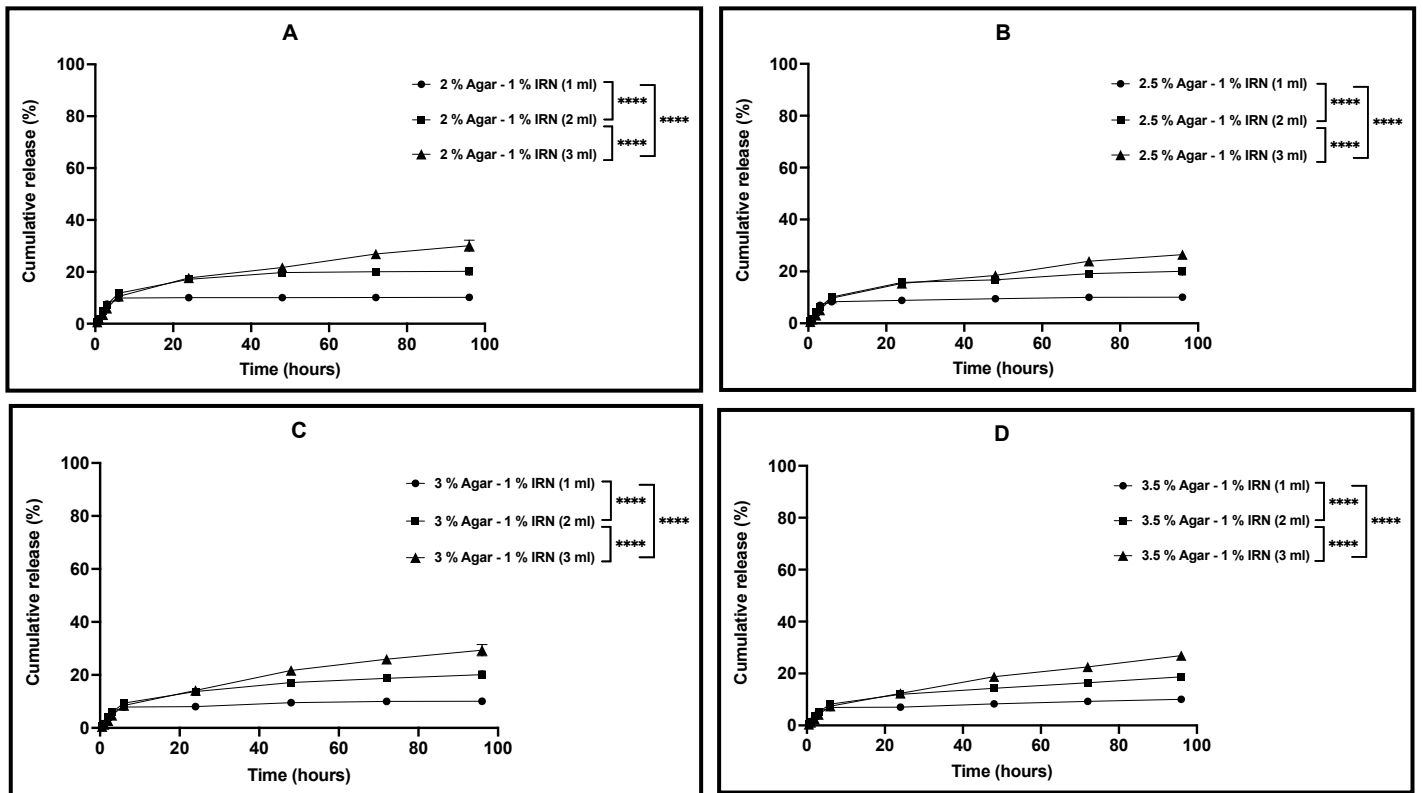


Figure 4-10: *In vitro* cumulative release profiles of different volumes (1, 2, and 3 ml) of 1% IRN from four different post-loaded agar aerogels (2, 2.5, 3, and 3.5%) in water at pH 6.5 over 96 hours in the shaking incubator at 60 rpm and 37°C. Results shown as mean \pm SD, n= 3, significance found using a two-way ANOVA with a Tukey's post-hoc test, * = P<0.05 ** = P<0.01, *** = P<0.001, **** = P<0.0001.

4.3.7 Cytotoxicity of the IRN-preloaded agar aerogels against MIA PaCa-2 and Panc-1 cells

The cytotoxicity evaluation of different agar aerogels (2, 2.5, 3, and 3.5%) preloaded with 5% IRN against MIA PaCa-2 and Panc-1 cells over 96 hours of treatment is presented in Figure 4-11. In MIA PaCa-2 cells, the IRN-preloaded aerogels demonstrated a significant ($p<0.05$) reduction in the cell viability with decreased agar concentration. The preloaded agar aerogels 2, 2.5, 3, and 3.5% achieved a cell viability of 37.7 ± 2.6 , 47.9 ± 3.4 , 53.1 ± 3.7 , and

60.4 ± 4.2% within six hours of treatment respectively, while after 96 hours of treatment they showed a cell viability of 19.7 ± 1.6% for 2% agar preloaded aerogel and about 27% for the rest IRN-preloaded aerogels (Figure 4-11 A). Comparably, the effect of IRN-preloaded agar aerogels was stronger on the Panc-1 cells viability (Figure 4-11 B). The 2 and 2.5% agar preloaded aerogels achieved lowest cell viability of 16.6 ± 1.1 and 44.5 ± 2% respectively after one hour of treatment and eliminated most of the Panc-1 cells post three hours treatment with a significant ($p < 0.05$) difference between both formulations. However, the 3 and 3.5% agar preloaded aerogels demonstrated higher cell viability of 61.1 ± 3.4 and 75 ± 3.5% within one hour treatment, while they required longer time to achieve almost complete eradication of the Panc-1 cells up to six hours after treatment.

4.3.8 Cytotoxicity of the IRN post-loaded agar aerogels against MIA PaCa-2 and Panc-1 cells

The cytotoxicity assay of different agar aerogels (2, 2.5, 3, and 3.5%) post-loaded with different volumes (1, 2, and 3 ml) of 1% IRN against MIA PaCa-2 and Panc-1 cells over 96 hours of treatment is presented in Figures 4-12 and 4-13. Results demonstrated that the rate of reduction in the MIA PaCa-2 cell viability is directly related to the agar and IRN loading concentrations simultaneously. The 1 ml post-loaded aerogels showed faster reduction in the cell viability with the lower agar aerogels concentrations (2 and 2.5%) (Figures 4-12 A and B), while slower reduced cell viability was associated with the post-loaded aerogels of higher agar concentrations (3 and 3.5%) (Figures 4-12 C and D). Subsequently, all agar aerogel formulations post-loaded with 1 ml of 1% IRN achieved significantly ($p < 0.05$) reduced cell viability around

60% after 96 hours treatment compared to untreated cells. Furthermore, the increased IRN post-loading (2 ml) into agar aerogels resulted in lower cell viability with varying reduction rates over the treatment duration based on the agar concentration. The 2, 2.5, 3, and 3.5% agar post-loaded aerogels achieved cell viability of 15.8 ± 0.3 , 16.5 ± 0.31 , 16.25 ± 0.3 , and $22 \pm 0.4\%$ after 96 hours treatment, respectively. As the IRN post-loading increased to 3 ml, the lowest cell viability (0%) was obtained with the 2, 2.5, and 3% agar aerogels post 72 hours treatment, while 3.5% agar post-loaded aerogels had a cell viability of $6.5 \pm .16\%$ within the same time frame.

In the Panc-1 cells, the 2 and 2.5% agar aerogels post-loaded with increased volumes (1, 2, and 3 ml) of 1% IRN resulted in almost complete cell death with non-significant ($p > 0.05$) between the formulations within 24 hours of treatment (Figures 4-13 A and B). However, the 3 and 3.5% agar aerogels post-loaded with 1 ml of 1% IRN resulted in significantly ($p < 0.05$) higher cell viability of 10.6 ± 1 and $21.8 \pm 1.5\%$, respectively compared to the same agar aerogels post-loaded with 2 and 3 ml of 1% IRN eliminated most of the cells following 24 hours treatment (Figures 4-13 C and D).

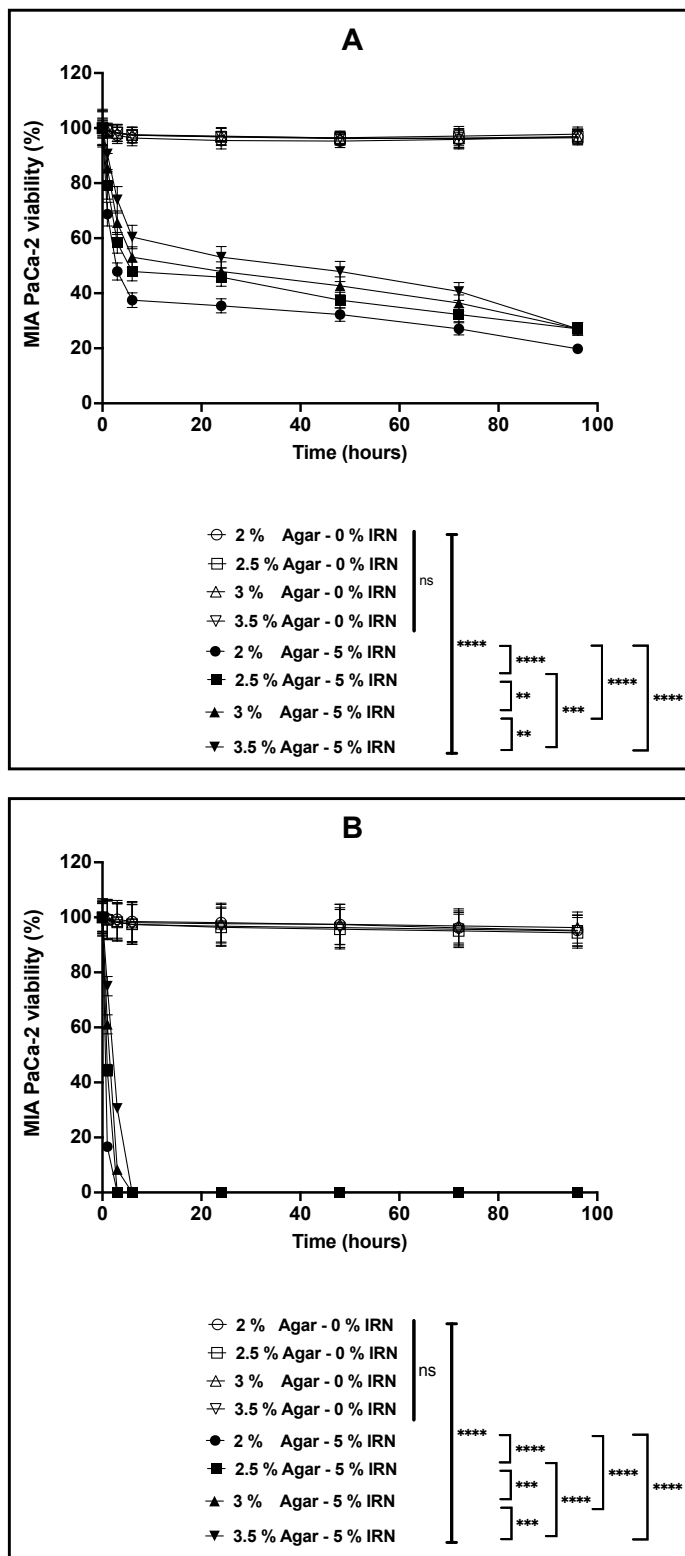


Figure 4-11: Viability of MIA PaCa-2 cells cultured with 5% IRN-preloaded aerogels using different agar concentrations (2, 2.5, 3, and 3.5%) (A). Viability of Panc-1 cells cultured with 5% IRN-preloaded aerogels using different agar concentrations (2, 2.5, 3, and 3.5%) (B). Results shown as mean \pm SD, n=3, significance found using a 2way ANOVA with a Tukey's post-hoc test, * = P<0.05 ** = P<0.01, *** = P<0.001, **** = P<0.0001.

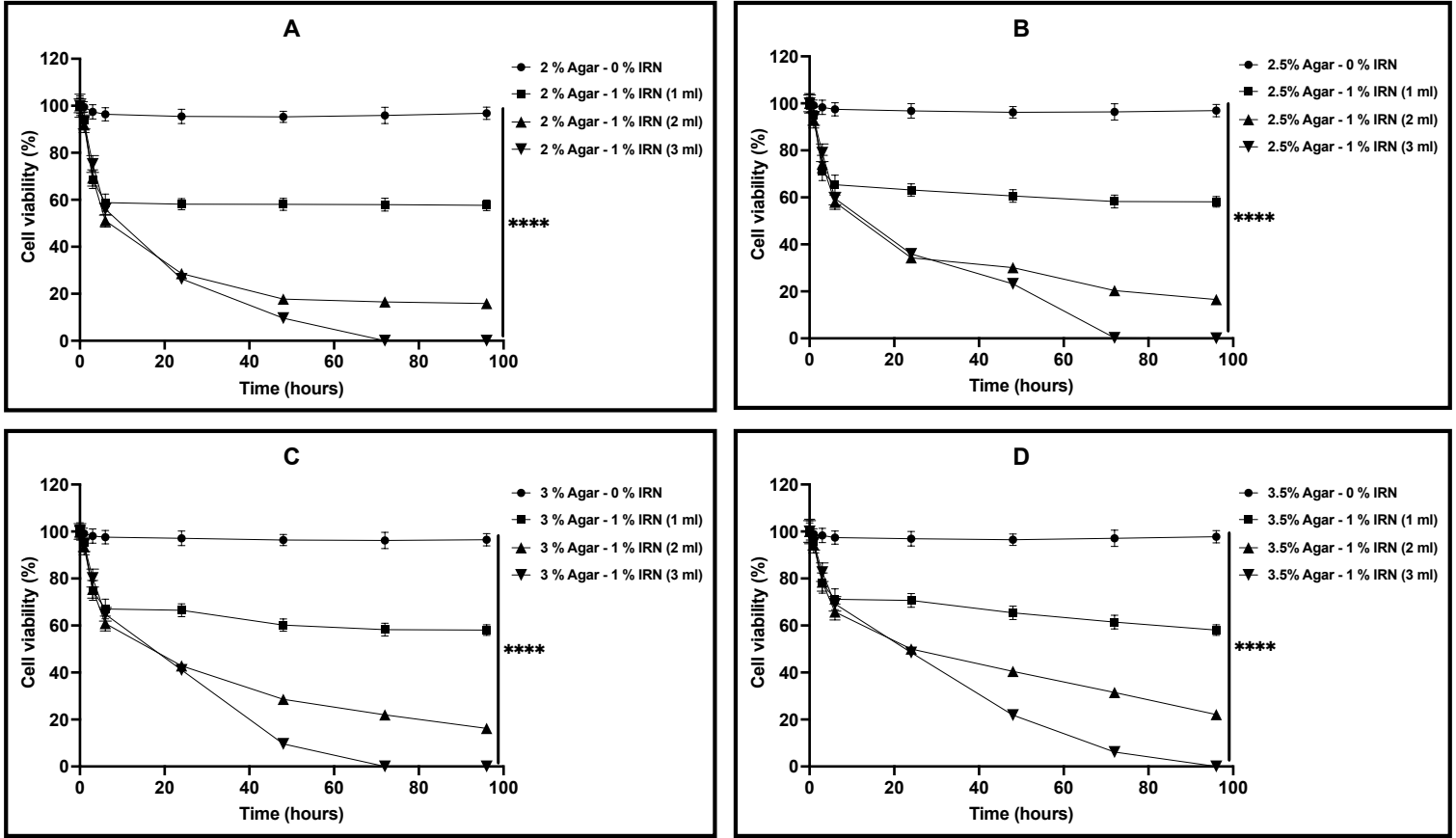


Figure 4-12: Viability of MIA PaCa-2 cells cultured with four different agar aerogels (2, 2.5, 3, and 3.5%) post-loaded with different volumes (1, 2, and 3 ml) of 1% IRN using over 96 hours. Results shown as mean \pm SD, n= 3, significance found using a two-way ANOVA with a Tukey's post-hoc test, * = P<0.05 ** = P<0.01, *** = P<0.001, **** = P<0.0001.

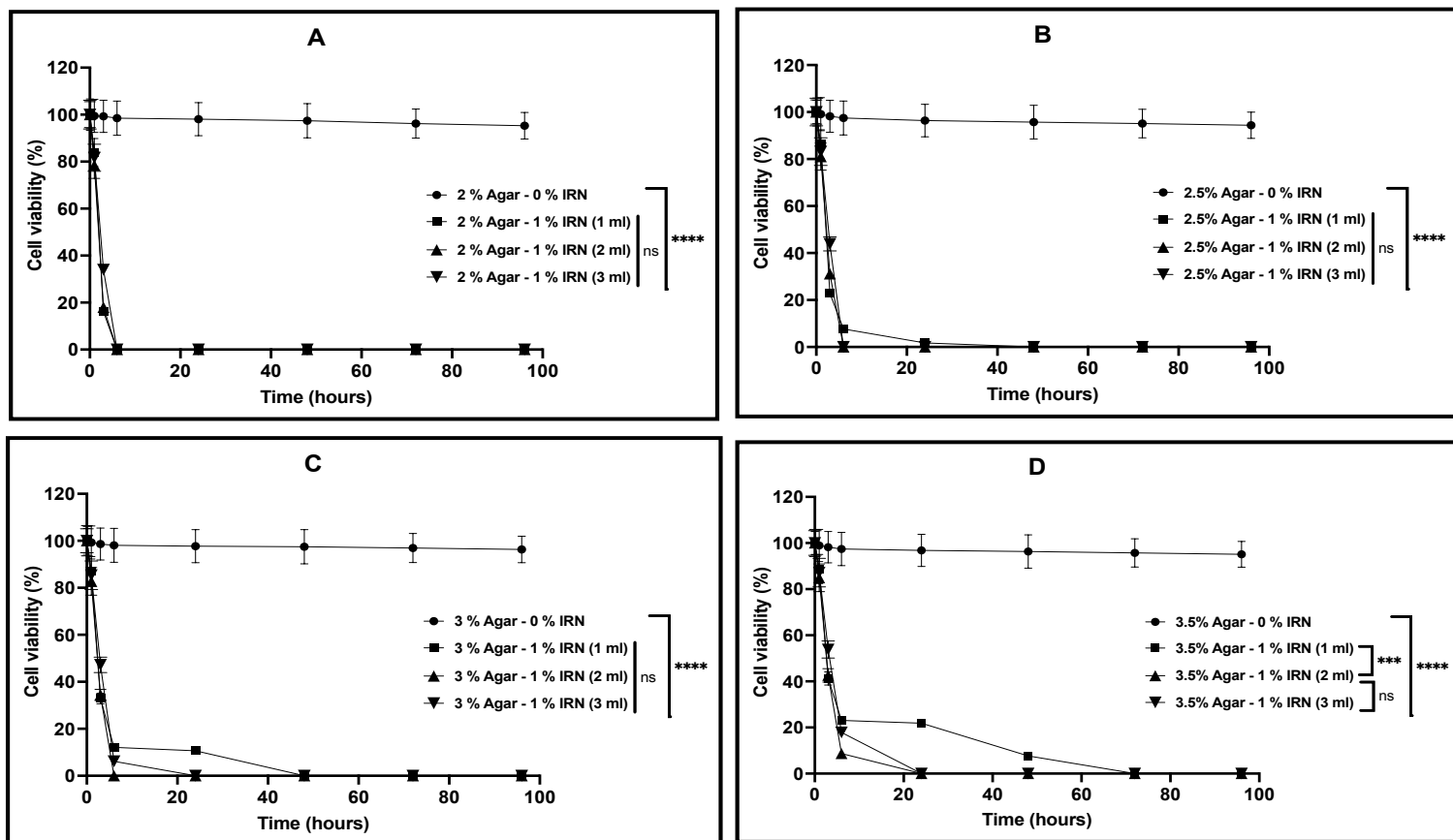


Figure 4-13: Viability of Panc-1 cells cultured with four different agar aerogels (2, 2.5, 3, and 3.5%) post-loaded with different volumes (1, 2, and 3 ml) of 1% IRN using over 96 hours. Results shown as mean \pm SD, n=3, significance found using a two-way ANOVA with a Tukey's post-hoc test, * = $P < 0.05$ ** = $P < 0.01$, *** = $P < 0.001$, **** = $P < 0.0001$.

4.4 Discussion

In this chapter, the agar hydrogels and aerogels were investigated as potential implantable drug delivery systems for post-surgical localised pancreatic cancer treatment. The agar hydrogels and aerogels were loaded with IRN using the sol-gel and post-loading methods. Several hydrogel and preloaded aerogel formulations were prepared with increased agar concentration 2, 2.5, 3, and 3.5% w/v, and IRN loading of 5% w/v, while post-loaded aerogels

were prepared using the similar increased agar concentration and loaded with different volumes (1, 2, and 3 ml) of 1% IRN. Hydrogels and aerogels were characterised for their mechanical properties, drug content, *in vitro* drug release.

The IRN-loaded hydrogels and preloaded aerogels mechanical strength data demonstrated that their increased mechanical strength is directly related to the increased agar concentration. This is due to the formation of higher intermolecular hydrogen bonds between the agar polymeric chains that form the double helical structures, which accumulate into thick swollen bundles and subsequently a stronger interconnected hydrogel network (Aymard, Martin et al. 2001, Xiong, Narayanan et al. 2005). Nevertheless, the IRN-preloaded agar aerogels were more flexible, with a lower mechanical strength due to the removal of water via lyophilization. As a result, a more flexible open porous network structure was obtained. Also, the IRN loading into the agar hydrogels and aerogels increased their mechanical strength. This can be attributed to IRN accumulation within the hydrogels network promoting a higher interpolymeric density, which results in a higher mechanical strength (Buckley, Thorpe et al. 2009, de Vries, Wesseling et al. 2017). Furthermore, the superiority of the elastic properties of the IRN-loaded hydrogels was also related to an increase in the agar concentration of the hydrogels, due to the presence of an increased amount of agar anhydrous units that enhance the elastic properties by increasing the number of crosslinking points within the hydrogel network (Bertasa, Dodero et al. 2020). In addition, the loaded drug may compete with the agar polymeric chains for water to form hydrogen bonds, which results in lower agar polymer hydrogen bonds with water causing increased interpolymeric bonding between agar chains. Consequently, more packed and reduced swelling network leading to highly elastic formulation (François, Rojas et al. 2005). Such

behaviour can be more dominant with IRN compared to caffeine. This is due to the presence of eight hydrogen bond acceptors for IRN, while caffeine has only three. The impact of drug loading on the hydrogel formulations mechanical strength is relatively lower compared to the increased agar concentration. However, an increased drug loading could have an influence on the hydrogel formulations mechanical properties as in 10% caffeine loading. Improved physical characteristics are useful for the development of an implantable hydrogel as a localised drug delivery system that will provide support and resistance to damage upon implantation. Also, such mechanical features will facilitate developing agar hydrogel desired shapes and sizes while maintaining their physical stability.

The IRN-loaded agar hydrogels demonstrated weak adhesion, which further reduced with higher agar concentrations. These findings are due to the strongly crosslinked solid agar hydrogels that do not provide liquid like properties required for essential molecular contact with mucin. Furthermore, the increased surface roughness produced by coil-like helical bundles that build up in the hydrogel network and the mechanical strength of the IRN-loaded hydrogels associated with higher agar concentrations increase the hydrogels surface resistance to deform needed to achieve sufficient contact with the mucin disc, and subsequently resulting in limited adhesive properties (Zosel 1989, Grillet, Wyatt et al. 2012, Rudge, Scholten et al. 2020). Therefore, improving the mucoadhesive properties of the agar hydrogels needs to be extensively investigated to promote their application as an implantable drug delivery system for post-surgical localised cancer chemotherapy. One of the reported techniques to improve agar hydrogel adhesive properties is based on the development of physically crosslinked synergistic double network hydrogel using agar and poly(*N*-acryloylaminoethoxyethanol) (PAAEE). The

PAAEE offers better hydrogel adhesive properties to both hard surfaces and soft tissues through improved hydrogen bonding and Vander der Waals interactions (Zhang, Ren et al. 2019).

The distribution of IRN within the agar preloaded aerogels (2, 2.5, 3, and 3.5%) was investigated using Raman spectroscopy. Results showed that aerogels with low agar concentration (2 and 2.5%) demonstrated better IRN distribution, while lower levels of IRN distribution were associated with higher agar concentrations aerogels (3 and 3.5%). These results are relatively in agreement with the IRN-loaded agar hydrogels content distribution findings, which demonstrated that the hydrogel formulations with lower agar concentrations (2 and 2.5%) produced better IRN distribution between the hydrogel different parts compared to higher agar hydrogels (3 and 3.5%). The IRN distribution variations within the agar hydrogel and aerogel formulations are possibly related to the increased viscosity of the hydrogel solution as a result of increased crosslinking density with higher agar concentrations, which may result in heterogenous network structure and consequently affecting the uniform drug distribution (Liang, Xu et al. 2006). Furthermore, the slight reduction in the IRN content in the hydrogels is mostly related to drug entrapment within the networks due to their reduced pores sizes as the agar content increased (Han, Choi et al. 2013). As a result, the IRN-loaded hydrogels and preloaded aerogels with lower agar concentrations (2 and 2.5%) yield better homogeneity and are thus more suitable for the development of uniform implantable drug delivery systems for post-surgical localised treatment of pancreatic cancer.

During the preparation to the in vitro release study experiment of the IRN, its solubility was tested using similar conditions of caffeine release (PBS at pH 7.4) and IRN demonstrated lower

solubility rate compared to caffeine that showed increased solubility within these conditions. Therefore, to ensure sink conditions with maintained release of IRN, it took place in an increased volume of deionized water instead of PBS at due to the increased solubility of IRN in water at lower acidic pH and to mimic the tumour tissue pH (Stella, Borchardt et al. 2007). The IRN is a HCL salt, which means the IRN is a base. Therefore, at lower pH it will be more ionised that will increase its solubility, while at higher pH (> 6.8) the IRN could show lower solubility and even reduce its cellular uptake at target tissues (Stella, Borchardt et al. 2007, Zashikhina, Volokitina et al. 2017). The pH of the normal tissue is in the range of 7.2 - 7.4, while tumour tissue ranges from 5.7 to 8.7 (Gerweck and Seetharaman 1996, Stubbs, McSheehy et al. 2000). Although caffeine solubility and release study were not investigated at lower pH, but it was reported that caffeine solubility increase and might accelerate its release at acidic media as its ionization is highly influence by the change in pH (Nikoo, Kadkhodae et al. 2018, Fakioglu and Kalpaklı 2022). The IRN showed a rapid 'burst' release during the first 6 hours from most of the agar hydrogels and preloaded aerogels. As the agar concentrations increases the release of IRN reduced within the first 3-6 hours with sustained release up to 96 hours. The initial 'burst' release phase is related to the presence of IRN on the surface of both formulations being released mediated via a concentration gradient, especially with lower agar formulations (2 and 2.5%) due to their large porous network. This was more obvious in the aerogels with low agar concentrations because of their large open porous network that allows higher penetration of the release media into the aerogels. The slower sustained release phase is associated with increased agar concentration of the formulations that results in a highly crosslinked denser network, corresponding with reduced pores and mesh size of the hydrogels and aerogels (Nordqvist and Vilgis 2011, Han, Choi et al. 2013). As a result, there is slower release media penetration into

the formulations and increasing resistance of IRN diffusion through the narrow pores of the higher agar aerogels and hydrogels (3 and 3.5%). Consequently, increasing the time required for the diffusion of the IRN through the agar hydrogel and aerogel polymeric networks (Franson and Peppas 1983, Brazel and Peppas 1999, Brazel and Peppas 1999). The hydrogels yielded slower sustained release of IRN compared to the aerogels as agar concentration increased. This is due to the swollen network matrix and water filled gaps that correspond with reduced pore sizes, while the aerogels provide an open porous network that facilitates faster IRN release. These results indicate that both agar hydrogels and aerogels are successfully capable to provide controllable sustained release of chemotherapy based on the agar concentration used in their preparations. The higher agar concentration hydrogels and aerogels (3 and 3.5%) offer slower burst and extended release, which could be up to greater than five days compared to the lower agar concentration formulations (2 and 2.5%). However, based on the previous findings they need to be further investigated for improved distribution and adhesion to be developed as implantable drug delivery systems for post-surgical localised treatment of cancer. The release profile of IRN from different post-loaded agar aerogels (2, 2.5, 3, and 3.5%) were evaluated and demonstrated almost similar release profiles over 96 hours. The increased volume of 1% IRN post-loaded into the agar aerogels (2, 2.5, 3, and 3.5%) is directly related to the improved sustained release from the aerogels. These results may indicate that there is an improvement in the IRN distribution within the agar aerogels associated with the increased loading rates, and thereby the IRN release of higher loading volumes (2 and 3 ml) from the lower side in contact with the release media was more efficient compared to the lower loading volume (1 ml). Furthermore, the post-loaded agar aerogels could provide extended sustained release of IRN possibly up to more than 7 days. The release of IRN showed slower release profiles compared

to caffeine possibly due to IRN higher molecular weight, and hence lower diffusion rate through the agar formulations. Therefore, the IRN loaded agar aerogels can have great potentials as an implantable drug delivery system for the post-surgical localised pancreatic cancer chemotherapy.

The cell viability of MIA PaCa-2 and Panc-1 cells using different agar aerogels (2, 2.5, 3, and 3.5%) preloaded with 5% IRN, and post-loaded with increased volumes (1, 2, and 3 ml) of 1% IRN were investigated. Generally, the MIA PaCa-2 cells demonstrated more aggressive behaviour and higher cell viability compared to the Panc-1 cells over 96 hours treatment. However, a higher sensitivity and reduced viability for MIA PaCa-2 cells toward different anti-cancer drugs like 5-FU, gemcitabine, and DOX compared to Panc-1 cell was reported (Ling, Xu et al. 2013, Daunys, Matulis et al. 2019). The cell viability results of MIA PaCa-2 are relatively in agreement with the IRN release profiles findings from the IRN pre- and post-loaded aerogels. However, the treatment using IRN-pre- and post-loaded aerogels with different agar concentrations (2, 2.5, 3, and 3.5%) provided more efficient cytotoxic effect on Panc-1 cells with non-significant ($p>0.05$) differences between the formulations. The cytotoxicity study using IRN-preloaded agar aerogels successfully showed their ability to reduce the cell viability of MIA PaCa-2 with significant ($p<0.05$) differences between all the formulations. The IRN-preloaded aerogel with low agar concentration (2%) has shown faster and lower reduction in the cell viability compared to the other IRN-preloaded aerogels with increased agar concentrations (2.5, 3, and 3.5%), which produced slower reduction in the MIA PaCa-2 viability. The rapid reduction rate in the cell viability with lower agar concentration is mainly due to the increased porosity of the aerogels, and thus faster diffusion of the preloaded IRN from the aerogels

matrices similarly to the release study findings. The cell viability of MIA PaCa-2 cells following their treatment using aerogels with higher agar concentrations (3 and 3.5%), as well as low post-loading of 1% IRN (1 ml) was higher compared to those aerogels of lower agar concentrations (2 and 2.5%) and higher post-loaded IRN (2 and 3 ml). The aerogel formulations varied significantly ($p < 0.05$) as the IRN post loading increased in every agar aerogel. Nevertheless, the cytotoxicity of low agar aerogels (2 and 2.5%) with varying 1% IRN post-loading rates (1, 2, and 3 ml) against Panc-1 cells resulted in a rapid reduced cell viability compared to the MIA PaCa-2 cell with non-significant ($p > 0.05$) between differently post-loaded agar aerogels. The higher agar aerogels (3 and 3.5%) of low 1% IRN post-loading (1 ml) demonstrated significantly ($p < 0.05$) higher cell viability within 24 hours of treatment compared to the same aerogels with increased post-loading rates (2 and 3 ml), and to the aerogels with lower agar concentrations (2 and 2.5%) with similar loading rate. However, all IRN post-loaded agar aerogels achieved the same cytotoxic effect against Panc-1 cells post 96 hours treatment. These findings indicate that lowering agar aerogels concentration and increasing the IRN post loading volume play an important role in improving the drug distribution and facilitating the IRN diffusion. Correspondingly, a possibly improved cytotoxic effect against cancer cells. Therefore, the aerogel formulations with low agar concentrations (2 and 2.5) and high post loading (3 ml) are preferable as a potential implantable drug delivery system for the post-surgical localised pancreatic cancer chemotherapy. Although higher cumulative release of the IRN from pre-loaded aerogels compared post-loaded aerogels was observed during in vitro release study, the IRN post-loaded aerogels demonstrated higher toxicity during the cell viability investigations. This is due to the variations in the conditions between the release and cell viability experiments. The release experiments for preloaded and post-loaded aerogels were performed using higher

volumes of water as release media with pH 6.5 at 37 °C in an orbital shaking incubator (60 rpm), while for the cell viability investigations different media was used with total volume of 3 ml for each well in 6-well plate. Therefore, the 5% IRN preloaded aerogels may require increased volume of media compared to 1% IRN post-loaded aerogels to achieve quicker drug diffusion and consequently higher cytotoxicity.

The sterilization process of aerogels by spraying 70% ethanol did not have any impact on the cell viability, as the drug free aerogels following their sterilization demonstrated no cytotoxicity on the cells. Also, the sterilization may not have any effect on IRN post-loaded aerogels as the aerogels were sterilized prior to the drug loading, while the effect on preloaded aerogels is probably limited as the sterilization could remove only small amount of the drug present on the surface of the aerogels.

4.5 Conclusion

The IRN-loaded agar hydrogels and aerogels were developed using the sol-gel and post-loading methods. The development and characterizations focused on two factors; the agar concentration used in the preparation and the IRN loading. Eight IRN-loaded hydrogel and preloaded aerogels formulations, as well as 12 IRN post-loaded agar aerogels were prepared. IRN-loaded hydrogel and preloaded aerogels were characterized for their mechanical features. Also, the IRN content distribution within loaded agar hydrogels and preloaded aerogels were assessed. The impact of agar concentration, loading method and concentration on the release of IRN from both agar hydrogels and aerogels were studied. The release profiles of IRN from

hydrogel and preloaded aerogel formulations demonstrated an initial ‘burst’ release followed by sustained release, while post-loaded aerogels showed slow sustained release. The release profiles and the mechanical properties varied depending on the agar concentration of the hydrogel and preloaded aerogel formulations. However, the release profiles from post-loaded aerogels varied mainly based on the IRN loading rate. The cytotoxicity assessment of the IRN pre- and post-loaded agar aerogel formulations against different pancreatic cancer cell lines showed that the reduction rate in the cell viability is directly related to the agar and IRN loading concentrations. Four IRN-loaded hydrogel and preloaded aerogel formulations, the 2 and 2.5% agar hydrogels and aerogels loaded with 5% IRN were considered to be the most optimised based on their mechanical properties, IRN content and distribution, as well as *in vitro* release profiles. Four IRN-loaded agar aerogel formulations, the 2 and 2.5% agar aerogels preloaded with 5% IRN and post-loaded with 3 ml of 1% IRN were chosen as the optimised formulations based on their cytotoxicity evaluation. Subsequently, these IRN-loaded agar hydrogels and aerogels (2 and 2.5%) could be efficient for post-surgical localised chemotherapy of pancreatic cancer as implantable drug delivery systems.

Chapter 5: Development of HEC and HPMC Hydrogels for Intravesical Delivery of Infigratinib for The Localised Treatment of Non-Muscle Invasive Bladder Cancer

5.1 Introduction

Bladder cancer is the 10th most common malignancy worldwide with more than 573,278 new cases diagnosed in 2020; incidence rates in Europe are amongst the highest in the world (Antoni, Ferlay et al. 2017, Saginala, Barsouk et al. 2020, Wen 2021). The majority of tumours (75-80%) are classified as non-muscle-invasive (NMIBC: stages Ta, T1 or Tis) at diagnosis; the remainder are muscle-invasive (MIBC: stages T2 to T4), a life-threatening disease necessitating radical treatment (Bryan 2013, Stewart 2020). Approximately one third of NMIBCs will progress to MIBC (Farling 2017, Hussein, Elsayed et al. 2021). Adjuvant intravesical therapy regimens for NMIBC are determined by the risk classification of the tumour(s); the most commonly utilised agents include mitomycin C (MMC) and bacillus Calmette-Guérin (BCG) (Porten, Leapman et al. 2015, Abufaraj, Mostafid et al. 2018). However, some cases do not respond to treatment, and there is currently a global shortage of BCG, while MMC is less effective than BCG in preventing progression to MIBC (Abufaraj, Mostafid et al. 2018). Accordingly, there is an urgent need to find new intravesical treatment of bladder cancer.

Infigratinib phosphate (INF) (formerly BGJ398, also known as BBP-831) is a bioavailable, potent, selective ATP-competitive inhibitor of fibroblast growth factor receptor (FGFR) (Merz, Zecchetto et al. 2020, Javle, Roychowdhury et al. 2021). The FGFR family of receptor tyrosine

kinases (RTKs) consist of four members (FGFR1, FGFR2, FGFR3, FGFR4) that serve as the high-affinity receptors for 22 FGF ligand. These are pleiotropic growth factors controlling cell proliferation, migration, angiogenesis, apoptosis, and differentiation that involved in both developmental and adult tissue homeostasis (Coumoul and Deng 2003, Cheng, Wang et al. 2017). Cancer epidemiological and molecular studies have reported various genetic alterations including gene amplifications, mutations, chromosomal translocations, as well as aberrant protein expression for this family of RTKs and ligands. A link between these genetic alterations and cancer has been established non-clinically (Haugsten, Wiedlocha et al. 2010, Network 2014).

Genetic alterations in some FGFR genes have been associated with bladder cancers, leading to altered FGFR proteins. Infrequently, alterations in FGFR occur, and can be identified through genetic testing. Mutations in FGFR constitute an active area of investigation in bladder and urothelial cancers. Clinical trials for treatment with FGFR inhibitors are ongoing (Packiam, Werntz et al. 2019, Bin Riaz, Khan et al. 2021). The genetic alterations in one of the FGFR genes that have been associated with bladder/urothelial cancers include activating mutations, gene fusions, and gene amplifications (Knowles 2007, Goebell and Knowles 2010).

In this chapter, we have investigated the preparation and characterization of two different hydrogels using hydroxyethyl cellulose (HEC) as well as hydroxypropyl methylcellulose (HPMC) as proposed formulations for intravesical treatment of bladder cancer. We evaluated the hydrogels physical properties with varying HEC and HPMC concentrations. Also, the effect of several INF loadings on the physical properties and the release profiles from both hydrogels

were studied. Furthermore, we have investigated the anti-tumour effect of INF on different bladder cancer cells lines and tried to demonstrate the potential application of the optimized hydrogel formulation for the intravesical therapy.

5.2 Materials and methods

5.2.1 Materials

Hydroxyl ethyl cellulose (HEC) (MW 250 000 Da), hydroxy propyl methyl cellulose (HPMC) (MW 120 000 Da), polyethylene glycol (PEG) (MW 300 Da), porcine gastric mucin, Dulbecco's Modified Eagle's Medium (DMEM-F12), fetal bovine serum (FBS), and phosphoric acid were purchased from Sigma (UK). Infigratinib (INF) anti-cancer drug was supplied by QED therapeutics. Dimethyl sulfoxide (DMSO), methanol 99%, and acetonitrile were obtained from Fisher Scientific. Ammonium phosphate dibasic from (VWR). CellTiter-Blue (Promega; Southampton, UK). Cell lines T24 (FGFRwt), VM-CUB1 (FGFRwt), SW-780 (FGFR3trans), MGH-U3 (FGFR3mut), RT4 (FGFR3 fusion with TACC3) are obtained from ATCC or DSMZ.

5.2.2 Preparation of the INF-loaded HEC and HPMC hydrogels

The INF-loaded HEC hydrogels were prepared by dispersing the appropriate amount of HEC (Table 5-1) into preheated distilled water at 75°C under continuous stirring until the hydrogels started to thicken. The hydrogels were subsequently removed from the heat and kept at room temperature to cool under continuous stirring. The HPMC hydrogels were prepared by dispersing the appropriate amount of HPMC (Table 5-2) into 25 ml of preheated distilled water at 90°C under continuous stirring. The remaining required amount of water was heated to 50°C

then added to the dispersion mixture and once the hydrogels began to thicken, they were allowed to cool under continuous stirring. The appropriate amount of INF was dispersed in PEG, then subsequently added to each hydrogel under stirring for 1 hour and dispersed producing HEC and HPMC hydrogels (1, 1.5, 2, and 2.5% w/v) with INF loadings of 1, 2.5, and 5% w/v. The INF-loaded hydrogels were collected and stored in the fridge until needed.

Table 5-1: Formulations of INF-loaded HEC hydrogels

Formulations	HEC % w/v	INF % w/v	PEG ml	Hydrogel ml
1	1	1	1.2	50
2	1	2.5	3	50
3	1	5	6	50
4	1.5	1	1.2	50
5	1.5	2.5	3	50
6	1.5	5	6	50
7	2	1	1.2	50
8	2	2.5	3	50
9	2	5	6	50
10	2.5	1	1.2	50
11	2.5	2.5	3	50
12	2.5	5	6	50

Table 5-2: Formulations of INF-loaded HPMC hydrogels

Formulations	HPMC % w/v	INF % w/v	PEG ml	Hydrogel ml
1	1	1	1.2	50
2	1	2.5	3	50
3	1	5	6	50
4	1.5	1	1.2	50
5	1.5	2.5	3	50
6	1.5	5	6	50
7	2	1	1.2	50
8	2	2.5	3	50
9	2	5	6	50
10	2.5	1	1.2	50
11	2.5	2.5	3	50
12	2.5	5	6	50

5.2.3 Characterization of the INF-loaded HEC and HPMC hydrogels

5.2.3.1 Injectability of INF-loaded HEC and HPMC hydrogels through a syringe

The injectability test was performed to investigate the forces required to push 10 ml of unloaded and INF loaded (1, 2.5, and 5%) HEC and HPMC hydrogels (1, 1.5, 2, and 2.5%) through disposable syringes. This test was performed using a texture analyser (TA.XT. Plus C) equipped with 20 mm cylindrical probe. 10 ml of each hydrogel formulation was loaded into 20 ml disposable syringes. The filled syringe was placed in a fixed position below the texture analyser probe and the distance required to move the probe downward to push the hydrogel completely through the syringe was measured. Then, the cylindrical probe was lowered to the syringe plunger at a constant speed of 10 mm/s until hydrogel pushed completely out of the

syringe and the resulted force required to push the hydrogel from the syringe was obtained. Experiments were conducted using one batch of every formulation including controls.

5.2.3.2 Injectability of INF-loaded HEC and HPMC hydrogels through a catheter

To identify the percentage of hydrogel that can be injected through a catheter, 10 ml of unloaded HEC and HPMC hydrogels (1, 1.5, 2, and 2.5%) and 1% INF-loaded hydrogels were loaded into pre-weighed 20 ml disposable syringes. Then, the hydrogels were injected slowly through different Foley urinary catheters with a diameter of 4 mm, while manually pressing along the catheter to push the injected hydrogels downward into pre-weighed weight boat plate. The weight of unloaded and 1% INF-loaded HEC and HPMC hydrogels that passed through the catheter were recorded and the percentage of the hydrogels that can be injected through the Foley catheters were calculated by dividing the weight of hydrogels in the weight boat by the initial hydrogels weight multiplied by 100. Experiments were conducted using one batch of every used formulation including controls.

5.2.3.3 Rheological evaluation of INF-loaded HEC and HPMC hydrogels

The rheological evaluation was performed on drug free the HEC and HPMC hydrogels (1, 1.5, 2, and 2.5%) as controls and with different INF loadings (1, 2.5, and 5%) for every gel. The experiments were performed using a discovery HR10 TA rotational rheometer equipped with a Peltier heating system. A plate-plate geometry with a diameter of 40 mm was used and the gap between the upper and lower stationary plate was 1 mm. The experiments were established by placing on the lower plate 1.5 ml of every hydrogel using disposable syringes.

The rheology tests were conducted at 37°C and repeated ramp mode with shear stress increased from 0 to 450 Pa over 13 minutes.

5.2.3.4 Mucoadhesive Properties of the INF-loaded HEC and HPMC hydrogels

The mucoadhesive properties of the unloaded and INF loaded HEC as well as HPMC hydrogels were investigated using the same procedures described earlier (Chapter 2, section 2.2.3.2). All measurements were conducted in triplicate using separate batches and drug free hydrogels were tested as controls.

5.2.3.5 INF Content of the HEC and HPMC hydrogels

2 ml of each INF loaded HEC and HPMC hydrogels were collected using disposable syringes and placed in a glass vial containing 30 ml of (80:20) DMSO:methanol under vigorous stirring for 30 minutes and subsequently vortexed until hydrogels completely dissolved, to ensure complete extraction of the INF. 1 ml of the extraction solution was collected and centrifuged at 13500 rpm for 15 minutes and filtered using a 0.45 µm membrane filter and analysed by HPLC.

5.2.4 In vitro release of the INF from HEC and HPMC hydrogels

The INF release from HEC and HPMC hydrogels (1, 1.5, 2, and 2.5%) was performed by collecting 2 ml of each hydrogel with different INF loadings (1, 2.5, and 5%) using disposable syringes. Each INF-loaded hydrogel was placed at the bottom of an empty glass vial and kept for 5 minutes to ensure the hydrogel spread over the lower surface of the vial prior the addition

of release media. 30 ml of (80:20) DMSO:methanol was slowly added to each formulation as release media and each vial was placed in an orbital shaker at 37°C and 60 rpm. At time intervals of 0.5, 1, 3, 6, and 24 hour 1 ml sample was collected and replaced with 1 ml of fresh DMSO:methanol. Each sample was stored at 4°C until analysed. The release study was conducted in triplicate and the percentage of cumulative released INF calculated relatively to the loaded INF concentration of the hydrogels.

5.2.5 HPLC analysis

5.2.5.1 INF chromatographic conditions

HPLC analysis was performed using an Agilent HPLC System (Agilent Technologies 1260 infinity II, Santa Clara, California, United States) equipped with a quadratic pump and autosampler. The separation was performed using a Thermo Scientific® 5 µm, C18 analytical HPLC column (150 mm *4.6 cm) at 25 °C with two mobile phases were used, mobile phase A composed of HPLC grade acetonitrile and mobile phases B 10 mM ammonium phosphate dibasic buffer (NH₄)₂HPO₄ in water pH 6.5 at flow rate of 1ml/ min. the UV detection was achieved at wavelength of 230 nm with injection volume 10 ul and a run time of 15 minutes.

5.2.5.2 Stock solution and calibration curve

10 mg of INF was transferred into a 10 ml volumetric flask and dissolved in acetonitrile to produce a stock solution with a final concentration of 1 mg/ml. The stock solution was then used to prepare standard solutions with concentrations of 0.005, 0.01, 0.05, 0.1, 0.5, and 1 mg/ml. The calibration curve was prepared by plotting the area under the curve versus the concentration. All measurements were conducted in triplicate.

5.2.6 Cell lines

T24 and MGH-U3 were cultured with RPMI-1640 media with 10% FBS. SW780 and VM-CUB1 were cultured with DMEM media with 10% FBS. Rt4 was cultured with McCoy's 5A medium with 10% FBS. All the cell lines were cultured in the 37°C with 5% CO₂ incubator in a humid environment.

5.2.7 Cell viability

The cell viability studies were performed by Bladder Cancer Research Centre at the University of Birmingham. Cell viability was quantified using the CellTiter-Blue assay according to the manufacturer's protocol. 2000 cells were plated in 96-well plates and treated the following day at the indicated concentrations. Two-hour pulse experiments were performed by removing the drug-containing media, replacing it with fresh media and measuring viability after 72h.

5.2.8 Statistical analysis

Statistical analysis was performed using a one-way or two-ways analysis of variance dependent on the presence of one variable or two independent variables respectively (ANOVA) (GraphPad Prism version 9.0.2 for MacOS, GraphPad Software, San Diego, CA). Post-hoc comparisons of the means were performed using Tukey's Honestly Significance Difference test. A significance level of $p < 0.05$ was accepted to denote significance in all cases.

5.3 Results

5.3.1 Evaluation of the INF-loaded HEC and HPMC hydrogels injectability

The injectability for the unloaded and the INF-loaded HEC as well as HPMC hydrogels was investigated. Results showed that the required forces to push the hydrogels are increasing as the hydrogels polymers concentrations and INF loadings simultaneously increased compared to the unloaded hydrogels (Figures 5-1 A and B).

5.3.2 Injectability of the INF-loaded HEC and HPMC hydrogels through catheter

Results in Figure 5-2 describe the percentage of the unloaded and the 1% INF-loaded HEC and HPMC hydrogels (1, 1.5, 2, and 2.5%) injected through the catheters. The results show that approximately 80% of the 1% unloaded HEC and HPMC hydrogels passed through the catheters, while the addition of 1% INF to both hydrogels had no impact. However, as the concentrations of the HEC and HPMC in the hydrogels increased, they became more difficult with less than 40 and 20% passing through the catheter for both the unloaded and 1% INF-loaded HEC and HPMC hydrogels, respectively.

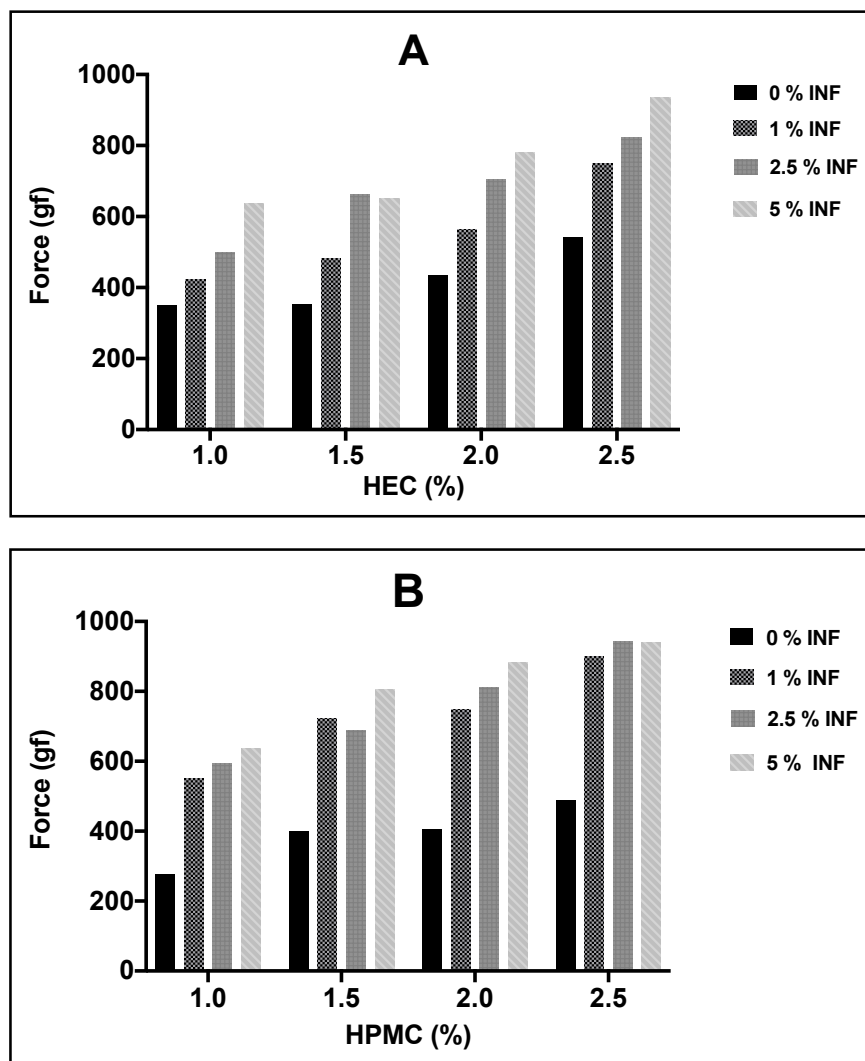


Figure 5-1: Effect of HEC and HPMC concentrations (1, 1.5, 2, and 2.5%) and INF loadings (1, 2.5, and 5%) on the injectability of HEC hydrogels (A), and HPMC hydrogels (B). Data represents n=1 experiment.

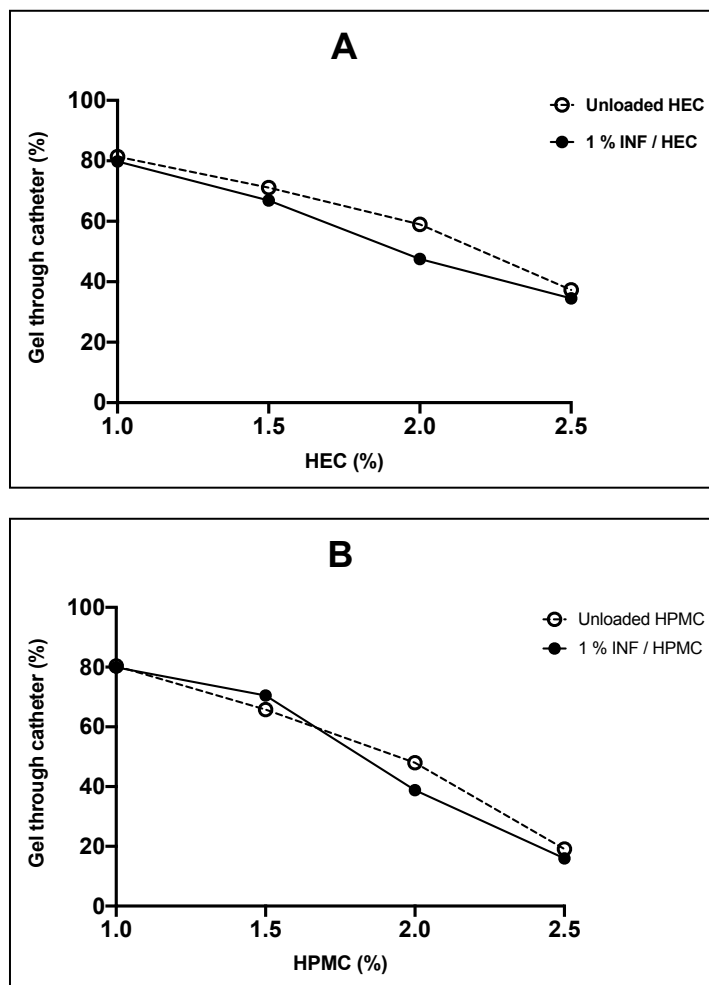


Figure 5-2: The percentage of unloaded HEC and HPMC hydrogels (1, 1.5, 2, and 2.5%) and 1% INF-loaded HEC hydrogels (A), and HPMC hydrogels (B) pushed through the urinary catheter. Data represents n=1 experiment.

5.3.3 Rheological evaluation of the INF-loaded HEC and HPMC hydrogels

The rheological analysis of the HEC and HPMC hydrogels with different polymer concentrations, as well as INF loadings is presented in Figures 5-3 to 5-5. The effect of the HEC and HPMC concentrations (1, 1.5, 2, and 2.5%) on the viscosity of the unloaded hydrogels upon increasing shear stress is demonstrated in Figures 5-3 A and B. Higher viscosity levels were observed with an increase HEC and HPMC concentrations. As the applied stress increased, the viscosity of the hydrogels decreased, especially for the 1 and 1.5% concentrations of both

hydrogels representing shear thinning behaviour. The shear stress results for the HEC hydrogels (1, 1.5, 2, and 2.5%) with different INF loadings (1, 2.5, and 5%) are shown in Figure 5-4, while the HPMC hydrogels with similar concentrations and INF loadings are illustrated in Figure 5-5. Generally, the INF-loaded hydrogels showed an increased viscosity with the dual increase in HEC/HPMC concentrations and INF loading. The 1% INF-loaded HEC hydrogels exhibited a slight increase in their initial viscosities at low shear stress compared to their unloaded hydrogels especially at higher HEC concentrations (2 and 2.5%) as seen in Figure 5-4 A. However, the simultaneous increase in both INF loadings (2.5 and 5%) and HEC concentration yielded hydrogels with higher viscosity (Figures 5-4 B and C). The 1% INF-loaded HPMC hydrogels showed shear thinning behaviour relatively similar to the 1% INF-loaded HEC hydrogels (Figure 5-5 A). The 2.5% INF-loaded HPMC hydrogels demonstrated an increased initial viscosity, followed by rapid shear thinning as the stress increased in the 1 and 1.5% HPMC hydrogels. The higher HPMC hydrogel concentrations (2 and 2.5%) showed higher viscosities compared to the lower HPMC concentration hydrogels with the same INF loading, and to 1% INF-loaded hydrogels of similar HPMC concentrations (Figure 5-5 B). Subsequently, the HPMC hydrogels with the 5% INF loading demonstrated higher initial viscosity rates mainly at low stress compared to the same hydrogels with the 1% INF loading. Nevertheless, the reduced viscosity levels compared to the 2.5% INF loading were observed as the stress increases especially in 1 and 1.5% HPMC hydrogels (Figure 5-4 C).

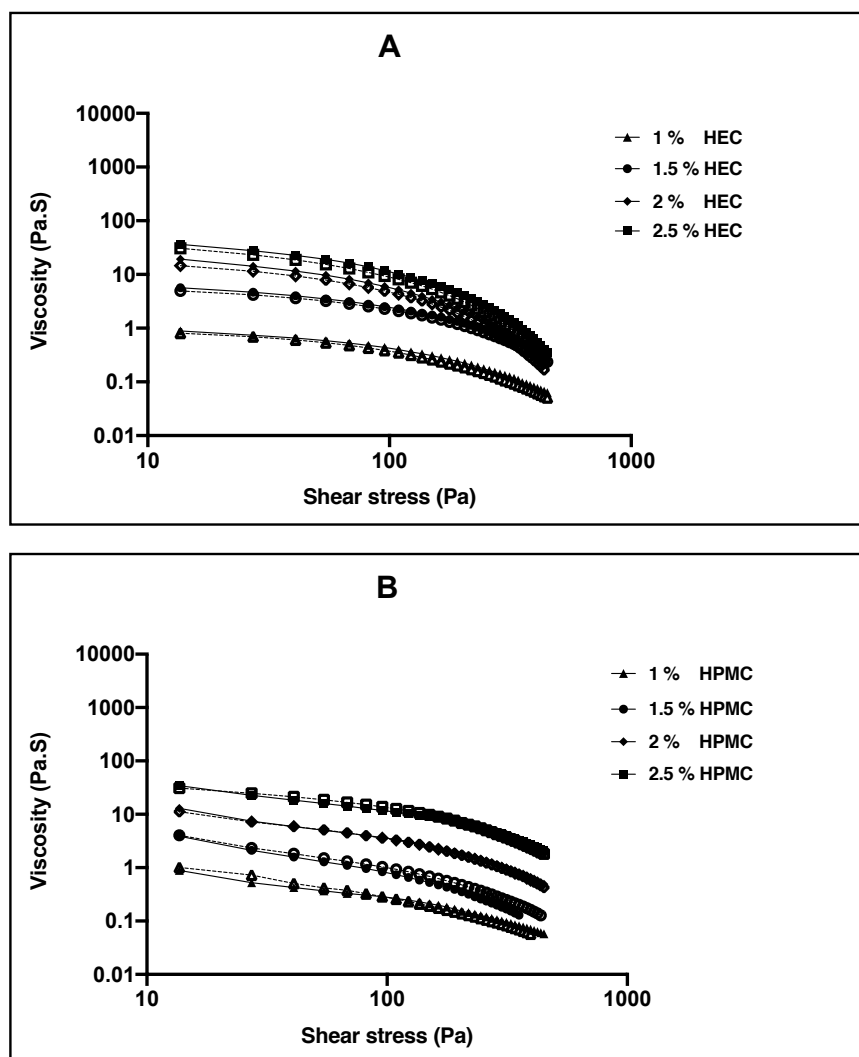


Figure 5-3: Shear stress ramps for different formulations, (A) different concentrations of unloaded HEC hydrogels (1, 1.5, 2, and 2.5%). (B) different concentrations of unloaded HPMC hydrogels (1, 1.5, 2, and 2.5%). Solid and empty points represent the effect of first and second ramp runs respectively.

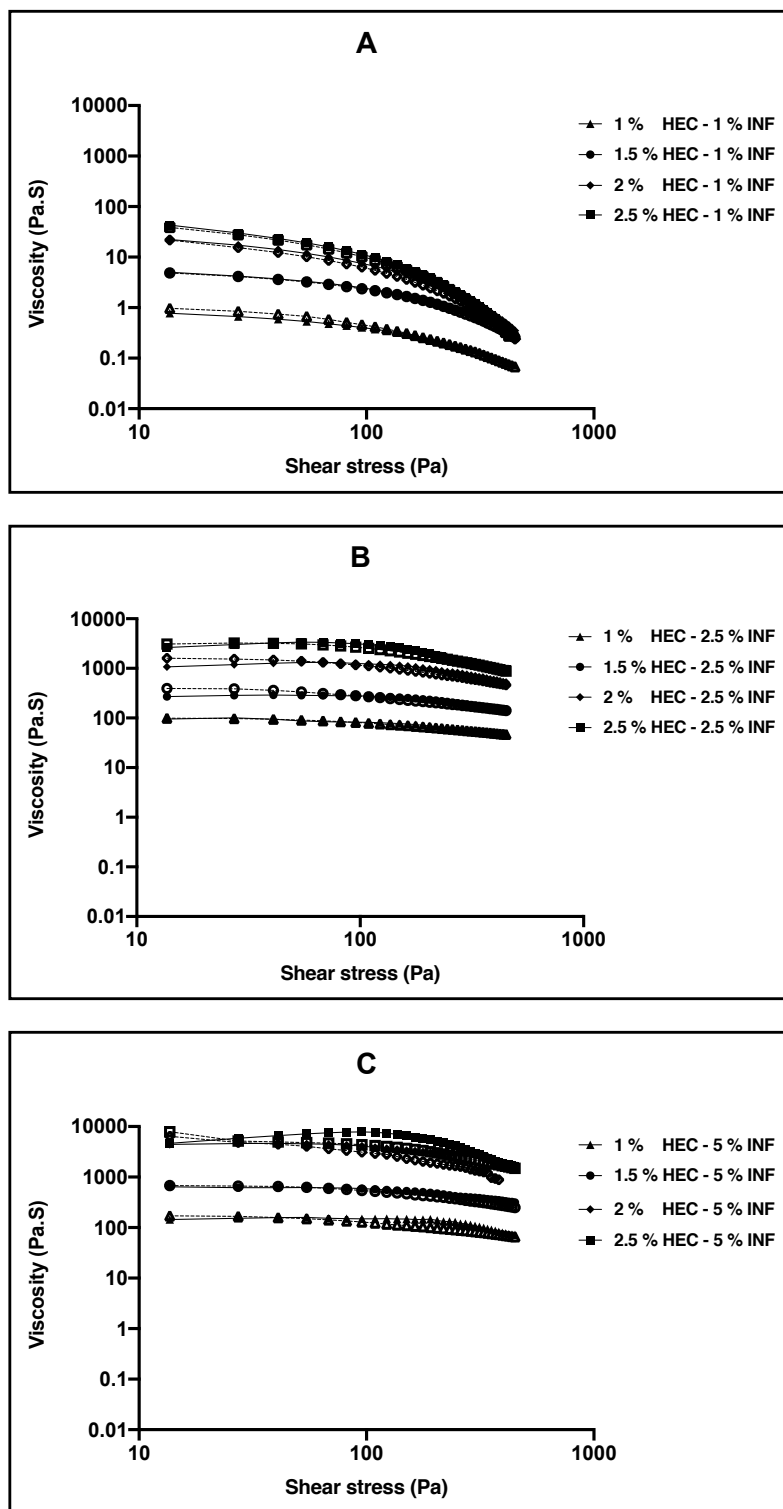


Figure 5-4: Shear stress ramps for different formulations, (A) 1% INF-loaded HEC hydrogels (1, 1.5, 2, and 2.5%). (B) 2.5% INF-loaded HEC hydrogels (1, 1.5, 2, and 2.5%). (C) 5% INF-loaded HEC hydrogels (1, 1.5, 2, and 2.5%). Solid and empty points represent the effect of first and second ramp runs respectively.

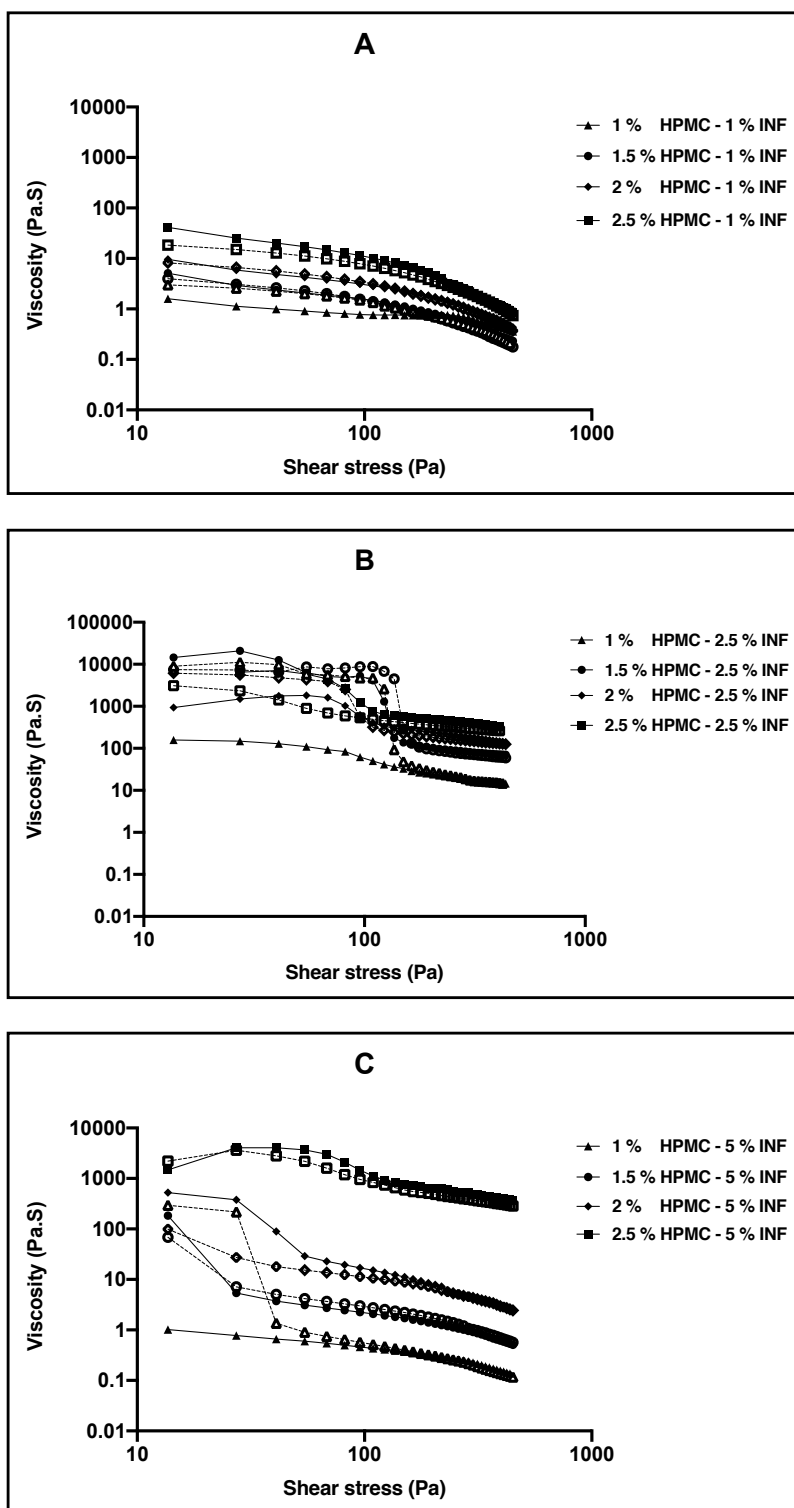


Figure 5-5: Shear stress ramps for different formulations, (A) 1% INF-loaded HPMC hydrogels (1, 1.5, 2, and 2.5%). (B) 2.5% INF-loaded HPMC hydrogels (1, 1.5, 2, and 2.5%). (C) 5% INF-loaded HPMC hydrogels (1, 1.5, 2, and 2.5%). Solid and empty points represent the effect of first and second ramp runs respectively.

5.3.4 Mucoadhesive properties of the INF-loaded HEC and HPMC hydrogels

The effect of increased HEC and HPMC hydrogels concentrations, as well as INF loading on their muco-adhesive properties was investigated. Results showed that the adhesive forces are directly related to the HEC and HPMC concentrations as well as the INF loadings. Generally, the INF-loaded HEC hydrogels had greater mucoadhesion compared to the INF-loaded HPMC hydrogels. The 1% HEC hydrogels did not show significant differences in their measured adhesion forces regardless of the increase in INF loading (Figure 5-6 A). However, as the HEC concentration and INF loading increased simultaneously, they showed significantly higher adhesive properties. Comparably, the increased concentration of HPMC hydrogels resulted in higher levels of mucoadhesion, while the increased INF loadings denoted statistically non-significant increase in their adhesive properties (Figure 5-6 B).

5.3.5 HPLC analysis of INF

Figure 5-7 demonstrated the INF standard curve at 6 different concentrations quantified by HPLC. The correlation between the INF concentrations and the HPLC area under the curve AUC was excellent with the R value at 0.99 from 0.005 to 1 mg/ml. The retention time was approximately 7 minutes (Figure 5-8).

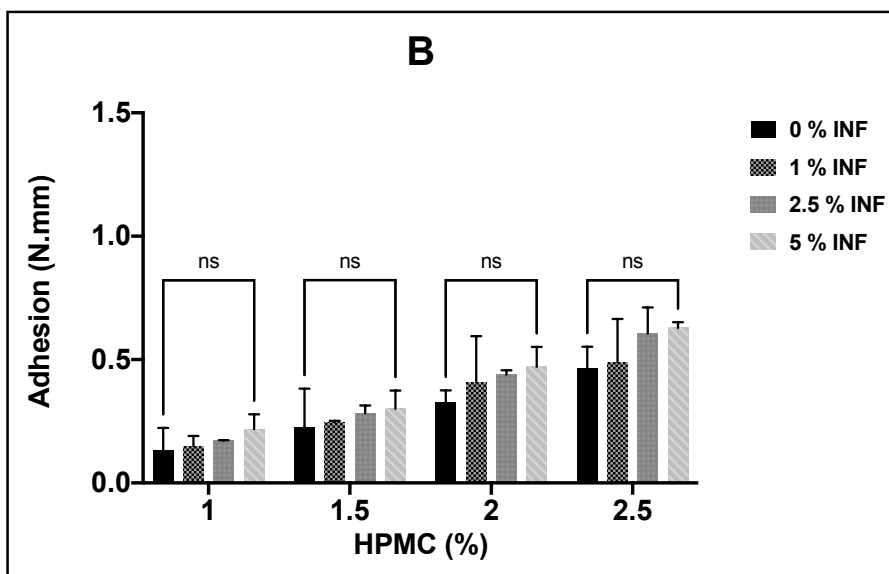
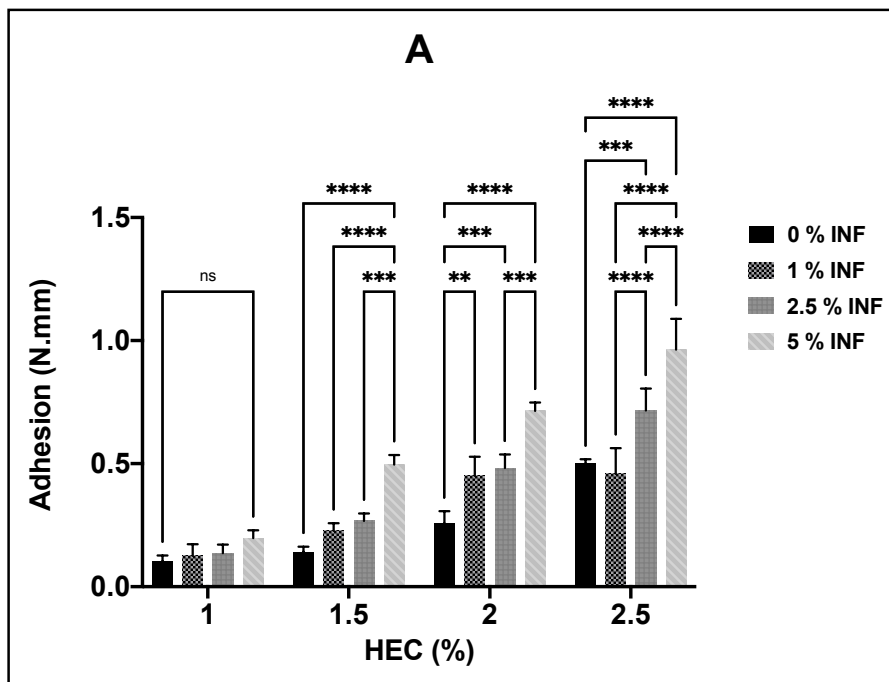


Figure 5-6: Mucoadhesion evaluation of HEC hydrogels (A) and HPMC hydrogels (B), based on different polymeric concentrations (1, 1.5, 2, and 2.5%) and INF loadings (1, 2.5, and 5%) for both hydrogels. Results shown as mean \pm SD, n= 3, significance found using a two-way ANOVA with a Tukey’s post-hoc test, * = P<0.05 ** = P<0.01, *** = P<0.001, **** = P<0.0001.

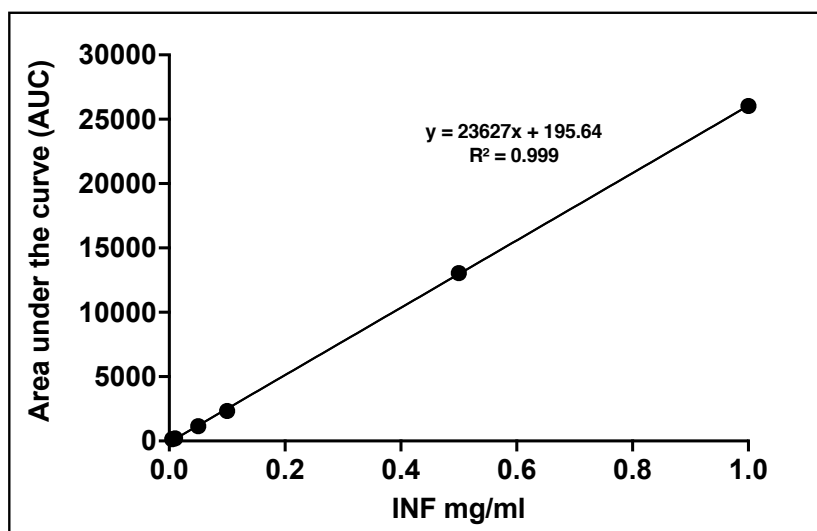


Figure 5-7: Standard curve for INF using HPLC (n=3).

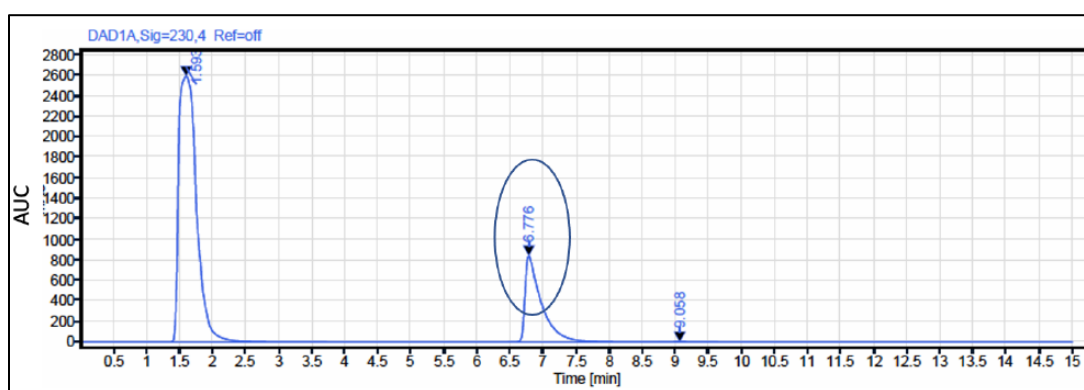


Figure 5-8: The HPLC chromatogram depicting the peak of INF at 230 nm wavelength.

5.3.6 INF content of the HEC and HPMC hydrogels

The INF content of the HEC and HPMC hydrogels (1, 1.5, 2, and 2.5%) loaded with INF (1, 2.5, and 5%) is presented in Figure 5-9 A. The INF content of the 1% HEC loaded hydrogel reduced from 116 ± 10.1 to $99.8 \pm 4.6\%$ as the INF loading increased from 1 to 5%. The 1.5% HEC loaded hydrogels demonstrated a relatively similar reduction in their INF contents as the

INF loading increased. They had INF contents of 115.4 ± 2.5 , 107.5 ± 4 , and $96.07 \pm 1.7\%$ for 1, 2.5, and 5% INF loadings, respectively. The INF content of the 2% HEC loaded hydrogels did not significantly vary ($p>0.05$), and demonstrated contents of 100.3 ± 3.1 , 106.2 ± 2.1 , and 99.1 ± 3.1 for 1, 2.5, and 5% INF loadings, respectively. Furthermore, the INF contents of the 2.5% HEC loaded hydrogels were 104.6 ± 2.9 , 105.8 ± 6.4 , and $97 \pm 4.1\%$ for the 1, 2.5 and 5% INF loadings. The INF-loaded HPMC hydrogels demonstrated varying INF contents among different formulations (Figure 5-9 B). The INF content of the 1% HPMC loaded hydrogels demonstrated a reduction from 96.3 ± 7.5 to $77 \pm 9.2\%$ as the INF loading increased from 1 to 5%, while in the 1.5% HPMC loaded hydrogels as the INF loading increased from 1 to 5% their contents varied from 88.4 ± 7.5 to $101 \pm 18.7\%$. Moreover, the 2 and 2.5% HPMC loaded hydrogels showed non-significant ($p>0.05$) difference in their INF contents with increased loadings. For the 1, 2.5, and 5% INF loadings, the 2% HPMC hydrogels had contents of 106.4 ± 1.8 , 97.6 ± 5.8 , and $110.5 \pm 6.4\%$ respectively, while the 2.5% HPMC hydrogels contents were 113 ± 3.1 , 101.2 ± 6.1 , and $116.4 \pm 8.7\%$ for the 1, 2.5 and 5% loadings.

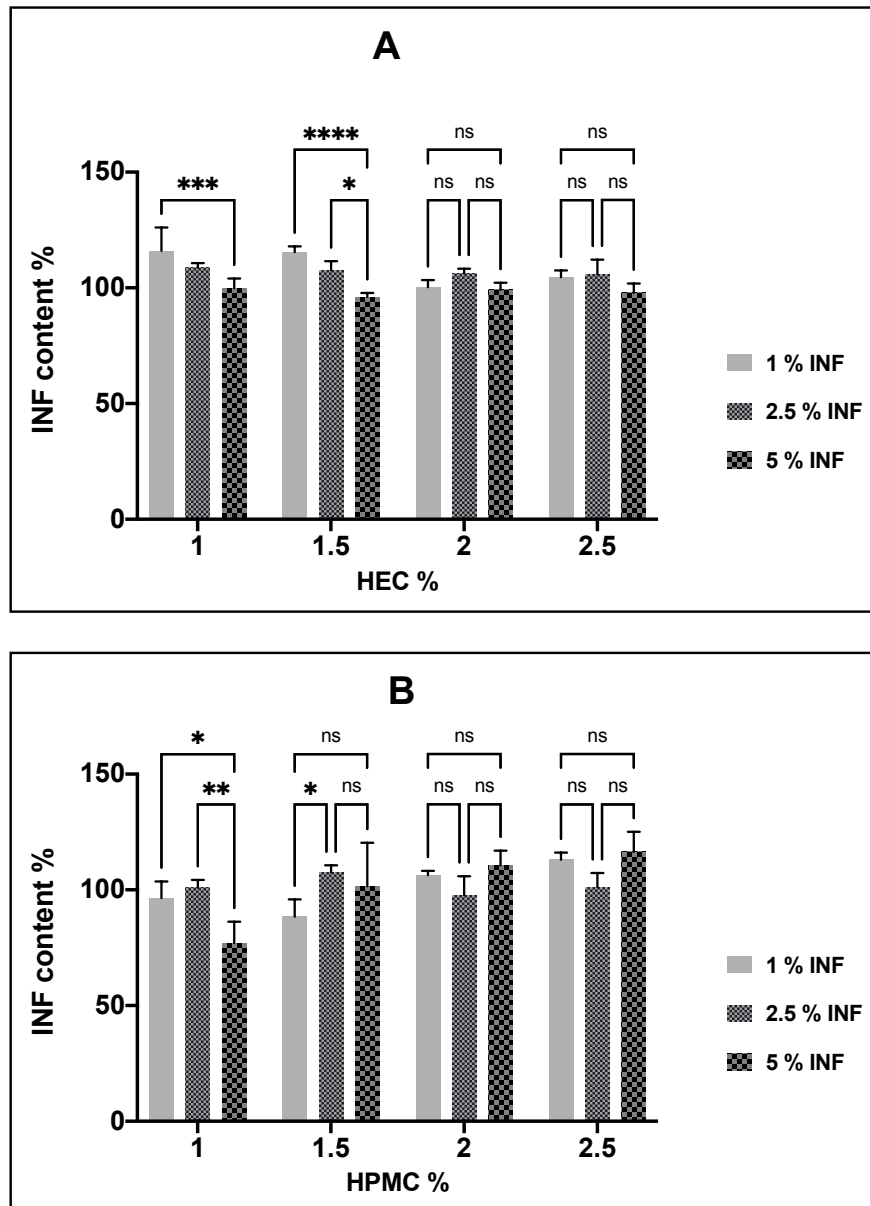


Figure 5-9: The content of different INF loadings (1, 2.5, and 5%) in four different HEC hydrogels (1, 1.5, 2, and 2.5%) (A), and four different HPMC hydrogels (1, 1.5, 2, and 2.5%) (B). Results shown as mean \pm SD, $n = 3$, significance found using a two-way ANOVA with a Tukey's post-hoc test, * = $P < 0.05$ ** = $P < 0.01$, *** = $P < 0.001$, **** = $P < 0.0001$.

5.3.7 In vitro release of INF from the HEC and HPMC hydrogels

The percentage cumulative *in vitro* release profiles for the INF-loaded HEC and HPMC hydrogels are presented in Figures 5-10 and 5-11. The release profiles of the 1% INF from the different HEC hydrogels over 24 hours vary and mainly depend on the HEC concentration of the hydrogels (Figure 5-10 A). The INF-loaded HEC hydrogels with lower HEC concentrations (1 and 1.5%) demonstrated a rapid 'burst' release and released most of their content within 6 hours. At 24 hours, 101.5 ± 4.9 and $89.4 \pm 8.5\%$ of the INF was released from the 1 and 1.5% HEC hydrogels respectively with no significant ($p > 0.05$) differences between the two formulations. However, the INF-loaded HEC hydrogels with higher HEC concentrations (2 and 2.5%) showed significantly ($p < 0.05$) slower and sustained release profiles compared to the previous formulations by releasing only 45.3 ± 18.7 and $38.3 \pm 24\%$ of their INF contents respectively after 24 hours. The HEC hydrogel formulations loaded with 2.5% INF exhibited very slow and sustained release over the 24 hours, with the 1% HEC hydrogel having faster release compared to the other formulations releasing $14.8 \pm 7.3\%$ after 24 hours (Figure 5-10 B). Moreover, the release profiles from different HEC hydrogels loaded with 5% INF illustrated demonstrated limited (less than 10%) INF release from all formulations after 24 hours (Figure 5-10 C). Alternatively, the release profiles from the HPMC hydrogels (1, 1.5, 2, and 2.5%) loaded with 1% INF over 24 hours showed slower relative release compared to the 1% INF-loaded HEC hydrogels (Figure 5-11 A). The 1% HPMC hydrogel demonstrated the fastest cumulative release of INF among all formulations by releasing $91.1 \pm 13\%$ at 24 hours, while the 1.5% HPMC hydrogel demonstrated significantly ($p < 0.05$) slower release profile by releasing $42.2 \pm 9.3\%$ of its INF after 24 hours (Figure 5-11 A). The 2 and 2.5% HPMC hydrogels demonstrated statistically non-significant ($p > 0.05$) slower release after 24 hours

compared to the 1.5% HPMC hydrogels, releasing 24.1 ± 23.6 and $37.1 \pm 7.2\%$, respectively. In contrast, the higher INF loading (2.5%) showed reduced release profiles for all HPMC hydrogels over 24 hours (Figure 5-11 B). Similarly, the HPMC hydrogels loaded with 5% INF showed limited release with 13.1 ± 4.3 , 11.3 ± 6.1 , 22.5 ± 12.4 , and $3.3 \pm 2.4\%$ of the INF released from 1, 1.5, 2, and 2.5% HPMC hydrogels, respectively after 24 hours (Figure 5-11 C).

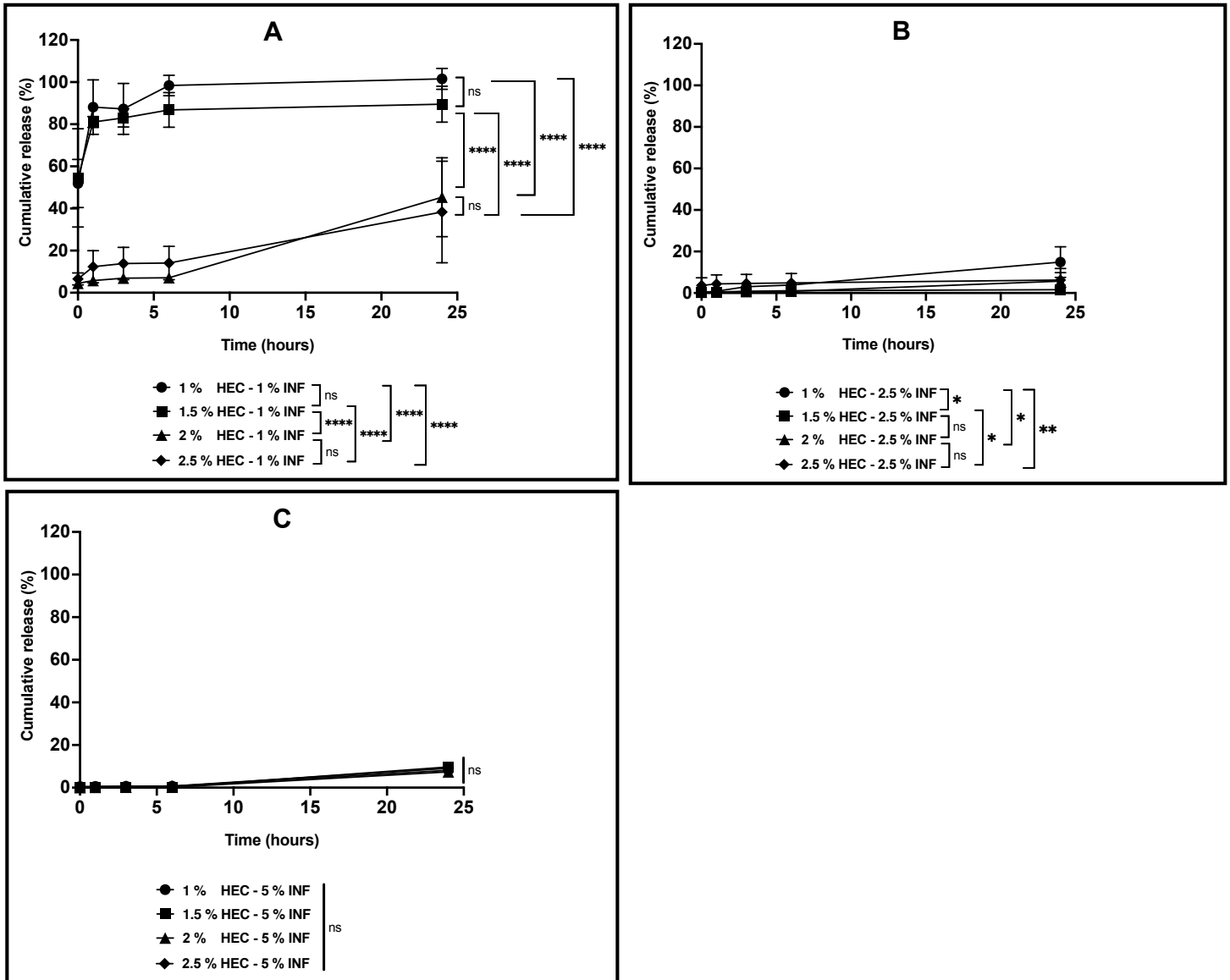


Figure 5-10: *In vitro* cumulative release profiles of 1% INF (A), 2.5% INF (B), and 5% INF (C) from four different HEC hydrogels (1, 1.5, 2, and 2.5%) in (80:20) DMSO:methanol over 24 hours in the shaking incubator at 60 rpm and 37 °C. Results shown as mean \pm SD, n= 3, significance found using a two-way ANOVA with a Tukey's post-hoc test, * = P<0.05 ** = P<0.01, *** = P<0.001, **** = P<0.0001.

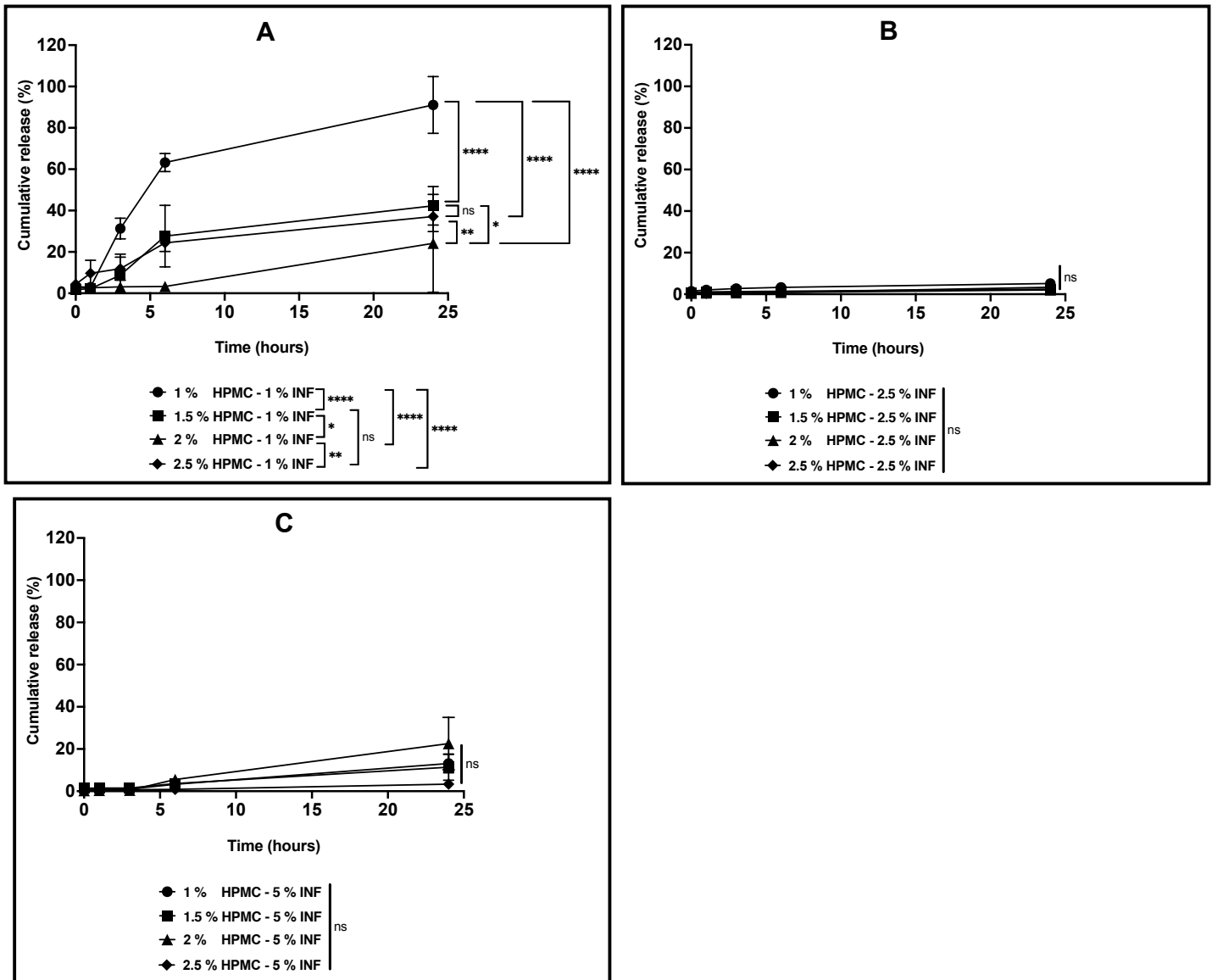


Figure 5-11: *In vitro* cumulative release profiles of 1% INF (A), 2.5% INF (B), and 5% INF (C) from four different HPMC hydrogels (1, 1.5, 2, and 2.5%) in (80:20) DMSO:methanol over 24 hours in the shaking incubator at 60 rpm and 37 °C. Results shown as mean \pm SD, n= 3, significance found using a two-way ANOVA with a Tukey's post-hoc test, * = P<0.05 ** = P<0.01, *** = P<0.001, **** = P<0.0001.

5.3.8 Dose titration on bladder cancer cell lines

The INF dose titration against different cell lines with continuous exposure for 72 hours is illustrated in Figure 5-12. The IC_{50} of INF against VM-CUB1(*FGFR*wt), SW780(*FGFR3*trans), and T24(*FGFR*wt) was 2.266 nM, 2.903 nM and 3.852 nM, respectively. We also tested the INF for the 2-hour pulse schedule to simulate intravesical delivery. However, there was no significant ($p>0.05$) cytotoxicity shown below 1000 nM. In contrast, the IC_{50} of INF against RT4(*FGFR3* fusion with TACC3) and MGH-U3(*FGFR3*mut) cells was 13.34 and 9.58 nM. The 2 hour pulse also showed an IC_{50} at 1.53 nM and 1.61 nM. These results demonstrate a significant ($p<0.05$) difference between the *FGFR* mutant and non-mutant cell lines (Figure 5-13).

5.3.9 Evaluation of INF-loaded HEC hydrogel formulation on *FGFR* mutant cell lines

Considering the cytotoxicity difference between the *FGFR*wt and *FGFR*mut cell lines, we focused on the *FGFR* mutant cell lines for the further evaluation of the anti-tumour efficacy of the INF-loaded HEC hydrogel. To test whether the hydrogel itself would affect the anti-tumour effect of the INF, we also put the equivalent amount of the INF-free HEC hydrogel formulation onto the cells. As shown in Figure 5-14, there is no difference of the anti-tumour efficacy between the INF and its hydrogel loaded formulation.

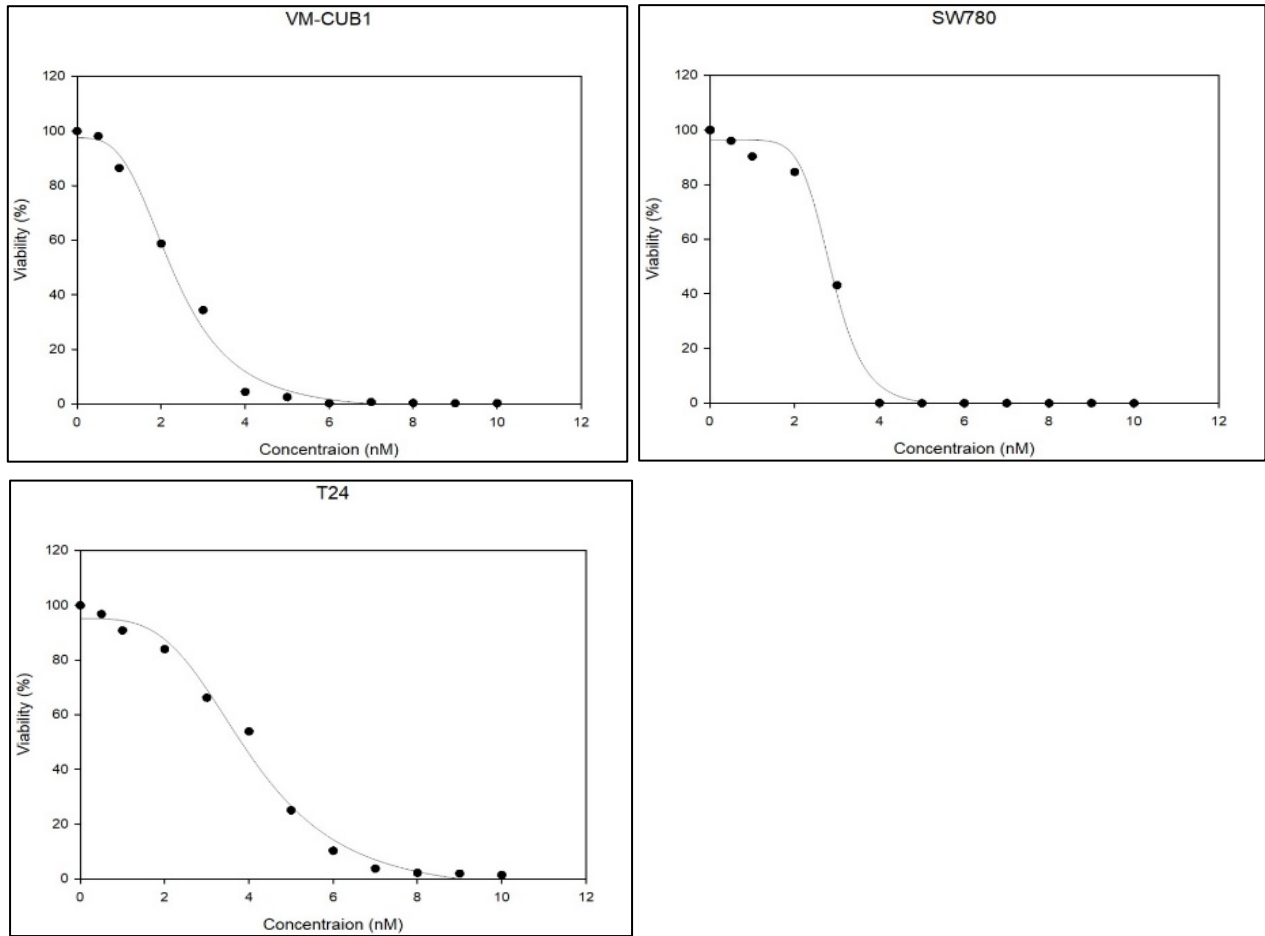


Figure 5-12: INF dose titration on VM-CUB1, SW780 and T24 cells for continues exposure of 72 hours. Cells viability was tested by Cell Titre Blue assay. Results shown as mean \pm SD, n= 3, significance found using a two-way ANOVA with a Tukey’s post-hoc test.

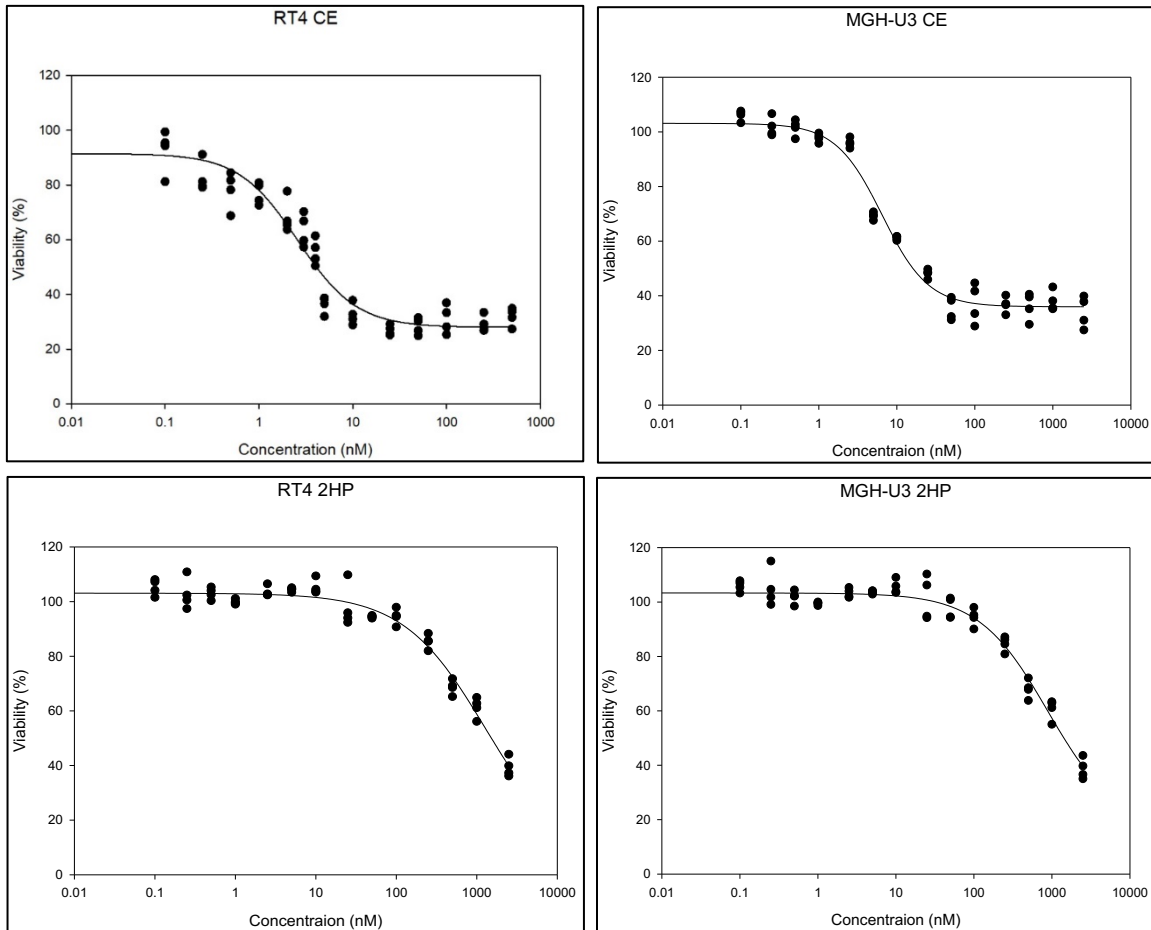


Figure 5-13: INF dose titration on RT4 and MGH-U3 cells for continues exposure of 72 hours (CE) or 2-hour pulse (2HP). Cell viabilities were tested by Cell Titre Blur assay. Results shown as mean \pm SD, n= 3, significance found using a two-way ANOVA with a Tukey’s post-hoc test.

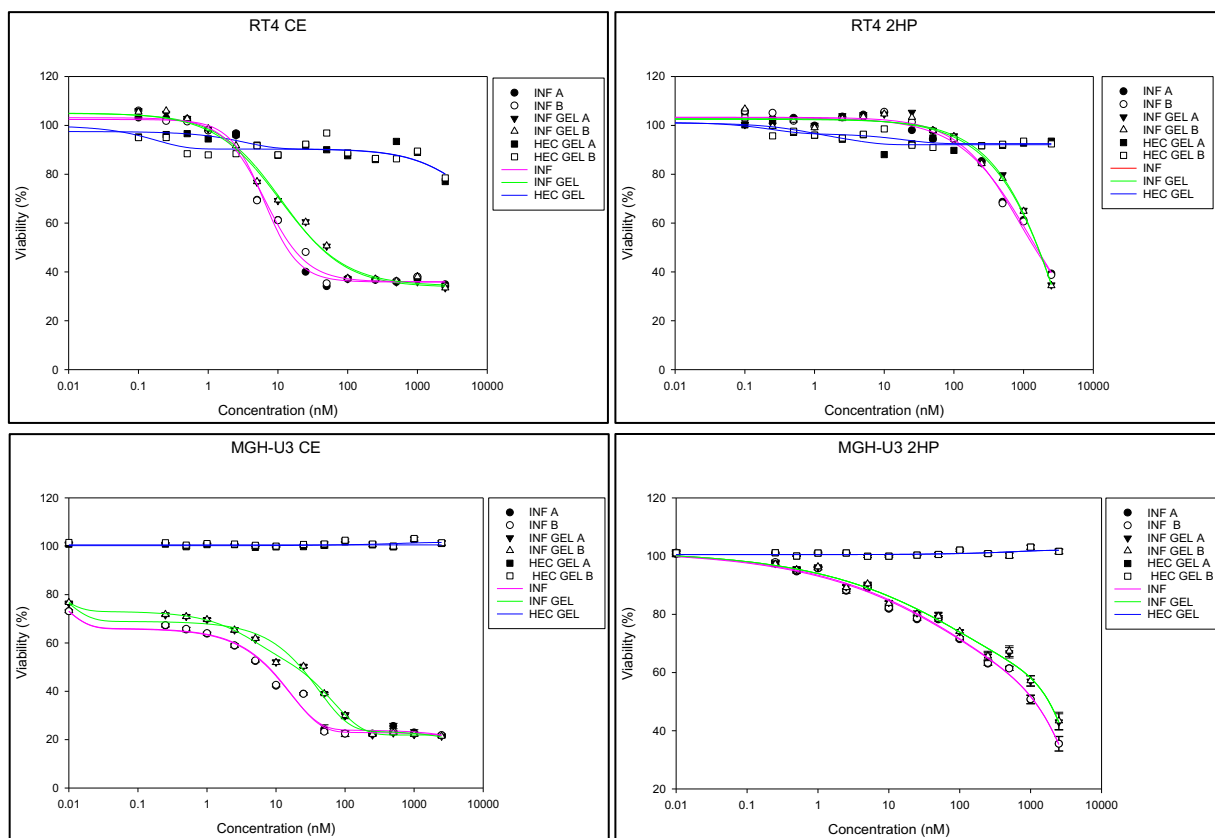


Figure 5-14: RT4 and MGH-U3 cells were treated with the INF, INF-loaded HEC hydrogel formulation (INF GEL) or the INF-free gel (HEC hydrogel) for continuous exposure of 72 hours (CE) or the 2 hour pulse (2HP). Cell viability was tested by Cell Titre Blue assay. Data represents n=2 experiments.

5.3.10 Discussion

The HEC and HPMC hydrogels were studied for their potential as an intravesical delivery of the anti-cancer drug INF for the treatment of bladder cancer. The HEC and HPMC hydrogels were loaded with INF using the sol-gel method. Hydrogel formulations were prepared with increasing HEC and HPMC concentrations (1, 1.5, 2, and 2.5% w/v) and INF loadings (1, 2.5 and 5% w/v), which were dispersed in the hydrogels using PEG that is commonly used as a cosolvent/dispersing agent (Ozkan, Esim et al. 2021). The INF-loaded HEC and HPMC

hydrogels were characterised for their syringe and catheter injectability, rheology, mucoadhesion, drug content, *in vitro* drug release, and cytotoxicity.

The unloaded and INF-loaded HEC, as well as HPMC hydrogels injectability results indicated that the force required to push them through the Foley catheter as well as the amount that passes through the catheter are directly related to the polymer concentration. Correspondingly, the hydrogels prepared using lower HEC and HPMC concentrations (1 and 1.5%) required lower forces to inject. Subsequently, more hydrogels can be pushed through the catheter due to their reduced viscosities. In contrast, the hydrogels with increased HEC and HPMC concentrations (2 and 2.5%) became more viscous and difficult to push through the catheter resulting in lower amounts of the hydrogels passing through the catheter. Therefore, using low concentrations (1%) of HEC and HPMC to develop INF-loaded hydrogels is more suitable for the intravesical delivery of INF for the treatment of bladder cancer to ensure that enough of the hydrogels will be delivered to the bladder. Although a 1% INF loading provided a slight reduction in the amount of hydrogel that could be pushed through the catheter, higher INF loadings will result in a more viscous hydrogel and consequently reduced hydrogel injectability based on the syringe injectability findings.

The use of repeated ramp runs mimicking continuous ramp mode to evaluate the rheological and thixotropic properties of the HEC and HPMC hydrogels supported the previously suggested theory. The results demonstrated that increased semi-solid hydrogel viscosities are associated with increased HEC and HPMC concentrations and INF loadings. The unloaded and 1% INF-loaded hydrogels with increased HEC and HPMC concentrations (2 and 2.5%) showed an

increased viscosity before demonstrating shear thinning behaviour, with the viscosity decreasing as the applied shear stress increased. Such rheological behaviour is undesirable to achieve good intravesical drug delivery, since the increased viscosity of the hydrogels will result in more difficulty to administer the INF-loaded hydrogels through the catheter. However, shear thinning may allow for more of the hydrogel to pass through the catheter as the shear increases. This will require enough force being applied to overcome the initial high viscosity. In contrast, both sets of hydrogels with lower polymeric concentrations (1 and 1.5%) and a 1% INF loading had greater shear thinning behaviour at low shear stresses due to their lower viscosity levels compared to the previous formulations, allowing for improved intravesical delivery through the catheter. However, increasing the INF loadings (2.5 and 5%) produced semi-solid hydrogels with higher viscosities, which further increased with an increase in polymer concentrations.

The increase in hydrogel viscosity and semi-solid thicker texture associated with increased HEC and HPMC concentrations is due to several factors. First, the increased inter- and intramolecular hydrogen bonds within the HEC polymeric chains and with the water (Meadows, Williams et al. 1995, Yamane, Aoyagi et al. 2006, Arfin and Bohidar 2012, Xu, Wang et al. 2021). Moreover, the presence of increased hydrophilic and hydrophobic groups with higher HPMC concentration allows it to form increased hydrogen bonds with water, as well as forming water cages over the hydrophobic clusters of HPMC chains leading to polymer extension forming coil-shaped structures. These structures form more hydrogen bonds with water and other coiled molecules, and subsequently increase hydrogels viscosity levels (Zarmpi, Flanagan et al. 2017, Hiremath, Nuguru et al. 2019, Petkova, Borlinghaus et al. 2020). Also, the increased *Van der Waals* forces with higher polymeric concentrations may also contribute significantly to link and

pack the cellulose network chains together along with the hydrogen bonding (Li, Lin et al. 2011, Chami Khazraji and Robert 2013). The increased viscosity levels of the HEC hydrogels with increased INF loadings (2.5 and 5%) can be attributed to the increased PEG, which can interact with the hydrogels polymeric chains through hydrogen bonding between the -OH groups of the HEC and -OH groups of the PEG forming highly crosslinked network, especially with higher HEC concentrations (Kim and Jung 2007, Reddy, Babu et al. 2013). Also, the presence of an increased concentration of INF drug itself may have an influence over the hydrogel rheological properties that require further investigations to identify. On the other hand, the 2.5% INF-loaded HPMC hydrogels rheological investigation results demonstrated an altered thixotropic behaviour during the second ramp run, mainly with lower HPMC hydrogel concentrations (1 and 1.5%) as the stress increased. In addition, the HPMC hydrogels showed a reduction in their viscosity levels with higher INF loading (5%), as well as decreased HPMC concentration, but with an increased initial viscosity at lower shear stress. This behaviour may be related to the presence of PEG, which at increased levels with higher HPMC hydrogel loadings (2 and 2.5%) can increase their viscosities through the same mechanism as with the HEC hydrogels. However, the reduced miscibility of higher PEG levels with decreased HPMC hydrogel concentration (1%) influences the hydrogel homogeneity and has a greater impact on its viscosity under an applied stress, which also suggest that hydrogel texture was affected as the stress increased and observed during the second ramp run (Illiger, Fadnis et al. 2009). As a result, the hydrogel formulations based on low HEC and HPMC concentration (1%), as well as low loading (1%) are more suitable for the development of INF-loaded hydrogels for the intravesical delivery in the treatment of bladder cancer.

The unloaded and INF-loaded HEC hydrogels demonstrated concentration dependent mucoadhesive properties that increase with higher viscosity levels (Jones, Woolfson et al. 1996, Jones, Woolfson et al. 1996, Jones, Woolfson et al. 1997, Ivarsson and Wahlgren 2012, Tang, Shan et al. 2019). This is related to the higher molecular adhesive bonds between the mucin and the increased HEC concentrations, as well as to the increased adhesive interaction between the crosslinked HEC hydrogels and higher INF/PEG loadings. The unloaded and INF-loaded HPMC hydrogels showed relatively similar trend to the HEC hydrogels. However, the impact of increased INF loadings on their increased adhesive properties were not significant ($p>0.05$) compared to their unloaded and INF-loaded HEC hydrogels. This behaviour may be due to the reduced molecular bonding between the more concentrated HPMC loaded hydrogels and the mucin, as their mucoadhesive properties are related to the physical interlocking with mucus (Bravo-Osuna, Noiray et al. 2012, da Silva, dos Santos et al. 2021). The higher INF/PEG loadings in the HPMC hydrogels have non-significantly ($p>0.05$) increased their adhesive features by improving the molecular interaction with the mucin. Generally, the hydrogels with increased HEC and INF loadings offered greater mucoadhesion compared to the HPMC hydrogels, which can provide further improved adhesive profiles with extended contact duration with the mucin (Jones, Woolfson et al. 1997). However, their increased viscosity and thick texture make them difficult to use for intravesical delivery for the treatment of bladder cancer.

The INF content investigations were performed on all HEC and HPMC hydrogels (1, 1.5, 2 and 2.5%) loaded with INF (1, 2.5, and 5%). The INF-loaded HEC hydrogels results demonstrated a reduction in their INF contents as the drug loading increased from 1 to 5% in the hydrogels with lower HEC concentrations (1 and 1.5%). However, the higher HEC hydrogel

concentrations (2 and 2.5%) showed non-significant ($p>0.05$) differences between their INF contents. The reduction in the INF content as the HEC and INF loading increased is due to the increased hydrogel chains swelling density as well as viscosity, thereby entrapping and limiting the INF movement following its dispersion (Ramadan, Elbakry et al. 2018). The INF-loaded hydrogels with increased HPMC hydrogel concentrations (2 and 2.5%) showed a non-significant ($p>0.05$) difference in the INF content between different formulations, while the lower HPMC hydrogel concentrations (1 and 1.5%) demonstrated a significant ($p<0.05$) reduction and reduced INF homogeneity as the drug loading increased to 5%. This can be confirmed by the rheology results, which suggest reduced HPMC/PEG miscibility as the concentration of HPMC decreases and PEG/INF loading increases. Subsequently, a reduced hydrogels viscosity, and thus limited INF entrapment within the hydrogels especially with the hydrophobic nature of INF. Overall, these findings indicate that both HEC and HPMC loaded hydrogels utilized improved INF content homogeneity at higher hydrogel polymeric concentrations (2 and 2.5%), while the HEC loaded hydrogels offered better INF content at lower polymeric concentrations compared to the HPMC loaded hydrogels. Therefore, the formulations based on low HEC hydrogel concentration (1%) and INF loading (1%) is more suitable for the intravesical delivery of INF for the treatment of bladder cancer due to its higher INF content and easier administration through a catheter.

The release of INF from the HEC and HPMC hydrogels showed a rapid ‘burst’ release associated with the low HEC (1 and 1.5%), HPMC (1%) hydrogels concentrations, as well as INF loading (1%). As the HEC and HPMC concentrations and INF loadings increased the percent release of INF reduces over 24 hours. This can be related to the different phases of INF

release from the hydrogels. First, the erosion phase of the outer surface of the hydrogels by the release media, followed by gradual penetration through the hydrogels' swollen and interconnected chains, followed by INF dissolution in the release media, diffusion through the gel and release. Thereby, the release rate is governed by the rate of release media penetration into the hydrogels, and correspondingly the INF diffusion into the release media (Dias, SAKHARE et al. 2009, Ramadan, Elbakry et al. 2018). Therefore, the fast release rate from the hydrogels is mainly related to the reduced viscosity and swelling of the hydrogels with the lower polymer concentrations allowing for faster hydrogel erosion, and diffusion of the INF decreasing the time to diffuse into the release media. In contrast, the slower release profiles of the loaded hydrogels were related to the increased polymer chain swelling and viscosity in the higher HEC and HPMC concentration (2 and 2.5%) and higher INF loading (2.5 and 5%) hydrogels. Consequently, increased media penetration and erosion times of the hydrogels as well as the high loading of INF within the formulations resulted in reduced diffusion and thus slower release profiles (Abd-Allah, Dawaba et al. 2010). These results demonstrate that the 1% HEC and HPMC hydrogels with a 1% INF loading released most of their INF content within 24 hours. However, the 1% HEC hydrogel with a 1% INF loading had a more sustained release profile over 24 hours compared to the same HPMC hydrogel, which is the maximum duration for the INF-loaded hydrogels inside the urinary bladder. Accordingly, it is considered to be the more preferable formulation for the intravesical delivery of INF for the treatment of bladder cancer.

Overall, the potentially ideal hydrogel for the intravesical delivery of INF for the treatment of NMIBC should provide a shear thinning and stable thixotropic behaviour during the rheological evaluation rather than an increase in the viscosity levels following drug loading. The shear thinning property of lower viscosity INF-loaded hydrogel under shear stress and the rapid recovery to their original condition (<5 s) after the strain removal facilitates an easier extrusion. This is considered to be a self-healing feature that allow their injection through catheter without clogging, making them highly desirable for localised and sustained drug delivery and release at the target site of action while minimizing the side effects often associated with systemic delivery (Uman, Dhand et al. 2020, Gruschwitz, Hausig et al. 2022). Unlike more viscous INF-loaded hydrogel that may accumulate at certain areas without covering the urinary bladder wall completely following its administration, the shear thinning behaviour is helpful for the injected hydrogels to take the local shape of the bladder leading to obtain maximal interfacial contact between the hydrogel and the bladder tissue wall, and hence improving the chemotherapeutic drug distribution over the bladder wall. Correspondingly, this will lead to improving the INF retention time to achieve better delivery across the bladder wall and its complete release within 24 hours from the hydrogel compared to the free drug without hydrogel. Ultimately, using hydrogel of low viscosity rates facilitates its easy elimination during urination process. Therefore, our findings suggested that 1% HEC hydrogel loaded with 1% INF is considered to be the most optimal formulation that meets the previously indicated properties to be used for the intravesical delivery for the localised treatment of NMIBC. The increased residence time of INF in the bladder by the loaded HEC hydrogel need to be investigated using an *in-vitro* model, followed by an animal study to evaluate its efficacy and toxicity for NIMBC treatment.

In the cellular antiproliferation assays, the INF selectively inhibited proliferation of cancer cells with FGFR genetic alterations and/or protein overexpression, while it was not efficacious on cancer cell lines in which FGFRs were either not expressed or not altered. It was suggested that 45% of cases of NMIBC exhibit mutations in FGFR, indicating that a targeted therapy of INF may be a suitable candidate if it can be effectively delivered via intravesical administration. This route of administration is likely to be well-tolerated and may present a means to circumvent the dose-limiting toxicities associated with systemic administration. The INF-loaded HEC hydrogel formulation showed the equivalent anti-tumour effect of the free INF and would be predicted to prolong the residence time of INF in the bladder. The data indicated that the INF-loaded HEC hydrogel formulation has a promising anti-bladder cancer effect on the FGFR mutant cell lines which provide the potential application in clinical practice.

The cell viability assays on bladder cancer cell lines were performed using CellTiter Blue method as reported for bladder cancer cells, while MTT method has been reported to be commonly used with pancreatic cancer cell lines (Kim, Park et al. 2015, Sathe and Nawroth 2018, Guzmán, Pitts et al. 2019, Hindupur, Schmid et al. 2020, Whyard, Liu et al. 2020, Sevgin, Coban et al. 2021). There are some limitations related to MTT assay including lack of sensitivity compared to other fluorescent and luminescent methods for detecting viable cell number. Also, an increased background absorbance values can be resulted from varying assays conditions that affect the chemical or enzymatic reduction of MTT. The MTT reagent may results in cytotoxic effects upon adding the reagent to estimate the cell viability as reported for eukaryotic cells (Riss 2017).

5.4 Conclusion

The INF-loaded HEC and HPMC hydrogels were prepared using the sol-gel method. 24 INF-loaded hydrogel formulations were developed and investigated. The INF-loaded HEC and HPMC hydrogels were characterized for their physical properties, injectability, and drug content distribution within the hydrogels. Both hydrogel properties are varied depending on their polymeric concentration and the INF loading rate. The influence of polymers and loading concentrations on the INF release profiles from both hydrogels were investigated. The rate of INF release of from both HEC and HPMC hydrogels was inversely related to the polymers and drug loading concentrations. One INF-loaded hydrogel formulation, the 1% HEC hydrogel loaded with 1% INF was selected as the most optimised formulation for cytotoxicity evaluation against several bladder cancer cell lines based on its mechanical properties, INF content, as well as *in vitro* release profile. The cytotoxicity evaluation suggested that the INF-loaded HEC hydrogel formulation has a promising anti-bladder cancer effect on the FGFR mutant cell lines which provide a potential application in clinical practice for the bladder cancer treatment.

Chapter 6: General discussion and future work

6.1 General discussion

6.1.1 Pancreatic cancer

Pancreatic cancer is one of the most common types of cancer, which is associated with high mortality and low survival rates despite the amount of research into this malignant disease. This increases the need for the development of novel techniques for the delivery of chemotherapeutic drugs following surgical resection in order to achieve better treatment outcomes. IRN has been used as a part of the FOLFIRINOX regimen (IRN, 5-Fluorouracil, Leucovorin, and Oxaliplatin) for systemic treatment of pancreatic cancer (Suker, Beumer et al. 2016). The drug delivery system in our study was designed for post-operative localised delivery of IRN at the tumour resection margins. The drug delivery system consisted of hydrogel and aerogel implants using agar polymer. These implants were expected to improve the delivery of IRN, while minimizing its systemic toxic effect on healthy tissues by their direct implantation at the resection tissue margins to eradicate any remaining cancer cells and preventing their metastasis.

In this study, the IRN loaded agar hydrogels, pre- and post-loaded agar aerogels implants were developed as drug delivery systems for the post-surgical localised treatment of pancreatic cancer. These loaded agar hydrogels and aerogels have been characterised for their physical properties, while the pre- and post-loaded agar aerogels were assessed for their cytotoxicity against different pancreatic cancer cells.

6.1.1.1 The IRN-loaded agar hydrogels

Prior to the development of the IRN-loaded agar hydrogels, several hydrogel formulations were prepared with increasing agar (2, 2.5, 3, and 3.5%) and model drug (caffeine) (1, 5, and 10%) loadings using the sol-gel method. The hydrogels were investigated for their mechanical strength, adhesion, rheology, content distribution, as well as *in vitro* drug release. Based on the characterization, the mechanical properties, drug content distribution, as well as the drug release were most affected by changes in the amount of the agar and drug loading. Generally, the hydrogels mechanical strength and elastic properties increased with increasing agar concentration and drug loading. The adhesive properties of the hydrogels decreased with increasing agar concentration and drug loading, which is related to their increased elastic properties (Zosel 1989, Grillet, Wyatt et al. 2012). In addition, the drug content distribution within the hydrogels was varied based on the agar and drug loading concentrations. The release of caffeine from most hydrogels showed an initial ‘burst’ release for most formulations. As both the caffeine and agar loadings increase, the release percentage of caffeine reduces within the first 3-6 hours with sustained release over the remaining 48 hours. From the 12 caffeine loaded agar hydrogel formulations, Four agar hydrogels 2, 2.5, 3 and 3.5% with drug loading of 5% were chosen for further analysis in this project. The mechanical features, content distribution, and *in vitro* drug release profiles were the main criteria to determine the optimised agar hydrogel formulations to take forward using IRN.

The selected hydrogel formulations were prepared with agar concentrations of 2, 2.5, 3, and 3.5%, and IRN loading of 5% using the same sol-gel method and characterized for their mechanical strength, adhesion, rheology, content distribution, as well as *in vitro* drug release.

The investigations results were relatively in agreement with the previous findings using caffeine as a model drug. Two IRN-loaded hydrogel formulations, the 2 and 2.5% agar hydrogels loaded with 5% IRN were determined to be the most optimised formulations.

6.1.1.2 The IRN pre- and post-loaded agar aerogels

The development process for obtaining the optimised agar loaded aerogels took several steps. They were loaded with a model drug caffeine using two different techniques. First, the sol-gel method, followed by lyophilization technique. Different preloaded aerogel formulations were prepared with increased agar (2, 2.5, 3, and 3.5%) and caffeine (1, 5 and 10%) loadings. Second, the aerogels were prepared using the same sol-gel, freeze-drying methods and agar concentrations. The aerogels were then post-loaded with the caffeine. Several post-loaded aerogels were prepared with increased agar (2, 2.5, 3, and 3.5%) and increased caffeine loadings (1, 2, and 3 ml) of every caffeine concentration (1, 5, and 10% w/v). The pre- and post-loaded agar aerogels were investigated for strength, porosity, swelling, drug content, as well as *in vitro* drug release to evaluate the effect of loading method and rate. Generally, the aerogels demonstrated more flexibility and lower mechanical strength compared to the hydrogels. The improved mechanical properties were associated with aerogels prepared using a high agar concentration and drug loadings, while those prepared using a decreased agar concentration and drug loading produced aerogels with a reduced mechanical strength. The post-loading method into aerogels produced aerogels with lower mechanical strength compared to free aerogels. The porosity and swelling rates of the agar aerogels was reduced as the agar concentration increased. The preloaded agar aerogels demonstrated relatively better caffeine content distribution

compared to the loaded agar hydrogels, while the post-loaded agar aerogels showed an improved homogenous caffeine distribution as the post-loading concentration increased.

Most preloaded aerogels demonstrated a rapid 'burst' release of caffeine for all drug loadings. However, the initial release rate of caffeine reduces hours with sustained release over the 48 hours as the agar concentration and caffeine loadings increased. The release rate is controlled by the rate of release media diffusion into the aerogels, and accordingly the caffeine diffusion through the network pores towards the release media. However, the slower sustained release from preloaded aerogels were associated with the reduced porous network in the aerogels with higher agar concentrations and higher drug loading. The post-loaded agar aerogels were able to decrease the release rate of caffeine as the agar concentration increased. Four agar preloaded aerogels 2, 2.5, 3 and 3.5% with drug loading of 5%, while 12 agar post-loaded aerogels 2, 2.5, 3 and 3.5% with drug loading of 1% of increased volume were selected as the optimised formulations for additional investigation in this study using IRN.

The IRN pre- and post-loaded agar aerogels were prepared using the chosen optimized concentrations. The IRN preloaded aerogels mechanical features were improved as the agar concentration increased, while their IRN distribution levels were improved as the agar concentration of the aerogels decreased. The effect of agar concentration loading method and concentration on the release of IRN from both pre- and post-loaded agar aerogels were studied. The release profiles of IRN from preloaded aerogel formulations varied depending on the agar concentration, while post-loaded aerogels showed slower sustained release rates varied based on the IRN loading volume.

The cytotoxicity of the optimised IRN pre- and post-loaded agar aerogels against two cancer cell lines MIA PaCa-2 and Panc-1 cells were investigated. Generally, both types of IRN-loaded agar aerogels demonstrated more cytotoxic effect against Panc-1 cells compared to MIA PaCa-2 cells. The IRN-preloaded aerogel with reduced agar concentration demonstrated faster and lower reduction in the cell viability compared to the other IRN-preloaded aerogels with increased agar concentrations. However, all IRN-preloaded agar aerogels produced stronger cytotoxic effect against Panc-1 cells. Similarly, all IRN post-loaded agar aerogels achieved the same cytotoxic effect against Panc-1 cells. Nevertheless, the cytotoxicity of the aerogels with increased agar concentration and low post-loading of IRN against MIA PaCa-2 cells was lower compared to those aerogels of reduced agar concentrations and higher post-loaded IRN. As the IRN post loading increased in every agar aerogel, the formulations varied significantly ($p < 0.05$). However, the cytotoxicity of low agar aerogels with increased 1% IRN post-loading volumes against Panc-1 cells resulted in a rapid reduced cell viability compared to the MIA PaCa-2 cells. The higher agar aerogels of low 1% IRN post-loading (1 ml) demonstrated lower cytotoxicity within 24 hours treatment compared to the same aerogels with increased post-loading rates, and to the aerogels with lower agar concentrations (2 and 2.5%) with similar IRN post-loading. Subsequently, four IRN-loaded agar aerogel formulations, the 2 and 2.5% agar aerogels preloaded with 5% IRN, and post-loaded with 3 ml of 1% IRN were determined to be the most optimised formulations as implantable drug delivery systems for post-surgical localised treatment of pancreatic cancer based on their cytotoxicity assessment.

6.1.2 Bladder cancer

Bladder cancer is a complicated disease, as the majority of cases are diagnosed with NMIBC tumours. However, approximately one third of NMIBCs will progress to MIBCs that require radical treatment and associated with substantial rate of morbidity and mortality if not managed and treated properly (Bryan 2013, Farling 2017, Stewart 2020, Hussein, Elsayed et al. 2021). It was reported that some patients with high risk NMIBC are not responding to the current treatment based on immunotherapy. Therefore, there is an urgent need to develop a new alternative chemotherapy, while ensuring the delivery of chemotherapeutic drugs at sufficient concentrations to the bladder in order to yield improved treatment outcomes. The treatment of bladder cancer using FGFR inhibitors is under investigation. In this study, we designed a drug delivery system based on hydrogels of HEC and HPMC for the intravesical delivery of INF, which is a potent FGFR inhibitor. These hydrogels were supposed to potentially improve the efficacy of the INF by facilitating their delivery into the urinary bladder by a catheter, while they spread across the bladder wall and increasing the INF retention in the bladder.

In this project, the INF-loaded HEC and HPMC hydrogels were developed to enhance the INF delivery to the bladder and to achieve better NMIBC treatment. These hydrogels were evaluated for their physical properties, INF content and release profiles, as well as cytotoxicity against different FGFR mutant and non-mutant cell lines.

6.1.2.1 INF-loaded HEC and HPMC hydrogels

Different hydrogel formulations were prepared with increased HEC and HPMC concentrations (1, 1.5, 2, and 2.5%) and INF loading (1, 2.5, and 5%) using the sol-gel method.

All hydrogels were characterized for their injectability, rheology, adhesion, content distribution, *in vitro* release, and cytotoxicity. The characterization outcomes showed that all these parameters were affected by varying the HEC and HPMC polymeric concentrations and INF loadings.

The injectability of INF-loaded hydrogels with lower HEC and HPMC concentrations (1 and 1.5%) and INF loading (1%) required lower forces and higher hydrogel amount can be pushed through the catheter due to their reduced viscosities and good shear thinning properties based on the rheological analysis. The viscosity and semi-solid thick texture of the hydrogels increased with higher HEC and HPMC concentrations (2 and 2.5%). Higher INF loadings into the HEC hydrogels has led to higher viscosities resulted from of the additional hydrogen bonding with PEG, while altered thixotropic behaviour and reduced viscosities were observed in the hydrogels with lower HPMC (1 and 1.5) and higher INF loadings (2.5 and 5%).

The INF-loaded HEC hydrogels showed concentration dependent mucoadhesive features. The higher INF/PEG loadings in the HPMC hydrogels have non-significantly ($p>0.05$) increased their adhesive features by improving the molecular interaction with the mucin. The higher HEC and HPMC hydrogel concentrations showed non-significant ($p>0.05$) differences between their INF contents. The lower HPMC hydrogel concentrations showed a significant ($p<0.05$) reduction and reduced INF homogeneity as the drug loading increased. The release of INF from the HEC and HPMC hydrogels showed a rapid 'burst' release associated with the low HEC (1 and 1.5%), HPMC (1%) hydrogels concentrations, as well as INF loading (1%). As the HEC and HPMC concentrations and INF loadings increased, the percent release of INF reduces over

24 hours. One INF-loaded hydrogel formulation, the 1% HEC hydrogel loaded with 1% INF was chosen as the optimised formulation for cytotoxicity evaluation against different bladder cancer cell lines based on its mechanical properties, INF content, as well as *in vitro* release profile.

The cytotoxicity of the optimised INF-loaded HEC hydrogel against FGFR mutant and non-mutant cancer cells demonstrated that the INF selectively inhibited proliferation of FGFR mutant cancer cells, while it was not efficacious on non-mutant FGFRs cancer cell lines. The targeted therapy of INF by intravesical administration can be an effective for NMIBC cases associated with FGFR mutations. The INF-loaded HEC hydrogel formulation demonstrated similar cytotoxic effect of the free INF and would prolong the INF residence time in the bladder. The INF-loaded HEC hydrogel formulation demonstrated an encouraging anti-bladder cancer effect on the FGFR mutant cell lines which provide the possible application in clinical application.

6.2 Future work

The cytotoxicity study using IRN-loaded agar hydrogels should be performed soon. An *in vivo* study to evaluate the IRN-loaded agar hydrogels and aerogels efficacy and toxicity should be investigated for post-surgical treatment of pancreatic cancer. Modification in the hydrogels and aerogels structural components could improve their physical features. The agar hydrogel solution needs to be mixed with PAAEE to produce physically crosslinked synergistic double network capable to enhance the mechanical strength for both formulations especially post-loaded aerogels and self-recovery under physical stress, as well as the adhesive properties of the

hydrogels through increased hydrogen bonding and Vander der Waals interactions (Zhang, Ren et al. 2019). Some experiments should be carried out to investigate the effect of agar-PAAEE complex on the formulations swelling, porosity, drug content distribution, the release profiles of IRN from hydrogels and aerogels, and cytotoxicity and compared to IRN-loaded agar hydrogels and aerogels. The agar and agar-PAAEE hydrogels and aerogels should be studied using the remaining FOLFIRINOX drugs either individually and/or as combination regimen through different loading methods. The increased residence time of INF in the bladder by the loaded HEC hydrogel need to be investigated using an *in-vitro* model, followed by an animal study to evaluate its efficacy and toxicity for NIMBC treatment.

References

- Abbas, M., et al. (2017). "Antitumor photodynamic therapy based on dipeptide fibrous hydrogels with incorporation of photosensitive drugs." *ACS Biomaterials Science & Engineering* 4(6): 2046-2052.
- Abd-Allah, F. I., et al. (2010). "Preparation, characterization, and stability studies of piroxicam-loaded microemulsions in topical formulations." *Drug Discov Ther* 4(4): 267-275.
- Abdelaty, M. S. (2022). "The Influence of pH/Salt Concentrations on Tuning Lower Critical Solution Temperature of Poly (NIPAAm-co-DMAA-co-DTBAVA) Multi-Environmentally Terpolymer." *Journal of Polymers and the Environment*: 1-16.
- Abufaraj, M., et al. (2018). "What to do during Bacillus Calmette–Guérin shortage? Valid strategies based on evidence." *Current opinion in urology* 28(6): 570-576.
- Ahmad, V., et al. (2021). Chapter 3 - Biomedical applications of aerogel. *Advances in Aerogel Composites for Environmental Remediation*. A. A. P. Khan, M. O. Ansari, A. Khan and A. M. Asiri, Elsevier: 33-48.
- Ahmed, E. M. (2013). "Hydrogel: preparation, characterization, and applications." *Journal of advanced research*.
- Ahuja, G. and K. Pathak (2009). "Porous carriers for controlled/modulated drug delivery." *Indian journal of pharmaceutical sciences* 71(6): 599-607.
- Akala, E. O., et al. (1998). "Novel pH-sensitive hydrogels with adjustable swelling kinetics." *Biomaterials* 19(11): 1037-1047.
- Ali, A., et al. (2021). "Control of Glucose-Induced Degradation and Cargo Release in Multi-Responsive Polymer Hydrogels." *Macromolecular Chemistry and Physics* 222(16): 2100121.
- Ali, O. A., et al. (2009). "Infection-mimicking materials to program dendritic cells in situ." *Nature materials* 8(2): 151-158.
- Allen, T. M. and P. R. Cullis (2004). "Drug delivery systems: entering the mainstream." *Science* 303(5665): 1818-1822.
- Alnaief, M., et al. (2012). "A novel process for coating of silica aerogel microspheres for controlled drug release applications." *Microporous and mesoporous materials* 160: 167-173.
- Alnaief, M., et al. (2012). "A novel process for coating of silica aerogel microspheres for controlled drug release applications." *Microporous and Mesoporous Materials* 160: 167-173.

- Alnaief, M. and I. Smirnova (2010). "Effect of surface functionalization of silica aerogel on their adsorptive and release properties." *Journal of Non-Crystalline Solids* 356(33): 1644-1649.
- Andersson, J., et al. (2004). "Influences of Material Characteristics on Ibuprofen Drug Loading and Release Profiles from Ordered Micro- and Mesoporous Silica Matrices." *Chemistry of Materials* 16(21): 4160-4167.
- Andrade, F., et al. (2021). "Stimuli-responsive hydrogels for cancer treatment: The role of pH, light, ionic strength and magnetic field." *Cancers* 13(5): 1164.
- Antoni, S., et al. (2017). "Bladder cancer incidence and mortality: a global overview and recent trends." *European urology* 71(1): 96-108.
- Araki, C. (1956). "Structure of the agarose constituent of agar-agar." *Bulletin of the Chemical Society of Japan* 29(4): 543-544.
- Arango, D., et al. (2004). "Molecular mechanisms of action and prediction of response to oxaliplatin in colorectal cancer cells." *British Journal of Cancer* 91(11): 1931-1946.
- Arends, T. J., et al. (2016). "Results of a randomised controlled trial comparing intravesical chemohyperthermia with mitomycin C versus bacillus Calmette-Guérin for adjuvant treatment of patients with intermediate-and high-risk non-muscle-invasive bladder cancer." *European urology* 69(6): 1046-1052.
- Arfin, N. and H. B. Bohidar (2012). "Concentration selective hydration and phase states of hydroxyethyl cellulose (HEC) in aqueous solutions." *International Journal of Biological Macromolecules* 50(3): 759-767.
- Armisen, R. and F. Gaiatas (2009). *Agar. Handbook of hydrocolloids*, Elsevier: 82-107.
- Armisen, R. and F. Galatas (1987). "Production, properties and uses of agar." *Production and utilization of products from commercial seaweeds. FAO Fish. Tech. Pap* 288: 1-57.
- Arruebo, M. (2012). "Drug delivery from structured porous inorganic materials." *Wiley Interdisciplinary Reviews: Nanomedicine and Nanobiotechnology* 4(1): 16-30.
- Ashtikar, M. and M. G. Wacker (2018). "Nanopharmaceuticals for wound healing – Lost in translation?" *Advanced drug delivery reviews* 129: 194-218.
- Atma, Y. (2021). "Synthesis and Application of Fish Gelatin for Hydrogels/Composite Hydrogels: A Review." *peptides* 22: 23.
- Au, J. L.-S., et al. (2002). "Clinical aspects of drug delivery to tumors." *Journal of Controlled Release* 78(1-3): 81-95.

Avramis, V. I., et al. (2002). "A randomized comparison of native *Escherichia coli* asparaginase and polyethylene glycol conjugated asparaginase for treatment of children with newly diagnosed standard-risk acute lymphoblastic leukemia: a Children's Cancer Group study." *Blood* 99(6): 1986-1994.

Aymard, P., et al. (2001). "Influence of thermal history on the structural and mechanical properties of agarose gels." *Biopolymers: Original Research on Biomolecules* 59(3): 131-144.

Bailly, C. (2019). "Irinotecan: 25 years of cancer treatment." *Pharmacological Research* 148: 104398.

Bao, X., et al. (2010). "Novel agarose and agar fibers: Fabrication and characterization." *Materials Letters* 64(22): 2435-2437.

Barrios, E., et al. (2019). "Nanomaterials in Advanced, High-Performance Aerogel Composites: A Review." *Polymers* 11(4): 726.

Berio, M., et al. (2021). "Synthesis and applications of graphene oxide aerogels in bone tissue regeneration: a review." *Materials Today Chemistry* 20: 100422.

Bertasa, M., et al. (2020). "Agar gel strength: A correlation study between chemical composition and rheological properties." *European Polymer Journal* 123: 109442.

Betz, M., et al. (2012). "Preparation of novel whey protein-based aerogels as drug carriers for life science applications." *The Journal of Supercritical Fluids* 72: 111-119.

Bilensoy, E., et al. (2009). "Intravesical cationic nanoparticles of chitosan and polycaprolactone for the delivery of Mitomycin C to bladder tumors." *International Journal of Pharmaceutics* 371(1-2): 170-176.

Bilimoria, K. Y., et al. (2007). "Extent of surgery affects survival for papillary thyroid cancer." *Annals of surgery* 246(3): 375-384.

Bin Riaz, I., et al. (2021). "Bladder cancer: shedding light on the most promising investigational drugs in clinical trials." *Expert Opinion on Investigational Drugs* 30(8): 837-855.

Birder, L. A. (2005). "More than just a barrier: urothelium as a drug target for urinary bladder pain." *American Journal of Physiology-Renal Physiology* 289(3): F489-F495.

Bosetti, C., et al. (2014). "Diabetes, antidiabetic medications, and pancreatic cancer risk: an analysis from the International Pancreatic Cancer Case-Control Consortium." *Annals of Oncology* 25(10): 2065-2072.

Brannon-Peppas, L. and N. A. Peppas (1990). "Dynamic and equilibrium swelling behaviour of pH-sensitive hydrogels containing 2-hydroxyethyl methacrylate." *Biomaterials* 11(9): 635-644.

Brausi, M., et al. (2014). "Side effects of Bacillus Calmette-Guerin (BCG) in the treatment of intermediate-and high-risk Ta, T1 papillary carcinoma of the bladder: results of the EORTC genito-urinary cancers group randomised phase 3 study comparing one-third dose with full dose and 1 year with 3 years of maintenance BCG." *European urology* 65(1): 69-76.

Bravo-Osuna, I., et al. (2012). "Interfacial Interaction between Transmembrane Ocular Mucins and Adhesive Polymers and Dendrimers Analyzed by Surface Plasmon Resonance." *Pharmaceutical research* 29(8): 2329-2340.

Brazel, C. and N. Peppas (1999). "Recent studies and molecular analysis of drug release from swelling-controlled devices." *STP pharma sciences* 9(5): 473-485.

Brazel, C. S. and N. A. Peppas (1999). "Mechanisms of solute and drug transport in relaxing, swellable, hydrophilic glassy polymers." *Polymer* 40(12): 3383-3398.

Bromberg, L. E. and E. S. Ron (1998). "Temperature-responsive gels and thermogelling polymer matrices for protein and peptide delivery." *Advanced drug delivery reviews* 31(3): 197-221.

Bryan, R. T. (2013). "Update on bladder cancer diagnosis and management." *Trends in Urology & Men's Health* 4(5): 7-11.

Buckley, C. T., et al. (2009). "The effect of concentration, thermal history and cell seeding density on the initial mechanical properties of agarose hydrogels." *Journal of the Mechanical Behavior of Biomedical Materials* 2(5): 512-521.

Cacicedo, M. L., et al. (2018). "Bacterial cellulose hydrogel loaded with lipid nanoparticles for localized cancer treatment." *Colloids and Surfaces B: Biointerfaces* 170: 596-608.

Caló, E. and V. V. Khutoryanskiy (2015). "Biomedical applications of hydrogels: A review of patents and commercial products." *European Polymer Journal* 65: 252-267.

Cambier, S., et al. (2016). "EORTC nomograms and risk groups for predicting recurrence, progression, and disease-specific and overall survival in non-muscle-invasive stage Ta-T1 urothelial bladder cancer patients treated with 1-3 years of maintenance bacillus Calmette-Guérin." *European urology* 69(1): 60-69.

Cao, H., et al. (2021). "Current hydrogel advances in physicochemical and biological response-driven biomedical application diversity." *Signal transduction and targeted therapy* 6(1): 1-31.

Carreño, G., et al. (2021). "Development of "on-demand" thermo-responsive hydrogels for anti-cancer drugs sustained release: Rational design, in silico prediction and in vitro validation in colon cancer models." *Materials Science and Engineering: C* 131: 112483.

Chami Khazraji, A. and S. Robert (2013). "Self-Assembly and Intermolecular Forces When Cellulose and Water Interact Using Molecular Modeling." *Journal of Nanomaterials* 2013: 745979.

Chang, L.-C., et al. (2009). "Optimization of epirubicin nanoparticles using experimental design for enhanced intravesical drug delivery." *International Journal of Pharmaceutics* 376(1-2): 195-203.

Chang, S., et al. (2022). "Advances of Stimulus-Responsive Hydrogels for Bone Defects Repair in Tissue Engineering." *Gels* 8(6): 389.

Chaudhary, J., et al. (2020). "Development of Biodegradable Agar-Agar/Gelatin-Based Superabsorbent Hydrogel as an Efficient Moisture-Retaining Agent." *Biomolecules* 10(6): 939.

Chen, J., et al. (2009). "Synthesis, swelling and drug release behavior of poly (N, N-diethylacrylamide-co-N-hydroxymethyl acrylamide) hydrogel." *Materials Science and Engineering: C* 29(7): 2116-2123.

Chen, P.-Y., et al. (2012). "Biological materials: Functional adaptations and bioinspired designs." *Progress in Materials Science* 57(8): 1492-1704.

Chen, P. C., et al. (2004). "Injectable microparticle-gel system for prolonged and localized lidocaine release. II. In vivo anesthetic effects." *Journal of Biomedical Materials Research Part A* 70(3): 459-466.

Chen, P. C., et al. (2004). "Injectable microparticle-gel system for prolonged and localized lidocaine release. I. In vitro characterization." *Journal of Biomedical Materials Research Part A* 70(3): 412-419.

Chen, S.-C., et al. (2004). "A novel pH-sensitive hydrogel composed of N,O-carboxymethyl chitosan and alginate cross-linked by genipin for protein drug delivery." *Journal of Controlled Release* 96(2): 285-300.

Cheng, L., et al. (2012). "Histologic grading of urothelial carcinoma: a reappraisal." *Human pathology* 43(12): 2097-2108.

Cheng, W., et al. (2017). "An overview of the binding models of FGFR tyrosine kinases in complex with small molecule inhibitors." *European journal of medicinal chemistry* 126: 476-490.

Choueiri, T. K., et al. (2014). "Neoadjuvant dose-dense methotrexate, vinblastine, doxorubicin, and cisplatin with pegfilgrastim support in muscle-invasive urothelial cancer: pathologic, radiologic, and biomarker correlates." *Journal of Clinical Oncology* 32(18): 1889.

Collaboration, G. B. o. D. C. (2017). "Global, Regional, and National Cancer Incidence, Mortality, Years of Life Lost, Years Lived With Disability, and Disability-Adjusted Life-years

for 32 Cancer Groups, 1990 to 2015: A Systematic Analysis for the Global Burden of Disease Study." *JAMA Oncology* 3(4): 524-548.

Compton, C. C., et al. (2012). Urinary bladder. *AJCC Cancer Staging Atlas*, Springer: 575-582.

Conroy, T., et al. (2011). "FOLFIRINOX versus gemcitabine for metastatic pancreatic cancer." *New England Journal of Medicine* 364(19): 1817-1825.

Conroy, T., et al. (2011). "FOLFIRINOX versus Gemcitabine for Metastatic Pancreatic Cancer." *New England Journal of Medicine* 364(19): 1817-1825.

Cook, M. T., et al. (2021). "Polymers exhibiting lower critical solution temperatures as a route to thermoreversible gelators for healthcare." *Advanced functional materials* 31(8): 2008123.

Coumoul, X. and C. X. Deng (2003). "Roles of FGF receptors in mammalian development and congenital diseases." *Birth Defects Research Part C: Embryo Today: Reviews* 69(4): 286-304.

Cox, E., et al. (2020). "Effects of Bladder Cancer on UK Healthcare Costs and Patient Health-Related Quality of Life: Evidence From the BOXIT Trial." *Clinical Genitourinary Cancer* 18(4): e418-e442.

Creemers, G. J., et al. (1994). "Topoisomerase I inhibitors: topotecan and irinotecan." *Cancer Treatment Reviews* 20(1): 73-96.

Cunningham, D., et al. (1998). "Randomised trial of irinotecan plus supportive care versus supportive care alone after fluorouracil failure for patients with metastatic colorectal cancer." *The Lancet* 352(9138): 1413-1418.

da Silva, J. B., et al. (2021). "Interaction between mucoadhesive cellulose derivatives and Pluronic F127: Investigation on the micelle structure and mucoadhesive performance." *Materials Science and Engineering: C* 119: 111643.

Dai, X. and C. Tan (2015). "Combination of microRNA therapeutics with small-molecule anticancer drugs: Mechanism of action and co-delivery nanocarriers." *Advanced drug delivery reviews* 81: 184-197.

Danenberg, P. V., et al. (2016). "Folates as adjuvants to anticancer agents: Chemical rationale and mechanism of action." *Crit Rev Oncol Hematol* 106: 118-131.

Dash, R., et al. (2013). "Improving the mechanical and thermal properties of gelatin hydrogels cross-linked by cellulose nanowhiskers." *Carbohydrate Polymers* 91(2): 638-645.

Daunys, S., et al. (2019). "Synergistic activity of Hsp90 inhibitors and anticancer agents in pancreatic cancer cell cultures." *Scientific reports* 9(1): 16177.

- Davis, M. E. (2002). "Ordered porous materials for emerging applications." *Nature* 417(6891): 813-821.
- De Jong, W. H. and P. J. Borm (2008). "Drug delivery and nanoparticles: applications and hazards." *International journal of nanomedicine* 3(2): 133.
- De Marco, I., et al. (2018). "An environmental study on starch aerogel for drug delivery applications: effect of plant scale-up." *The International Journal of Life Cycle Assessment* 23(6): 1228-1239.
- De Marco, I., et al. (2019). "Life cycle assessment of supercritical impregnation: Starch aerogel + α -tocopherol tablets." *The Journal of Supercritical Fluids* 143: 305-312.
- de Morais Zanata, D. and M. I. Felisberti (2022). "Thermo- and pH-responsive POEGMA-b-PDMAEMA-b-POEGMA triblock copolymers." *European Polymer Journal* 167: 111069.
- de Sousa Cavalcante, L. and G. Monteiro (2014). "Gemcitabine: Metabolism and molecular mechanisms of action, sensitivity and chemoresistance in pancreatic cancer." *European Journal of Pharmacology* 741: 8-16.
- de Vries, A., et al. (2017). "Protein oleogels from heat-set whey protein aggregates." *Journal of Colloid and Interface Science* 486: 75-83.
- Deszczynski, M., et al. (2003). "Effect of sugars on the mechanical and thermal properties of agarose gels." *Food Hydrocolloids* 17(6): 793-799.
- Dharunya, G., et al. (2016). "Curcumin cross-linked collagen aerogels with controlled anti-proteolytic and pro-angiogenic efficacy." *Biomedical Materials* 11(4): 045011.
- Di Stasi, S. M., et al. (2006). "Sequential BCG and electromotive mitomycin versus BCG alone for high-risk superficial bladder cancer: a randomised controlled trial." *The lancet oncology* 7(1): 43-51.
- Dias, R. J., et al. (2009). "Design and development of mucoadhesive acyclovir tablet."
- Divrik, R. T., et al. (2006). "The effect of repeat transurethral resection on recurrence and progression rates in patients with T1 tumors of the bladder who received intravesical mitomycin: a prospective, randomized clinical trial." *The Journal of urology* 175(5): 1641-1644.
- Du, A., et al. (2013). "A special material or a new state of matter: a review and reconsideration of the aerogel." *Materials* 6(3): 941-968.
- Edge, S. B., et al. (2010). *AJCC cancer staging manual*, Springer New York.

Edge, S. B. and C. C. Compton (2010). "The American Joint Committee on Cancer: the 7th Edition of the AJCC Cancer Staging Manual and the Future of TNM." *Annals of Surgical Oncology* 17(6): 1471-1474.

Edsman, K., et al. (1998). "Rheological evaluation of poloxamer as an in situ gel for ophthalmic use." *European journal of pharmaceutical sciences* 6(2): 105-112.

El-Aneed, A. (2004). "An overview of current delivery systems in cancer gene therapy." *Journal of Controlled Release* 94(1): 1-14.

Ethun, C. G. and D. A. Kooby (2016). "The importance of surgical margins in pancreatic cancer." *Journal of Surgical Oncology* 113(3): 283-288.

Fabra, M. J., et al. (2021). "Effect of biopolymer matrices on lactose hydrolysis by enzymatically active hydrogel and aerogels loaded with β -galactosidase nanoflowers." *Food Hydrocolloids* 111: 106220.

Faivre, S., et al. (2003). "DNA strand breaks and apoptosis induced by oxaliplatin in cancer cells." *Biochemical pharmacology* 66(2): 225-237.

Fakioğlu, M. and Y. Kalpaklı (2022). "Mechanism and behavior of caffeine sorption: affecting factors." *RSC advances* 12(41): 26504-26513.

Falamarzian, M. and J. Varshosaz (1998). "The effect of structural changes on swelling kinetics of polybasic/hydrophobic pH-sensitive hydrogels." *Drug development and industrial pharmacy* 24(7): 667-669.

Farling, K. B. (2017). "Bladder cancer: risk factors, diagnosis, and management." *The Nurse Practitioner* 42(3): 26-33.

Fathi, M., et al. (2019). "Dual thermo-and pH-sensitive injectable hydrogels of chitosan/(poly(N-isopropylacrylamide-co-itaconic acid)) for doxorubicin delivery in breast cancer." *International Journal of Biological Macromolecules* 128: 957-964.

Fatimi, A., et al. (2022). "Natural Hydrogel-Based Bio-Inks for 3D Bioprinting in Tissue Engineering: A Review." *Gels* 8(3): 179.

Feil, H., et al. (1992). "Mutual influence of pH and temperature on the swelling of ionizable and thermosensitive hydrogels." *Macromolecules* 25(20): 5528-5530.

Ferlay, J., et al. (2015). "Cancer incidence and mortality worldwide: Sources, methods and major patterns in GLOBOCAN 2012." *International Journal of Cancer* 136(5): E359-E386.

Ferlay, J., et al. (2013). "Cancer incidence and mortality patterns in Europe: Estimates for 40 countries in 2012." *European Journal of Cancer* 49(6): 1374-1403.

Finnbladder, N. B. C. S. G., et al. (1999). "Neoadjuvant cisplatin, methotrexate, and vinblastine chemotherapy for muscle-invasive bladder cancer: a randomised controlled trial." *The Lancet* 354(9178): 533-540.

François, N. J., et al. (2005). "Rheological and drug-release behaviour of a scleroglucan gel matrix at different drug loadings." *Polymer international* 54(12): 1613-1619.

Frangos, D. N., et al. (1990). "The development of liposomes containing interferon alpha for the intravesical therapy of human superficial bladder cancer." *The Journal of urology* 143(6): 1252-1256.

Fransen, M. F., et al. (2013). "Local targets for immune therapy to cancer: Tumor draining lymph nodes and tumor microenvironment." *International Journal of Cancer* 132(9): 1971-1976.

Franson, N. M. and N. A. Peppas (1983). "Influence of copolymer composition on non-fickian water transport through glassy copolymers." *Journal of applied polymer science* 28(4): 1299-1310.

Freedman, B. R., et al. (2021). "Degradable and removable tough adhesive hydrogels." *Advanced Materials* 33(17): 2008553.

Fuge, O., et al. (2015). "Immunotherapy for bladder cancer." *Research and reports in urology* 7: 65.

Gakis, G., et al. (2013). "ICUD-EAU International Consultation on Bladder Cancer 2012: Radical cystectomy and bladder preservation for muscle-invasive urothelial carcinoma of the bladder." *Eur Urol* 63(1): 45-57.

Gall, T. M. H., et al. (2015). "Pancreatic cancer: current management and treatment strategies." *Postgraduate Medical Journal* 91(1080): 601-607.

Gandhi, V., et al. (1996). "Excision of 2',2'-Difluorodeoxycytidine (Gemcitabine) Monophosphate Residues from DNA." *Cancer research* 56(19): 4453.

García-González, C. A., et al. (2011). "Polysaccharide-based aerogels—Promising biodegradable carriers for drug delivery systems." *Carbohydrate Polymers* 86(4): 1425-1438.

García-González, C. A., et al. (2015). "Processing of Materials for Regenerative Medicine Using Supercritical Fluid Technology." *Bioconjugate chemistry* 26(7): 1159-1171.

García-González, C. A. and I. Smirnova (2013). "Use of supercritical fluid technology for the production of tailor-made aerogel particles for delivery systems." *The Journal of Supercritical Fluids* 79: 152-158.

García-González, C. A., et al. (2021). "Aerogels in drug delivery: From design to application." *Journal of Controlled Release* 332: 40-63.

Gerweck, L. E. and K. Seetharaman (1996). "Cellular pH gradient in tumor versus normal tissue: potential exploitation for the treatment of cancer." *Cancer research* 56(6): 1194-1198.

Giannantoni, A., et al. (2006). "New frontiers in intravesical therapies and drug delivery." *European urology* 50(6): 1183-1193.

Giray, S., et al. (2012). "Controlled drug delivery through a novel PEG hydrogel encapsulated silica aerogel system." *Journal of Biomedical Materials Research Part A* 100A(5): 1307-1315.

Goebell, P. J. and M. A. Knowles (2010). *Bladder cancer or bladder cancers? Genetically distinct malignant conditions of the urothelium. Urologic Oncology: Seminars and Original Investigations*, Elsevier.

Gontero, P., et al. (2015). "Prognostic factors and risk groups in T1G3 non-muscle-invasive bladder cancer patients initially treated with bacillus Calmette-Guérin: results of a retrospective multicenter study of 2451 patients." *European urology* 67(1): 74-82.

Grillet, A. M., et al. (2012). "Polymer gel rheology and adhesion." *Rheology* 3: 59-80.

Grossman, H. B., et al. (2003). "Neoadjuvant chemotherapy plus cystectomy compared with cystectomy alone for locally advanced bladder cancer." *New England Journal of Medicine* 349(9): 859-866.

Gruschwitz, F. V., et al. (2022). "Shear-Thinning and Rapidly Recovering Hydrogels of Polymeric Nanofibers Formed by Supramolecular Self-Assembly." *Chemistry of Materials* 34(5): 2206-2217.

Guevara, A., et al. (2010). "The role of tumor-free status in repeat resection before intravesical bacillus Calmette-Guerin for high grade Ta, T1 and CIS bladder cancer." *The Journal of urology* 183(6): 2161-2164.

GuhaSarkar, S. and R. Banerjee (2010). "Intravesical drug delivery: Challenges, current status, opportunities and novel strategies." *Journal of Controlled Release* 148(2): 147-159.

Guiseley, K. B. (1970). "The relationship between methoxyl content and gelling temperature of agarose." *Carbohydrate Research* 13(2): 247-256.

Guo, S. and L. A. DiPietro (2010). "Factors Affecting Wound Healing." *Journal of Dental Research* 89(3): 219-229.

Gurunathan, S., et al. (2018). "Nanoparticle-mediated combination therapy: two-in-one approach for cancer." *International journal of molecular sciences* 19(10): 3264.

Güven, M. N., et al. (2021). "Bisphosphonate-functionalized poly (amido amine) crosslinked 2-hydroxyethyl methacrylate hydrogel as tissue engineering scaffold." *European Polymer Journal* 159: 110732.

Guzmán, E. A., et al. (2019). "The marine natural product Scalarin inhibits the receptor for advanced glycation end products (RAGE) and autophagy in the PANC-1 and MIA PaCa-2 pancreatic cancer cell lines." *Investigational new drugs* 37(2): 262-270.

Haimer, E., et al. (2010). "Loading of Bacterial Cellulose Aerogels with Bioactive Compounds by Antisolvent Precipitation with Supercritical Carbon Dioxide." *Macromolecular Symposia* 294(2): 64-74.

Han, X., et al. (2020). "PVA/Agar Interpenetrating Network Hydrogel with Fast Healing, High Strength, Antifreeze, and Water Retention." *Macromolecular Chemistry and Physics* 221(22): 2000237.

Han, Y., et al. (2013). "Control of pore and window size of ceramic foams with tri-modal pore structure: Influence of agar concentration." *Materials Letters* 110: 256-259.

Hanauer, N., et al. (2015). "2D, 3D and 4D Active Compound Delivery in Tissue Engineering and Regenerative Medicine." *Current pharmaceutical design* 21(12): 1506-1516.

Haugsten, E. M., et al. (2010). "Roles of fibroblast growth factor receptors in carcinogenesis." *Molecular Cancer Research* 8(11): 1439-1452.

He, J., et al. (2014). "Management of borderline and locally advanced pancreatic cancer: where do we stand?" *World journal of gastroenterology* 20(9): 2255-2266.

Helenius, M., et al. (2015). "Bladder cancer detection in patients with gross haematuria: computed tomography urography with enhancement-triggered scan versus flexible cystoscopy." *Scandinavian journal of urology* 49(5): 377-381.

Hidalgo, M. (2010). "Pancreatic Cancer." *New England Journal of Medicine* 362(17): 1605-1617.

Hina, M., et al. (2021). "Fabrication of aqueous solid-state symmetric supercapacitors based on self-healable poly (acrylamide)/PEDOT: PSS composite hydrogel electrolytes." *Materials Chemistry and Physics* 273: 125125.

Hindupur, S. V., et al. (2020). "STAT3/5 inhibitors suppress proliferation in bladder cancer and enhance oncolytic adenovirus therapy." *International journal of molecular sciences* 21(3): 1106.

Hiremath, P., et al. (2019). Chapter 8 - Material Attributes and Their Impact on Wet Granulation Process Performance. *Handbook of Pharmaceutical Wet Granulation*. A. S. Narang and S. I. F. Badawy, Academic Press: 263-315.

Hirotsu, S. (1993). Coexistence of phases and the nature of first-order phase transition in poly-N-isopropylacrylamide gels. *Responsive Gels: Volume Transitions II*, Springer: 1-26.

Hoare, T. R. and D. S. Kohane (2008). "Hydrogels in drug delivery: progress and challenges." *Polymer* 49(8): 1993-2007.

Hoffman, A. S. (2012). "Hydrogels for biomedical applications." *Advanced drug delivery reviews* 64: 18-23.

Horvat, G., et al. (2022). "A Brief Evaluation of Pore Structure Determination for Bioaerogels." *Gels* 8(7): 438.

Hossen, S., et al. (2019). "Smart nanocarrier-based drug delivery systems for cancer therapy and toxicity studies: A review." *Journal of advanced research* 15: 1-18.

Hruban, R. H., et al. (2010). "Update on Familial Pancreatic Cancer." *Advances in Surgery* 44(1): 293-311.

Hu, B.-H. and P. B. Messersmith (2003). "Rational design of transglutaminase substrate peptides for rapid enzymatic formation of hydrogels." *Journal of the American chemical society* 125(47): 14298-14299.

Hu, Q., et al. (2021). "Recent advances in dextran-based drug delivery systems: From fabrication strategies to applications." *Carbohydrate Polymers* 264: 117999.

Huang, D., et al. (2011). "Antibacterial chitosan coating on nano-hydroxyapatite/polyamide66 porous bone scaffold for drug delivery." *Journal of Biomaterials Science, Polymer Edition* 22(7): 931-944.

Huang, P., et al. (1991). "Action of 2',2'-Difluorodeoxycytidine on DNA Synthesis." *Cancer research* 51(22): 6110.

Huang, X. and C. S. Brazel (2001). "On the importance and mechanisms of burst release in matrix-controlled drug delivery systems." *Journal of Controlled Release* 73(2): 121-136.

Huang, Y., et al. (2007). "pH-sensitive cationic guar gum/poly (acrylic acid) polyelectrolyte hydrogels: Swelling and in vitro drug release." *Carbohydrate Polymers* 69(4): 774-783.

Huang, Z., et al. (2018). "Enhanced photo/chemo combination efficiency against bladder tumor by encapsulation of DOX and ZnPC into in situ-formed thermosensitive polymer hydrogel." *International journal of nanomedicine* 13: 7623.

Huisman, S. A., et al. (2016). "Fasting protects against the side effects of irinotecan treatment but does not affect anti-tumour activity in mice." *British journal of pharmacology* 173(5): 804-814.

Huncharek, M., et al. (2000). "Intravesical chemotherapy prophylaxis in primary superficial bladder cancer: a meta-analysis of 3703 patients from 11 randomized trials." *Journal of clinical epidemiology* 53(7): 676-680.

Hüsing, N. and U. Schubert (1998). "Aerogels—Airy Materials: Chemistry, Structure, and Properties." *Angewandte Chemie International Edition* 37(1-2): 22-45.

Hussein, A. A., et al. (2021). Investigating the association between the urinary microbiome and bladder cancer: an exploratory study. *Urologic Oncology: Seminars and Original Investigations*, Elsevier.

Hutmacher, D., et al. (2001). "An introduction to biodegradable materials for tissue engineering applications." *Annals of the Academy of Medicine, Singapore* 30(2): 183-191.

Hutmacher, D. W. (2001). "Scaffold design and fabrication technologies for engineering tissues—state of the art and future perspectives." *Journal of Biomaterials Science, Polymer Edition* 12(1): 107-124.

Iizawa, T., et al. (2007). "Synthesis of porous poly (N-isopropylacrylamide) gel beads by sedimentation polymerization and their morphology." *Journal of applied polymer science* 104(2): 842-850.

Illiger, S. R., et al. (2009). "Miscibility studies of HPMC/PEG blends in water by viscosity, density, refractive index and ultrasonic velocity method." *Carbohydrate Polymers* 75(3): 484-488.

Iodice, S., et al. (2008). "Tobacco and the risk of pancreatic cancer: a review and meta-analysis." *Langenbeck's Archives of Surgery* 393(4): 535-545.

Ivarsson, D. and M. Wahlgren (2012). "Comparison of in vitro methods of measuring mucoadhesion: Ellipsometry, tensile strength and rheological measurements." *Colloids and Surfaces B: Biointerfaces* 92: 353-359.

Jabbari-Gargari, A., et al. (2021). "Carboxylic acid decorated silica aerogel nanostructure as drug delivery carrier." *Microporous and mesoporous materials* 323: 111220.

Jahanmir, G. and Y. Chau (2019). Chapter 9 - Mathematical models of drug release from degradable hydrogels. *Biomedical Applications of Nanoparticles*. A. M. Grumezescu, William Andrew Publishing: 233-269.

Jancke, G., et al. (2011). "Impact of tumour size on recurrence and progression in Ta/T1 carcinoma of the urinary bladder." *Scandinavian journal of urology and nephrology* 45(6): 388-392.

Javle, M., et al. (2021). "Infigratinib (BGJ398) in previously treated patients with advanced or metastatic cholangiocarcinoma with FGFR2 fusions or rearrangements: mature results from a

multicentre, open-label, single-arm, phase 2 study." *The Lancet Gastroenterology & Hepatology* 6(10): 803-815.

Jayakumar, R., et al. (2011). "Biomaterials based on chitin and chitosan in wound dressing applications." *Biotechnology advances* 29(3): 322-337.

Jaywant, P., et al. (2017). "Biodegradable Porous Starch Spheres as a Novel Carrier for Enhancement of Dissolution Rate and Oral Bioavailability of Itraconazole." *Current Drug Delivery* 14(7): 944-954.

Jin, R., et al. (2007). "Enzyme-mediated fast in situ formation of hydrogels from dextran-tyramine conjugates." *Biomaterials* 28(18): 2791-2800.

Jo, S. D., et al. (2017). "Harnessing designed nanoparticles: Current strategies and future perspectives in cancer immunotherapy." *Nano Today* 17: 23-37.

Jones, D. S., et al. (1997). "Textural, viscoelastic and mucoadhesive properties of pharmaceutical gels composed of cellulose polymers." *International Journal of Pharmaceutics* 151(2): 223-233.

Jones, D. S., et al. (1996). "Texture profile analysis of bioadhesive polymeric semisolids: Mechanical characterization and investigation of interactions between formulation components." *Journal of applied polymer science* 61(12): 2229-2234.

Jones, D. S., et al. (1996). "Development and Mechanical Characterization of Bioadhesive Semi-Solid, Polymeric Systems Containing Tetracycline for the Treatment of Periodontal Diseases." *Pharmaceutical research* 13(11): 1734-1738.

Jones, R., et al. (2007). "Alarm symptoms in early diagnosis of cancer in primary care: cohort study using General Practice Research Database." *Bmj* 334(7602): 1040.

Kaasinen, E., et al. (2002). "Factors explaining recurrence in patients undergoing chemoimmunotherapy regimens for frequently recurring superficial bladder carcinoma." *European urology* 42(2): 167-174.

Kamat, A. M., et al. (2015). "Consensus statement on best practice management regarding the use of intravesical immunotherapy with BCG for bladder cancer." *Nature Reviews Urology* 12(4): 225-235.

Kamat, A. M., et al. (2016). "Bladder cancer." *The Lancet* 388(10061): 2796-2810.

Kamat, A. M., et al. (2016). "Bladder cancer." *Lancet* 388(10061): 2796-2810.

Kamat, A. M. and S. Orten (2014). "Myths and mysteries surrounding bacillus Calmette-Guérin therapy for bladder cancer." *European urology* 65(2): 267.

- Kamisawa, T., et al. (2016). "Pancreatic cancer." *The Lancet* 388(10039): 73-85.
- Kang, J. H., et al. (2021). "Temperature and pH-responsive in situ hydrogels of gelatin derivatives to prevent the reoccurrence of brain tumor." *Biomedicine & Pharmacotherapy* 143: 112144.
- Kanokpanont, S., et al. (2012). "An innovative bi-layered wound dressing made of silk and gelatin for accelerated wound healing." *International Journal of Pharmaceutics* 436(1): 141-153.
- Karoyo, A. H. and L. D. Wilson (2021). "A review on the design and hydration properties of natural polymer-based hydrogels." *Materials* 14(5): 1095.
- Kashyap, N., et al. (2005). "Hydrogels for pharmaceutical and biomedical applications." *Critical Reviews™ in Therapeutic Drug Carrier Systems* 22(2).
- Kayahara, M., et al. (1993). "An evaluation of radical resection for pancreatic cancer based on the mode of recurrence as determined by autopsy and diagnostic imaging." *Cancer* 72(7): 2118-2123.
- Kesharwani, P., et al. (2021). "Biomedical applications of hydrogels in drug delivery system: An update." *Journal of Drug Delivery Science and Technology* 66: 102914.
- Khare, A. R. and N. A. Peppas (1993). "Release behavior of bioactive agents from pH-sensitive hydrogels." *Journal of Biomaterials Science, Polymer Edition* 4(3): 275-289.
- Kharkar, P. M., et al. (2013). "Designing degradable hydrogels for orthogonal control of cell microenvironments." *Chemical Society Reviews* 42(17): 7335-7372.
- Kharkar, P. M., et al. (2015). "Design of thiol-and light-sensitive degradable hydrogels using Michael-type addition reactions." *Polymer chemistry* 6(31): 5565-5574.
- Kim, D.-J. and J.-Y. Jung (2007). "Granule performance of zirconia/alumina composite powders spray-dried using polyvinyl pyrrolidone binder." *Journal of the European Ceramic Society* 27(10): 3177-3182.
- Kim, S. E., et al. (2015). "Autophagy sustains the survival of human pancreatic cancer PANC-1 cells under extreme nutrient deprivation conditions." *Biochemical and Biophysical Research Communications* 463(3): 205-210.
- Kin, N. and W. Yaphe (1972). "Properties of agar: Parameters affecting gel-formation and the agarose-iodine reaction." *Carbohydrate Research* 25: 379-385.
- Kistler, S. S. (1931). "Coherent Expanded Aerogels and Jellies." *Nature* 127(3211): 741-741.
- Kleeff, J., et al. (2007). "Surgery for Recurrent Pancreatic Ductal Adenocarcinoma." *Annals of surgery* 245(4): 566-572.

- Knowles, M. A. (2007). "Role of FGFR3 in urothelial cell carcinoma: biomarker and potential therapeutic target." *World journal of urology* 25(6): 581-593.
- Kooby, D. A., et al. (2014). "Value of Intraoperative Neck Margin Analysis During Whipple for Pancreatic Adenocarcinoma: A Multicenter Analysis of 1399 Patients." *Annals of surgery* 260(3): 494-503.
- Kopecek, J. (2009). "Hydrogels: From soft contact lenses and implants to self-assembled nanomaterials." *Journal of Polymer Science Part A: Polymer Chemistry* 47(22): 5929-5946.
- Kost, J. and R. Langer (2012). "Responsive polymeric delivery systems." *Advanced drug delivery reviews* 64: 327-341.
- Kuhlmann, K. F. D., et al. (2004). "Surgical treatment of pancreatic adenocarcinoma: actual survival and prognostic factors in 343 patients." *European Journal of Cancer* 40(4): 549-558.
- Kurahara, H., et al. (2007). "Impact of Lymph Node Micrometastasis in Patients with Pancreatic Head Cancer." *World Journal of Surgery* 31(3): 483-490.
- Kurisawa, M., et al. (2005). "Injectable biodegradable hydrogels composed of hyaluronic acid–tyramine conjugates for drug delivery and tissue engineering." *Chemical communications*(34): 4312-4314.
- Kweekel, D., et al. (2008). "Clinical and pharmacogenetic factors associated with irinotecan toxicity." *Cancer Treatment Reviews* 34(7): 656-669.
- Kwon, D. Y., et al. (2016). "Synergistic anti-tumor activity through combinational intratumoral injection of an in-situ injectable drug depot." *Biomaterials* 85: 232-245.
- Lavan, D. A., et al. (2003). "Small-scale systems for in vivo drug delivery." *Nature biotechnology* 21(10): 1184-1191.
- Lavelle, J., et al. (2002). "Bladder permeability barrier: recovery from selective injury of surface epithelial cells." *American Journal of Physiology-Renal Physiology* 283(2): F242-F253.
- Lázár, I., et al. (2020). "Mechanism of hydration of biocompatible silica-casein aerogels probed by NMR and SANS reveal backbone rigidity." *Applied Surface Science* 531: 147232.
- Leakakos, T., et al. (2003). "Intravesical administration of doxorubicin to swine bladder using magnetically targeted carriers." *Cancer chemotherapy and pharmacology* 51(6): 445-450.
- Lee, J., et al. (2008). "Three-dimensional cell culture matrices: state of the art." *Tissue Engineering Part B: Reviews* 14(1): 61-86.

- Lee, K. Y. and D. J. Mooney (2001). "Hydrogels for tissue engineering." *Chemical reviews* 101(7): 1869-1880.
- Lerouge, S., et al. (2018). "314 - Injectable T cell delivery scaffolds for cancer immunotherapy." *Cytotherapy* 20(5, Supplement): S106-S107.
- Lewis, S. (1986). "The mammalian urinary bladder: it's more than accommodating." *Physiology* 1(2): 61-65.
- Lewis, S. A. (2000). "Everything you wanted to know about the bladder epithelium but were afraid to ask." *American Journal of Physiology-Renal Physiology* 278(6): F867-F874.
- Li, C., et al. (2019). "Recent progress in drug delivery." *Acta pharmaceutica sinica B* 9(6): 1145-1162.
- Li, J. and D. J. Mooney (2016). "Designing hydrogels for controlled drug delivery." *Nature Reviews Materials* 1(12): 1-17.
- Li, L., et al. (2015). "Injectable and biodegradable pH-responsive hydrogels for localized and sustained treatment of human fibrosarcoma." *ACS Applied Materials & Interfaces* 7(15): 8033-8040.
- Li, L., et al. (2009). "Flexible Nanofiber-Reinforced Aerogel (Xerogel) Synthesis, Manufacture, and Characterization." *ACS Applied Materials & Interfaces* 1(11): 2491-2501.
- Li, Y., et al. (2010). "The effect of strontium-substituted hydroxyapatite coating on implant fixation in ovariectomized rats." *Biomaterials* 31(34): 9006-9014.
- Li, Y., et al. (2011). "Ab initio studies of cellulose I: crystal structure, intermolecular forces, and interactions with water." *The Journal of Physical Chemistry C* 115(23): 11533-11539.
- Li, Y., et al. (2012). "Injectable and biodegradable hydrogels: gelation, biodegradation and biomedical applications." *Chemical Society Reviews* 41(6): 2193-2221.
- Liang, S., et al. (2006). "Protein diffusion in agarose hydrogel in situ measured by improved refractive index method." *Journal of Controlled Release* 115(2): 189-196.
- Liang, Y., et al. (2022). "pH/glucose dual responsive metformin release hydrogel dressings with adhesion and self-healing via dual-dynamic bonding for athletic diabetic foot wound healing." *ACS nano* 16(2): 3194-3207.
- Lin, C.-C. and A. T. Metters (2006). "Hydrogels in controlled release formulations: network design and mathematical modeling." *Advanced drug delivery reviews* 58(12): 1379-1408.

- Ling, Q., et al. (2013). "The diversity between pancreatic head and body/tail cancers: clinical parameters and in vitro models." *Hepatobiliary & Pancreatic Diseases International* 12(5): 480-487.
- Liu, H. and X. Zhu (1999). "Lower critical solution temperatures of N-substituted acrylamide copolymers in aqueous solutions." *Polymer* 40(25): 6985-6990.
- Liu, L., et al. (2021). "Facile synthesis of calcium carbonate/polyacrylic acid hydrogels for pH-responsive delivery of cytarabine." *Journal of Saudi Chemical Society* 25(11): 101344.
- Liu, M., et al. (2000). "Water-soluble dendritic unimolecular micelles:: Their potential as drug delivery agents." *Journal of Controlled Release* 65(1): 121-131.
- Liu, X., et al. (2019). "Targeted and Sustained Corelease of Chemotherapeutics and Gene by Injectable Supramolecular Hydrogel for Drug-Resistant Cancer Therapy." *Macromolecular Rapid Communications* 40(5): 1800117.
- Liu, Z., et al. (2020). "Polymeric hybrid aerogels and their biomedical applications." *Soft Matter* 16(40): 9160-9175.
- Longley, D. B., et al. (2003). "5-Fluorouracil: mechanisms of action and clinical strategies." *Nature Reviews Cancer* 3(5): 330-338.
- López-Iglesias, C., et al. (2019). "Vancomycin-loaded chitosan aerogel particles for chronic wound applications." *Carbohydrate Polymers* 204: 223-231.
- López-Iglesias, C., et al. (2019). "From the printer to the lungs: Inkjet-printed aerogel particles for pulmonary delivery." *Chemical Engineering Journal* 357: 559-566.
- Lu, Z., et al. (2004). "Paclitaxel-loaded gelatin nanoparticles for intravesical bladder cancer therapy." *Clinical Cancer Research* 10(22): 7677-7684.
- Lutolf, M., et al. (2003). "Synthetic matrix metalloproteinase-sensitive hydrogels for the conduction of tissue regeneration: engineering cell-invasion characteristics." *Proceedings of the National Academy of Sciences* 100(9): 5413-5418.
- Lutolf, M. P., et al. (2003). "Cell-Responsive Synthetic Hydrogels." *Advanced Materials* 15(11): 888-892.
- Ma, H., et al. (2015). "Localized co-delivery of doxorubicin, cisplatin, and methotrexate by thermosensitive hydrogels for enhanced osteosarcoma treatment." *ACS Applied Materials & Interfaces* 7(49): 27040-27048.
- Ma, J., et al. (2022). "Hydrogels for localized chemotherapy of liver cancer: a possible strategy for improved and safe liver cancer treatment." *Drug delivery* 29(1): 1457-1476.

- Ma, W., et al. (2021). "Sprayable β -FeSi₂ composite hydrogel for portable skin tumor treatment and wound healing." *Biomaterials* 279: 121225.
- Maleki, H., et al. (2016). "Synthesis and biomedical applications of aerogels: Possibilities and challenges." *Advances in colloid and interface science* 236: 1-27.
- Malmstrom, P.-U., et al. (1996). "Five-year followup of a prospective trial of radical cystectomy and neoadjuvant chemotherapy: Nordic Cystectomy Trial 1." *The Journal of urology* 155(6): 1903-1906.
- Malmström, P.-U., et al. (2009). "An individual patient data meta-analysis of the long-term outcome of randomised studies comparing intravesical mitomycin C versus bacillus Calmette-Guérin for non-muscle-invasive bladder cancer." *European urology* 56(2): 247-256.
- Malvezzi, M., et al. (2014). "European cancer mortality predictions for the year 2014." *Annals of Oncology* 25(8): 1650-1656.
- Mano, J., et al. (2007). "Natural origin biodegradable systems in tissue engineering and regenerative medicine: present status and some moving trends." *Journal of the Royal Society Interface* 4(17): 999-1030.
- Månsson, Å., et al. (1993). "Time lag to diagnosis of bladder cancer—influence of psychosocial parameters and level of health-care provision." *Scandinavian journal of urology and nephrology* 27(3): 363-369.
- Martens, P. J., et al. (2003). "Tailoring the degradation of hydrogels formed from multivinyl poly (ethylene glycol) and poly (vinyl alcohol) macromers for cartilage tissue engineering." *Biomacromolecules* 4(2): 283-292.
- Martin-Doyle, W., et al. (2015). "Improving selection criteria for early cystectomy in high-grade t1 bladder cancer: a meta-analysis of 15,215 patients." *J Clin Oncol* 33(6): 643-650.
- Mason, M. N., et al. (2001). "Predicting controlled-release behavior of degradable PLA-b-PEG-b-PLA hydrogels." *Macromolecules* 34(13): 4630-4635.
- Matricardi, P., et al. (2013). "Interpenetrating Polymer Networks polysaccharide hydrogels for drug delivery and tissue engineering." *Advanced drug delivery reviews* 65(9): 1172-1187.
- McCrorie, P., et al. (2020). "Etoposide and olaparib polymer-coated nanoparticles within a bioadhesive sprayable hydrogel for post-surgical localised delivery to brain tumours." *European journal of pharmaceuticals and biopharmaceutics* 157: 108-120.
- Meadows, J., et al. (1995). "Comparison of the extensional and shear viscosity characteristics of aqueous hydroxyethyl cellulose solutions." *Macromolecules* 28(8): 2683-2692.

- Mehling, T., et al. (2009). "Polysaccharide-based aerogels as drug carriers." *Journal of Non-Crystalline Solids* 355(50): 2472-2479.
- Melo, M. N., et al. (2021). "Chitosan and chitosan/PEG nanoparticles loaded with indole-3-carbinol: Characterization, computational study and potential effect on human bladder cancer cells." *Materials Science and Engineering: C* 124: 112089.
- Merril, E. and R. W. Pekala (1987). "Hydrogel for blood contact." *Hydrogels in medicine and pharmacy* 3.
- Merz, V., et al. (2020). "Pemigatinib, a potent inhibitor of FGFRs for the treatment of cholangiocarcinoma." *Future Oncology* 17(4): 389-402.
- Metters, A. T., et al. (2001). "A statistical kinetic model for the bulk degradation of PLA-b-PEG-b-PLA hydrogel networks: Incorporating network non-idealities." *The Journal of Physical Chemistry B* 105(34): 8069-8076.
- Metters, A. T., et al. (2000). "A statistical kinetic model for the bulk degradation of PLA-b-PEG-b-PLA hydrogel networks." *The Journal of Physical Chemistry B* 104(30): 7043-7049.
- Mishra, B. and J. Singh (2021). *Hydrogel-based drug delivery systems for cancer therapy. Advanced Drug Delivery Systems in the Management of Cancer*, Elsevier: 63-74.
- Mizrahi, J. D., et al. (2020). "Pancreatic cancer." *The Lancet* 395(10242): 2008-2020.
- Moch, H., et al. (2016). "Tumours of the urinary tract." *WHO Classification of Tumours of the Urinary System and Male Genital Organs*, 4th ed. Lyon, France: IARC.
- Moghimi, S. M., et al. (2001). "Long-Circulating and Target-Specific Nanoparticles: Theory to Practice." *Pharmacological Reviews* 53(2): 283-318.
- Molineux, G. (2004). "The design and development of pegfilgrastim (PEG-rmetHuG-CSF, Neulasta®)." *Current pharmaceutical design* 10(11): 1235-1244.
- Mostofi, F. K., et al. (2012). *Histological typing of urinary bladder tumours*, Springer Science & Business Media.
- Murillo-Cremaes, N., et al. (2013). "Nanostructured silica-based drug delivery vehicles for hydrophobic and moisture sensitive drugs." *The Journal of Supercritical Fluids* 73: 34-42.
- Murphy, W. M., et al. (2002). "Interobserver discrepancy using the 1998 World Health Organization/International Society of Urologic Pathology classification of urothelial neoplasms: practical choices for patient care." *The Journal of urology* 168(3): 968-972.

- Nagy, G., et al. (2019). "Controlled release of methotrexate from functionalized silica-gelatin aerogel microparticles applied against tumor cell growth." *International Journal of Pharmaceutics* 558: 396-403.
- Narayanan, J., et al. (2006). Determination of agarose gel pore size: Absorbance measurements vis a vis other techniques. *Journal of Physics: Conference Series*, IOP Publishing.
- Navya, P., et al. (2019). "Current trends and challenges in cancer management and therapy using designer nanomaterials." *Nano Convergence* 6(1): 1-30.
- Negrete, H., et al. (1996). "Permeability properties of the intact mammalian bladder epithelium." *American Journal of Physiology-Renal Physiology* 271(4): F886-F894.
- Neoptolemos, J. P., et al. (2004). "A Randomized Trial of Chemoradiotherapy and Chemotherapy after Resection of Pancreatic Cancer." *New England Journal of Medicine* 350(12): 1200-1210.
- Network, C. G. A. R. (2014). "Comprehensive molecular characterization of urothelial bladder carcinoma." *Nature* 507(7492): 315.
- Ngadaonye, J. I., et al. (2012). "Photopolymerised thermo-responsive poly (N, N-diethylacrylamide)-based copolymer hydrogels for potential drug delivery applications." *Journal of Polymer Research* 19(3): 1-15.
- Nguyen, K. T. and J. L. West (2002). "Photopolymerizable hydrogels for tissue engineering applications." *Biomaterials* 23(22): 4307-4314.
- Nicodemus, G. D. and S. J. Bryant (2008). "Cell encapsulation in biodegradable hydrogels for tissue engineering applications." *Tissue Engineering Part B: Reviews* 14(2): 149-165.
- Nikoo, A. M., et al. (2018). "Electrospray-assisted encapsulation of caffeine in alginate microhydrogels." *International Journal of Biological Macromolecules* 116: 208-216.
- Nita, L. E., et al. (2020). "New trends in bio-based aerogels." *Pharmaceutics* 12(5): 449.
- Nordli, H. R., et al. (2016). "Producing ultrapure wood cellulose nanofibrils and evaluating the cytotoxicity using human skin cells." *Carbohydrate Polymers* 150: 65-73.
- Nordqvist, D. and T. A. Vilgis (2011). "Rheological Study of the Gelation Process of Agarose-Based Solutions." *Food Biophysics* 6(4): 450.
- Norouzi, M., et al. (2016). "Injectable hydrogel-based drug delivery systems for local cancer therapy." *Drug discovery today* 21(11): 1835-1849.
- Nussinovitch, A. (2019). *Cooking innovations: Using hydrocolloids for thickening, gelling, and emulsification*, CRC Press.

Nweke, M. C., et al. (2017). "Drying techniques for the visualisation of agarose-based chromatography media by scanning electron microscopy." *Biotechnology journal* 12(3): 1600583.

O'Reilly, D., et al. (2018). "Diagnosis and management of pancreatic cancer in adults: A summary of guidelines from the UK National Institute for Health and Care Excellence." *Pancreatology* 18(8): 962-970.

Oettle, H., et al. (2013). "Adjuvant Chemotherapy With Gemcitabine and Long-term Outcomes Among Patients With Resected Pancreatic Cancer: The CONKO-001 Randomized Trial." *JAMA* 310(14): 1473-1481.

of Trialists, I. C. (2011). "International phase III trial assessing neoadjuvant cisplatin, methotrexate, and vinblastine chemotherapy for muscle-invasive bladder cancer: long-term results of the BA06 30894 trial." *Journal of Clinical Oncology* 29(16): 2171.

Okutucu, B. (2021). "The medical applications of biobased aerogels: 'Natural aerogels for medical usage'." *Medical Devices & Sensors* 4(1): e10168.

Osorno, L. L., et al. (2021). "Review of Contemporary Self-Assembled Systems for the Controlled Delivery of Therapeutics in Medicine." *Nanomaterials* 11(2): 278.

Ozkan, C. K., et al. (2021). "An overview of excipients classification and their use in pharmaceuticals." *Current Pharmaceutical Analysis* 17(3): 360-374.

Packiam, V. T., et al. (2019). "Current clinical trials in non-muscle-invasive bladder cancer: heightened need in an era of chronic BCG shortage." *Current urology reports* 20(12): 1-11.

Palmer, L. C., et al. (2008). "Biomimetic Systems for Hydroxyapatite Mineralization Inspired By Bone and Enamel." *Chemical reviews* 108(11): 4754-4783.

Pantić, M., et al. (2020). "Preparation and Characterization of Chitosan-Coated Pectin Aerogels: Curcumin Case Study." *Molecules* 25(5): 1187.

Park, H., et al. (2011). *Biodegradable hydrogels for drug delivery*, CRC Press.

Patel, V. G., et al. (2020). "Treatment of muscle-invasive and advanced bladder cancer in 2020." *CA: A Cancer Journal for Clinicians* 70(5): 404-423.

Pawlik, T. M., et al. (2008). "Evaluating the Impact of a Single-Day Multidisciplinary Clinic on the Management of Pancreatic Cancer." *Annals of Surgical Oncology* 15(8): 2081-2088.

Pekarek, K. J., et al. (1993). "Double-walled microspheres for drug delivery." *MRS Online Proceedings Library* 331(1): 97-101.

Pelosi, E., et al. (2017). "Pancreatic Cancer: Molecular Characterization, Clonal Evolution and Cancer Stem Cells." *Biomedicines* 5(4): 65.

Peppas, N. A. (1986). *Hydrogels in medicine and pharmacy*, CRC press Boca Raton, FL.

Pereira, N. P. and J. R. Corrêa (2018). "Pancreatic cancer: treatment approaches and trends." *Journal of Cancer Metastasis and Treatment* 4: 30.

Petkova, D., et al. (2020). "Hydrophobic Pockets of HPMC Enable Extremely Short Reaction Times in Water." *ACS Sustainable Chemistry & Engineering* 8(33): 12612-12617.

Petrelli, F., et al. (2015). "FOLFIRINOX-Based Neoadjuvant Therapy in Borderline Resectable or Unresectable Pancreatic Cancer: A Meta-Analytical Review of Published Studies." *Pancreas* 44(4): 515-521.

Pham, Q. P., et al. (2006). "Electrospinning of polymeric nanofibers for tissue engineering applications: a review." *Tissue engineering* 12(5): 1197-1211.

Piazza, L. and S. Benedetti (2010). "Investigation on the rheological properties of agar gels and their role on aroma release in agar/limonene solid emulsions." *Food Research International* 43(1): 269-276.

Plamper, F. A., et al. (2007). "Tuning the thermoresponsive properties of weak polyelectrolytes: aqueous solutions of star-shaped and linear poly (N, N-dimethylaminoethyl methacrylate)." *Macromolecules* 40(23): 8361-8366.

Plimack, E. R., et al. (2014). "Accelerated methotrexate, vinblastine, doxorubicin, and cisplatin is safe, effective, and efficient neoadjuvant treatment for muscle-invasive bladder cancer: results of a multicenter phase II study with molecular correlates of response and toxicity." *Journal of Clinical Oncology* 32(18): 1895.

Poggi, M. M., et al. (2000). Glycosaminoglycan content of human bladders: a method of analysis using cold-cup biopsies. *Urologic Oncology: Seminars and Original Investigations*, Elsevier.

Porcelli, L., et al. (2011). "The impact of folate status on the efficacy of colorectal cancer treatment." *Curr Drug Metab* 12(10): 975-984.

Porten, S. P., et al. (2015). "Intravesical chemotherapy in non-muscle-invasive bladder cancer." *Indian journal of urology: IJU: journal of the Urological Society of India* 31(4): 297.

Pourjavadi, A., et al. (2009). "Synthesis and investigation of swelling behavior of new agar based superabsorbent hydrogel as a candidate for agrochemical delivery." *Journal of Polymer Research* 16(6): 655.

Prasher, P., et al. (2021). "Current-status and applications of polysaccharides in drug delivery systems." *Colloid and Interface Science Communications* 42: 100418.

Qiu, Y. and K. Park (2012). "Environment-sensitive hydrogels for drug delivery." *Advanced drug delivery reviews* 64: 49-60.

Rafael, D., et al. (2021). "Thermo-responsive hydrogels for cancer local therapy: Challenges and state-of-art." *International Journal of Pharmaceutics* 606: 120954.

Raimondi, S., et al. (2010). "Pancreatic cancer in chronic pancreatitis; aetiology, incidence, and early detection." *Best Practice & Research Clinical Gastroenterology* 24(3): 349-358.

Rajanna, S. K., et al. (2015). "Silica Aerogel Microparticles from Rice Husk Ash for Drug Delivery." *Industrial & Engineering Chemistry Research* 54(3): 949-956.

Ramadan, A. A., et al. (2018). "Pharmaceutical and pharmacokinetic evaluation of novel rectal mucoadhesive hydrogels containing tolmetin sodium." *Journal of Pharmaceutical Investigation* 48(6): 673-683.

RAO, T. and P. CHVS (2021). "Hydrogels the three dimensional networks: a review." *Int J Curr Pharm Res* 13(1): 12-17.

Reddy, C. S., et al. (2013). "Miscibility studies of hydroxyethyl cellulose and poly (ethylene glycol) polymer blends." *Journal of Polymer Research* 7: 253-266.

Richter, A., et al. (2003). "Long-term Results of Partial Pancreaticoduodenectomy for Ductal Adenocarcinoma of the Pancreatic Head: 25-Year Experience." *World Journal of Surgery* 27(3): 324-329.

Abstract

Riss, T. (2017). "Is your MTT assay really the best choice." Promega™, Madison, Wisconsin, United States).

Rodríguez-Cabello, J. C., et al. (2018). "Bioactive scaffolds based on elastin-like materials for wound healing." *Advanced drug delivery reviews* 129: 118-133.

Rossi, S. M., et al. (2020). "Evaluation of the activity of a chemo-ablative, thermoresponsive hydrogel in a murine xenograft model of lung cancer." *British Journal of Cancer* 123(3): 369-377.

Rothenberg, M. L. (2001). "Irinotecan (CPT-11): Recent Developments and Future Directions—Colorectal Cancer and Beyond." *The oncologist* 6(1): 66-80.

Rudge, R. E. D., et al. (2020). "Natural and induced surface roughness determine frictional regimes in hydrogel pairs." *Tribology International* 141: 105903.

Safarzadeh Kozani, P., et al. (2021). "Polysaccharide-based hydrogels: Properties, advantages, challenges, and optimization methods for applications in regenerative medicine." *International Journal of Polymeric Materials and Polymeric Biomaterials*: 1-15.

Saginala, K., et al. (2020). "Epidemiology of Bladder Cancer." *Medical sciences (Basel, Switzerland)* 8(1): 15.

San Biagio, P., et al. (1984). "Cooperative interaction of polysaccharide molecules in water: A role of connectivity properties of H-Bonds within the solvent?" *Le Journal de Physique Colloques* 45(C7): C7-225-C227-233.

Sanli, O., et al. (2017). "Bladder cancer." *Nature Reviews Disease Primers* 3(1): 17022.

Sathe, A. and R. Nawroth (2018). "Targeting the PI3K/AKT/mTOR pathway in bladder cancer." *Urothelial carcinoma*: 335-350.

Schild, H. G. (1992). "Poly (N-isopropylacrylamide): experiment, theory and application." *Progress in polymer science* 17(2): 163-249.

Segal, R., et al. (2012). "Prognostic factors and outcome in patients with T1 high-grade bladder cancer: can we identify patients for early cystectomy?" *BJU international* 109(7): 1026-1030.

Senapati, S., et al. (2018). "Controlled drug delivery vehicles for cancer treatment and their performance." *Signal transduction and targeted therapy* 3(1): 1-19.

Sercombe, L., et al. (2015). "Advances and challenges of liposome assisted drug delivery." *Frontiers in pharmacology* 6: 286.

Sevgin, B., et al. (2021). "AMPK Is the Crucial Target for the CDK4/6 Inhibitors Mediated Therapeutic Responses in PANC-1 and MIA PaCa-2 Pancreatic Cancer Cell Lines." *Stresses* 1(1): 48-68.

Sfakianos, J. P., et al. (2014). "The effect of restaging transurethral resection on recurrence and progression rates in patients with nonmuscle invasive bladder cancer treated with intravesical bacillus Calmette-Guérin." *The Journal of urology* 191(2): 341-345.

Shao, J., et al. (2018). "Black-Phosphorus-Incorporated hydrogel as a sprayable and biodegradable photothermal platform for postsurgical treatment of cancer." *Advanced Science* 5(5): 1700848.

Shao, L., et al. (2018). "Dual responsive aerogel made from thermo/pH sensitive graft copolymer alginate-g-P(NIPAM-co-NHMAM) for drug controlled release." *International Journal of Biological Macromolecules* 114: 1338-1344.

Sheikholeslam, M., et al. (2018). "Biomaterials for Skin Substitutes." *Advanced Healthcare Materials* 7(5): 1700897.

Sheikhpour, M., et al. (2017). "Biomimetics in drug delivery systems: A critical review." *Journal of Controlled Release* 253: 97-109.

Sher, P., et al. (2007). "Low density porous carrier: Drug adsorption and release study by response surface methodology using different solvents." *International Journal of Pharmaceutics* 331(1): 72-83.

Sherif, A., et al. (2002). "Neoadjuvant cisplatin-methotrexate chemotherapy for invasive bladder cancer-Nordic cystectomy trial 2." *Scandinavian journal of urology and nephrology* 36(6): 419-425.

Shi, Q., et al. (2021). "Recent Advances in Enhancement of Dissolution and Supersaturation of Poorly Water-Soluble Drug in Amorphous Pharmaceutical Solids: A Review." *AAPS PharmSciTech* 23(1): 16.

Shibanuma, T., et al. (2000). "Thermosensitive Phase-Separation Behavior of Poly (acrylic acid)-g raft-poly (N, N-dimethylacrylamide) Aqueous Solution." *Macromolecules* 33(2): 444-450.

Siegel, R. A., et al. (1988). "pH-controlled release from hydrophobic/polyelectrolyte copolymer hydrogels." *Journal of Controlled Release* 8(2): 179-182.

Silberfeld, T., et al. (2014). "An updated classification of brown algae (Ochrophyta, Phaeophyceae)." *Cryptogamie, Algologie* 35(2): 117-156.

Smirnova, I., et al. (2004). "Feasibility study of hydrophilic and hydrophobic silica aerogels as drug delivery systems." *Journal of Non-Crystalline Solids* 350: 54-60.

Smith, A. A., et al. (2021). "Controlling properties of thermogels by tuning critical solution behaviour of ternary copolymers." *Polymer chemistry* 12(13): 1918-1923.

Smith, T. T., et al. (2017). "Biopolymers codelivering engineered T cells and STING agonists can eliminate heterogeneous tumors." *The Journal of Clinical Investigation* 127(6): 2176-2191.

Sobczak, M. (2022). "Enzyme-Responsive Hydrogels as Potential Drug Delivery Systems—State of Knowledge and Future Prospects." *International journal of molecular sciences* 23(8): 4421.

Soler, R., et al. (2008). "Urinary glycosaminoglycans as biomarker for urothelial injury: is it possible to discriminate damage from recovery?" *Urology* 72(4): 937-942.

Song, S. W., et al. (2005). "Functionalized SBA-15 Materials as Carriers for Controlled Drug Delivery: Influence of Surface Properties on Matrix–Drug Interactions." *Langmuir* 21(21): 9568-9575.

Sonpavde, G., et al. (2009). "Quality of pathologic response and surgery correlate with survival for patients with completely resected bladder cancer after neoadjuvant chemotherapy." *Cancer: Interdisciplinary International Journal of the American Cancer Society* 115(18): 4104-4109.

Sordi, M. B., et al. (2021). "Three-dimensional bioactive hydrogel-based scaffolds for bone regeneration in implant dentistry." *Materials Science and Engineering: C* 124: 112055.

Stein, J. P., et al. (2001). "Radical cystectomy in the treatment of invasive bladder cancer: long-term results in 1,054 patients." *Journal of Clinical Oncology* 19(3): 666-675.

Stella, V., et al. (2007). *Prodrugs: challenges and rewards*, Springer Science & Business Media.

Stergar, J. and U. Maver (2016). "Review of aerogel-based materials in biomedical applications." *Journal of Sol-Gel Science and Technology* 77(3): 738-752.

Sternberg, C. N., et al. (2015). "Immediate versus deferred chemotherapy after radical cystectomy in patients with pT3–pT4 or N+ M0 urothelial carcinoma of the bladder (EORTC 30994): an intergroup, open-label, randomised phase 3 trial." *The lancet oncology* 16(1): 76-86.

Stewart, R. (2020). "Illness perceptions, coping and psychological distress. The lived experience of non muscle invasive bladder cancer: a mixed methods approach."

Stubbs, M., et al. (2000). "Causes and consequences of tumour acidity and implications for treatment." *Molecular medicine today* 6(1): 15-19.

Suker, M., et al. (2016). "FOLFIRINOX for locally advanced pancreatic cancer: a systematic review and patient-level meta-analysis." *The lancet oncology* 17(6): 801-810.

Sun, T.-W., et al. (2018). "Hydroxyapatite nanowire/collagen elastic porous nanocomposite and its enhanced performance in bone defect repair." *RSC advances* 8(46): 26218-26229.

Sun, Z., et al. (2020). "Hydrogel-Based Controlled Drug Delivery for Cancer Treatment: A Review." *Molecular pharmaceutics* 17(2): 373-391.

Sylvester, R. J., et al. (2016). "Systematic review and individual patient data meta-analysis of randomized trials comparing a single immediate instillation of chemotherapy after transurethral resection with transurethral resection alone in patients with stage pTa–pT1 urothelial carcinoma of the bladder: which patients benefit from the instillation?" *European urology* 69(2): 231-244.

Sylvester, R. J., et al. (2006). "Predicting recurrence and progression in individual patients with stage Ta T1 bladder cancer using EORTC risk tables: a combined analysis of 2596 patients from seven EORTC trials." *European urology* 49(3): 466-477.

Ta, H. T., et al. (2008). "Injectable chitosan hydrogels for localised cancer therapy." *Journal of Controlled Release* 126(3): 205-216.

Takimoto, C. H. and A. Awada (2008). "Safety and anti-tumor activity of sorafenib (Nexavar®) in combination with other anti-cancer agents: a review of clinical trials." *Cancer chemotherapy and pharmacology* 61(4): 535-548.

Tang, B., et al. (2019). "Hydroxypropylcellulose enhanced high viscosity endoscopic mucosal dissection intraoperative chitosan thermosensitive hydrogel." *Carbohydrate Polymers* 209: 198-206.

Tertuliano, O. A. and J. R. Greer (2016). "The nanocomposite nature of bone drives its strength and damage resistance." *Nature materials* 15(11): 1195-1202.

Tong, H., et al. (2018). "The benefits of modified FOLFIRINOX for advanced pancreatic cancer and its induced adverse events: a systematic review and meta-analysis." *Scientific reports* 8(1): 1-8.

Tuna, B., et al. (2011). "Histologic grading of urothelial papillary neoplasms: impact of combined grading (two-numbered grading system) on reproducibility." *Virchows Archiv* 458(6): 659-664.

Tyagi, P., et al. (2008). "Structural aspects of the anti-cancer drug oxaliplatin: A combined theoretical and experimental study." *Polyhedron* 27(18): 3567-3574.

Tyagi, P., et al. (2006). "Recent advances in intravesical drug/gene delivery." *Molecular pharmaceutics* 3(4): 369-379.

Ubeyitogullari, A., et al. (2018). "In Vitro Digestibility of Nanoporous Wheat Starch Aerogels." *Journal of Agricultural and Food Chemistry* 66(36): 9490-9497.

ud Din, F., et al. (2017). "Effective use of nanocarriers as drug delivery systems for the treatment of selected tumors." *International journal of nanomedicine* 12: 7291.

Uhrich, K. E., et al. (1999). "Polymeric systems for controlled drug release." *Chemical Reviews-Columbus* 99(11): 3181-3198.

Ulker, Z. and C. Erkey (2014). "An emerging platform for drug delivery: Aerogel based systems." *Journal of Controlled Release* 177: 51-63.

Uman, S., et al. (2020). "Recent advances in shear-thinning and self-healing hydrogels for biomedical applications." *Journal of applied polymer science* 137(25): 48668.

Vale, C. (2005). "Neoadjuvant chemotherapy in invasive bladder cancer: update of a systematic review and meta-analysis of individual patient data: advanced bladder cancer (ABC) meta-analysis collaboration." *European urology* 48(2): 202-206.

Valo, H., et al. (2013). "Drug release from nanoparticles embedded in four different nanofibrillar cellulose aerogels." *European journal of pharmaceutical sciences* 50(1): 69-77.

van Valenberg, F. J. P., et al. (2021). "DPPG2-based thermosensitive liposomes with encapsulated doxorubicin combined with hyperthermia lead to higher doxorubicin concentrations in the bladder compared to conventional application in pigs: A rationale for the treatment of muscle-invasive bladder cancer." *International journal of nanomedicine* 16: 75.

Vemulakonda, V. M., et al. (2005). "Inhibitory effect of intravesically applied botulinum toxin A in chronic bladder inflammation." *The Journal of urology* 173(2): 621-624.

Veres, P., et al. (2017). "Mechanism of drug release from silica-gelatin aerogel—Relationship between matrix structure and release kinetics." *Colloids and Surfaces B: Biointerfaces* 152: 229-237.

Veronovski, A., et al. (2013). "Preparation of multi-membrane alginate aerogels used for drug delivery." *The Journal of Supercritical Fluids* 79: 209-215.

Veronovski, A., et al. (2012). "Synthesis and Use of Organic Biodegradable Aerogels as Drug Carriers." *Journal of Biomaterials Science, Polymer Edition* 23(7): 873-886.

Vihola, H., et al. (2005). "Cytotoxicity of thermosensitive polymers poly (N-isopropylacrylamide), poly (N-vinylcaprolactam) and amphiphilically modified poly (N-vinylcaprolactam)." *Biomaterials* 26(16): 3055-3064.

Wagner, M., et al. (2004). "Curative resection is the single most important factor determining outcome in patients with pancreatic adenocarcinoma." *BJS* 91(5): 586-594.

Wagner, V., et al. (2006). "The emerging nanomedicine landscape." *Nature biotechnology* 24(10): 1211-1217.

Wang, A. Z., et al. (2008). "Biofunctionalized targeted nanoparticles for therapeutic applications."

Wang, B., et al. (2020). "Poly(amidoamine)-modified mesoporous silica nanoparticles as a mucoadhesive drug delivery system for potential bladder cancer therapy." *Colloids and Surfaces B: Biointerfaces* 189: 110832.

Wang, C., et al. (2009). "In vitro performance of an injectable hydrogel/microsphere based immunocyte delivery system for localised anti-tumour activity." *Biomaterials* 30(36): 6986-6995.

Wang, H., et al. (2015). "Doxorubicin conjugated phospholipid prodrugs as smart nanomedicine platforms for cancer therapy." *Journal of Materials Chemistry B* 3(16): 3297-3305.

Wang, R., et al. (2017). "pH-Controlled drug delivery with hybrid aerogel of chitosan, carboxymethyl cellulose and graphene oxide as the carrier." *International Journal of Biological Macromolecules* 103: 248-253.

- Wang, X. and Z. Guo (2013). "Targeting and delivery of platinum-based anticancer drugs." *Chemical Society Reviews* 42(1): 202-224.
- Wegst, U. G. K., et al. (2015). "Bioinspired structural materials." *Nature materials* 14(1): 23-36.
- Wei, M., et al. (2021). "Injectable poly (γ -glutamic acid)-based biodegradable hydrogels with tunable gelation rate and mechanical strength." *Journal of Materials Chemistry B* 9(16): 3584-3594.
- Wei, S., et al. (2020). "Synthesis of chitosan aerogels as promising carriers for drug delivery: A review." *Carbohydrate Polymers* 231: 115744.
- Weiden, J., et al. (2018). "Synthetic immune niches for cancer immunotherapy." *Nature Reviews Immunology* 18(3): 212-219.
- Wen, X. (2021). Mathematical model for the change of the protein profiles in urine during the bladder cancer development.
- Wheate, N. J., et al. (2010). "The status of platinum anticancer drugs in the clinic and in clinical trials." *Dalton transactions* 39(35): 8113-8127.
- Whyard, T., et al. (2020). "Organoid model of urothelial cancer: Establishment and applications for bladder cancer research." *Biotechniques* 69(3): 193-199.
- Willis, D. L., et al. (2015). "Clinical outcomes of cT1 micropapillary bladder cancer." *The Journal of urology* 193(4): 1129-1134.
- Witjes, J. A., et al. (2014). "EAU guidelines on muscle-invasive and metastatic bladder cancer: summary of the 2013 guidelines." *European urology* 65(4): 778-792.
- Wright, B., et al. (2012). "Enhanced viability of corneal epithelial cells for efficient transport/storage using a structurally modified calcium alginate hydrogel." *Regenerative medicine* 7(3): 295-307.
- Wu, S., et al. (2017). "High strength, biocompatible hydrogels with designable shapes and special hollow-formed character using chitosan and gelatin." *Carbohydrate Polymers* 168: 147-152.
- Wu, W., et al. (2011). "Drug release behaviors of a pH sensitive semi-interpenetrating polymer network hydrogel composed of poly (vinyl alcohol) and star poly [2-(dimethylamino) ethyl methacrylate]." *International Journal of Pharmaceutics* 416(1): 104-109.
- Xia, J.-Y., et al. (2015). "Gemcitabine-Loaded Nanocarrier for the Potential Treatment of Bladder Cancers: A Nanomedicine Approach." *Journal of Biomaterials and Tissue Engineering* 5(2): 128-134.

- Xing, Q., et al. (2014). "Increasing Mechanical Strength of Gelatin Hydrogels by Divalent Metal Ion Removal." *Scientific reports* 4(1): 4706.
- Xiong, J.-Y., et al. (2005). "Topology evolution and gelation mechanism of agarose gel." *The Journal of Physical Chemistry B* 109(12): 5638-5643.
- Xu, J., et al. (2021). "Preparation of Cellulose Hydrogel Dressing with Evenly Dispersed Hydrophobic Drugs by Hydrogen Bonding and Encapsulation Methods." *Macromolecular Materials and Engineering* 306(10): 2100286.
- Xu, X., et al. (2020). "Near-infrared light-triggered degradable hyaluronic acid hydrogel for on-demand drug release and combined chemo-photodynamic therapy." *Carbohydrate Polymers* 229: 115394.
- Xu, Y. and M. Villalona-Calero (2002). "Irinotecan: mechanisms of tumor resistance and novel strategies for modulating its activity." *Annals of Oncology* 13(12): 1841-1851.
- Xu, Y. and M. A. Villalona-Calero (2002). "Irinotecan: mechanisms of tumor resistance and novel strategies for modulating its activity." *Annals of Oncology* 13(12): 1841-1851.
- Yafi, F. A., et al. (2011). "Contemporary outcomes of 2287 patients with bladder cancer who were treated with radical cystectomy: a Canadian multicentre experience." *BJU international* 108(4): 539-545.
- Yahya, E. B., et al. (2021). "Insights into the role of biopolymer aerogel scaffolds in tissue engineering and regenerative medicine." *Polymers* 13(10): 1612.
- Yamane, C., et al. (2006). "Two different surface properties of regenerated cellulose due to structural anisotropy." *Polymer journal* 38(8): 819-826.
- Yang, G., et al. (2018). "Assessment of the characteristics and biocompatibility of gelatin sponge scaffolds prepared by various crosslinking methods." *Scientific Reports* 8(1): 1616.
- Yoo, C., et al. (2017). "Efficacy and safety of neoadjuvant FOLFIRINOX for borderline resectable pancreatic adenocarcinoma: improved efficacy compared with gemcitabine-based regimen." *Oncotarget* 8(28): 46337-46347.
- Yuan, Y., et al. (2018). "Effects of konjac glucomannan on the structure, properties, and drug release characteristics of agarose hydrogels." *Carbohydrate Polymers* 190: 196-203.
- Zabot, G. L. (2020). Chapter 11 - Decaffeination using supercritical carbon dioxide. *Green Sustainable Process for Chemical and Environmental Engineering and Science*. Inamuddin, A. M. Asiri and A. M. Isloor, Elsevier: 255-278.

Zargarzadeh, M., et al. (2022). "Self-glucose feeding hydrogels by enzyme empowered degradation for 3D cell culture." *Materials Horizons* 9(2): 694-707.

Zarmpi, P., et al. (2017). "Biopharmaceutical aspects and implications of excipient variability in drug product performance." *European journal of pharmaceutics and biopharmaceutics* 111: 1-15.

Zashikhina, N. N., et al. (2017). "Self-assembled polypeptide nanoparticles for intracellular irinotecan delivery." *European journal of pharmaceutical sciences* 109: 1-12.

Zhang, J., et al. (2007). "Dual thermo- and pH-sensitive poly (N-isopropylacrylamide-co-acrylic acid) hydrogels with rapid response behaviors." *Polymer* 48(6): 1718-1728.

Zhang, K., et al. (2021). "Thermo-responsive hydrogels: from recent progress to biomedical applications." *Gels* 7(3): 77.

Zhang, X., et al. (2021). "Locally Injectable Hydrogels for Tumor Immunotherapy." *Gels* 7(4): 224.

Zhang, Y., et al. (2019). "Multiple Physical Cross-Linker Strategy To Achieve Mechanically Tough and Reversible Properties of Double-Network Hydrogels in Bulk and on Surfaces." *ACS Applied Polymer Materials* 1(4): 701-713.

Zhang, Y., et al. (2021). "Strong, Self-Healing Gelatin Hydrogels Cross-Linked by Double Dynamic Covalent Chemistry." *Chempluschem* 86(11): 1524-1529.

Zhang, Y.-G., et al. (2018). "Bioinspired Ultralight Inorganic Aerogel for Highly Efficient Air Filtration and Oil–Water Separation." *ACS Applied Materials & Interfaces* 10(15): 13019-13027.

Zhao, W., et al. (2013). "Degradable natural polymer hydrogels for articular cartilage tissue engineering." *Journal of Chemical Technology and Biotechnology* 88(3): 327-339.

Zhao, Y., et al. (2014). "In situ cross-linked polysaccharide hydrogel as extracellular matrix mimics for antibiotics delivery." *Carbohydrate Polymers* 105: 63-69.

Zheng, K. and D. Du (2021). "Recent advances of hydrogel-based biomaterials for intervertebral disc tissue treatment: A literature review." *Journal of Tissue Engineering and Regenerative Medicine* 15(4): 299-321.

Zheng, L., et al. (2020). "Engineering of aerogel-based biomaterials for biomedical applications." *International journal of nanomedicine* 15: 2363.

Zhu, D., et al. (2021). "Single injection and multiple treatments: an injectable nanozyme hydrogel as AIEgen reservoir and release controller for efficient tumor therapy." *Nano Today* 37: 101091.

Zosel, A. (1989). "Adhesive failure and deformation behaviour of polymers." *The journal of adhesion* 30(1-4): 135-149.

Zou, F. and T. Budtova (2021). "Polysaccharide-based aerogels for thermal insulation and superinsulation: An overview." *Carbohydrate Polymers* 266: 118130.